Armed Services Technical Information Agency

Because of our limited supply, you are requested to return this copy WHEN IT HAS SERVED YOUR PURPOSE so that it may be made available to other requesters. Your cooperation will be appreciated.

AD 36782

NOTICE: WHEN GOVERNMENT OR OTHER DRAWINGS, SPECIFICATIONS OR OTHER DATA ARE USED FOR ANY PURPOSE OTHER THAN IN CONNECTION WITH A DEFINITELY RELATED GOVERNMENT PROCUREMENT OPERATION, THE U. S. GOVERNMENT THEREBY INCURS NO RESPONSIBILITY, NOR ANY OBLIGATION WHATSOEVER; AND THE FACT THAT THE GOVERNMENT MAY HAVE FORMULATED, FURNISHED, OR IN ANY WAY SUPPLIED THE SAID DRAWINGS, SPECIFICATIONS, OR OTHER DATA IS NOT TO BE REGARDED BY IMPLICATION OR OTHERWISE AS IN ANY MANNER LICENSING THE HOLDER OR ANY OTHER PERSON OR CORPORATION, OR CONVEYING ANY RIGHTS OR PERMISSION TO MANUFACTURE, USE OR SELL ANY PATENTED INVENTION THAT MAY IN ANY WAY BE RELATED THERETO.

Reproduced by

DOCUMENT SERVICE CENTER

KNOTT BUILDING, DAYTON, 2, OHIO

UNCLASSIFIED

AD No. 36 782
ASTIA FILE COPY

ATTENUATORS

by

ANTHONY B. GIORDANO

FINAL REPORT R-351-53, PIB-285
BUREAU OF SHIPS
CONTRACT NO-bsr-43360
INDEX NO. 100-402

December 11, 1953

FURTHER DISSEMINATION IS AUTHORIZED ONLY TO MILITARY AGENCIES.

MRI

POLYTECHNIC INSTITUTE OF BROOKLYN
MICROWAVE RESEARCH INSTITUTE

Microwave Research Institute
Polytechnic Institute of Brooklyn
55 Johnson Street
Brooklyn 1, New York

Report R-351-53, PIB-285
Contract No. NObsr-43360
Index No. 100-402

FINAL REPORT
ON
ATTENUATORS

Contract No. NObsr-43360
Index No. 100-402
Bureau of Ships
Navy Department

The research reported in this document has been made possible through support and sponsorship extended by the Bureau of Ships under Contract No. NObsr-43360, Index No. 100-402. It is published for technical information only and does not represent recommendations or conclusions of the sponsoring agency.

Author: Anthony B. Giordano
Anthony B. Giordano
Research Supervisor

Title Page
Acknowledgment
Abstract
Table of Contents
58 Pages of Text
112 Pages of Figures

Approved: Ernst Weber
Ernst Weber
Director

Brooklyn 1, New York
December 11, 1953

ACKNOWLEDGMENT

This report has been prepared in connection with the Bureau of Ships Contract No. NObsr-43360, Index No. 100-402 carried on at the Microwave Research Institute of the Polytechnic Institute of Brooklyn.

ABSTRACT

This final report is devoted to the presentation of design principles and /or data relating to metallized-glass attenuators, dissipating matching networks, the measurement of waveguide attenuator phase-shifts, high power probe attenuators, a variable broadband 7/8" coaxial attenuator, fixed attenuators for 3/8" coaxial line, magnetic attenuators, the fabrication and mechanical testing of coaxial attenuators, and the evaporation of uniform metallic film attenuator plates.

TABLE OF CONTENTS

TABLE OF CONTENTS
(Continued)

CHAPTER I

INTRODUCTION

1.1 Summary of Objectives: Since its inception on June 1, 1949, Contract No. NObsr-43360, Index No. 100-402, has provided for the development of

a. broadband continuously variable metallized film glass attenuators for

Waveguide	Frequency Range	Maximum Attenuation
RG-48/U (3" x 1 1/2")	2.60 - 3.95 kmc/sec	40 db
RG-50/U (1 1/2" x 3/4")	5.85 - 8.20 kmc/sec	40 db
RG-50/U (1 1/2" x 3/4")	5.4 - 5.9 kmc/sec	20 db
RG-50/U (1 1/2" x 3/4")	5.4 - 5.9 kmc/sec	70 db

b. fixed high-power probe attenuators for

Coaxial Line	Frequency Range	Maximum Attenuation
7/8" (49.45 ohms)	1.0 - 4.0 kmc/sec	40 db
1 5/8" (53.65 ohms)	1.0 - 3.0 kmc/sec	50 db

c. fixed metallized film glass attenuators for 3/8" (49.45 ohms) coaxial line

d. variable metallized film glass attenuator for 7/8" (49.45 ohms) coaxial line

e. synthesis theory of broadband matching networks

f. techniques for the measurement of phase-shift characteristics of variable waveguide attenuators

g. magnetic coaxial attenuators

h. shock and vibration data of coaxial attenuators

1.2 Staff and Special Reports Issued: The following personnel were associated with the activities of the contract:

Anthony B. Giordano
Herbert J. Carlin
Salvatore Ammiratti
Philip Kantrowitz

Paul G. Mariotti
Moe Wind
Lucio M. Vallese
Hubert W. Schleuning
Clifford Graham
Richard LaRosa
Harold Rapaport
Mary Eschwei
Eugene Torgow
Milton A. Treuhaft
Carl Bollinger
Rose Scarpa
Walter Huebner
Dorothy Iverson
Goldie Altstock
Lula Harisiades
Marie Seifert
Morris Cohen
Walter Cornetz

Special research reports have been issued in connection with specific phases. They are as follows:

1. "Development of a Rotary Evaporation Jig for Thin Film Attenuators", (R-241-51) by C. Graham.

2. "Shock and Vibration Tests on Coaxial Attenuators", (R-242-51) by H.W. Schleuning.

3. "On the Uniformity of Evaporated Metallic Film Attenuator Plates", (R-252-51, PIB-193) by H.W. Schleuning.

4. "A Class of Broadband Dissipative Matching Networks Designed on an Insertion Loss Basis", (R-264-52, PIB-203) by R. LaRosa and H.J. Carlin.

5. "20 DB and 70 DB Attenuator Plates for 1 1/2" x 3/4" Waveguide", (R-283-52, PIB-222) by A.B. Giordano.

6. "Preliminary Report on 7/8" Broadband Variable Coaxial Attenuator", (R-354-53, PIB-288) by L.M. Vallese.

In addition, some of the earlier work on dissipative matching networks carried on by R.LaRosa and H.J. Carlin under the sponsorship of this contract was included in the Doctor's Dissertation of R. LaRosa. It was issued as

"Broadband Dissipative Matching Networks", D.E.E. Thesis, Polytechnic Institute of Brooklyn, June 1953,

with an acknowledgment to the Bureau of Ships Contract No. NObsr-43360.

CHAPTER II

DEVELOPMENT OF METALLIZED-GLASS ATTENUATORS FOR WAVEGUIDES 3" x 1 1/2" AND 1 1/2" x 3/4"

2.1 Summary: Four variable attenuators were developed for the following waveguides, frequency limits, and maximum attenuation;

1. RG-48/U (3" x 1 1/2"); 2.60 - 3.95 kmc/sec; 40 db
2. RG-50/U (1 1/2" x 3/4"); 5.85 - 8.20 kmc/sec; 40 db
3. RG-50/U (1 1/2" x 3/4"); 5.4 - 5.9 kmc/sec; 20 db
4. RG-50/U (1 1/2" x 3/4"); 5.4 - 5.9 kmc/sec; 70 db

The maximum VSWR of the first three units was within 1.1 while the last unit had a maximum VSWR of approximately 1.15. These attenuators were designed for a minimum of insertion loss as well as a minimum of frequency sensitivity.

2.2 Design Principles: The dissipative element of the developed attenuators is comprised of a glass plate coated with an evaporated film of nichrome. The thickness of the deposit is small in comparison to the depth of penetration. A coating of magnesium fluoride is applied during the fabrication process to protect the film from chemical deterioration and accidental scratching. Such films have been proven to be extremely stable and insensitive to atmospheric changes.

The element is inserted into a waveguide casing parallel to the electric field of the TE_{10} mode from one of the narrow side walls of the casing. The casing incorporates a precision mechanism for varying the position of the plate in order to realize variability in attenuation.

Each element is so constructed that the attenuator is bilaterally matched. By matching is meant that the input impedance of the attenuator is approximately equal to the characteristic impedance of the waveguide line used. A good match is necessary for proper loading on preceding equipment and is important for the accurate calibration and interchangeability of various calibrated attenuators. The mismatch is measured as a voltage-standing-wave-ratio, abbreviated VSWR. The desired match is achieved by providing a film transforming section at either end of the plate.

The design of the plate is based upon an optimization of plate dimensions, plate dielectric, and film resistivity for desired attenuation and VSWR characteristic. The casing is comprised of properly spaced struts which support the metallized-glass element. Usually, two struts are used spaced an odd multiple of the mean waveguide wavelength since they introduce shunting capacitance. A precision screw mechanism controls the insertion of the plate into the guide.

2.3 Development of 3" x 1 1/2" 40 DB Attenuator

1. Frequency Range

For dominant mode transmission in waveguide size 3" x 1 1/2" x .080", the prescribed maximum limits of frequency operation is 2.6 to 3.95 kmc/sec or, in terms of free-space wavelength, 7.60 to 11.54 cm. This bandwidth has been subdivided into four spot wavelengths at which measurements have been performed to ascertain broadband characteristics; the wavelengths are 7.60 cm, 9.16 cm, 10.07 cm, and 11.54 cm. Wavelength 9.16 cm represents the average between the two wavelengths at the edges of the bandwidth in free-space. Wavelength 10.07 cm is the free-space wavelength corresponding to the mean waveguide wavelength.

2. Preliminary Scaling Design

The preliminary design of the attenuator element was ascertained by scaling one of the acceptable metallized glass plates designed for guide size 2"x1"x0.064". Details of this attenuator are presented in Report R-206-49 issued by MRI.

The scaling principle used is that the ratio of plate dimensions to the mean waveguide wavelength remains invariant, assuming that the characteristic impedance and glass dielectric remain constant. The scaled data for the element of guide size 3" x 1 1/2" x 0.080" are shown by Table I

TABLE I

Guide Size Inner Dimension a by b (in.)	Ratio a/b	Mean Ratio λ_g/λ	Mean λ_g (in.)	Z_c (ohms)	Glass Length (in.)	Glass Width (in.)	Glass Thickness (in.)	Film Resistivity (ohms/sq.)	Length of Matching Section (in.)
1.872x0.872	2.15	1.4	3.685	303	9.50	0.795	0.062	187.5	0.50
2.840x1.340	2.12	1.41	5.545	309	14.30	1.20	0.0933	187.5	0.753

The 2" x 1" x 0.064" plate data are shown by Fig. PIB-C-504-U.

Since the scaled plate length was 14.3 inches, it became nesessary to fabricate the plate in two halves since the evaporating chamber at MRI could not accommodate plate lengths of greater than 9.8 inches. The preliminary specifications of one half-plate are given by Fig. MRI-10704.

The casing was constructed so that each half-plate would be attached to a pair of struts. The casing, therefore, employed four struts. They were displaced along the guide length by a distance corresponding to a quarter of the mean waveguide wavelength. These struts were attached to a common base so that they moved in unison. An assembly view of this casing is illustrated by Dwg. No. PIB-A-515-A.

The scaled plate was fabricated and attenuation measurements were performed. The results of these measurements are illustrated by Fig. MRI-10927.

3. Experimental Data Including Final Design

Since the total attenuation spreads of the scaled plate at the upper db range was appreciable, additional measurements were performed to determine the optimum plate-width corresponding to

lime glass width - 0.091 inch
film resistivity - 187.5 ohms/square
glass length per half section 7.156 inches
insertion into guide 500 mils

The results of these measurements are shown by Fig. MRI-10923. These data indicate that the optimum plate width is 1.215 inch.

A plate having a width of 1.215 inch was tested. The attenuation and VSWR responses are given by Figures. MRI-11147 and MRI-11148. In the upper db range, the results were not within desired specifications.

A series of plates were tested to determine the optimum design. The final design data are shown below

lime glass width - 0.068 inch
glass length per half section- 7.2 inches
film resistivity - 195 ohms/square

The plate specifications with tolerances are illustrated by Dwg. PIB-C-515-U the corresponding attenuation and VSWR characteristics are given by Figs. MRI-12218 and MRI-12219. These characteristics are acceptable and hold only if the narrow dimension of the waveguide falls within a value $1.340^{+0.005}_{-0.002}$.

2.4 Development of 1 1/2" x 3/4" Attenuator (40 DB)

1. Frequency Range

The first attenuator developed was for a maximum attenuation of 40 db over the frequency range of 3.66 to 5.13 kmc/sec. This range corresponds to a wavelength coverage of 3.66 to 5.13 cm. Four wavelengths were selected for attenuation and VSWR measurements, namely, 3.66 cm, 4.28 cm, 4.25 cm and 5.13 cm. Wavelength 4.28 is the mean between the two edges and 4.52 cm represents the free-space wavelength equivalent of the mean waveguide wavelength.

2. Preliminary Scaling Design

The scaling procedure discussed in Section 2.3 was utilized in determining the preliminary dimensions. The 2" x 1" x 0.064" plate was used as reference. The dimensions of the scaled plate for guide size 1 1/2" x 3/4" x 0.064" are shown by Table II

TABLE II

Guide Size Inner Dimension a by b (in.)	Ratio a/b	Mean Ratio λ_g/λ	Mean λ_g (in.)	Z_c (ohms)	Glass Length (in.)	Glass Width (in.)	Glass Thickness (in.)	Film Resistivity (ohms/sq.)	Length of Matching Section (in.)
1.872x0.872	2.15	1.43	3.685	303	9.50	0.795	0.062	187.5	0.50
1.372x0.622	2.21	1.325	2.35	278.8	6.0	0.50	0.040	187.5	0.317

The scaled plate is illustrated by Fig. MHI-10833. The step-film sections represent the matching transformer.

3. Experimental Data Including Final Design

The scaled plate described above was tested for attenuation and VSWR responses. A nominal glass thickness of 50 mils was used instead of 40 mils, the scaled value, since the 50 mil glass was commercially available.

Fig. MRI-10937 shows the resulting attenuation response which is rather sensitive to frequency. However, the corresponding VSWR response, which is not reported, possessed a maximum value of less than 1.1.

In order to improve the attenuation response, a series of plates were tested to determine the attenuation vs. plate width curves for

lime glass thickness	-	0.048 - 0.052 inch
nominal film resistivity	-	187 ohms/square
glass length	-	6.0 inches
insertion into guide	-	250 mils

The results of these measurements are illustrated by Fig. MRI-10934, which shows that the optimum plate width is approximately 0.534 inch. At this width, the total attenuation spread is 4 db in the region of 30 db and quite appreciable at attenuations of 40 db.

In order to decrease the attenuation spread, a series of plates were tested by varying the glass length, the glass width, and the surface resistivity of the film. It was finally concluded that the following specifications would lead to optimum results:

lime glass thickness	-	0.048 inch
film resistivity	-	150 ohms/square
glass length	-	7.65 inches

The attenuation and VSWR characteristics of such an optimum plate are shown by Figures MRI-11666 and MRI-11667. These were considered acceptable. The plate dimensions are given by Dwg. No. PIB-C-519-18. The assembly view of the final casing design is illustrated by Dwg. No. PIB-A-519-A. It is necessary that the narrow dimension of the guide be kept within $0.622 \pm .002$ in order to realize an acceptable response.

2.5 Development of 1 1/2" x 3/4" Attenuators (20 DB and 70 DB)

1. Specifications

The specifications of the development of metallized-glass plates capable of yielding 20 db and 70 db over the frequency range of 5.4 - 5.9 kmc/sec were set by the Bureau to be

a. Plate for 0 - 20 DB Attenuator

maximum insertion loss	- 0.5db
maximum bilateral VSWR	- 1.10 or better
maximum casing length	- 8 1/2" from flange to flange
calibration accuracy	- $\pm$ 0.1db from 0 to 8db
	$\pm$ 0.2db from 8 to 20db

b. Plate for 0 - 70 DB Attenuator

maximum insertion loss	- 1.0db
bilateral VSWR	- 1.15 or better
maximum casing length	- 10" from flange to flange
calibration accuracy	- ± 1.0db, from 0 to 40db
	± 1.5db, from 40 to 70db

2. Response Data of 40DB Attenuator

As a first step in this development, the 40db attenuator discussed in Section 2.4 was tested over the frequency range of 5.4 - 5.9 kmc.sec. The results were:

attenuation curves	-	Fig. MRI-12717
VSWR curves	-	Fig. MRI-12718

The attenuation curves revealed that the response was excellent from 0 - 20db. However, difficulties may arise in the range of 40 - 70db.

The VSWR curves indicated that the maximum VSWR in the attenuation range of 0 - 20db was approximately 1.16. However, from 40 - 70 db, the maximum VSWR was more than 1.24.

These data demonstrated the unsuitability of the 40db attenuator to meet desired specifications.

3. Design of 20DB Metallized-Glass Plate

The basic intent was to design a 20db attenuator possessing an over-all length of less than 8.5 inches. Based upon preliminary computations, a plate length of 5 inches was selected as most promising.

The 40db plate discussed in Section 2.4 was scaled to 5 inches. The results of attenuation and VSWR measurements are given by Figs. MRI-12702 and MRI-12703. In the neighborhood of 20db, the attenuation spread with frequency is 1.4db. The maximum VSWR is 1.16. To reduce these values, a series of plates were tested with the surface resistivity and plate width as variables. The length of the matching film section was increased from 0.317 inch to 0.432 inch in order to improve the VSWR. A study of the results yielded the optimum design specifications as given by Fig. MRI-12729. Two plates were fabricated and tested in casings with different average guide heights. The results are illustrated by the following figures

average guide height	=	0.621 inch
attenuation curves	-	Fig. MRI-12730
VSWR curves	-	Fig. MRI-12731
average guide height	=	0.626 inch
attenuation curves	-	Fig. MRI-12732
VSWR curves	-	Fig. MRI-12733

These results were satisfactory. The average insertion loss of the attenuator over the frequency range was approximately 0.43 db.

4. Design of 70DB Metallized-Glass Plate

A procedure was applied to improving the characteristics of the 40db plate in order to realize a 70db response. The matching length of the film step was increased to 0.432 and various plates were tested to obtain the optimum plate width and surface resistivity. These results yielded an optimum surface resistivity of 160 ohms per square. The optimum plate width was chosen from Fig. MRI-12734 to be 0.580 inch. The final design specifications are given by Fig. MRI-12735.

Two plates were constructed in accordance with Fig. MRI-12735 and tested in two casings having different average guide heights. The VSWR and attenuation responses are shown by the following curves.

average guide height	=	0.621 inch
VSWR curves	-	Fig. MRI-12736
attenuation curves	-	Fig. MRI-12737
average guide height	=	0.626 inch
VSWR curves	-	Fig. MRI-12738
attenuation curves	-	Fig. MRI-12739

These results met desired characteristics. The insertion loss, on the average over the frequency range, was about 0.62 db.

2.6 Uniformity of Evaporated Metallic Film Attenuator Plates: Difficulties were experienced in producing uniformly distributed evaporated metallic films on large size attenuator plates of lime glass. Theoretical and experimental investigations were made to determine what distribution can be expected and what might cause variations in that distribution.

The studies led to the conclusion that geometry, cleaning, and speed of evaporation are of great importance for the attainment of uniform evaporated films.

1. Geometry of the System

The geometry of the system should be such that all pieces of work that are to receive an evaporated film are equi-distant from the source. They should be located far enough from the source so that particles of essentially the same size will fall on the receiving surfaces and will all receive a film deposition of the same thickness according to the cosine cubed law. An acceptable distance from the source is approximately 15 inches.

2. Cleaning of the Substrate

In the recommended method, the substrate is first washed to remove any grease accumulated from handling during the grinding process which shapes the glass to size. The blanks are then polished with calcium carborate, such as, Bon Ami, followed by a thorough rinse. This polishing is followed by a wash with 10 percent Aerosol solution and then another rinse, following which the blanks are submerged in hot distilled water in which they are kept until they are ready to be placed on their supporting jig in the vacuum system. Before placing the blanks on the jig, they are taken from the hot distilled water by means of clean forceps. While holding the blanks with the forceps, the blanks are subjected to a blast of hot distilled water from a wash bottle and then a blast of freshly distilled acetone from another wash bottle. After the acetone spray, the blanks should be perfectly clean but should be inspected with reflected light for any surface contamination. Surface contamination, if present, is usually visible as a light grayish film. If any contamination is visible, the cleaning process is repeated until a clean surface is seen.

3. Speed of Evaporation

The most uniform and stable films, considering the speed of evaporation of the metallic film, are those that are formed from a combination of high speed evaporation at the start of the formation period and low speed evaporation at the end of the period. The reasoning behind this sequence is that the high initial rate of evaporation produces a finely aggregated uniform film. The lower speed final evaporation then builds up the preliminary film, filling in the spaces between the fine aggregates by a growth process, to produce a more homogeneous uniform film. It is well to reduce the speed of evaporation at the end of the deposition period for one other reason. When attenuator plates are being evaporated, their final resistance must be of a definite value. If the speed of evaporation is decreased near the end of the deposition period, the resistance of the test strip may be followed closely by a resistance measurement bridge and stopped sharply when the correct resistance value is reached. If the speed of evaporation is high at that time, it is almost impossible to stop the process at the correct resistance value.

2.7 References: Details of the above developments are presented in issued progress reports and in the following special Research Reports:

1. "On the Uniformity of Evaporated Metallic Film Attenuator Plates" (R-252-51, PIB-293) by H.W. Schleuning.

2. "20 DB and 70DB Attenuator Plates for 1 1/2" x 3/4" Waveguide" (R-283-52, PIB-222) by A. Giordano.

CHAPTER III

A CLASS OF BROADBAND DISSIPATIVE MATCHING NETWORKS DESIGNED ON AN INSERTION-LOSS BASIS

by R. LaRosa and H.J. Carlin

3.1 Summary: The design of broadband lossless matching networks is fairly well understood. Dissipative networks can perform functions which are not possible with lossless networks. The development of dissipative matching networks is presented from a preliminary viewpoint. Various types of procedures are discussed.

3.2 Application of Dissipative Matching Networks: In designing microwave equipment, it is often necessary to match the input impedance of some component to a resistive generator or to the characteristic impedance of a lossless line. When this match is required over a narrow band, a pair of reactive elements, (stubs, tuning screws, etc.) or a single element placed at a particular point on the line, can be used to give a perfect match at the mid-frequency. The mismatch at the edges of the band may be small enough (because of the narrowness of the band) so that a "single-frequency" match is adequate. When the load which is to be matched has an impedance which varies slowly as a function or frequency, tuning elements which store a minimum amount of energy are used in order to obtain the greatest bandwidth. When the load has some particular change with frequency, it is possible to pick tuning elements whose reactance change with frequency compensates for the load impedance change and thus gives a satisfactory match over a band.

The simple procedure outlined above is adequate for many situations encountered in the design of radars, communication facilities, and some narrow band test equipment. When antennas are connected to transmitters by long transmission lines, it is often necessary to match more carefully to avoid frequency pulling. In this case, more effort is expended in the choice of line lengths, transformers and stubs in order to give as nearly perfect match as possible in the transmitter band.

The above remarks apply to problems where simple lossless elements are adequate to give the required match. As the maximum permitted VSWR becomes smaller, or the required bandwidth becomes greater, the design becomes more difficult. Eventually, a point is reached when it is impossible to obtain required performance. When lossless matching networks are used, it is not possible, with physical elements, to match perfectly over any finite bandwidth. The question of what amount of mismatch must be tolerated for a particular load impedance and specified frequency band has been treated by R.M. Fano (Journal, Franklin Institute, Jan. 1950)

When the required performance is greater than the possible limit for lossless matching networks, it is necessary to include dissipative elements in the matching network. One simple method of doing this is known as "padding". A dissipative attenuator can be placed in front of the load and if the attenuation is large enough, the input impedance of the attenuator can be matched to the generator or transmission line. This is a common procedure because (1) there may be more than sufficient power available and (2) broadband matched attenuators are usually available. This process is not good when signal strength is at a premium because it is wasteful of power. It simply consists of putting in enough insertion loss so that the load cannot be "seen" from the input terminals of the matching or so-called buffer attenuator. It is therefore desirable to investigate matching networks which include dissipative elements which are inserted in such a way that power waste is minimized.

3.3 Properties of Matching Four-Poles

1. Specification of the Matching Problem

A load is given which has an impedance $Z(p)$ where $p = \sigma + j\omega$ is the complex frequency variable. Power is supplied by a generator whose internal resistance is R_o. A lossy four-terminal network (four-pole) is connected between generator and load as in Fig. MRI-11968a. The matching network is to be composed of linear, passive elements and should do the following:

(a) The imput impedance of the load and matching network, i.e., the impedance presented to the generator, should be constant and equal to R_o for all values of p.

(b) In a specified range of simusoidal frequencies ($\sigma = 0$, $0 \leq \omega \leq \omega_c$), the power in the load should be constant to within a certain tolerance and this constant should be as large as possible.

The above requirements are more restrictive than would be desirable in many practical problems, but they provide sufficient latitude for the present study. Note that although low-pass performance is usually not desirable in microwave work, many loads encountered in practice have geometric symmetry about some center frequency. These loads have low-pass equivalents: knowledge obtained for the low-pass problem can be applied to them. Results of the present investigation can also be extended by means of high-pass transformers.

In what follows, all impedances are normalized to R_o so that the generator has a one ohm internal impedance, and the load is $z(p) = Z(p)/R_o$. The open circuit voltage of the generator is arbitrarily fixed at 2 volts (RMS) so that the available power from the generator is 1 watt.

The power that is dissipated in the load is of physical significance only when $\sigma = 0$, since the $j\omega$ axis of the p-plane corresponds to sinusoidal frequencies (steady-state a.c.). This power is written as a function of ω or $P(\omega)$. $P(\omega)$ is the actual power in watts for the normalized system. $P(\omega)$ is identically the ratio of power dissipated in the load to the available power of the generator. Note that the power entering the input terminal of the four-pole is the available power of the generator (because it is perfectly matched). Therefore, $P(\omega)$, can also be interpreted as the ratio of power leaving the output terminals of the matching network to the power entering the input terminal of the matching four-pole.

2. Network Equations of Matching Four-Poles

The four-pole is characterized by three parameters, $z_{11}(p)$, $z_{22}(p)$, $z_{12}(p)$ which are the open circuit input, output, and transfer impedances, respectively. When the four-pole is terminated in z, its input impedance is:

$$z_{in} = z_{11} - \frac{z_{12}^2}{z_{22} + z} \qquad (1)$$

$z_{in} = 1$ to satisfy requirement (a) of Part 1 so that the three parameters are related by the following equations:

$$z_{11} = 1 + \frac{z_{12}^2}{z_{22} + z} \qquad (2a)$$

$$z_{12}^2 = (z_{11} - 1)(z_{22} + z) \qquad (2b)$$

If $z(p=j\omega) = r(\omega) + jx(\omega)$: the expression for $P(\omega)$ is:

$$P(\omega) = \left| \frac{z_{12}}{z_{22} + z} \right|^2 r(\omega) = \left| \frac{z_{11} - 1}{z_{22} + z} \right| r(\omega) \qquad (3)$$

Thus, there are two general relations; one of them (Equations 2a, 2b) is algebraic, but the other one (Equation 3) involves magnetides of sums of impedances and the real part of $z(j\omega)$. One of the four-pole parameters can be arbitrarily picked because there are only two relations. It is important to note that this arbitrary parameter is a function of the complex variable p.

One additional consideration makes the problem extremely difficult. The four-pole must be physically realizable as a linear, passive network. Whether it is composed of lumped inductance, capacitance, and resistance, or distributed elements is a question that need not be considered here. In some of the examples, the matching network will be composed of lumped elements, while in others, various impedances will be given as empirically determined functions of ω, and therefore might be synthesized by either lumped or distributed elements.

One ideal transformer will be allowed in the matching network, either at the output or input end. This avoids complication in the treatment of the problem and is justified in practice because,

(a) There is often considerable choice of impedance level at the terminals of a microwave load (where to tap into a cavity for instance). This freedom of choice corresponds to the availability of an ideal transformer.

(b) When sufficient physical space is available, an ideal transformer at the input of the matching network, for the input impedance of a long line terminated in a mismatched load is a complicated function of frequency and is difficult to match.

3.4 Realizability of Matching Networks Without Regard to Insertion Loss: Given any realizable load function $z(p)$, it is always possible to provide a four-pole which will, when terminated in $z(p)$ have unit input impedance. To show this, a simple method of matching will be described which makes use of the following theorem:

If $Z_1(p)$ is a physically realizable minimum reactance impedance (i.e., $Z_1(p)$ has no pole on the $j\omega$ axis of the p-plane), it is possible to find a $Z_2(p)$ such that

$$Z_1(p) + Z_2(p) = R \qquad (4)$$

If $Z_1(j\omega) = R_1(\omega) + jX_1(\omega)$, then

$$R \geq \text{maximum value of } R_1(\omega) \qquad (5)$$

The proof of this theorem is given by Bode. ("Network Analysis and Feedback Amplifier Design", VanNostrand Co.)

Applying this to a given minimum reactance load $z(p)$, it is clear that if the real part of $z(p)$ along $j\omega$ obeys:

$$\text{maximum } r(\omega) \leq 1 \qquad (6)$$

then a two-terminal impedance connected in series with the load can be designed to give a perfect match to a 1 ohm generator.

If Max $r(\omega) > 1$, a transformer can precede or follow the series matching impedance to adjust the impedance level to the unit value required.

If $z(p)$ is not minimum reactance, a new $z'(p)$ function can be formed by placing a resistor of any value in parallel with $z(p)$. This new $z'(p)$ function will then be minimum reactance and an impedance, $z_1(p)$, can be put in series with $z'(p)$ to give a perfect match to some constant resistance. This constant resistance can be transformed to unity as before by means of an ideal transformer.

3.5 Some Matching Structures: As discussed in Section 3.3, Part 3, it is always possible to match any load, $Z(p)$, to a 1 ohm generator by means of a realizable dissipative four-pole. These matching structures are in the forms shown by Figures MRI-11968b and MRI-11968c. For design details refer to the report by Richard LaRosa and Herbert J. Carlin "A Class of Broad-Band Dissipative Matching Networks Designed On an Insertion-Loss Basis", Report R-264-52, PIB-203.

This work was continued under the auspices of ONR Contract NOnr-292(00). For latest results refer to Research Report R-308-53, PIB-247 on "A General Theory of Wideband Matching With Dissipative Four-Poles" by R. LaRosa and H.J. Carlin.

Examples of derived matching structures are illustrated by Figures MRI-13041 and MRI-13402.

CHAPTER IV

PHASE SHIFT DATA OF 1 1/4" x 5/8" ATTENUATOR

4.1 Summary: The insertion of a metallized-glass plate within a waveguide casing introduces not only attenuation but also phase-shifts. A phase-shift measuring system was designed for waveguide 1 1/4" x 5/8" to ascertain phase-shifts for an attenuation range of 0 - 20 db approximately. It was observed that an attenuation of 20 db yields a maximum phase-shift of 40 degrees.

4.2 Historical Notes: Under the Watson Contract No. WLENG-W28-099-ac-197, the Microwave Research Institute investigated techniques for measuring phase-shifts introduced by a metallized-glass attenuator for waveguide size 1/2" x 1/4" over a frequency range of 18.0 - 25.5 kmc/sec. These techniques have been summarized in a research report entitled "Phase-Shift Data of Metallized-Glass Attenuator for Frequency Range 18,000 - 25,500 mc/sec", R-228; PIB-173. Various methods were investigated and one selected as most feasible from the point of view of simplicity and ease of operation. The procedure has been named the comparison method and it is described below.

4.3 Comparison Method of Measuring Phase-Shifts: The line set-up for the comparison method of measuring phase-shifts is illustrated in Part A of Fig. MRI-11422. It contains a split-section to divide the signal power equally into two branches, one containing a phase-shift reference standard, and the other the unknown attenuator. The branches are recombined through another split-section which leads to a spectrum analyzer detector, where the resulting signal is measured.

The phase-shift measurement is based upon the principle that the magnitude of the final signal depends upon the relative phase of the component signals as they leave the output split-section. With the unknown attenuator replaced by a line section, the phase-shift standard is set to yield zero output at the detector. This will occur at the setting for which the electric filed components of the two branches, E_a and E_b, are 180 electrical degrees out of phase. This is shown in Part B of Fig. MRI-11422. When the unknown attenuator is inserted, the electric field component of that branch, E_a, is reduced in magnetide and shifted in phase, as shown in Part C. The phase-shift standard is thereupon varied until the detector indicates that E_r is a minimum. This will occur when E_a and E_d are again 180 degrees out of phase, i.e., when the change of phase introduced by the phase-shift standard equals the change in phase introduced by the unknown attenuator, as illustrated in Part E, and the latter can thus be measured.

The line set-up as finally used in measuring the phase-shift of a test attenuator is shown in Fig. MRI-11423. To realize it, it was necessary to design buffers, bends, connectors, and a phase-shift standard.

4.4 Phase-Shift Standard: A phase-shift standard was developed for guide size 1 1/4" x 5/8" using the mechanism of the casing designed for the 1 1/4" x 5/8" waveguide attenuator. The development was based upon the use of a bilaterally tapered dielectric glass plate. Various lengths of lime glass and pyrex glass were measured. These data showed that it would be necessary to use glass lengths of about 10 inches to realize reasonable VSWR's. Fig. MRI-12547, illustrates the VSWR characteristics of the lime glass plate with four inch tapers at both ends. Fig. MRI-12643 corresponds to a similar pyrex glass plate. Comparing, it is noted that the pyrex glass plate yields smoother VSWR variations with higher values at 3 cm. The maximum phase-shift response with frequency of the pyrex glass plate is shown by Fig. MRI-12644. The lime glass plate yielded slightly lower values in maximum phase-shifts. The latter plate was selected as the best compromise.

4.5 Final Data: The bridge system shown by Fig. MRI-11423 was assembled and the phase-shift characteristics of attenuator 1 1/4" x 5/8" were measured. The results are shown by Fig, MRI-13030. The lower range of these curves were checked by the short-circuit method and these results are given by Fig. MRI-13029. They compared favorably.

Referring to Fig. MRI-11359 which represents the attenuation response of the 1 1/4" x 5/8" attenuator, it is noted that a plate insertion of 140 mils yields approximately an attenuation of 20 db at 4.25 cm. From Fig. MRI-13030, the corresponsing phase-shift is around 40 degrees.

CHAPTER V

HIGH POWER PROBE ATTENUATORS

by M. Wind and C. Bollinger

5.1 Summary: The objectives of this phase of the program were:

(a) Modification of an existent probe attenuator design in 7/8" coaxial line to increase its power handling capacity.

(b) Development of a broadband probe attenuator to present a relatively constant attenuation and low VSWR over the frequency range of operation in 1 5/8" coaxial line and incorporating the high power handling capacity feature of item (a) above.

The broadband probe attenuator (See Fig. MRI-11161) is a device which utilizes a capacitance-divider principle to reduce power levels by a predictable amount to a level where power can be monitored by standard bolometric techniques. The units consist basically of a probe (penetrating into the main transmission line), buffing attenuator and matched dissipative load. In this phase of the program interest is confined to the probe section.

1. 7/8" Coaxial High Power Broadband Probe Attenuator

Modification of the design of a 7/8" coaxial probe attenuator has led to a power monitor with increased power handling capacity and with the following characteristics:

Insertion VSWR	< 1.10	1000 - 4000 mc/sec
Decoupling from main line (without equalization)	35.0db ± 1.5db	1000 - 4000 mc/sec

Breakdown at 60 ~ 10 KV rms corresponsing to 3.5 Megawatts Peak Power

Breakdown at rf (2800 mcs) 830 KW peak power

2. 1 5/8" Coaxial High Power Probe Attenuator

A 1 5/8" Coaxial Line Probe Attenuator was developed having the following characteristics:

Insertion VSWR	1.13	1000 - 3000 mc/sec
Decoupling from main line (without equalization)	49.0db ± 2db	1000 - 3000 mc/sec
Breakdown at 60	10 KV rms corresponding to 3.5 megawatts Peak Power	
Breakdown at r-f (2800mc)	1.1 Megawatts Peak Power	

These results are tabulated in Table I of this Chapter. In addition the VSWR and decoupling characteristics for the 7/8" and 1 5/8" coaxial probe attenuators are plotted in Fig. MRI-13694.

5.2 Principle of Operation: For a detailed analytical discussion of the principles of operation reference is made to the work performed previously in connection with broadband probe attenuators[1,2]. Briefly, however, it can be shown that the device acts as a capacitive voltage divider. Fig. MRI-13695a is a schematic diagram of the basic probe construction, and Fig. MRI-13695b shows an approximate equivalent circuit. The probe-to-inner conductor capacitance is small and is represented by C_1. The shunt capacitance consists of discontinuity capacitance, and the capacity that exists between the face of the probe line disc and the milled flat surface of the outer conductor which surrounds the hole through which the probe enters the main line. Hence if the probe inductance is neglected it can be seen that the device acts as a capacitive voltage divider. The output of the probe may be fed (through an equalizing attenuator) to standard bolometer power measuring instruments. Thus the power delivered by the main transmission line to a matched load can be measured providing the decoupling characteristic of the probe is known. An equalization buffer attenuator may be added in tandem to the probe to compensate for the change in the probe decoupling characteristic with frequency. The equalization attenuator would then be required to have a variation of the same magnitude but of opposite sense to that of the probe in order that constant output be maintained.

5.3 Design Considerations: Presented here is the detailed final design procedure for the 1 5/8" coaxial line probe attenuator which is analagous to the design procedure for the original 7/8" coaxial unit.[1,2]

The following assumptions must be made: (Referring to Fig. MRI-13695)

---

[1] H.J. Carlin and E.N. Torgow, Broadband Attenuators for Powers Up to 1000 Watts, Report R-210-49, PIB-154, BuShips Contract No. 28376 with Polytechnic Institute of Brooklyn, May 26, 1946.

[2] E.N. Torgow, A Broadband High Power Probe for Microwave Power Measurements, Thesis for the Degree of Master of Electrical Engineering, Polytechnic Institute of Brooklyn, June 1949.

(a) The input capacitive reactance $X_{e_1} >>$ load impedance the shunt capacitive reactance $X_{e_2} <<$ detector impedance.

(b) Load and detector are matched terminations, R_o.

(c) The lumped parameter circuit closely approximates the actual case of distributed capacitances, and

(d) the series inductance is negligible.

The upper frequency limit (for dominant mode propagation) of 1 5/8" coaxial line is approximately 3230 Mc/s so that a design point at 3000 mc/s is suitable.

Under assumptions (a) and (b) above let $P_1 \geqslant 10$ and $P_2 \geqslant 10$ so that $1/\omega C_1 = P_1 R_o$ and $1/\omega C_2 = R_o/P_2$ from which $P_1 P_2 = C_2/C_1$.

The decoupling characteristic is given by:[1,2]

$$\text{Decoupling (in db)} = 10 \log \left[\left(1 + \frac{C_2}{C_1}\right)^2 + \frac{1}{\omega^2 C_1 R_o} \right] \qquad (1)$$

$$\text{for } \frac{C_2}{C_1} >> \frac{1}{\omega^2 C_1 R_o}$$

$$50 \text{ db} = 20 \log \frac{C_2}{C_1} \qquad \frac{C_2}{C_1} = 316$$

then if $P_1 = P_2 = \sqrt{316} = 17.8$ (trial and error figure for physically realizable capacitances)

$$C_1 = \frac{1}{\omega P_1 R_o} = \frac{1}{2\pi \times 3 \times 10 \times 17.8 \times 53.5} = 0.0558 \ \mu\mu\text{fd.}$$

$$C_2 = 316\, C_1 = 17.60 \ \mu\mu\text{fd} \qquad (2)$$

Referring to Fig. MRI-13696 from design assumption (c):

$$C_1 = C_A + C_B$$

$$C_2 = C_E + C_F + C_G + C_C$$

then setting

$$\left.\begin{aligned} d_2 &= 1.327'' \\ d_3 &= 0.300'' \\ d_5 &= 0.050'' \end{aligned}\right\} \quad \text{ARBITRARILY CHOSEN FOR MECHANICAL STRENGTH}$$

$$C_E = \varepsilon_o \varepsilon_r \frac{A}{d_5} \quad \text{and} \quad C_F = \frac{\varepsilon_r}{v} \frac{L}{60 \ln \frac{1.527}{1.327}}$$

where
- L = length of plate in meters
- ε_o = dielectric constant of free space = $\frac{10^{-9}}{39\pi} \frac{f}{in}$
- ε_r = relative dielectric constant of teflon = 2
- A = cross-sectional area of condenser plates in inch^2
- V = velocity of light.

Step (1) $C_E = 0.353 \frac{(d_2^2 - d_3^2)}{d_5} = 11.8$ μμ fd

Step (2) $C_F = 20.15\, d_6 = 4.03$ μμ fd for d_6 chosen to be 0.200"

Step (3) $C_G = 2\pi \varepsilon_r \frac{1.527}{2} C_G' = 1.46$ μμ fd

where

$C_G' = 0.06$ μμ fd/cm^3

Step (4) Setting $d_4 = .200''$ and evaluating C_C similarly to C_F

$C_C = 0.34$ μμ f

Now

$$C_2 = C_E + C_F + C_G + C_C$$

$\therefore$ $C_2 = 11.8 + 4.03 + 1.46 + 0.34 = 17.63$ μμ fd (approximately C_2 of Equation 2)

---

[3] J.E. Whinnery, E.W. Jamieson and T.E. Robbins, Coaxial Line Discontinuities.

Step (5) Determination of $d_1 + d_8$

$$\frac{1}{C_A} = \frac{1}{C_{air}} + \frac{1}{C_{teflon}} = \frac{d_1}{\varepsilon_o A} + \frac{d_7}{2\varepsilon_o A}$$

$$C_A = \frac{2\varepsilon_o A}{2d_1 + d_7} = \frac{0.353\, d_4^2}{2d_1 + d_7} \quad \mu\mu f$$

Let

$$d_7 = \frac{d_3 - d_4}{2} = \frac{0.300 - 0.200}{2} = 0.050"$$

Since C_B is difficult to determine C_A is assumed to be 1/3 C_1 so that

$$C_A = \frac{C_1}{3} = \frac{0.0558}{3} = \frac{0.353\, d_4^2}{2d_1 + d_7} \quad \mu\mu fd.$$

solving for d_1

$$d_1 = \frac{3(0.353\, d_4^2) - 0.0558\, d_7}{2 \times 0.0558} = 0.356"$$

Shown in Fig. MRI-13224 are the measured decoupling characteristics of the 1 5/8" coaxial line probe attenuator for different probe depths, d. The probe diameter, d_4, was held constant at an abritrary value of .201". For the assumed value of d = 0.191, corresponding to the calculated value of d_1 = 0.356" the measured decoupling characteristic approximated the anticipated attenuation value of within 2 db. Finally selected, however was a probe depth of d = 0.161" since the mean attenuation value was close to 50 decibels (See Fig. MRI-13224).

It is to be noted that the high power broadband coaxial probe attenuator features a dieletric sleeved pin which increases the dielectric strength between the probe pin and the inner conductor of the main line and also increases the discharge path of a breakdown arc, hence increases the breakdown voltage and power handling capacity. Both the 7/8" and 1 5/8" coaxial units have this feature. The addition of the dielectric sleeve to the 7/8" coaxial unit modified the VSWR and attenuation characteristics of the probe attenuators as shown in Figs. MRI- 12746 and MRI-12747. The VSWR characteristics can be seen is negligibly affected. The attenuation characteristic is considerably reduced, as expected, since C_1, the capacitance between the probe pin and the inner conductor of the main line is changed with the addition of the dielectric sleeve. Although, the original characteristic could have been returned to by simple adjustment of the probe depth

corresponding to the value of C_1 desired, it was felt that the increased output was equally acceptable.

In addition, a 1 5/8" compensated coaxial line teflon bead support was designed whose VSWR characteristic is less than 1.03 over the measured frequency band from 1000 - 3000 megacycles. The dimensions of bead support structure and its VSWR characteristic is shown in Fig. MRI-13644. Assembly drawings of the 7/8" and 1 5/8" coaxial units are given in Figs. PIB-B-522-A and Fig. PIB-A-713-A.

5.4 Final Test Data

1. VSWR and Attenuator Characteristics

The final test data is summarized in Table I and Fig. MRI-13694 of this Section for both the 7/8" and 1 5/8" coaxial line probe attenuators. The maximum VSWR value over the measured frequency band for the 7/8" coax unit is 1.10 and 1.13 for the 1 5/8 coaxial unit . (The insertion VSWR's were measured with the probe attenuator looking into a matched load.) Correspondingly the decoupling characteristics for the units are seen to be 35 ± 1.5db and 49 ± 2.0db for the 7/8" and 1 5/8" coaxial units respectively.

2. Breakdown Strength

Breakdown tests at 60 cycles disclosed the fact that the 7/8" and 1 5/8" units break down at approximately the same voltage (10 KV rms) with the potential applied between the probe pin and the inner conductor of the main line. In addition, breakdown tests were performed at r-f utilizing the facilities of the Microwave Tube Laboratory, Materials Testing Laboratory, New York Naval Shipyards, Brooklyn, New York. The results of the tests are summarized in Table I of this section.

The test of the 7/8" coaxial bare pin indicated breakdown between the probe pin and the inner conductor of the main line occurring at approximately 750 KW of peak power. With teflon or polystyrene sleeves covering the probe pin and using Dow Corning No. 4 Ignition Sealing Compound to eliminate air spaces between the pin and the sleeve, the breakdown point of the probe attenuator is limited by surface flashover across the 7/8" coaxial line teflon bead supports, occurring at ~833 KW peak power.

The maximum available r-f power at the Material Testing Laboratories (1.1 megawatts peak) was insufficient to cause breakdown of the 1 5/8" coaxial probe attenuator unit.

TABLE I

CHARACTERISTICS OF COAXIAL HIGH POWER

PROBE ATTENUATORS

	7/8" Line Unit	1 5/8" Line Unit
VSWR	<1.10 1000 - 4000 Mc/s	<1.13 1000 - 3000 Mc/s
Decoupling From Main Line (Without Equalization)	35. db ± 1.5 db	49. db ± 2.0 db
Measured RF Breakdown	>833. KW Peak Power (Line Breakdown)	>1113. KW Peak Power (Maximum Power Available)
Measured 60 Cycle Breakdown	Approximately 10. KV RMS	Approximately 10. KV RMS
RF Breakdown (Extrapolated From 60 Cycle)	Approximately 3.5 MW Peak Power	Approximately 3.5 MW Peak Power

CHAPTER VI

VARIABLE BROADBAND 7/8" COAXIAL ATTENUATOR

by L.M. Vallese

6.1 Summary: Various ideas and data are discussed regarding the development of a variable broadband 7/8" coaxial attenuator. A most promising design appears to be one in which the lossy element is fixed between the inner and outer conductors of the coaxial line. Variability in attenuation is achieved by inserting a metallic sheet parallel to the element. Attenuation and VSWR characteristics are presented.

6.2 Preliminary Discussion: Work for the design of a variable coaxial attenuator began in January 1951. At first, the design was started along criteria which had proved successful in the case of attenuators for rectangular waveguides. Consequently, it was thought to insert a resistive strip parallel to the electric field in the direction of propagation and to control the amount of attenuation by varying the depth of insertion into the electric field. However, it was immediately found that the amount of attenuation obtainable by inserting such a strip in a diametral plane of a center symmetric coaxial line was very small. In order to increase the magnitude of the electric field without changing the value of the characteristic impedance, a section of eccentric coaxial line was provided and the resistive strip was inserted in the region of minimum spacing between inner and outer conductor. The intensity of the electric field in such a region varies with the eccentricity e (e is the ratio of the distance between centers to the radius of the outer conductor). The field at the inner surface of the outer conductor varies as indicated in the graph of Fig. MRI-11989. The ordinate of this graph indicates the normalized ratio E(e)/E(o) and the abscissa the eccentricity e. Since the impedance of the eccentric line is given by

$$Z = \frac{60}{\sqrt{\epsilon_0}} \cosh^{-1}\left[\frac{D}{2d} + \frac{d}{2D} - \frac{e^2 D}{2d}\right]$$

where D is the outer diameter, d the inner diameter of the inner conductor, one can choose two out of the three variables D, d, e for fixed Z. In the present design Z = 49.4 ohms; in addition it is convenient to make either D or d equal to the corresponding values of the center symmetric coaxial line. Therefore, the design is obtained, once the value of e has been chosen. For instance, assuming e = 0.595, one has the following designs according if the internal diameter of the outer conductor or the external diameter of the inner conductor are kept equal to the corresponding ones for the center symmetric lines:

	Coaxial Line	Eccentric Line
Internal Diameter of Outer Cond.	0.811"	0.811"
External " " Inner "	0.352"	0.220"
Minimum Interconductor Distance	0.2295"	0.055"
Internal Diameter of Outer Cond.	0.811"	1.30"
External " " Inner "	0.352"	0.352"
Minimum Interconductor Distance	0.2295"	0.088"

Both designs were actually realized. It was found that the second one was more convenient for the purpose of providing matching sections at the junctions eccentric-to-center-symmetric line. Since the inner conductor in this case is kept of constant diameter, the outer conductor is offset with respect to the main line. (Fig. MRI-12130) The corresponding discontinuity in the line is equivalent to a capacitive reactance, whose value may be computed approximately assuming that the capacitance per unit width is equal to that of a pair of plane transmission line with a corresponding step discontinuity. With this assumption one obtains the total equivalent capacitance multiplying the capacitance per unit width by the length of the arc along the edge of the junction cross-section. For the design in question a value of $C = 0.20\ \mu\mu F$ was found. Since such a capacitance is small enough, it is possible to compensate it by means of a series inductance of a short section of coaxial line.

Although such matching was actually realized, details are not given here because further experimentation showed that practically all the maximum attenuation realizable was not a function of the eccentricity. In other words, the complications introduced in the design in order to obtain a higher intensity of the electric field are not beneficial for the design and, as a consequence, the design had to be modified following different criteria. Actually, if it is assumed that only the principal mode is predominant in the operation of the attenuator section of the line, and if the length of the section and the matching junctions are satisfactory the analysis of its behavior can be made by means of the simple transmission line theory and the results agree satisfactorily with the experiments.

6.3 Design Data and Final Results: The differential equations of a transmission line are

$$\frac{dV}{dx} = -I(R + jX) = -IZ$$

$$\frac{dI}{dx} = -V(G + jB) = -VY \qquad (1)$$

or equivalently in one variable only

$$\frac{d^2V}{dx^2} = \frac{d}{dx} \ln Z \frac{dV}{dx} - YZV = 0$$

$$\frac{d^2I}{dx^2} = \frac{d}{dx} \ln Y \frac{dI}{dx} - YZL = 0 \qquad (2)$$

For a uniform line, where Z and Y are constants, the solutions of (1) are

$$V = V_o \varepsilon^{-\gamma x} \quad , \quad I = I_o \varepsilon^{-\lambda x}$$

where

$$\gamma = \pm \sqrt{YZ} = \pm (\alpha + jB)$$

and in general

$$\alpha^2 = + \frac{GR - BX}{2} \pm \frac{1}{2} \sqrt{|Z|^2 |Y|^2} \qquad (3)$$

As attenuation of a section of length L we assume the quantity $A = L\alpha$ therefore it is α, the attenuation constant, which determines the operation of the attenuator.

If in (1) we let $G = 0$, but $R \neq 0$, we have

$$\alpha^2 = - \frac{BX}{2} + \frac{B}{2} \sqrt{X^2 + R^2} = \frac{\omega^2 CL}{2} \left[\sqrt{1 + \left(\frac{R}{\omega L}\right)^2} - 1 \right] \qquad (4)$$

In other words it is possible to obtain variable attenuation by inserting a variable resistance R (per unit length of line) in series with one or both conductors of the line. Such design was actually utilized by Weber and Johnson*, who inserted in the inner conductor a section of metallized glass tubing properly matched at both ends with the inner conductor of the line. The variation of the value of R was obtained by shunting the resistive coating of the inner section with a metal sleeve sliding over its surface, or with a metal rod penetrating inside the glass tubing. The mechanical control of the movement of the metal sleeve can be obtained by means of a slide outlet in the outer conductor, while that of the metal

*E. Weber, Precision Metallized-Glass Attenuators - Technique of Microwave Measurements, MIT Radiation Laboratory, Vol. II, p. 769, McGraw-Hill, New York.

rod must be obtained from the far end of the attenuator. Large values of attenuation up to 50 db can be obtained with these designs; however, the corresponding values of the VSWR are in average less than 1.25 in a bandwidth of 10 per cent.

Formula (3) suggests another type of design where one lets $R = 0$ but $G \neq 0$. Then one has

$$\alpha^2 = -\frac{BX}{2} + \frac{X}{2}\sqrt{G^2 + B^2} = \frac{\omega^2 CL}{2}\left[\sqrt{1 + \left|\frac{G}{\omega C}\right|^2} - 1\right] \quad (5)$$

There are two ways by which a variable conductance can be shunted across the coaxial transmission line. If one lowers from the outer conductor a resistive strip until it contacts the inner conductor, a variation of the total conductance per unit length is obtained by varying the areas of the contact. It is seen that this operation corresponds practically to that adopted in the first approach to the design of the attenuator. However, no attenuation is practically obtained until actual contact between the strip and the inner conductor is realized; for this reason it is not important that the value of the electric field in the interspacing be made especially large. In an actual design of this type of attenuator an IRC resistive strip of length nine inches and resistivity 50 ohms/square was used. In order to protect its conductive coating, it has been necessary to provide a capacitive coupling between it and the inner conductor of the line. This is obtained by covering the IRC card with a cellophane tape of proper thickness. The shape of the card is made convex of circular or even triangular form, according to the indications of Fig. MRI-13706. The slot in the outer conductor of the line has been shielded carefully and also provided with internal absorbing material like polyiron, to prevent radiation losses. The section of attenuator line built for these experiments is represented in Fig. MRI-13697. The vertical drive for the IRC card is obtained by means of a micrometer gauge. During the experimentation some disturbing resonance phenomena were encountered, and these had to be eliminated by adjustment of the shape of the IRC card and increasing the capacitance between the card and the inner conductor. The final results obtained with the experimental unit are very satisfactory since they show uniform behavior of the attenuator over the frequency range 1500 - 5200 Mc/sec, with a maximum attenuation of 35 db or more and VSWR less than 1.3 in the range 2500 to 5200 Mc and less than 1.6 in the range 1500 to 2500 Mc. These results are shown in Figs. MRI-13022, MRI-13023, MRI-13139 and MRI-13140. It is of interest to observe that, according to formula (5) the attenuation is a function of G (i.e., of the penetration) but also of the frequency. The frequency spread of the various attenuation curves is not dependent upon the value of the coupling capacitance between IRC card and inner conductor, but rather is a result of intrinsic properties

of the attenuation of the fundamental mode. Although the type of design just described is satisfactory from the point of view of the electrical behavior, its operation is delicate from the mechanical point of view since it is required that such a flimsy element like the IRC card be introduced in the narrow slot of the inner conductor. It is evident that any accidental rotation of the inner conductor might bend and break the IRC card. In addition, this type of design does not permit use of metallized-glass plates in place of IRC cards.

There exists another method by which a variable conductance can be shunted across the coaxial transmission line. This consists in placing a fixed resistive strip across the line and then shunting it by means of a metal plate connected with the outer conductor. The metal plate is made to slide at close contact over the surface of the resistive element. To avoid scratching the conductive film of the glass plate this is covered by a protective layer of oxide; therefore, the shunting effect with the metal plate is capacitive. However, the corresponding capacitive susceptance is very small with respect to the shunt conductance of the fixed element so that, as a result, the variable shunt admittance is practically ohmic. Since formula (5) still applies, one would not expect that the electric behavior of this new type of attenuator be different from that of the previous one; however, the value of maximum attenuation depends upon G and G must be chosen compromising for a small insertion loss and a large maximum attenuation. Since the rate of increase of the attenuation is much larger when the penetration reaches the limit value, it is convenient to use a non-uniform mechanical drive for the insertion of the metal plate.

In the actual design the fixed strip (of IRC card or also of metalized glass plate) has been placed in a diametral plane in metallic contact with both inner and outer conductor. The same casing and the same drive used for the previously described type of attenuator has been adopted. A sketch with indication of the fundamental dimensions of the units is reported in Fig. MRI-13259. The insertion loss has been kept less than 5 db in all cases; this loss varies with frequency, as indicated by (5) and in one example, for instance, has been found to have the dependence indicated in Fig. MRI-13260.

In the final design of the attenuator a metallized-glass plate of resistivity 2500 ohms per square has been adopted. From Fig. MRI-13698 it appears that the maximum attenuation is 25 db and the corresponding VSWR less than 1.3. The range of frequencies in which the unit has been tested is 3100 - 4560 Mc/sec but, for the reasons mentioned, it is expected that the attenuator operates substantially like the previous one in a bandwidth 2000 to 5200 Mc/sec.

An attempt has been made to investigate the behavior of a fixed metal plate with non-uniform resistivity. For this purpose the film deposited on the plate was made of resistivity 3000 ohms per square for one half of the strip (the side closer to the outer conductor) and of resistivity 1000 ohms per square for the other half. The results of attenuation and VSWR are indicated in Fig. MRI-13698.

6.4 Conclusion: Two types of variable coaxial attenuators have been described. Both are of new design principle and both have been experimented successfully in the laboratory. They represent an improvement with respect to the existing variable coaxial attenuators with respect to the VSWR values that they present in the range of frequencies of operation. Of the two designs analyzed the second one appears to be based on a more sound engineering point of view than the first one, as the delicate resistive element is fixed, and so is not subject to stresses. The design of the attenuator for production purposes might require some refinement of the mechanical part, but it is felt that the electric characteristics have been investigated exhaustively.

CHAPTER VII

FIXED ATTENUATORS FOR 3/8" COAXIAL LINE

by M. Wind and C. Bollinger

7.1 Summary: The objective of this phase of the program was to make available fixed attenuators for 3/8" coaxial line to cover the frequency band from 0 - 4000 megacycles per second in the following attenuation range:

0 - 1.0 db in steps of 0.1 db

3 - 12.0db in steps of 1.0 db

10 - 40. db in steps of 10. db

In addition it was though to combine these units in a suitable arrangement to realize a precision decade attenuator (which could be used as a reference standard in the frequency range from 1 - 500 megacycles per second.)

Three types of attenuating units were developed to cover the frequency and attenuator range desired. These include a continuous series film type, a"chimney" type and a shunt "disc" type.

The VSWR response of each of the attenuator units is tabulated in the body of this chapter (See Tables I through V inclusive). Most of the attenuator units show VSWR values (including fittings) of less than 1.20 over the measured frequency band. VSWR values in excess of 1.20 only occur in the case of a discrete number of disc-type units and then only for frequencies greater than 3000 megacycles.

In addition to providing well-matched attenuators, the objective of the program was to provide attenuators a) having attenuation values reasonably close to the nominal value and b) having attenuator values reasonably constant over the specified frequency band.

The attenuation characteristics of each of the attenuator units are tabulated in Tables I through V inclusive of this chapter. These characteristics were measured as an insertion loss under matched load-matched generator conditions except in the case of the continuous series film units where the reported attenuation values were measured at d-c using bridge techniques.

Considering the continuous film and chimney type units only, most of the attenuator units showed a maximum attenuation within ± 10% of the nominal value. In most cases, the attenuator units, particularly the chimney type units had attenuator response characteristics considerably

superior to this. In addition, the excursion in attenuation value from the mean (where the mean value is equal to one-half the sum of the maximum and minimum attenuation values) over the measured frequency range is within ± 2% for all but two of the disc type units and well within ± 4% for all but the very low valued chimney type units.

7.2 Ranges and Types: Three types of units were developed to cover the frequency and attenuation ranges desired. These include a continuous metallic film type, a chimney type and a shunt disc type.

1. Continuous Film Type

The continuous film type attenuator (See Fig. PIB-C-691-A) consists of a single section of metallized glass. The ends of the film are connected to high conductivity platinized collars to which bullets are soldered so that the unit maybe inserted as the center conductor of a coaxial casing. Under this phase of the contract, a series of seven continuous film attenuators were developed with nominal attenuation values of 0.1, 0.2,....., 0.7 decibels at d-c, having a finite (but not yet accurately measurable) increment-characteristic from unit to unit over the measured r-f frequency band from 1000 - 4000 megacycles per second. VSWR and attenuation values for two sets of these units are tabulated in Table I.

2. Chimney Type Attenuators

The chimney type attenuator (See Fig. PIB-C-700-A) is a novel type of film attenuator which utilizes a lossy stub transmission line as a matching network to yield a broadband matched attenuator.

Thirteen units of the chimney type (single stub T-Pad) film attenuators designed to operate from d-c to 4000 megacycles were developed in 3/8" coaxial line under this phase of the contract having nominal attenuation values of 0.8, 0.9, 1.0, 3.0, 4.0, 5.0 ..... 12.0 db. The performance characteristics of these units measured at d-c and in the microwave region from 2500 - 4000 mc/sec are tabulated in Tables II and VI of this chapter.

3. Disc Type Attenuator

The disc type attenuator (See Fig. PIB-B-624-A) is an alternative form of a T-Pad attenuator which utilizes a metallized shunt mica disc to yield the desired broadband values of VSWR and attenuation. In contradistinction to the chimney attenuator, it has the advantage that the dimensions of the attenuator casings are the same for each of the attenuator units in the series.

Six disc-type attenuator units were designed (in 3/8" coaxial line) having nominal attenuation values of 10,11,12,20,30 and 40 decivels to operate over the frequency range from d-c to 4000 megacycles. The performance characteristics of the disc units are tabulated in Tables IV; V and VI of this Chapter.

7.3 Design Data

1. Continuous Film Attenuators

As was previously mentioned the continuous film attenuation (See PIB-C-691-A) is composed of a single section of metallized glass whose ends are terminated in connector bullets so that the unit may be incorporated into a coaxial casing (with a Type "N" or other coupling).

The total attenuation of the continuous film attenuator is given by:*

$$\alpha_T = \alpha \ell = \frac{2\pi\sigma\ell}{\lambda} \qquad (1)$$

α_T = total attenuation of the continuous film

α = attenuation constant in nepers per unit length

ℓ = total length of lossy film

λ = wavelength in air

σ = $-I_m\sqrt{1 - jX}$ (I_m denotes "imaginary part of")

and where

$$\frac{Z_c}{Z_o} = \sqrt{1 - jX} \qquad (2)$$

Z_o = characteristic impedance of the lossless section

Z_c = characteristic impedance of the continuous film section

X = a wavelength variable = $R\lambda/2\pi Z_o \ell$

R = total resistance of the lossy film

The design procedure was basically the selection of the resistance value, R, (R = the total resistance of the lossy film section) which was computed to meet the attenuator requirements on a d-c basis and the analutical verification of the corresponding attenuation value at the design frequency.

*H.J. Carlin, Final Report on the Development of Broadband Microwave Attenuators for Navy Contract NObs-28376, Section I - Coaxial Line Attenuators, Report R-217-49, PIB-161 Polytechnic Institute of Brooklyn, May 26, 1949.

From simple network theory, the total resistance value, R, of the attenuator for a specified value of attenuation at d-c is given by:

$$R = 98.90 \left[\left(\log^{-1} \frac{db}{20} \right) - 1 \right] \qquad (3)$$

db = nominal value of attenuation.

Shown in Table VII, Resistance Chart-Continuous Film Attenuators, are the (upper and lower) limit values of the resistance R, of the continuous film section designed to yield attenuation values at d-c to within 2% of the nominal value. (For optimum results, the resistance value selected should be nearer the lower tolerance value to allow for possible slight increases of resistance with temperature for prolonged operation of the unit.)

Shown below is an example illustrating the analytical corroboration of t he attenuation at r-f using a value of continuous resistance film R, from Table VII.

ILLUSTRATIVE EXAMPLE

To design the 0.7db attenuator, the Resistance Chart (Table VII) is consulted and a value of 8.13 Ω is selected. (NOTE: for practice, the technician endeavors to metallize the glass insert so that its d-c resistance value is between 8.13 Ω and 8.45 Ω, preferably near the lesser value for the reasons indicated above.)

Then X = wavelength variable = $\frac{R\lambda}{2\pi Z_o \ell}$

$$= \frac{(8.13)\ (30\ cm)}{2\pi(49.45)(2.54cm)} = 0.31$$

now $\alpha_T = \frac{2\pi\sigma\ell}{\lambda}$

and for low value of X

$$\sqrt{1-jX} \doteq 1 - j\frac{X}{2}$$

$$\therefore \sigma = -I_m \sqrt{1-jX} \doteq \frac{X}{2}$$

$$\therefore \alpha_T = \frac{2\pi \ell}{\lambda} \doteq \frac{2\pi X \ell}{2\lambda} \doteq \frac{R}{2Z_o}$$

$\therefore$ R = 8.13 Ω (corresponding to a 0.7db unit at d-c) and Z_o for 3/8" coaxial line equal to 49.45 Ω

$$\alpha_T \doteq \frac{8.13}{98.9} \doteq .0822 \text{ nepers} \doteq \underline{0.714 \text{ decibels}}$$

For test purposes and inserts were assembled in casings terminated in improved type "N" female connectors, consequently the measured values of VSWR reported in Table I include the reflections arising from the discontinuities associated with the fron and fack end connectors. The VSWR valuw of a mated pair of improved Type "N" (C series) connectors in the frequency region from 1000 - 4000 megacycles per second may very from 1.03 to 1.07.*

The assembly drawing of the continuous film attenuator is shown in PIB-C-691-A. The casing is simply designed to present an impedance of Z_o to 3/8" air coaxial line considering the glass insert as the inner conductor.

2. Chimney Attenuator

The basic design procedure in connection with the chimney T-pad attenuator designed to operate from 0 - 4000 megacycles is the specification of the resistance values of the series arms (which are metallized glass inserts) and the specification of the resistance value and characteristic impedance of the shunt arm of the structure.

Considering the T-pad attenuator as a lumped constant symmetrical-T network, it is easily shown that:**

$$R_1 = Z_o \left(\frac{\alpha - 1}{\alpha + 1}\right)$$

$$R_2 = Z_o \left(\frac{2\alpha}{\alpha^2 - 1}\right) \qquad (4)$$

where

R_1 = resistance of each of the series arm elements

R_2 = resistance of the shunt arm

α = $\frac{\text{load current without the attenuator}}{\text{load current with the attenuator}}$

*J.W.E. Griemsmann, Handbook of Design Data on Cable Connectors for Microwave Use, Report No. R-158-47, PIB-107, prepared under Navy Bu Ships Contract NObs 28372 with Polytechnic Institute of Brooklyn, July 1947.

**F.E. Terman, Radio Engineer Handbook, pp. 215-216, McGraw-Hill Co. New York.

where by definition the total attenuation α_T is:

$$\alpha_T = 20 \log \alpha \qquad (5)$$

Thus the resistance values of the metallized glass, series and shunt arms can be specified since at these frequencies (up to 4000 mc) the metallized films are essentially non-inductive and non-reactive. In order, however, for the attenuator to remain matched, the impedance presented to the main transmission line by the shunt arm must remain real despite the fact that the lossy stub is terminated in a short circuit. It can be shown*, however, that the reactance of a short circuited transmission line is very nearly zero for small values of ℓ/λ corresponding to the condition:

$$R/Z_o = \sqrt{3} \qquad (6)$$

where

R = total value of series resistance of the line (actually, the resistance of the metallized glass shunt element of the attenuator)

ℓ = length of the shunt or stub line

Z_o = characteristic impedance of the short circuited lossy stub

λ = free space wavelength

In addition, advantage is taken of the fact that when resistors (e.g., metallized glass insert) are used for terminating transmission lines as shown in the simplified schematic drawings at the right, Equation (6) gives the widest frequency response for a fixed minimum standing wave ratio and that the SWR introduced is very nearly zero for low values of ℓ/λ.

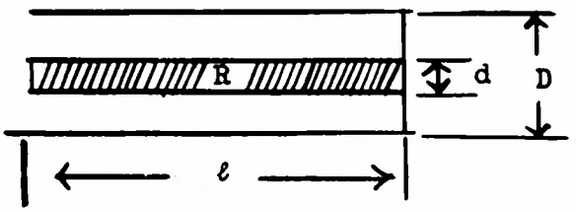

Thus after the resistance R, of the metallized shunt element is specified from the attenuation performance characteristics, the inner diameter of the stub casing can be calculated, since the characteristic impedance of the stub line is given by:

$$Z_{o_{stub}} = R/\sqrt{3} \qquad (6a)$$

Therefore D, the inner diameter of the stub casing can be specified as:

$$D = d \text{ antilog } \frac{Z_{o_{stub}}}{138}$$

where d = diameter of the metallized glass film resistor.

Thus, to reiterate, the advantage of this simple compensation procedure is two fold. By adding to the condition of Equation (6) and keeping the length of the lossy stub short, (1) a real impedance is presented at the terminals of the stub line and (2) the discontinuity introduced into the main line by the stub line is very near zero. Since the resistance, R, of the metallized shunt element must be maintained regardless of the length, ℓ, of the element, the shortness of the stub (and consequently the minimum value of ℓ/λ) is limited by the ability of the technician and the available technique and equipment to evaporate or burn on uniform, thinner metallic resistive films on shorter sections of glass with reasonable control and accuracy. A second limitation on the shortness of the lossy stub is the increased power handling/unit surface area required of the shortened stub.

Shown in Fig. PIB-C-634-F and J are the tabulated values of resistance of the metallized glass inserts for the series and shunt elements of the chimney T-pad attenuators corresponding to the nominal value of attenuation specified for the frequency range from 0 - 4000 megacycles.

Fig. MRI-11781 indicates the allowed tolerances in the resistance values of the shunt and series arms of the chimney T-pad attenuators for an allowed mismatch VSWR of 1.20. In addition, the excursion in attenuation from the nominal value corresponding to a deviation in the resistance values of either the series or shunt elements from the nominal value (tabulated in Fig. PIB-C-634-F and J) and be determined from the performance specification chart in Fig. MRI-11781.

The assembly drawing of the chimney attenuator is given in Fig. PIB-C-700-A. As in the case of the continuous film attenuators, the casings are terminated in type "N" female connectors consequently the measured values of VSWR reported in Table III include the reflections from the front and back end connectors.

3. Mica-disc Attenuators

The technique used in designing the shunt mica-disc attenuators (See Fig. PIB-B-624-A) is basically similar to that employed for the chimney type attenuators. The resistance values of the series and shunt arms were specifued by considering the d-c equivalent network of the

attenuator (as a symmetrical T structure) and computing the values of R_1 and R_2 (See Equation (4)) corresponding to the specified nominal values of attenuation (and characteristic impedance of 3/8" air coaxial line).

Chronologically, the shunt-mica disc attenuators covering the higher range of attenuation values (≥10 decibels) were developed prior to the chimney T-pad units and as can be seen from the assembly drawing (Fig. PIB-C-624-A) are much simpler to fabricate and assemble. The shunting element, a large mica disc (upon which is evaporated a metallic resistive film) provides a large surface area corresponding to the low resistive paths required of the shunt element at higher values of attenuation (See PIB-C-624-H and N). The lower valued attenuation units required correspondingly higher values of shunt resistances which in turn necessitated the evaporation of thinner resistive metallic films on the mica disc. Hence the introduction of the chimney T-pad attenuators to cover the mid-ranges of attenuation value despite the fact that several different casings are required and that the assembly is more difficult since it is required to short the shunting element by soldering the metallized glass resistive element to the stub casing.

In addition to specifying the resistance values of the elements, it was required to overcut the outer conductor of the 3/8" air coaxial line to compensate for the change in characteristic impedance as a result of the instroduction of the mica disc. No formal attempt was made to optimumally compensate for the capacitance discontinuity introduced by the line size change. An approximation to a suitable compensating gap is realized, however, by the existence of a small gap introduced for symmetry purposes in fabrication.

Shown in Fig. PIB-C-624-A is the assembly drawing of the shunt-mica disc attenuator unit. As in the case of the continuous film and chimney units, these have been fabricated with Type "N" female connectors hence the VSWR values of the attenuators reputed in Table IV include the reflections associated with the front and back end connectors.

Shown in Fig. PIB-C-624-H and N are the tabulated values of resistance of the metallized glass series arms and the metallized mica shunt arms for the mica disc attenuation to cover the range of attenuation values from 10, 11, 12, 20, 30 and 40 decibels and to operate over the specified frequency range from 0 to 4000 megacycles. In addition, Fig. MRI-11783 indicates the allowable tolerances in the resistance values of the elements for an allowed VSWR mismatch of 1.20. The excursion in attenuation corresponding to a variation in resistance from the nominal value (specified in Fig. PIB-C-624-H and N) can also be determined.

7.4 Performance

1. Continuous Film Attenuators

Table I of this section lists the VSWR response of two sets of continuous film attenuators covering the range of value from 0.1 to 0.7 db in 0.1 db steps.

The VSWR values measured from 1000 - 4000 mc/sec are seen to be less than 1.20 for all of the attenuating units in the first set and less than 1.20 for most of these in the second set. The difference in VSWR values between the two sets of attenuators can largely be ascribed to the difference in assembly technique between a skilled and a lesser skilled technician. Particularly critical is the area a-b in Fig. MRI-11260c which illustrates the bullet used to terminate the attenuator insert. Section a-b of this bullet is greater in diameter than the main line in order to permit the metallized glass to be slipped in and soldered. Though the effect of the resulting capacitive discontinuity is canceled by the neighboring reduced diameter section, b-c as shown in Fig. MRI-11260d, poor soldering technique in which "blobs" and "pimples" of solder are left on the oversized section a-b (Fig. MRI-11260c) may result in higher values of VSWR. It is felt that high VSWR values of some of the units are largely due to improper assembly.

It should be noted that attenuation values for the tenth decibel units are reported only at d-c. This is so because no system of evaluating the attenuation characteristic (of the 3/8" coaxial line tenth db attenuator terminated in type "N" connectors) attempted was considered to give reliable results.

In particular, two systems were tried which were based on (1) the relationship between the attenuation and the resultant voltage at the input terminal when the output is terminated in a short circuit and (2) the use of equal arm d-c Wheatstone bridge circuits with r-f bolometer power meters designed to yield accurate power measurements* Both these systems failed to accurately measure the attenuation values of the tenth db attenuator for two major reasons. These are:

(1) In both cases the instability of the r-f source (power and frequency wise) or the drift of the available d-c bolometer bias supply, or the effects of thermal instability on the bolometer level caused errors in the measurement of the order of magnitude of the attenuation value to be measured.

---

*For a description of The Precision Milli-db Method of Measurement, see Bi-monthly Progress Report for the Months of December 1951 and January 1952, Report R-222.16-52, PIB-167.16.
For a description of the technique using a bolometer power bridge reference is made to Two DC Power Bridges for Bolometer Power Measurements, by H.J. Carlin and E. Torgow, Report R-248-51, PIB-189, Contract No. W 28-029-ac-503, Polytechnic Institute of Brooklyn, June 18, 1951.

(2) It was literally impossible to reproduce measured results if the attenuators were removed from the test line (requiring disconnection of the Type "N" connectors) and then reinserted.

Hence no reliable data on the attenuation values of the continuous film units can be reported in the frequency region have 1000 - 4000 megacycles other than the fact that they apparently did display a finite increment-characteristic from unit to unit.

2. Chimney Attenuators

The VSWR values of the chimney type attenuators are reported in Table II of this section, but cover only the frequency range from 2500 - 4000 megacycles. No measurements on these units are available at the lower frequencies at the time of development were destroyed in a severe fire at the laboratories of the Polytechnic Institute of Brooklyn in the summer of this year. From the excellent VSWR response at the higher frequencies it is not unreasonable to assume that the VSWR response in the frequency region from 1000 - 2500 megacycles is equally satisfactory. The VSWR values are seen to be less than 1.10 for most of the chimney units and less than 1.20 for all of them.

The d-c and r-f attenuation characteristics of the chimney attenuators are tabulated in Table III of this Section. Except for the lower valued attenuators the chimney units show a maximum attenuation deviation from nominal well within ± 10%. In addition Table VI of this Section lists the mean* attenuation value of each chimney unit and the attenuation excursion from the mean at r-f. From this data it can be seen that the variation in attenuation of each of the chimney units (except for the tenth db series whose measured attenuation data, although reported, cannot be considered reliable for the reasons previously given) is held to within ± 4% for all the units and to within ± 2% for 70% of the units.

These values of attenuation were measured using the standard Ballantine Voltmeter technique.

3. Mica Disc Attenuators

The VSWR values for the mica-disc attenuator units are reported in Table IV of this Chapter. These cover the frequency range from 1000 to 4000 megacycles/second.

---

*Mean attenuation is arbitrarily defined here as one half the sum of the maximum value of attenuation and the minimum value of attenuation measured at r-f.

Except for a limited number of units (and then above approximately 3200 megacycles), the VSWR values of the units are seen to be less than 1.20. All of the VSWR values are less than 1.30. It is felt that if warranted the VSWR values in excess of 1.20 can be reduced by adjustment of the gap spacing in the mica disc attenuator to compensate for the capacitive discontinuity introduced by the line size change.

The attenuation characteristic of the mica disc units are tabulated in Table V of this Section, covering the d-c values and the r-f range from 1000 - 4000 megacycles. From the data it can be seen that the maximum attenuator is well within $\pm$ 10% of the nominal value for all (but one) of the disc units. The performance of most of the units was considerably superior to this. In addition, in Table VI of this Section is listed the mean for each disc attenuator unit. From this data it can be seen that the excursion in attenuation about the mean over the frequency range from 1000 - 4000 megacycles is well within $\pm$ 2% for all (but three) of the units.

TABLE I

VSWR AND D-C ATTENUATION CHARACTERISTICS
OF CONTINUOUS FILM ATTENUATORS

1000 - 4000 Mc/sec

< 1" Film Length

Nominal db	Frequency in Megacycles per second 1000	1500	2000	2500	3000	3500	4000	D-C	% Deviation from Nominal
	VSWR							db	
0.1	1.04	1.04	1.08	1.10	1.15	1.12	1.14	0.1156	15.6%
0.2	1.05	1.03	1.06	1.09	1.14	1.12	1.10	0.2128	6.4
0.3	1.09	1.08	1.03	1.03	1.12	1.1	1.08	0.3147	4.9
0.4	1.10	1.07	1.04	1.15	1.18	1.14	1.12	0.4229	5.7
0.5	1.10	1.08	1.03	1.15	1.18	1.15	1.10	0.5168	3.4
0.6	1.14	1.10	1.03	1.12	1.12	1.15	1.10	0.6209	2.5
0.7	1.20	1.12	1.08	1.18	1.18	1.20	1.09	0.7891	12.7

1" Film Length

Nominal db	Frequency in Megacycles per second 1000	1500	2000	2500	3000	3500	4000	D-C	% Deviation from Nominal
	VSWR							db	
0.1	1.07	1.06	1.15	1.16	1.12	1.15	1.27	0.1010	1.9%
0.2	1.05	1.05	1.03	1.06	1.09	1.05	1.05	0.1984	-0.8
0.3	1.09	1.03	1.05	1.13	1.08	1.10	1.18	0.3030	1.0
0.4	1.10	1.07	1.04	1.10	1.14	1.15	1.11	0.3998	-0.05
0.5	1.10	1.09	1.05	1.15	1.13	1.07	1.12	0.4963	-0.74
0.6	1.15	1.06	1.12	1.22	1.20	1.15	1.10	0.6006	0.1
0.7	1.16	1.04	1.15	1.25	1.25	1.26	1.30	0.6949	-0.7

TABLE II

VSWR CHARACTERISTICS OF CHIMNEY-TYPE ATTENUATORS

2500 - 4000 Mc/sec

Nominal db	Frequency in Megacycles per second 2500	3000	3500	4000
0.8	1.12	1.10	1.12	1.20
0.8	1.11	1.07	1.08	1.17
0.9	1.09	1.10	1.09	1.17
0.9	1.13	1.10	1.12	1.18
1.0	1.09	1.05	1.07	1.12
1.0	1.08	1.05	1.09	1.14
3.0	1.10	1.10	1.13	1.18
3.0	1.04	1.05	1.08	1.05
4.0	1.05	1.05	1.05	1.03
4.0	1.08	1.07	1.11	1.15
5.0	1.05	1.05	1.10	1.15
5.0	1.03	1.05	1.05	1.08
6.0	1.05	1.04	1.04	1.03
6.0	1.03	1.03	1.02	1.03
7.0	1.07	1.04	1.03	1.04
7.0	1.05	1.04	1.04	1.04
8.0	1.05	1.04	1.05	1.08
8.0	1.04	1.03	1.05	1.05
9.0	1.03	1.03	1.04	1.05
9.0	1.02	1.03	1.05	1.06
10.0	1.03	1.04	1.04	1.07
10.0	1.03	1.05	1.04	1.05
11.0	1.05	1.07	1.06	1.10
11.0	1.07	1.08	1.09	1.08
12.0	1.05	1.08	1.08	1.10
12.0	1.06	1.08	1.08	1.10

TABLE III

ATTENUATION CHARACTERISTICS OF CHIMNEY-TYPE ATTENUATORS

2500 - 4000 Mc/sec

Nominal db	D-C	Frequency in Megacycles per second				% Deviation of Largest Deviation from Nominal
		2500	3000	3500	4000	
0.8	0.82	1.15	1.2	1.2	1.2	+ 50%
0.8	0.80	0.9	0.9	0.95	1.0	+ 18.7%
0.9	0.87	1.05	1.1	1.2	1.0	+ 30%
0.9	0.91	1.05	1.1	1.1	1.1	+ 11.1%
1.0	0.98	0.9	1.0	1.05	1.05	- 10%
1.0	0.97	1.1	1.1	1.1	1.15	+ 11.5%
3.0	3.1	3.3	3.2	3.15	3.05	+ 10%
3.0	2.95	2.9	2.85	2.7	2.75	- 10%
4.0	3.8	4.0	3.8	3.8	3.8	- 5%
4.0	4.1	4.2	4.25	4.25	4.3	+ 7.5%
5.0	5.1	4.8	4.7	4.8	4.8	- 6%
5.0	4.9	4.55	4.5	4.4	4.35	- 12%
6.0	6.04	5.85	5.9	5.85	5.8	- 3.3%
6.0	5.97	5.65	5.6	5.5	5.5	- 8.3%
7.0	6.97	6.75	6.7	6.7	6.7	- 4.3%
7.0	6.95	6.9	6.7	6.6	6.5	- 7.1%
8.0	8.0	8.15	7.8	7.8	7.7	- 3.8%
8.0	8.1	7.8	7.7	7.65	7.6	- 5.0%
9.0	9.0	8.75	8.7	8.7	8.7	- 3.3%
9.0	9.2	8.9	8.75	8.75	8.7	- 3.3%
10.0	10.0	9.6	9.4	9.3	9.3	- 7.0%
10.0	10.2	9.8	9.75	9.7	9.8	- 3.0%
11.0	11.1	10.55	10.5	10.3	10.3	- 6.4%
11.0	11.14	10.85	10.8	10.8	10.8	- 1.8%
12.0	11.98	11.7	11.5	11.2	11.2	- 6.7%
12.0	12.0	11.75	11.7	11.7	11.8	- 2.5%

TABLE IV

VSWR CHARACTERISTICS OF DISC-TYPE ATTENUATORS

1000 - 4000 Mc/sec

Nominal db	Frequency in Megacycles per second 1000	1500	2000	2500	3000	3500	4000
10	1.20	1.10	1.05	1.06	1.12	1.18	1.10
10	1.05	1.10	1.08	1.07	1.14	1.15	1.18
11	1.08	1.08	1.05	1.02	1.06	1.13	1.2
11	<1.03	1.08	1.05	1.06	1.04	1.09	1.13
12	1.07	1.06	1.04	1.03	1.05	1.15	1.18
12	1.07	1.08	1.05	1.05	1.07	1.18	1.19
20	1.13	1.12	1.10	1.11	1.18	1.25	1.29
20	1.11	1.14	1.07	1.09	1.15	1.26	1.24
20	1.17	1.12	1.12	1.07	1.10	1.25	1.27
20	1.15	1.15	1.08	1.10	1.15	1.25	1.29
30	1.10	1.14	1.10	1.10	1.12	1.25	1.30
30	1.07	1.14	1.10	1.10	1.15	1.25	1.29
30	1.13	1.07	1.03	<1.01	1.12	1.22	1.28
30	1.10	1.15	1.10	1.10	1.09	1.25	1.29
40	1.05	1.12	1.07	1.05	1.09	1.20	1.26
40	1.10	1.10	1.10	1.03	1.12	1.15	1.28
40	1.06	1.09	1.10	1.05	1.06	1.13	1.20

TABLE V

ATTENUATION CHARACTERISTICS OF DISC-TYPE ATTENUATORS

1000 - 4000 Mc/sec

Nominal db	D-C	Frequency in Megacycles per second 1000	1500	2000	2500	3000	3500	4000	% Deviation from Nominal
10	8.7	9.4	9.9	10.2	10.4	10.6	10.7	10.6	- 13.0%
10	10.1	9.9	9.9	9.8	9.8	9.8	9.75	9.7	- 3.0
11	10.4	10.6	10.6	10.6	10.6	10.7	10.7	10.7	6.4
11	10.8	11.3	11.3	11.3	11.3	11.5	11.6	11.6	5.6
12	10.9	11.3	11.3	11.5	11.6	11.7	11.7	11.6	- 9.2
12	11.8	11.3	11.5	11.5		11.7	11.5	11.4	- 5.8
20	19.9	19.7	19.7	19.7	19.7	19.5	19.3	19.1	- 4.5
20	20.6	20.6	20.6	20.5		20.3	20.0	19.8	3.5
20	20.1	19.8	19.7	19.7	19.8	19.6	19.5	19.3	- 3.5
20	21.2	20.2	20.3	20.2	20.2	20.0	19.8	19.7	6.0
30	29.3	29.1	29.0	28.8		28.3	28.0	27.6	- 8.0
30	29.5	29.4	29.3	29.1		28.8	28.6	28.3	- 5.7
30		30.3	30.1	30.0		29.5	29.3	29.0	- 3.3
30	30.1	30.1	30.1	30.1		29.7	29.5	29.3	- 2.3
40	41.9	41.8	41.1	41.0		41.0	42.0	42.0	2.5
40	38.3	37.8	37.8	38.0		38.0	38.0	37.5	- 6.3
40	40.9	41.0	41.1	41.1		41.1	41.0	41.0	2.8

TABLE VI

CHIMNEY-TYPE

Nominal Attenuation (db)	Mean Attenuation (db)	Attenuation Excursion from the Mean
3.0	3.175	± 3.9%
3.0	2.8	± 3.5
4.0	3.9	± 2.7
4.0	4.25	± 1.8
5.0	4.75	± 1.1
5.0	4.45	± 2.2
6.0	5.85	± 1.0
6.0	5.575	± 1.4
7.0	6.725	± 0.5
7.0	6.7	± 0.5
8.0	7.975	± 3.4
8.0	7.7	± 1.2
9.0	8.725	± 0.5
9.0	8.8	± 1.1
10.0	9.45	± 1.6
10.0	9.75	± 0.5
11.0	10.425	± 1.2
11.0	10.825	± 0.5
12.0	11.45	± 2.2
12.0	11.775	± 0.5

TABLE VI
(Continued)

DISC-TYPE

Nominal Attenuation (db)	Mean Attenuation (db)	Attenuation Excursion from the Mean
10	10.05 db	6.4%
10	9.8	1.0
11	10.65	0.5
11	11.45	1.3
12	11.5	1.7
12	11.5	1.7
20	19.4	1.5
20	20.2	2.0
20	19.55	1.3
20	20.15	1.0
30	28.85	4.3
30	28.85	1.7
30	29.65	2.2
30	29.7	1.3
40	41.5	1.2
40	37.75	0.7
40	41.05	0.5

TABLE VII

RESISTANCE CHART - CONTINUOUS FILM ATTENUATORS

db (nominal)	db (actual)	Resistance ohms
0.1	0.098	1.13
	0.102	1.16
0.2	0.196	2.27
	0.204	2.34
0.3	0.294	3.42
	0.306	3.52
0.4	0.392	4.57
	0.408	4.74
0.5	0.490	5.75
	0.510	5.96
0.6	0.588	6.94
	0.612	7.21
0.7	0.686	8.13
	0.714	8.45

CHAPTER VIII

MAGNETIC ATTENUATOR

by H. Rapaport

8.1 Summary: Ferromagnetic materials have often been used in the construction of microwave components. For example, microscopic iron particles dispersed in a polystyrene matrix (Polyiron) have been employed as the dissapative element in waveguide loads. The many recent developments in ferromagnetic materials (ferrites, high μ irons, etc.) suggest even broader application of the principles of ferromagnetism toward the solution of microwave problems. Current literature indicates that many researches already well advanced are producing results of practical import as well as theoretical interest. A great variety of microwave devices is indicated.[1] Some are new - such as the gyrator - and some offer new methods for solving old problems - such as phase shifting.

The general objective of the NA-2 magnetic attenuator program has been to investigate the possibility of developing a ferromagnetic variable attenuator in coaxial line for use in millidecibel measurements. In concept, the attenuator is to be a continuously variable device (0db. 3db.) operating in the frequency range 1000 mcs to 4000 mcs. It is to have a low initial insertion loss and VSWR in this frequency region, and it is to be completely electrical in control.

The experimental results, described in detail below, indicate that considerable variations in attenuation can be obtained by varying the longitudinal magnetic field applied to a cylinder of ferromagnetic material in a rigid coaxial line. The ferromagnetic materials used were polyiron and ferrites in the form of cylinders. The relationship of the center conductor of the coaxial line to the test specimens was varied considerably (see 8.2). In almost every case, more than adequate variations in attenuation were obtained by variation of the longitudinal magnetic field. Both AC and DC magnetizing coil currents were used and produced similar results.

Although the initial insertion loss and VSWR obtained with the test specimens were unfavorable, it must be emphasized that no "shaping of the specimens or compensation for the geometry was attempted. It is felt that with proper compensation and further experiment these limitations can be overcome.

8.2 Principle of Operation: Because of the limited scope of the magnetic attenuator program, no formal theoretical analysis was performed. However, it is presumed that the variable attenuation of the polyiron is adequately

---

[1] Prof. IRE, Vol. 41, No. 1 Jan. 1953.

accounted for by the well known theory of the losses in spherical iron particles imbedded in an insulating matrix. The variable attenuation observed with ferrite specimens is assumed to be an aspect of the generalized theory of gyromagnetic phenomena in ferrites, and should be treated, in a formal analysis, by means of that theory.[2]

In order to facilitate experimentation, two specimen holders which approximated 3/8" rigid coaxial line were fabricated. The first holder (holder A) was a brass tube with an I.D. of 0.356" to which two type N male connectors were soldered as end pieces. The center conductor was of 0.120" diameter. A coil of 1200 turns of No. 22 wire, 1-3/4" long and 1-3/4" O.D. was wrapped around the brass cylinder to provide the magnetizing field. The second specimen holder (holder B) was similar to holder A but had an I.D. of approximately 0.286 so that the ferrite specimens (of 0.285 diameter) might fit snugly in the tube. The inner conductor was of 0.125" diameter, and the longitudinal magnetizing coil consisted of 3025 turns of No. 20 wire. To calibrate the field produced in both holders, a search coil of 10 turns of No. 40 wire wrapped on a 0.25" diameter insulator was made. A Ballantine VTVM was used to measure the induced voltage in the search coil.

To facilitate both a-c and d-c measurements of the characteristics of the various ferromagnetic materials, a special console was constructed. Figure MRI-13141 shows a schematic of the test console circuit.

8.3 Samples Tested: The original experimental program called for testing a great variety of ferromagnetic materials under different conditions of geometry and frequency (with, of course, different magnetizing fields). Because of the early curtailment of program (as reported in R-222.25-53, PIB-167.25) only the following materials were tested;

a) Polyiron D
b) Ferramic C
c) Ferramic G
d) Lavite F-4

and as described in 8.4 below, only the polyiron specimens were tested under different conditions of "center conductor geometry", i.e. with the center conductor butted against, recessed into, or continuous through the specimen.

8.4 Performance Data: The experimental data for the Polyiron D specimens were the most complete obtained. These data, obtained with the specimens placed in holder A described in 8.2, are summarized in Figs. MRI-12933 - MRI-12939 inclusive. The calibration curve for the magnetizing coil as given by Fig. MRI-12940 is applicable to these data. As illustrated by the figures, large variations in attenuation (of the order of 10db) can be

[2] H.J. Beljers and J.L. Snoek, Phillips Technical Review, Vol. 11, No. 11, May 1950.

produoed by variations in 60 cycle a-c magnetizing coil current (of the order of 5 amp.). The variation in attenuation depends directly on length and exhibits considerable dependence on the frequency of the incident miorowave energy. This frequency dependence is strikingly illustrated by comparison of Figs. MRI-12935 and MRI-12936 or Figs. MRI-12938 and MRI-13939. Comparison of these figures shows that for the same center conduotor geometry and magnetizing coil current, either an increase in attenuation or a decrease in attenuation can be achieved, depending on the microwave frequenoy. Measurements of VSWR, although not given explicitly as part of the figures, indicate that minimum values of VSWR (1.5-4.0) result when the center conductor is continuous through the specimen (See R-222.21-52, PIB-167.21). The data also indicate that the VSWR is a function of the magnitude of the magnitizing coil current.

Comparative data for specimens of Polyiron D, Ferramic C, Ferramic G, and Lavite F-4 at frequencies of 2000 mcs and 3000 mcs are summarized in Figs. MRI-13143 to MRI-13152 inclusive and Figs. MRI-13226 to MRI-13242 inclusive. The magnetizing coil calibration curve given in Fig. MRI-13142 is applicable to these data. Although both a-c and d-c magnetizing fields were used, the data is limited in that only the butted center conductor case was examined. The specimens and test unit were destroyed by fire before more measurements could be taken (See R-222.25-53, PIB-167.25). The Figures indioate that considerable variations in attenuation can be achieved by varying the longitudinal magnetio field. Both a-c and d-c magnetizing coil currents produce similar results. The magnitude of the attenuation variation depends on the type of ferromagnetic material, microwave frequency, length of speoimen, and magnitude of magnetizing current. For a given type of material the attenuation variation seems to inorease with frequency, with Favite F-4 apparently the most sensitive material. The VSWR measurements were uncertain, but the data displayed in Figs. MRI-13240 to MRI-13242 inclusive may be regarded as representative . It should be emphasized that although the insertion loss and VSWR are unfavorable, these data are for the butted oenter conduotor case and with no compensayion of any type employed.

CHAPTER IX

FABRICATION AND MECHANICAL TESTING OF COAXIAL ATTENUATORS

by C. Grahm and H. W. Schleuning

9.1 Summary: The production of metallized glass tubular units for use as attenuators in coaxial line by thermal evaporation imposes problems of physical support and measurement. The development of a fixture that permits rotation of the tubes during evaporation and continuous measurement of resistance of the deposited film while the evaporation is in progress is here described. Shock and vibration tests of coaxial attenuators is also included.

9.2 Introduction To The Evaporation Problem: Tubular units must have a resistive film of metal deposited evenly all around the circumference and along the axial length. The requirement indicates that the tubes be rotated on a spit and the metal source held stationary, or vice versa. The former approach was pursued since the mechanical problems were amenable to solutions.

Units made in the past had proved that the initial requirements of even coating could be very well met by this process. The difficulties had been in getting the units to the predetermined resistance. Theoretical considerations and a considerable amount of data proved it necessary to eliminate the effect of variations in ellipticity and lengths of the glass units.

9.3 Development Of The Rotary Evaporation Jig: One of the obvious solutions of controlling the end to end resistance was tried on a pilot model, that of using "brushes" on the ends of the unit being coated, and it proved successful with minor improvements.

A series of spindles were mounted in a bearing group at one end leaving most of the length of the spindle free of obstruction so that the glass tubes could be slipped over them. The center-lines of the spindles were arranged in an arc so that each spindle was parallel and equidistant from the filament from which the resistive metal was to be evaporated. The rotating drive for the spindles was accomplished by securing a spur gear to the spindle between the bearing supports at one end. Each spindle gear is meshed with its neighbor and thus constitutes an element in a train of gears across the arc of center-lines. The spur gears are all the same diameter and pitch so that the centers are evenly spaced and the speeds of

rotation are equal though alternating in direction. The central spindle has a long projection beyond the bearing block. The end of this shaft extension is turned by a bevel gear driven by a vertical shaft, offset in the base plate and driving through it through a Wilson Seal. The lower end of the vertical drive shaft is rotated by an electric motor with integral speed reducer.

The spindles are of steel drill rod and the bearing plates are hard steel. Softer metals were found to wear too quickly at the elevated temperatures to which the whole is subjected in the vacuum deposition process. Slight wear in the bearing holes causes the gears to move laterally thus placing the pitch circles out of tangency. This action and it's attendant change in gear thrust angles causes intermittent binding and vibration which is amplified many times by the drill rod spindles.

The units are slipped over the ends of the spindles and held in position tightly by conical shocks which also slip over the spindles and lock in position by means of a set screw. Once in place, the outboard ends of the spindles are supported on a combe-like rest that inhibits lateral motion and dampens vibrations of the spindles. This operation is identical whether the units are coaxial attenuators or tubular resistors.

The centrally mounted unit is used as the resistance indicator for the group. Two brushes are brought to bear on the platinized ends of the tube and the electrical connections lead from these through the base plate to a Wheatstone Bridge. The brush material may be hard silver wire or a thin strip of phosphor bronze. These are brought to bear in such a way that they do not cast a shadow on the units from the filament below. Ordinarily a shadow so cast would cause a discontinuous path through the element and be readily detected, but with rotating units the shadow just adds a high resistance section, spoiling the end to end uniformity.

Throughout the process of assembly and selection of materials for components, one must have in mind that the components must safely stand temperatures of 350°C, must not be zinc or zinc alloy coated metals that will "position" the vacuum system, must have a low vapor pressure, below 10^{-5} mm of mercury, must not be what is referred to in high vacuum parlance as "gassy," and lastly the assembly must be easily cleaned.

The only disadvantage with the fixture is that with the present set-up it is not possible to make tapered resistances or units with higher resistance or, compensated sections. However, since these units are not in large demand, this is not felt to be a limiting short coming. It is also felt that with a little ingenuity and practice a movable mask could be developed to satisfy this need.

9.4 Vibration Tests of Coaxial Attenuators: Various 3/8" and 7/8" coaxial attenuator units were subjected to vibration tests. The All American Tool and Mfg. Co., Model 10-HA, Vibration Fatigue Testing Machine was used for the tests. Units were clamped to the table and vibrated in a direction perpendicular to the long axis of the units. Each test consisted of 10 periods of one minute duration during which the frequency of vibration was varied from 12 cycles per sec. to 65 cycles per sec. Each unit was given four tests as follows:

(a) 10 cycles at 0.05 in. traverse - g accel. range 0.37 → 11

(b) " " " 0.109 " " " " " 0.80 → 24

(c) " " " 0.16 " " " " " 1.2 → 35

(d) Step (c) repeated with unit turned 90° on long axis. All units withstood the vibration tests without damage or change in resistance.

The units tested were:

MRI Units: 2- 3/8" , 50 ohms, 13 db units
2- 7/8" , 50 ohms, 6 db units
1- 7/8" , 20 db chimey unit

PRD Units 1- 3/8" , 20 db units
1- 7/8" , 3 db units
1- 7/8" , 6 db unit

9.5 Shock Tests Of Coaxial Attenuators: Each of the above units was dropped onto a cast iron block from heights starting at six inches and increasing the heights by six inch increments, with the following results: (units were dropped vertically onto female end fitting)

(a) 2 units; MRI-3/8"-13 db ; max. height reached, 10 ft.-4 in. units did not break

(b) 1 unit; MRI -7/8"-6 db ; max. height reached, 48 in. insert fractured at female end of casing

(c) 1 unit; MRI-7/8"-6 db ; max. height reached, 36 in. insert fractured at male end of casing

(d) 1 unit; PRD-3/8"-20db; max. height reached, 8 ft.- 6 in. insert broken at both ends

(e) 1 unit; PRD-3/8" -3db; max. height reached, 9 ft.- 6 in. insert broken at one bullet

(f) 1 unit; PRD-7/8"-6db; max. height reached, 12 in. insert broken at one bullet.

The two MRI units of part (a) were given an additional test by dropping them sidewise (long axis parallel to direction of all) onto the cast iron block with the following results:

(a) 1 unit; MRI-3/8"-13db; max. height reached, 60 in. insert broken at bullet; sharp break across insert

(b) 1 unit; MRI-3/8"-13 db; max. height reached 42 in. insert shattered at bullets

The above data indicated that the 3/8" units withstood shock tests which might be considered greater than one would normally impose on a piece of apparatus containing glass in its structure. The 7/8" units were definitely weak to shock.

9.6 References: The above data were abstracted from the following research reports:

1. "Development of A Rotary Evaporation Jig For Thin Film Attenuators" by Clifford Graham, R-241-51
2. "Shock And Vibration Tests On Coaxial Attenuators" by Hubert W. Schleuning, R-242-51

which have been issued by MRI.

CHAPTER X

RECOMMENDATIONS

As described by the preceding chapters, the Microwave Research Institute has developed and designed microwave components for precision test equipment needed by the Bureau of Ships and other Services. Many of the assigned tasks have been successfully completed while others remain to be engineered into final designs. Since the facilities of MRI are naturally adaptable to these activities, it is recommended that these facilities be utilized to the utmost in completing started developments and investigating newer ideas for the future benefit of our country. In this regard, the following suggestions are made:

1. development of rugged precision waveguide attenuators capable of absorbing high power
2. completion of phase-shift data of waveguide attenuators designed for standard waveguide lines
3. design of waveguide high power probe attenuators
4. engineering of variable broadband 7/8" coaxial attenuator
5. combining 7/8" coaxial fixed attenuators into a precision decade attenuation with a maximum frequency range of 4000 mc/sec.
6. development of magnetic attenuators for rugged applications
7. improvement of mechanical rigidity of coaxial attenuators for field applications
8. investigation of methods for measuring attenuation magnitudes of 0.1 db or less.

DWG. NO. P.I.B.-C 504-U

DWG. NO. P.I.B.-C 504-U

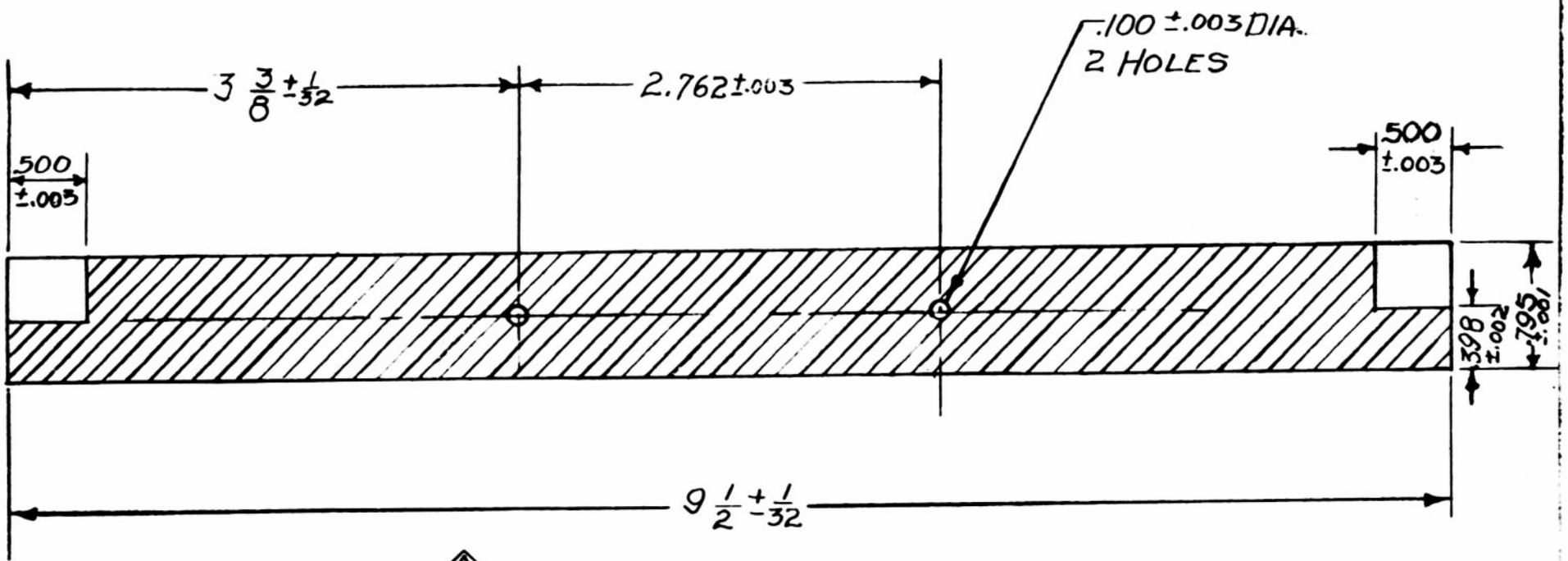

MAT'L: SOFT GLASS .062 ±.010 THICK
OHMS PER SQUARE: 187.5 ± 2.5 OHMS.
NICHROME FILM.

ITEM	DWG. NO.	DESCRIPTION	REQ'D	STOCK ITEMS

CHANGE	DATE
◇ WAS 1/16"	1-30-52

POLYTECHNIC INSTITUTE OF BROOKLYN
MICROWAVE RESEARCH INSTITUTE

DRAWN FOR	APPROVED BY
DRAWN BY F.Q.	SCALE 1 = 1
CHECKED BY	DATE 7-51

TITLE: METALLIZED PLATE.

DWG. No. P.I.B.-C 504-U

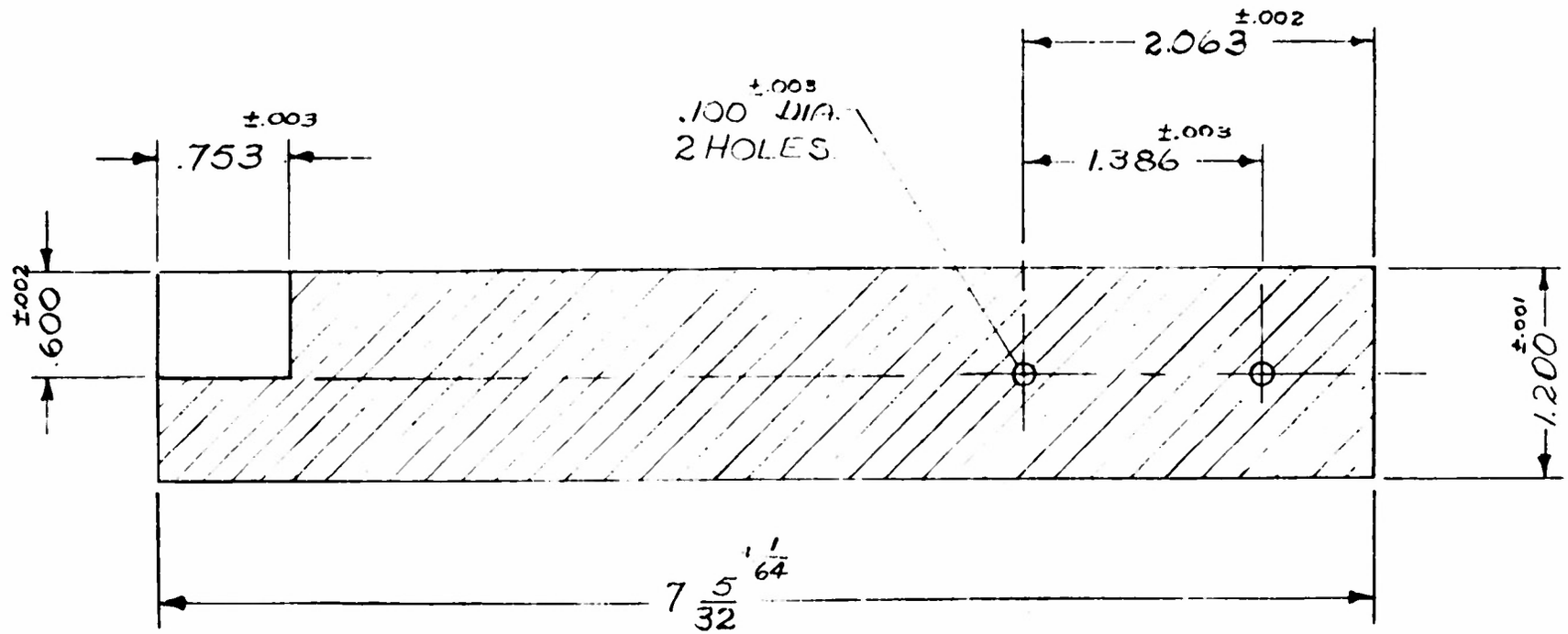

MAT'L: SOFT GLASS .091 ±.003
OHMS/SQUARE: 187.5 ± 2.5 OHMS
NICHROME FILM,
TWO REQ'D.

X1-1 METALLIZED PLATE

M.R.I. 10704

P.I.B-A-515-A

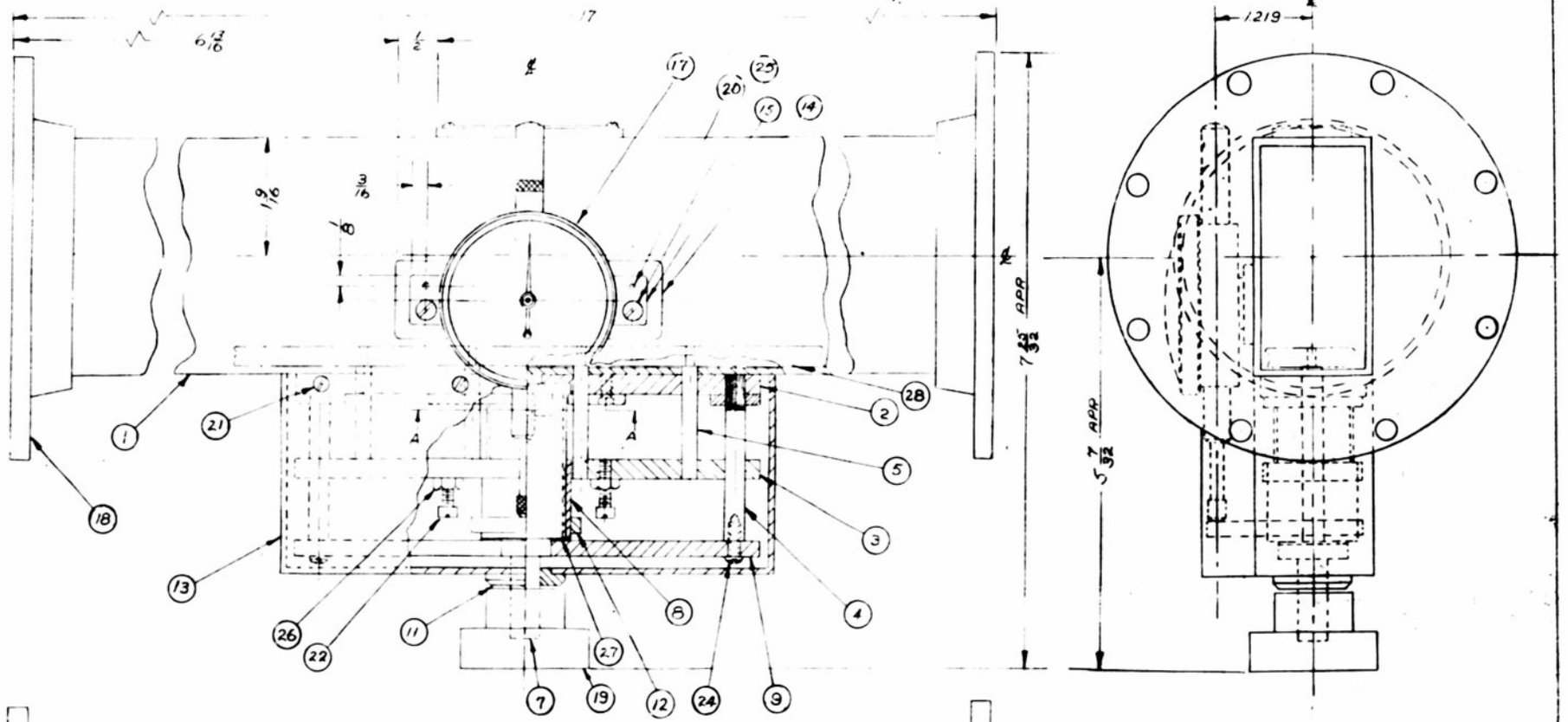

NOTE:
1) AFTER (17) HAS BEEN "ZERO SET" PRESSFIT (20) THRU (15) INTO (14) AS SHOWN & PEEN
2) PRESS FIT (5) INTO (3), (4) INTO (2) & (6) INTO (7)
3) HARD SOLDER (12) TO (8), (8) TO (3), (14) TO (1), (17) TO (15) & (11) TO (13)
4) AFTER FASTENING (6) TO (7) WITH (23), (23) IS TO BE DUTCH TINNED IN PLACE THEN LAP (6) TILL FLUSH WITH TOP OF (2) PAINT REAR BOSS OF FLANGE (18), EXTERIOR OF (13) & (1) WITH PR.D. GRAY.
5) FLANGES CHROME PLATED.

POLYTECHNIC INSTITUTE OF BROOKLYN MICROWAVE RESEARCH INSTITUTE	TYPE 1/2 x 3 VARIABLE ATTENUATOR CASING
	P.I.B.-A-515-A

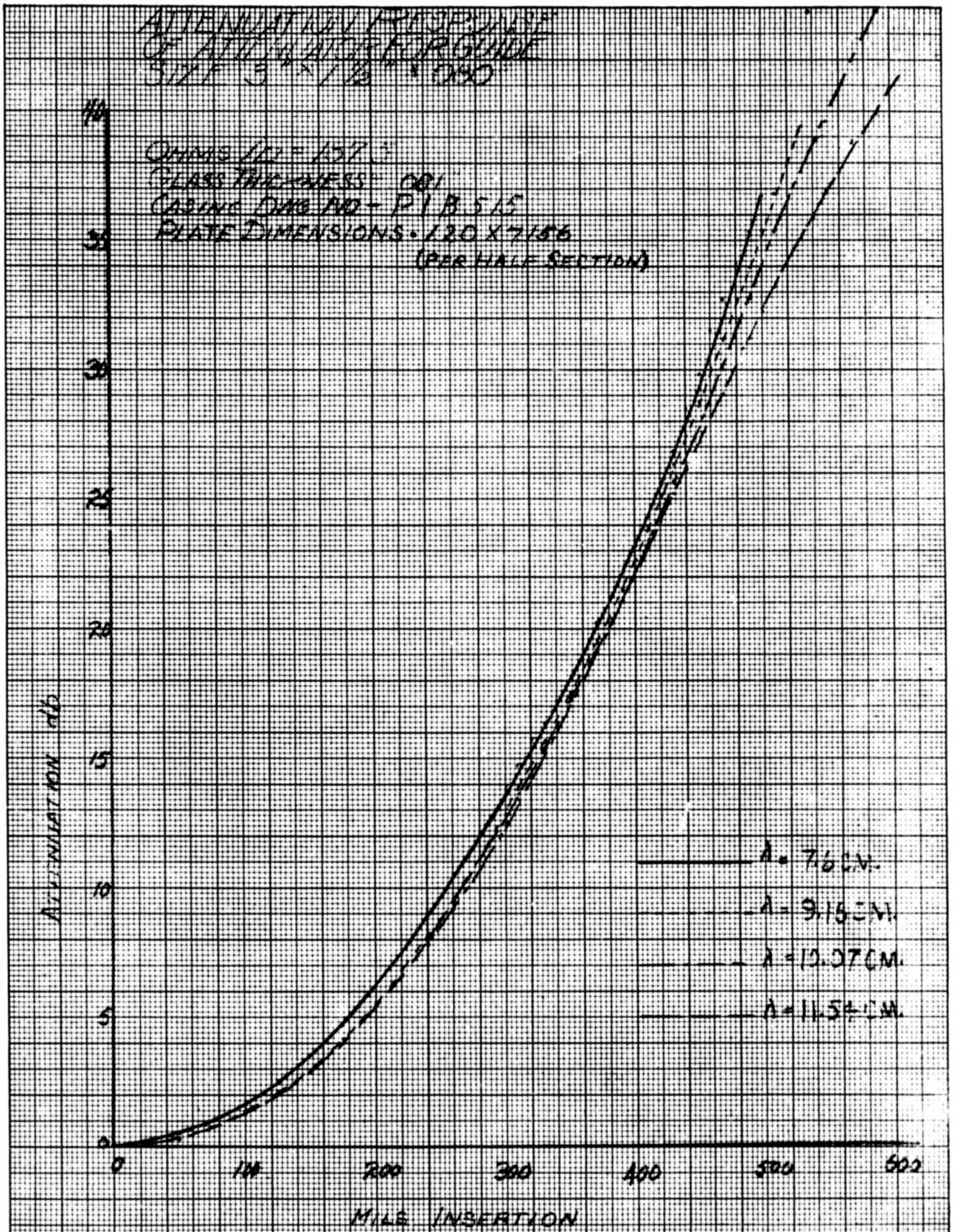
(PER HALF SECTION)
λ = 7.6 CM.
λ = 9.15 CM.
λ = 10.07 CM.
λ = 11.54 CM.
ATTENUATION db
MILS INSERTION
0
100
200
300
400
500
600
5
10
15
20
25
30
35
40

MR 110927

ATTENUATOR FOR GUIDE SIZE 3 x 1 1/2 x .080 ATTENUATION VS PLATE WIDTH

LIME GLASS THICKNESS = 0.091 INCH
NOMINAL FILM RESISTIVITY = 187.5 OHMS/SQ.
GLASS LENGTH PER HALF SECTION = 7.156 INCHES
INSERTION INTO GUIDE = 500 MILS

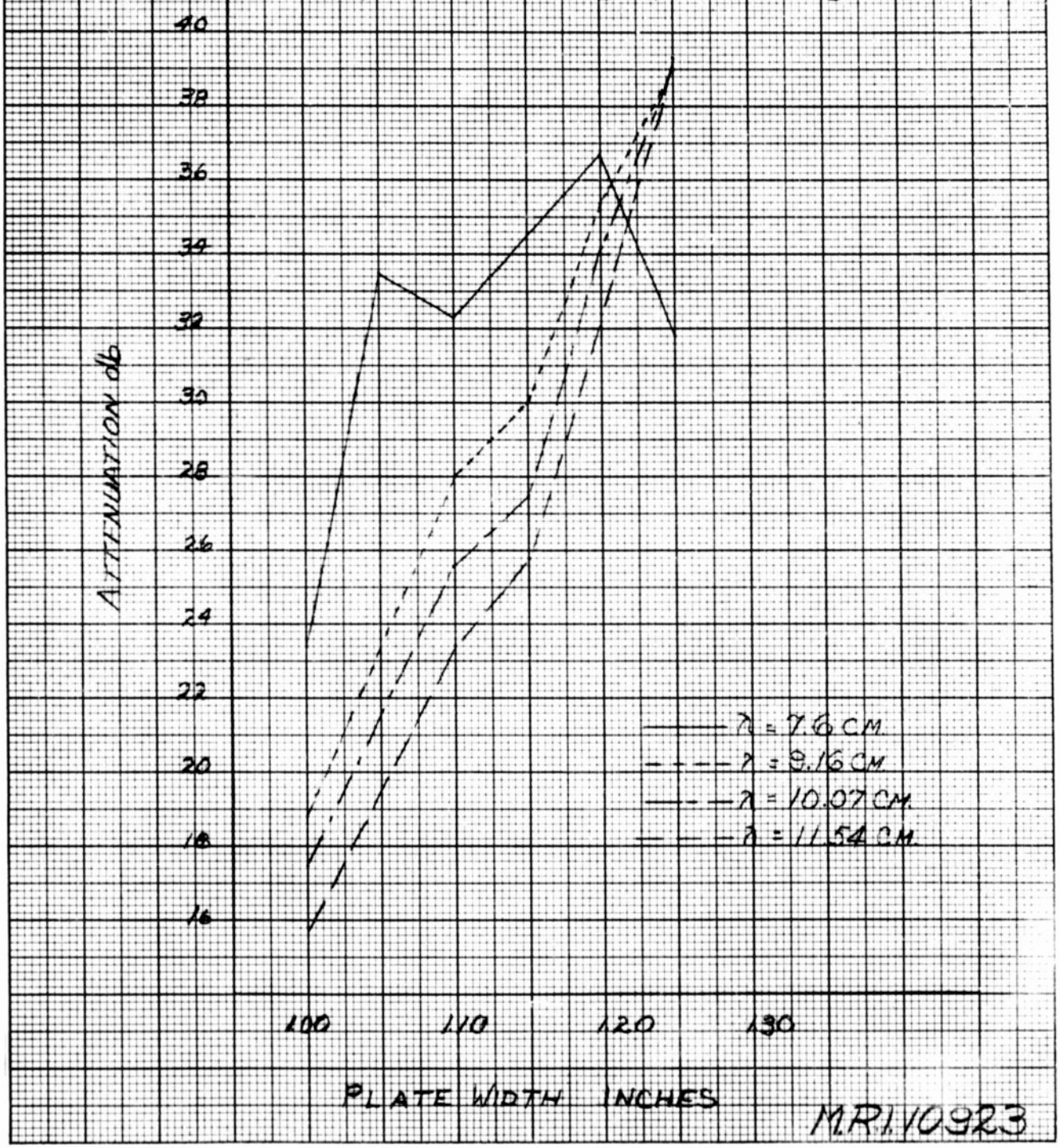

MR.10923

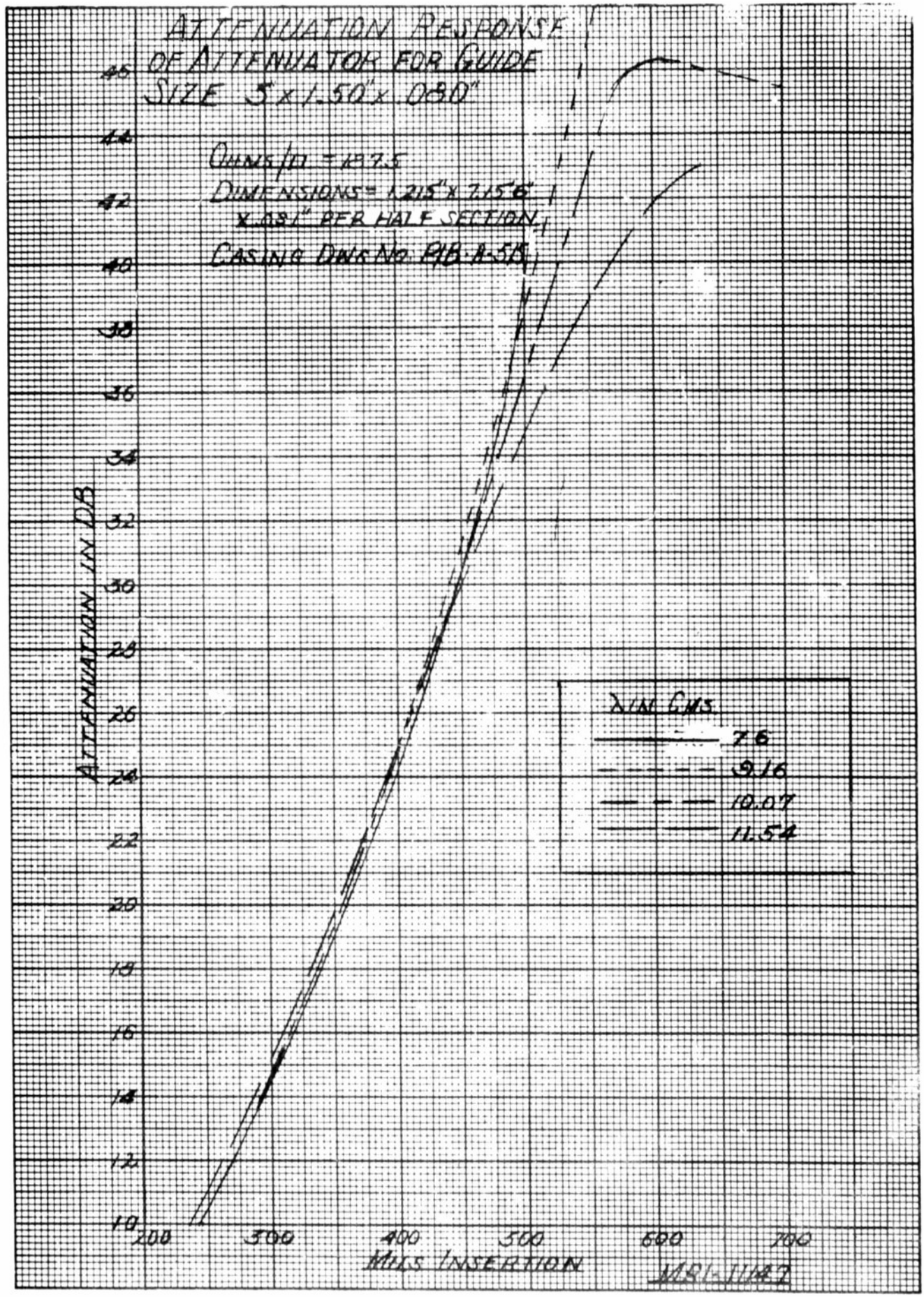
ATTENUATION RESPONSE OF ATTENUATOR FOR GUIDE SIZE 3" x 1.50" x .080"
QUENCHING = 187.5
DIMENSIONS = 1.215" x 2.156" x .081" PER HALF SECTION
CASING DWG NO. RIB A-58
ATTENUATION IN DB
MILS INSERTION
MRI-1142
λ IN CMS.
7.6
9.16
10.07
11.54
46
44
42
40
38
36
34
32
30
28
26
24
22
20
18
16
14
12
10
200
300
400
500
600
700

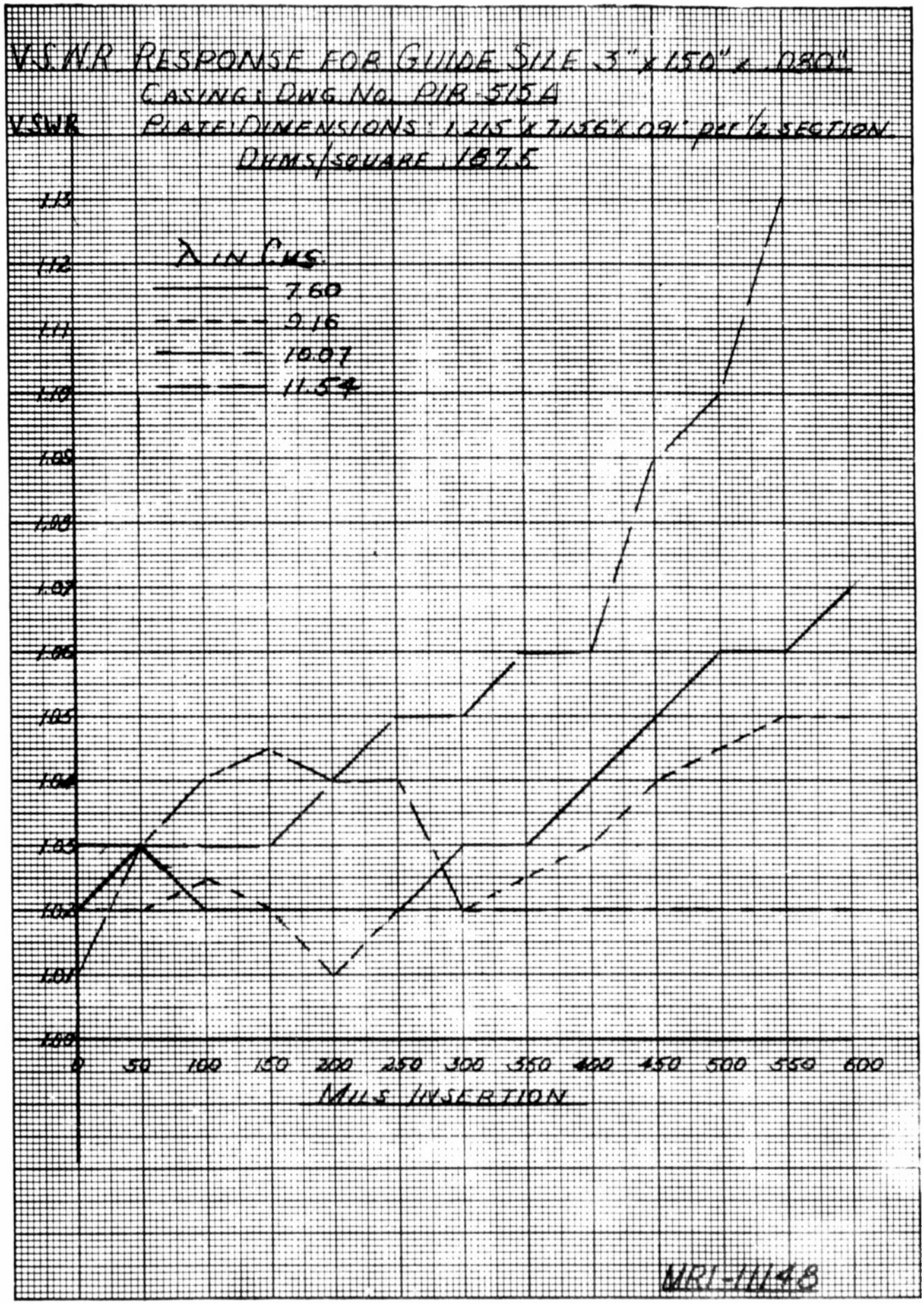
V.S.W.R RESPONSE FOR GUIDE SIZE 3" x 1.50" x .080"
CASING: DWG. NO. PIB-515A
PLATE DIMENSIONS: 1.215" x 1.156" x .091" per ½ SECTION.
DIMS/SQUARE .187.5
VSWR
λ IN CMS.
7.60
9.16
10.07
11.54
1.13
1.12
1.11
1.10
1.09
1.08
1.07
1.06
1.05
1.04
1.03
1.02
1.01
1.00
0
50
100
150
200
250
300
350
400
450
500
550
600
MILS INSERTION
MRI-1148

DWG. NO. P. I. B.-C- 515 U

DWG. NO. P. I. B.-C- 515 U

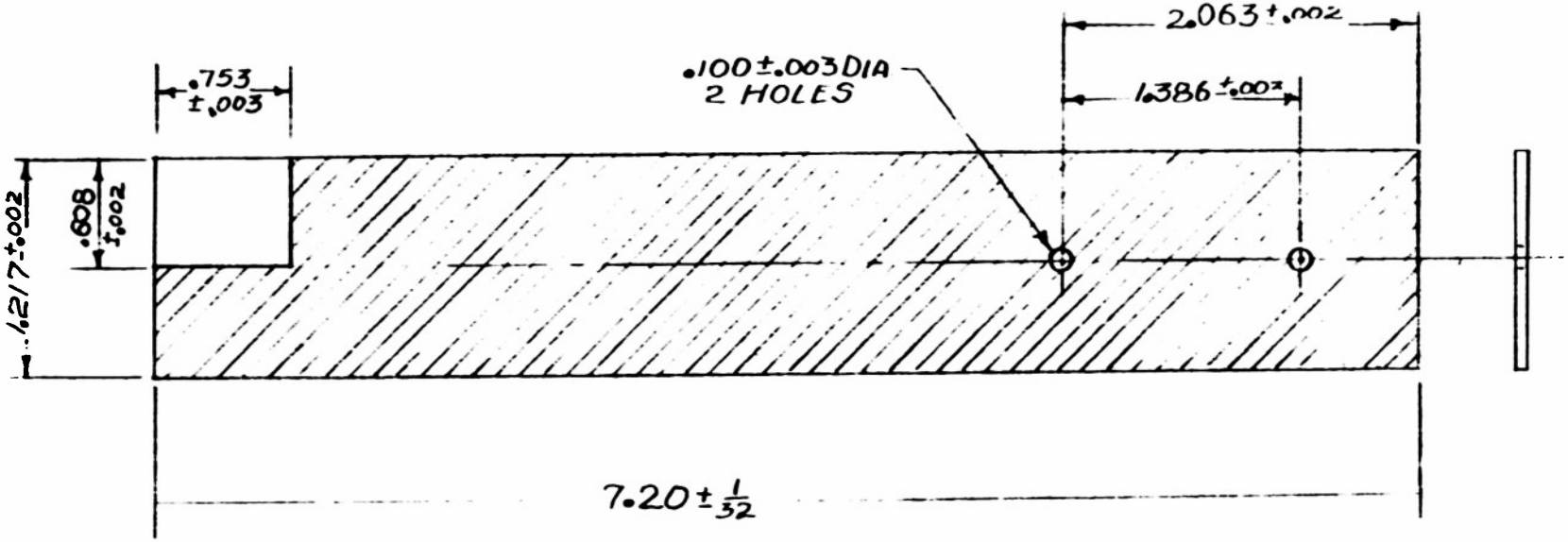

MAT'L: LIME GLASS .068 ±.002
NICHROME FILM RESISTIVITY 192.5 OHMS/□ ±2.5 OHMS/□
NARROW DIMENSION OF GUIDE 1.340 $\pm^{.005}_{.002}$

POLYTECHNIC INSTITUTE OF BROOKLYN MICROWAVE RESEARCH INSTITUTE	
DRAWN FOR	APPROVED BY
DRAWN BY F.Q.	SCALE 1=1
CHECKED BY	DATE 7-51

TITLE
METALLIZED GLASS PLATE

ITEM	DWG. NO.	DESCRIPTION	REQ'D	STOCK ITEMS	CHANGE	DATE	DWG. NO. P. I. B.-C- 515 U

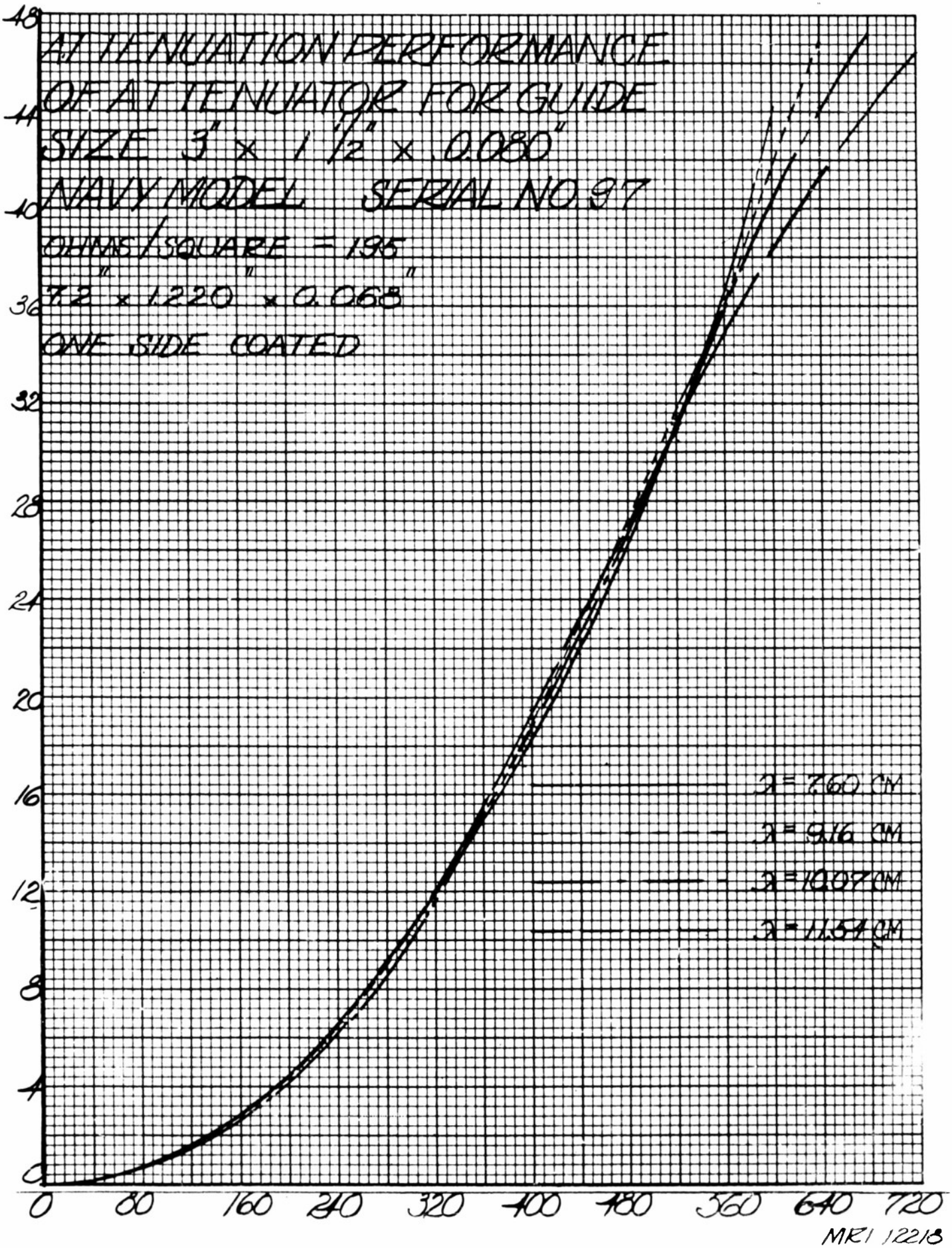
ATTENUATION PERFORMANCE OF ATTENUATOR FOR GUIDE SIZE 3" × 1 1/2" × .0080"
NAVY MODEL SERIAL NO. 97
OHMS/SQUARE = 195
7.2" × 1.220" × 0.068"
ONE SIDE COATED
λ = 7.60 CM
λ = 9.16 CM
λ = 10.07 CM
λ = 11.54 CM
0
4
8
12
16
20
24
28
32
36
40
44
48
0
80
160
240
320
400
480
560
640
720
MRI 12218

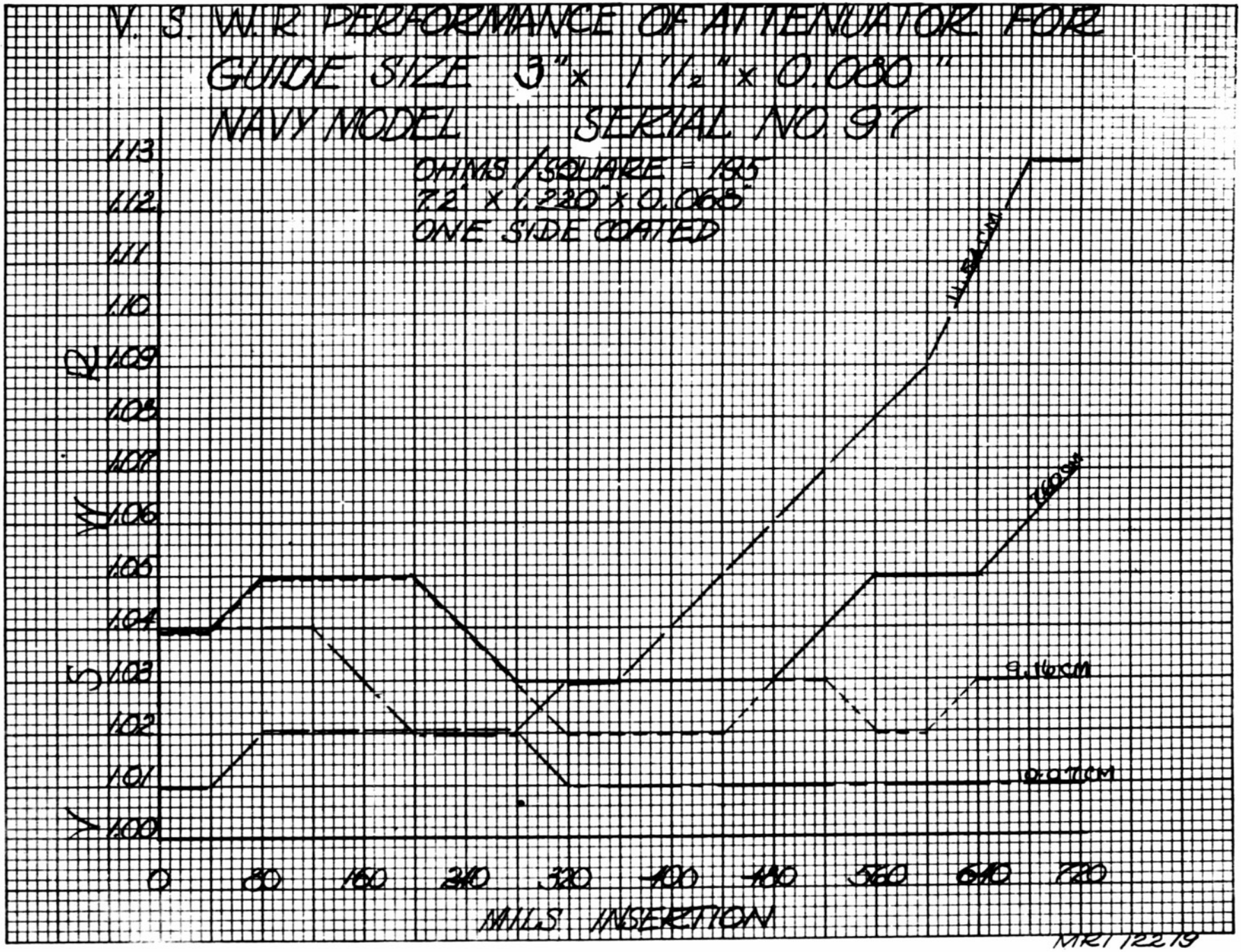
V. S. W. R. PERFORMANCE OF ATTENUATOR FOR
GUIDE SIZE 3" × 1 1/2" × 0.080"
NAVY MODEL SERIAL NO. 97
OHMS / SQUARE = 185
72" × 1.220" × 0.065"
ONE SIDE COATED
1.13
1.12
1.11
1.10
1.09
1.08
1.07
1.06
1.05
1.04
1.03
1.02
1.01
1.00
VSWR
1.54 CM
1.08 CM
9.16 CM
0.070 CM
0
80
160
240
320
400
480
560
640
720
MILS INSERTION
MR1 12219

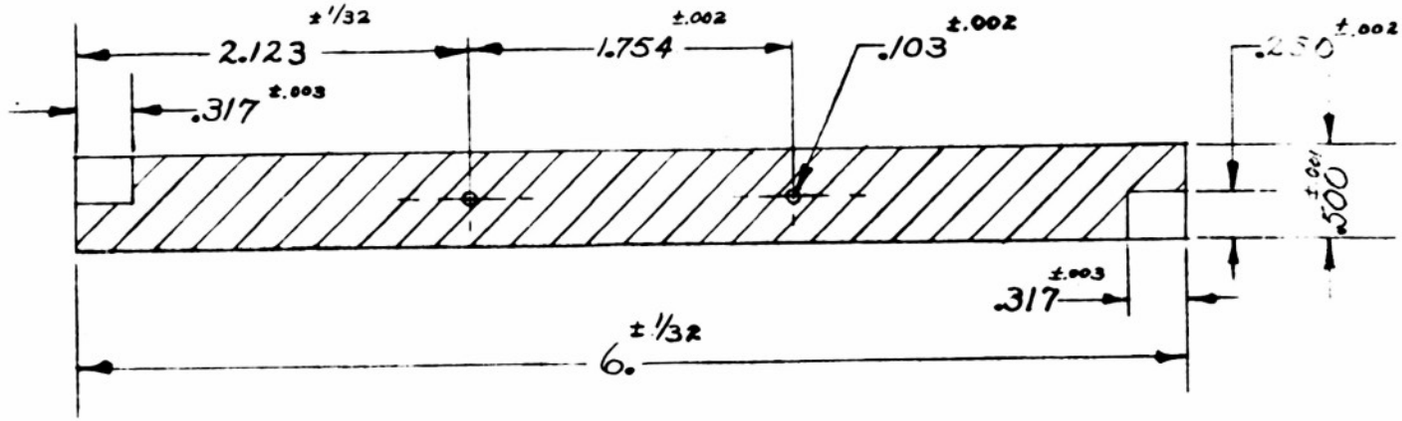

X4-1 METALLIZED PLATE

MAT'L: SOFT GLASS

THICKNESS: $.040^{+.000}_{-.002}$

OHMS PER SQUARE: 187.5 ± 2.5

NICHROME FILM

M.R.I. 10833

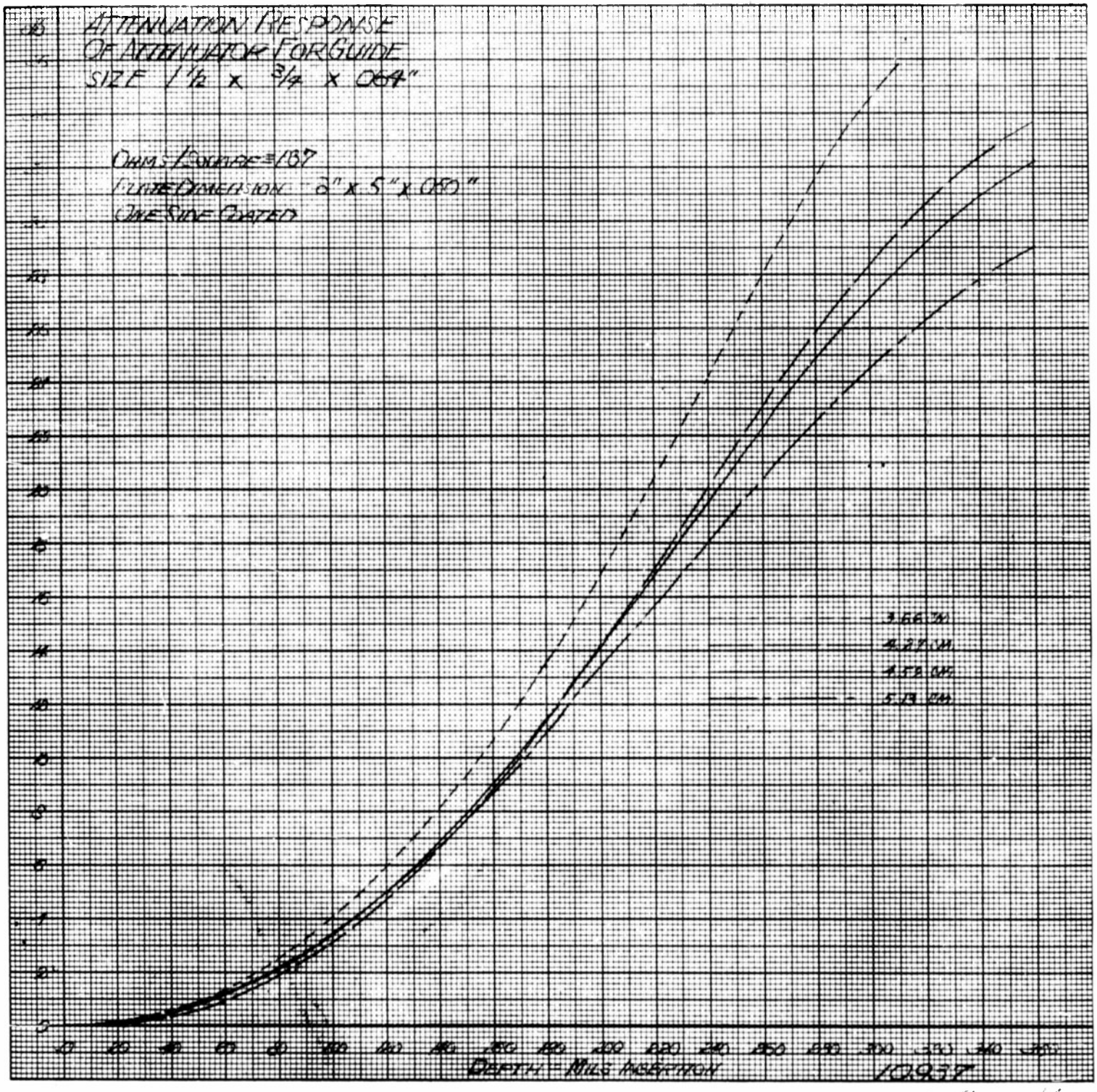
ATTENUATION RESPONSE
OF ATTENUATOR FOR GUIDE
SIZE 1 1/2 x 3/4 x .064"
OHMS LOADING = 137
FLANGE DIMENSION 2" x 5" x .080"
ONE SIDE COATED
3.66 (W)
4.22 (W)
4.52 (W)
5.13 (W)
DEPTH - MILS PENETRATION
10937

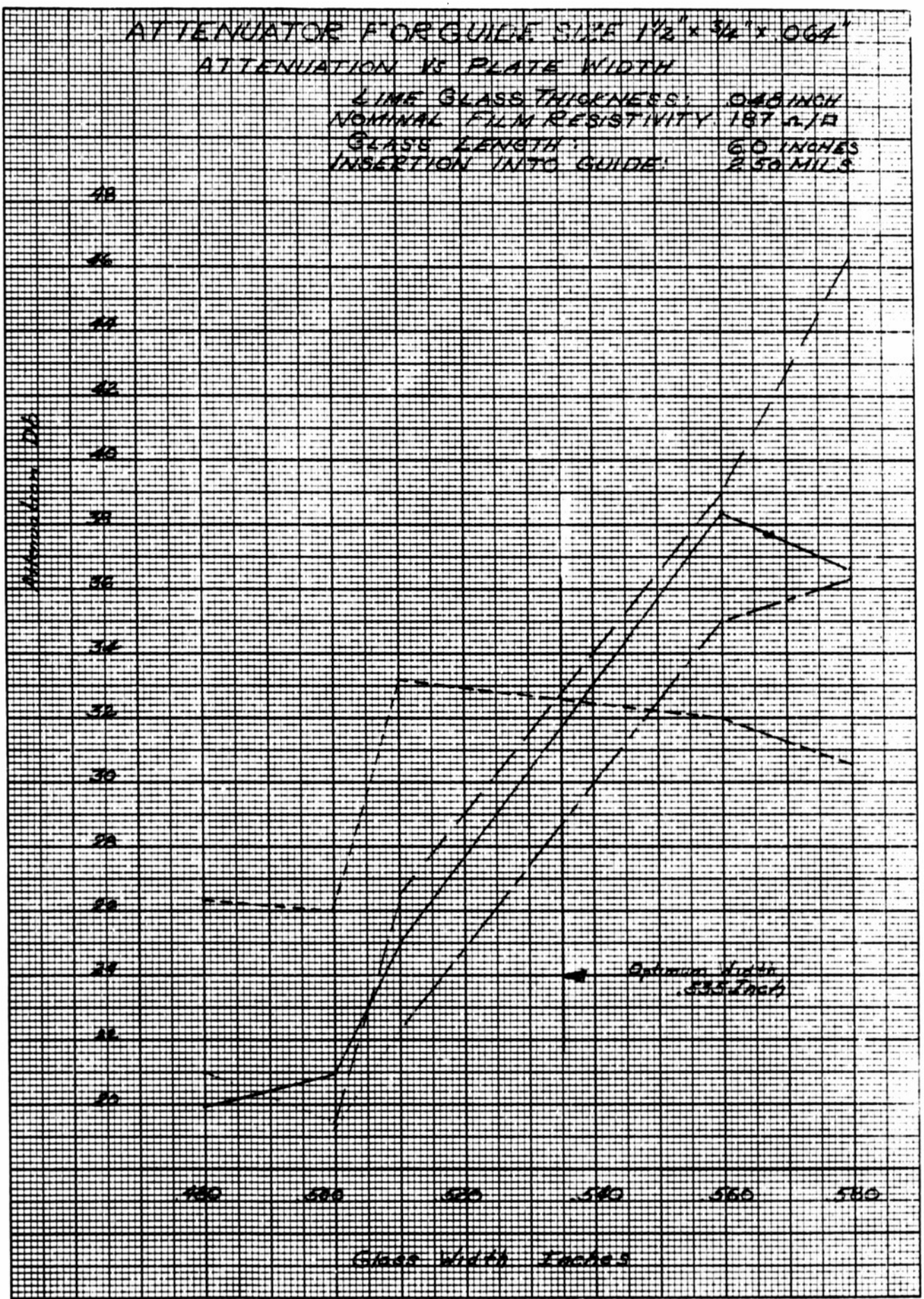
ATTENUATOR FOR GUIDE SIZE 1½" × ¾" × .064"
ATTENUATION VS PLATE WIDTH
LIME GLASS THICKNESS: .048 INCH
NOMINAL FILM RESISTIVITY 187 Ω/□
GLASS LENGTH: 6.0 INCHES
INSERTION INTO GUIDE: 2.50 MILS
Attenuation DB
48
46
44
42
40
38
36
34
32
30
28
26
24
22
20
Optimum Width .535 Inch
500
520
540
560
580
Glass Width Inches

MRI-10934

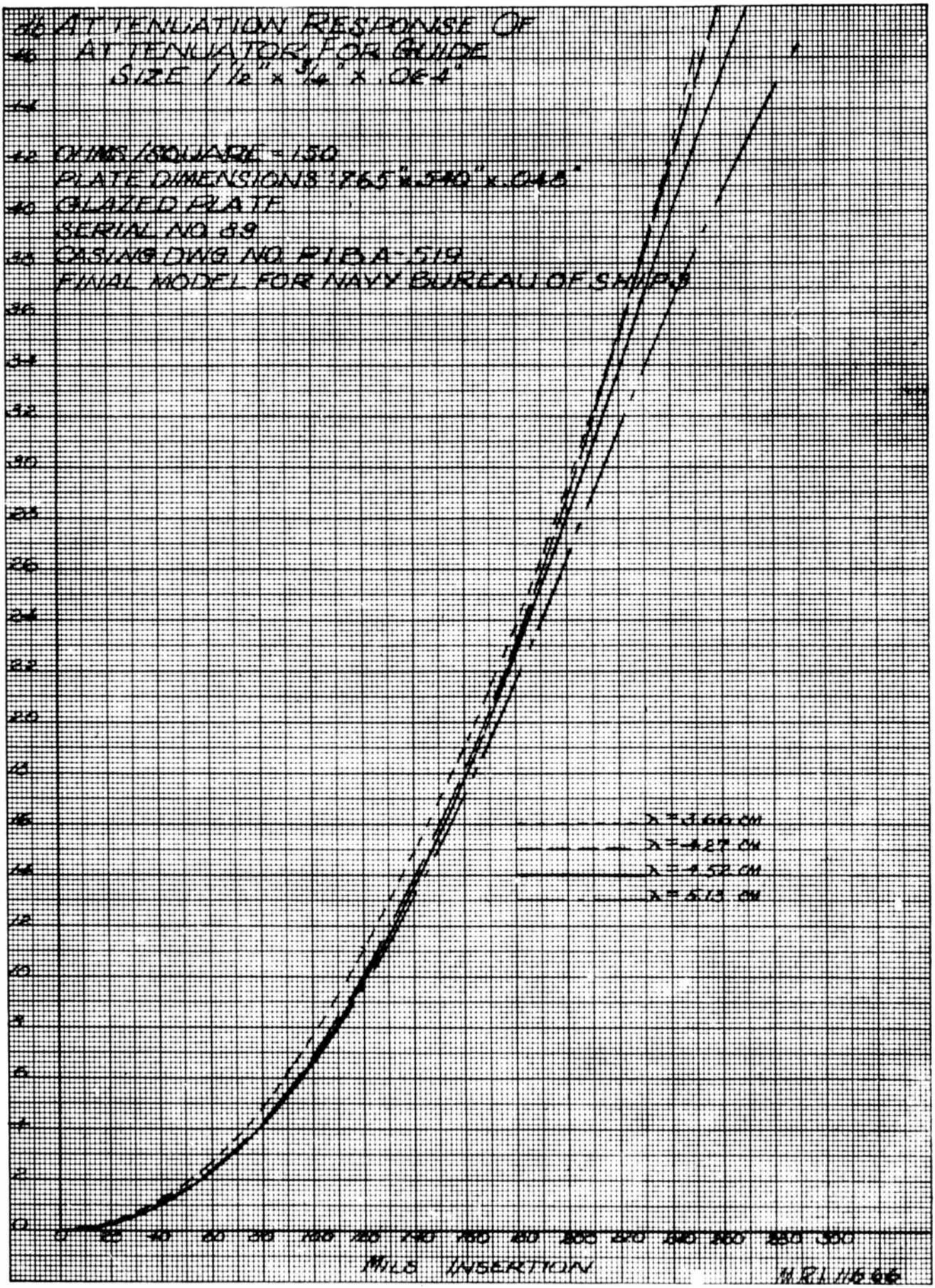
ATTENUATION RESPONSE OF
ATTENUATOR FOR GUIDE
SIZE 1 1/2" x 3/4" x .064"
OHMS/SQUARE = 150
PLATE DIMENSIONS .765" x .540" x .048"
GLAZED PLATE
SERIAL NO. 89
CASING DWG. NO. F1EA-519
FINAL MODEL FOR NAVY BUREAU OF SHIPS
λ = 3.66 cm
λ = 4.27 cm
λ = 4.52 cm
λ = 5.13 cm
MILS INSERTION
0
2
4
6
8
10
12
14
16
18
20
22
24
26
28
30
32
34
36
38
40
42
44
46
48
0
20
40
60
80
100
120
140
160
180
200
220
240
260
280
300
320
340
360

E.S.M.R. RESPONSE OF ATTENUATOR FOR GUIDE SIZE 1 1/2" x 3/4" x .064"

OHMS/SQUARE = 150
PLATE DIMENSIONS 7.65" x 5.40" x .048"
GLAZED PLATE
SERIAL NO. 89
CASING DWG NO. PIB A519
FINAL MODEL FOR NAVY BUREAU OF SHIPS

λ = 3.66 CM
λ = 4.25 CM
λ = 4.52 CM
λ = 5.13 CM

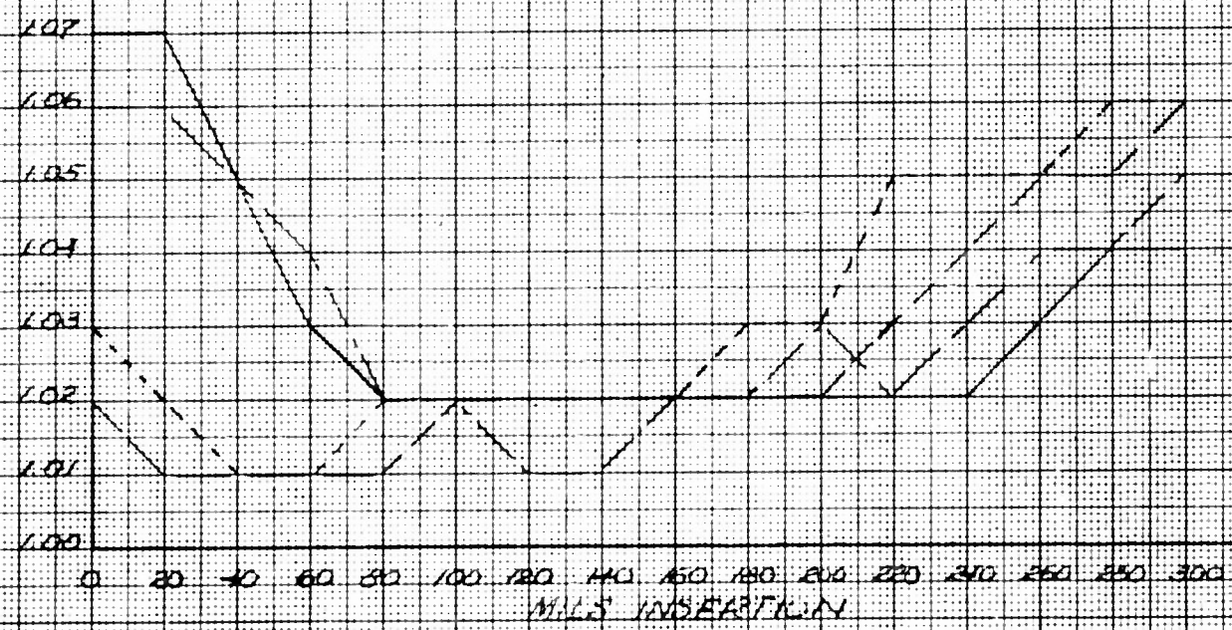

MR 11662

DWG. NO. P. I. B.-C- 519-18

DWG. NO. P. I. B.-C- 519

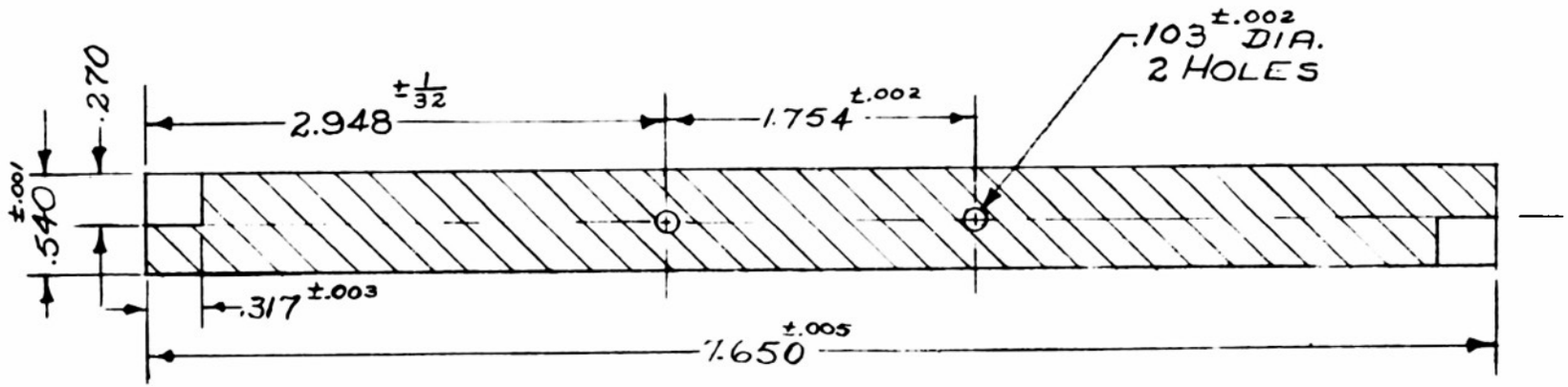

NOTE.
TO BE USED WITH WAVEGUIDE
TUBING WITH NARROW DIMENSION
.622 ±.002.
NICHROME RESISTIVITY = 150. ± 5. OHMS/SQ. (A)
LIME GLASS THICKNESS = .048 ±.002

ITEM	DWG. NO.	DESCRIPTION	REQ'D	STOCK ITEMS

	CHANGE	DATE
(A)	WAS. .155	6-52

POLYTECHNIC INSTITUTE OF BROOKLYN
MICROWAVE RESEARCH INSTITUTE

DRAWN FOR PM	APPROVED BY
DRAWN BY J.I	SCALE 1-1
CHECKED BY	DATE 5-50

TITLE
METALLIZED GLASS PLATE
DESIGN FOR 1½ x ¾ - .064 ATTEN.

DWG. No. P. I. B.-C- 519-18

P.I.B.-A-519-A

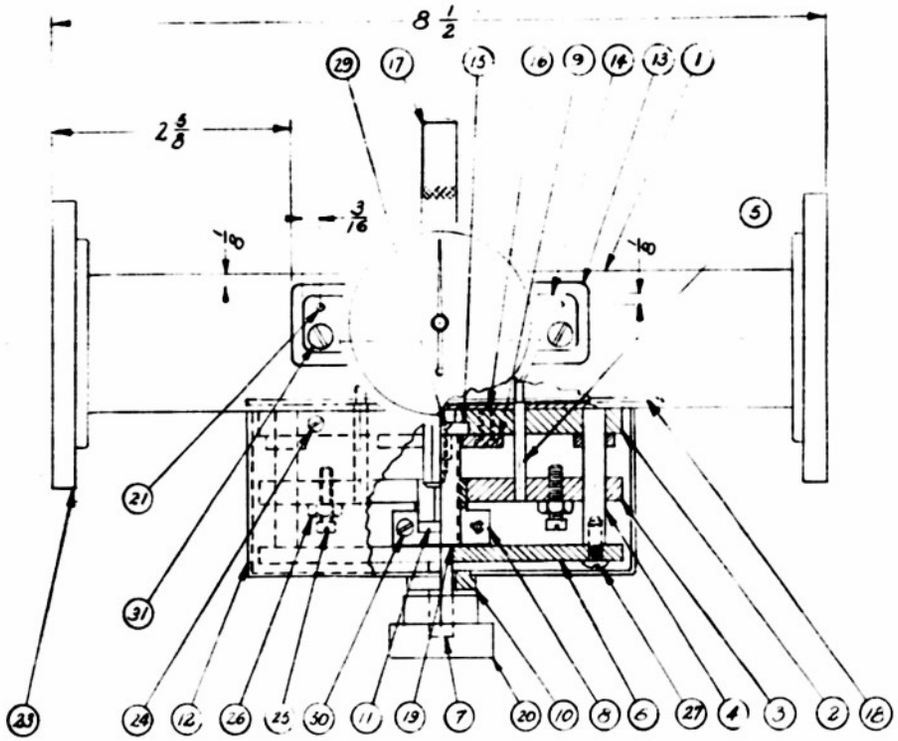

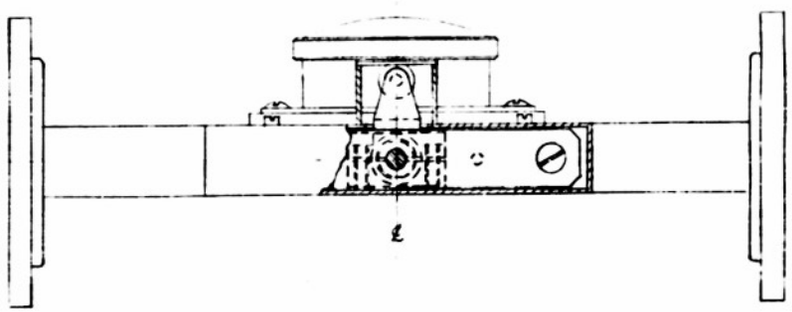

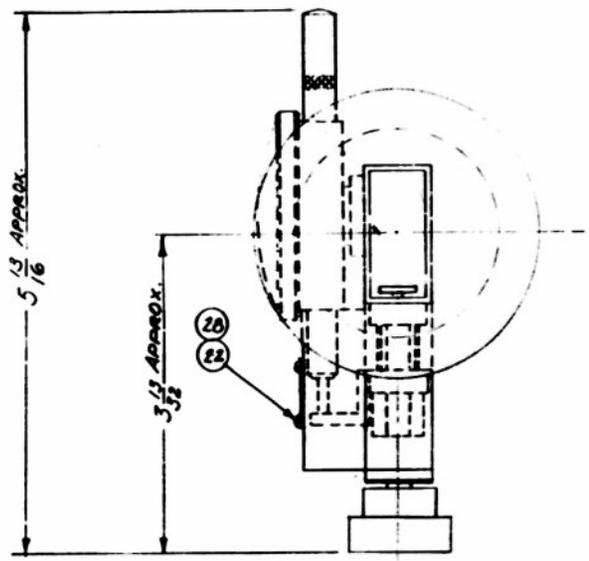

8 2/16" O.D. x 17/64" I.D. WITH A THICKNESS SO THAT BASE OF STRUT SHOULDER IS .010 INTO WAVEGUIDE AT MIN. INSERTION

NOTE: 1.- AFTER (17) HAS BEEN "ZERO SET" PRESS FIT (21) AS SHOWN & PEEN.
2.- PRESS (4) INTO (2) & (5) INTO (3), (15) INTO (7).
3.- HARD SOLDER (11) TO (3), (2) TO (1), (6) TO (3), (17) TO (14), (13) TO (1), & (10) TO (12)
4.- LAP (13) FLUSH WITH TOP OF PT. (2).
5.- CHROME PLATE PT. (23).
6.- PAINT REAR BOSS OF (23), EXTERIOR OF (16), (13) & (1)

NO	TITLE	REQ'D
18	METALLIZED GLASS PLATE	1
17	INDICATOR	1
16	RETAINER-SCREW	4
15	BEARING-THRUST	1
14	PAD INDICATOR	1
13	PAD-SUPPORT	1
12	COVER	1
11	PAD-DRIVE	1
10	BUSHING-COVER	1
9	PLATE-RETAINER	1
8	BUSHING-SPLIT	1
7	SHAFT	1
6	PLATE-BEARING	1
5	STRUT	2
4	ROD-GUIDE	2
3	PLATE-MOVABLE	1
2	PLATE-BASE	1
1	WAVE GUIDE	1

PARTS LIST

NO	DESCRIPTION	REQ'D
31	#6-32 BIND. HD. SC 3/16" LG. NI. PL.	2
30	#4-40 FIL. SC. NI. PL. 3/16" LG.	2
29	#6-32 FLT. HD. SC. NI. PL. 1/2 LG.	1
28	#00 DRIVE SC. NI. PL. 1/8 LG.	4
27	#6-32 BIND. HD. SC. NI. PL. 5/16 LG.	2
26	#6-32 HEX NUT NI. PL.	2
25	#6-32 FIL. HD. SC. . NI. PL. 9/16 LG.	2
24	#4-40 FIL. HD. SC. NI. PL. 7/16 LG.	4
23	FLANGE UG-344/U	2
22	NAME PLATE 3/4 x 7/16	1
21	.083 DIA. 37° LESS 37½ PIN 3/8 LG	1
20	1/8 FLUTED KNOB	1
19	SS WASHER	4

STOCK PARTS

MICROWAVE RESEARCH INSTITUTE
POLYTECHNIC INSTITUTE OF BROOKLYN

TYPE 178 PRECISION VARIABLE ATTENUATOR (1 5/8" x 3/4" x .064 WALL)

MATERIAL	FINISH	DRAWN BY	CHECKED BY	DATE
				6-48
NO. REQ.	SCALE 1:1	APPROVED BY	DWG NO P.I.B.-A- 519-A	

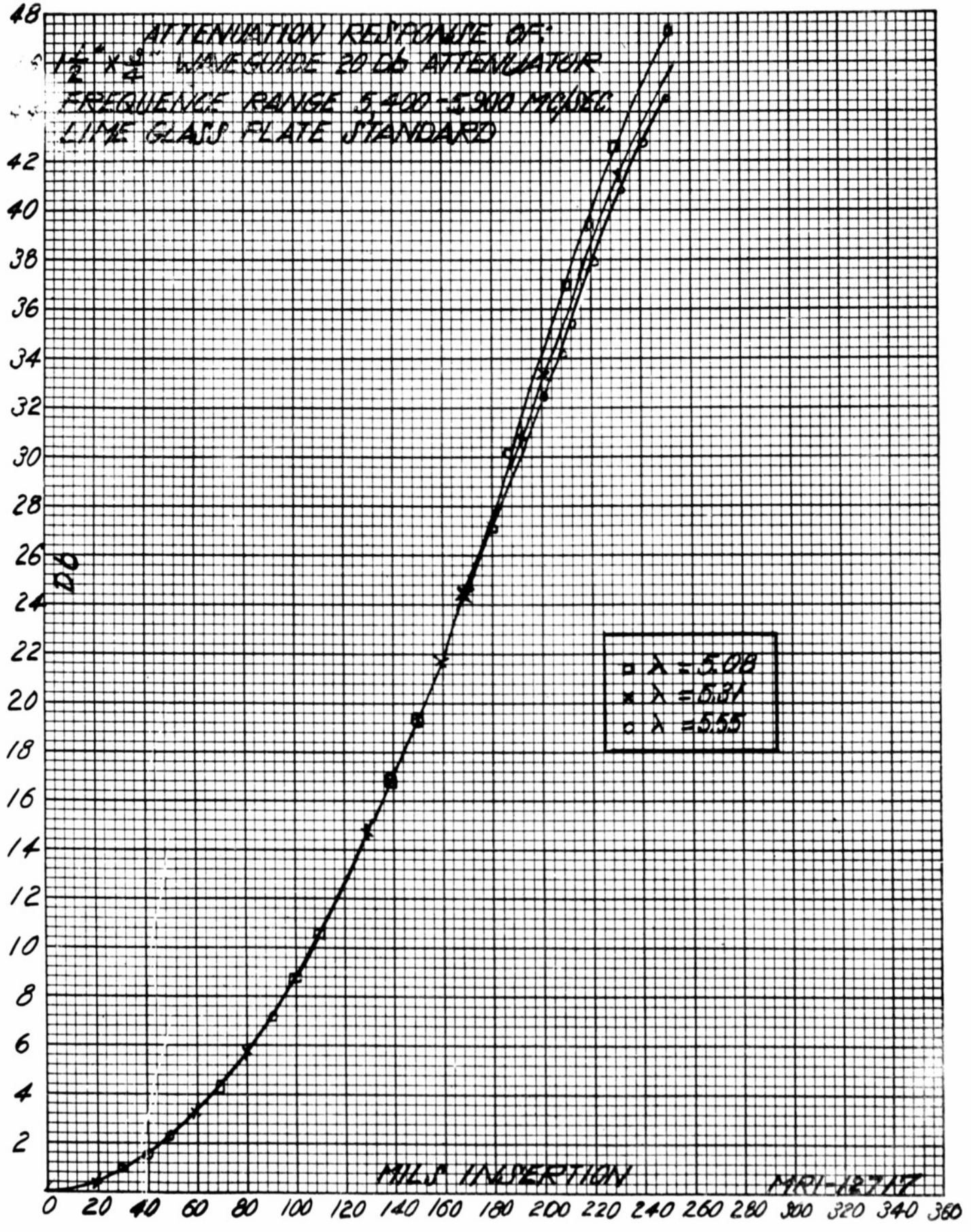
ATTENUATION RESPONSE OF:
1½" x ¾" WAVEGUIDE 20 DB ATTENUATOR
FREQUENCE RANGE 5.400-5.900 MC/SEC.
LIME GLASS PLATE STANDARD
DB
MILS INSERTION
MRI-12717
λ = 5.08
λ = 5.31
λ = 5.55
0 20 40 60 80 100 120 140 160 180 200 220 240 260 280 300 320 340 360
2 4 6 8 10 12 14 16 18 20 22 24 26 28 30 32 34 36 38 40 42 48

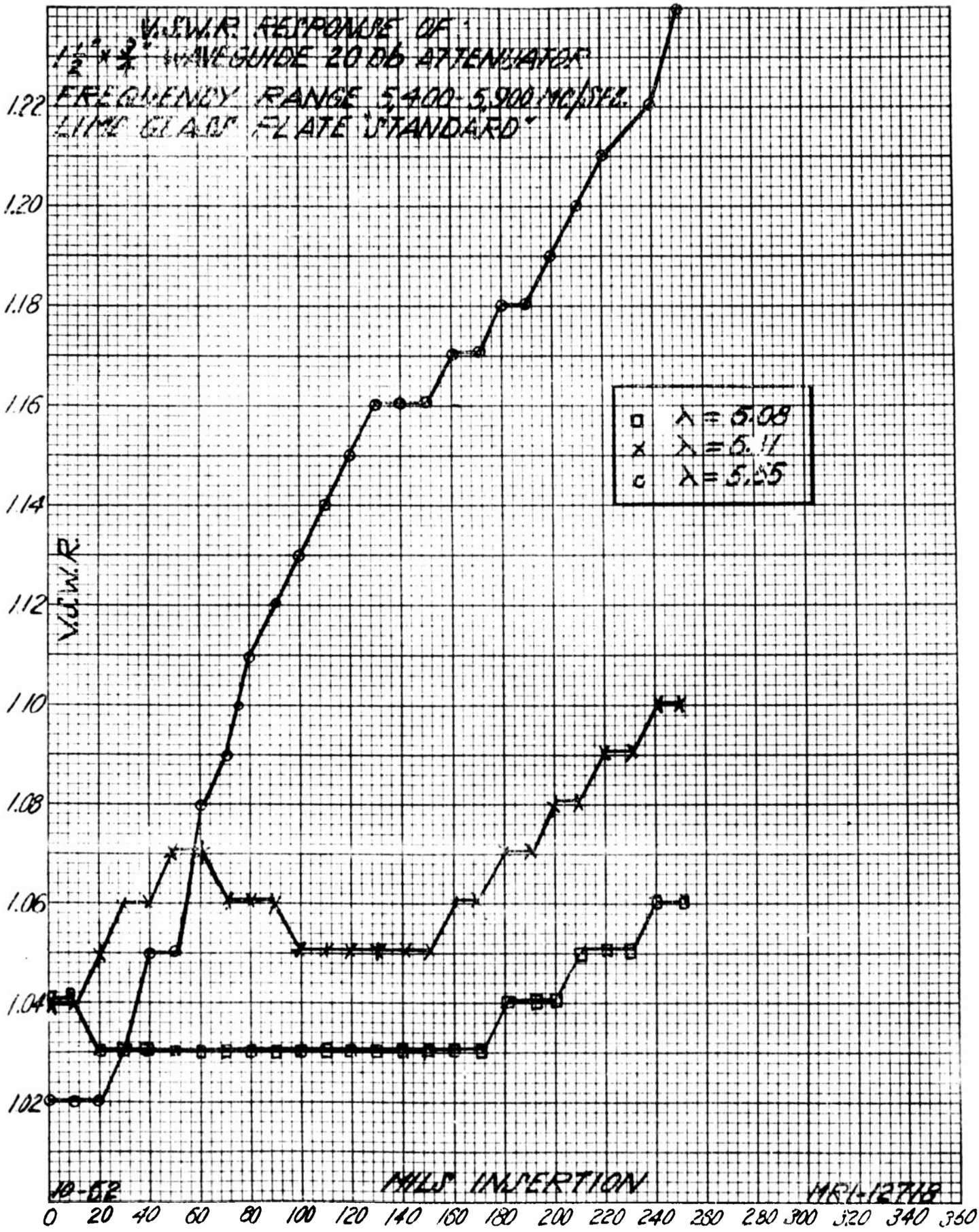
V.S.W.R. RESPONSE OF
1½" × ½" WAVEGUIDE 20 DB ATTENUATOR
FREQUENCY RANGE 5,400-5,900 MC/SEC.
LINE TO A.F. PLATE "STANDARD"
□ λ = 5.08
× λ = 5.11
○ λ = 5.25
V.S.W.R.
1.22
1.20
1.18
1.16
1.14
1.12
1.10
1.08
1.06
1.04
1.02
MILS INSERTION
0 20 40 60 80 100 120 140 160 180 200 220 240 260 280 300 320 340 360
10-62
MRL-12748

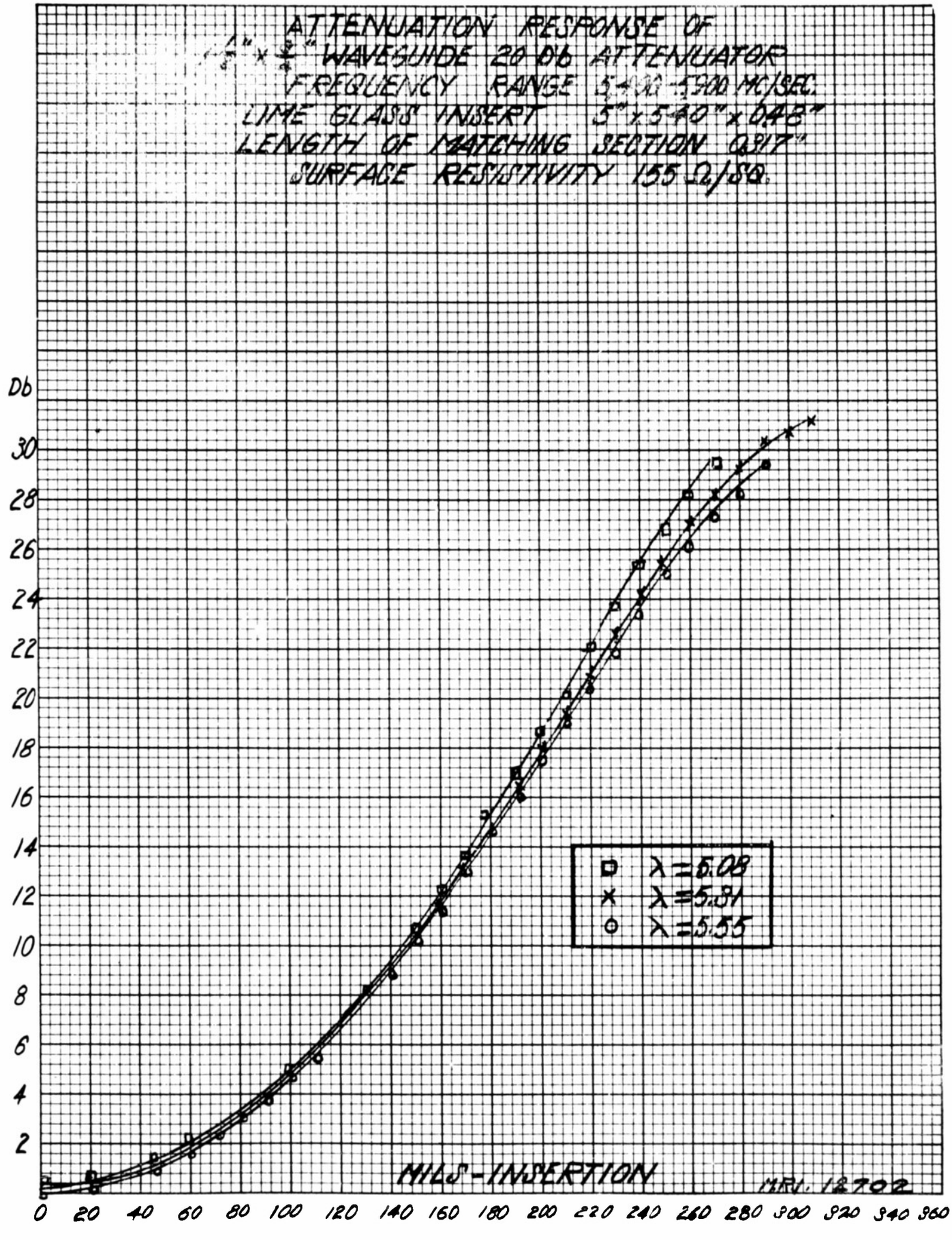
ATTENUATION RESPONSE OF
WAVEGUIDE 20 DB ATTENUATOR
FREQUENCY RANGE 5400-5900 MC/SEC.
LIME GLASS INSERT 5" x 5.40" x 0.46"
LENGTH OF MATCHING SECTION 0.81"
SURFACE RESISTIVITY 155 Ω/SQ.
Db
30
28
26
24
22
20
18
16
14
12
10
8
6
4
2
λ = 6.08
λ = 5.81
λ = 5.55
MILS-INSERTION
MRV. 12702
0 20 40 60 80 100 120 140 160 180 200 220 240 260 280 300 320 340 360

V.S.W.R. RESPONSE OF 1½" × ¾" WAVEGUIDE 20 DB ATTENUATOR

FREQUENCY RANGE 5,400-5,900 MC/SEC.
LIME GLASS INSERT 5" x .540" x .048"
LENGTH OF MATCHING SECTION 0.317"
SURFACE RESISTIVITY 155 Ω/SQ.

□ = λ 5.08
× = λ 6.31
○ = λ 5.55

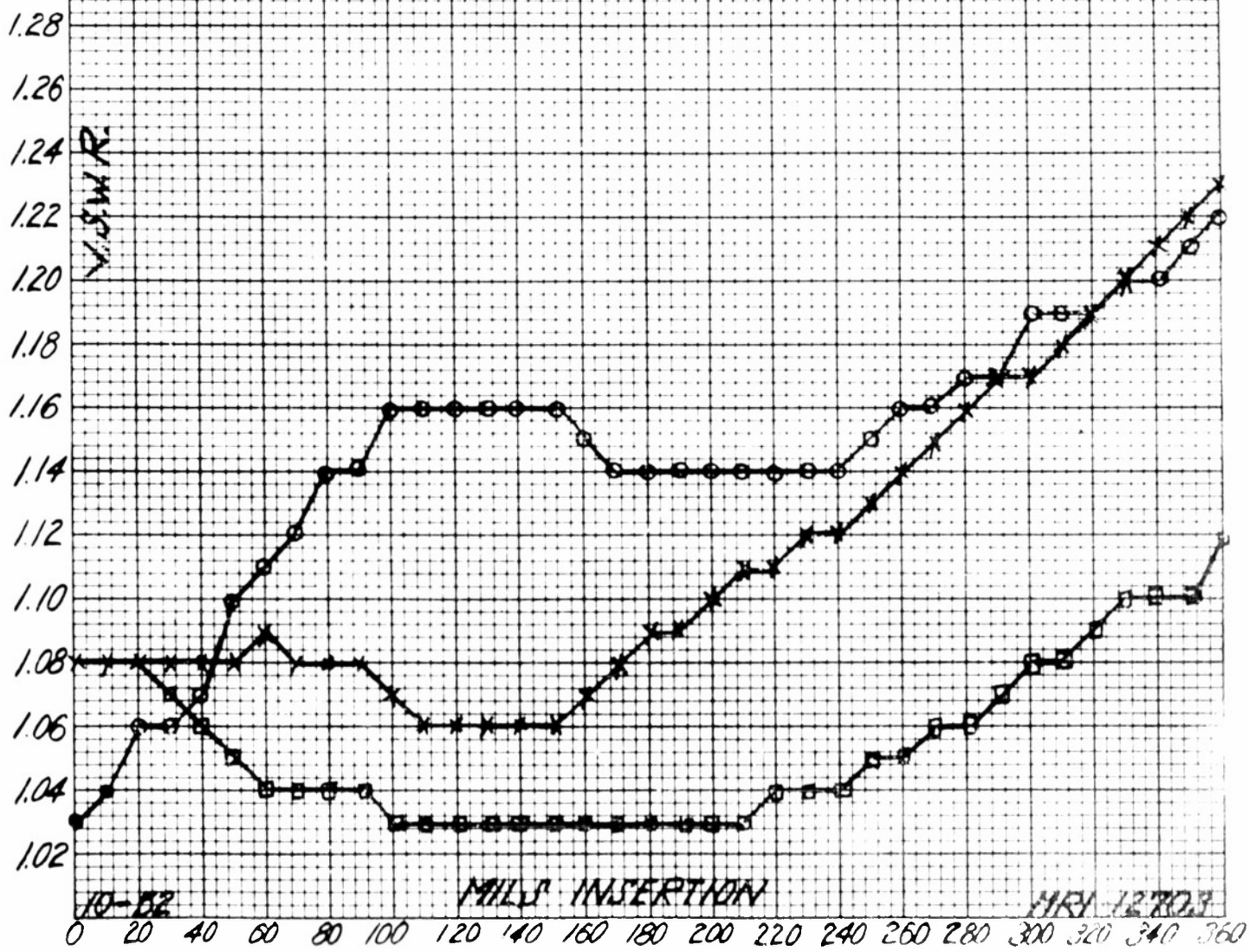

10-52

MRY 12703

SPECIFICATIONS OF 20 DB METALLIZED—GLASS PLATE DESIGNED FOR $1\frac{1}{2}$" x $\frac{3}{4}$" x 0.064" WAVEGUIDE

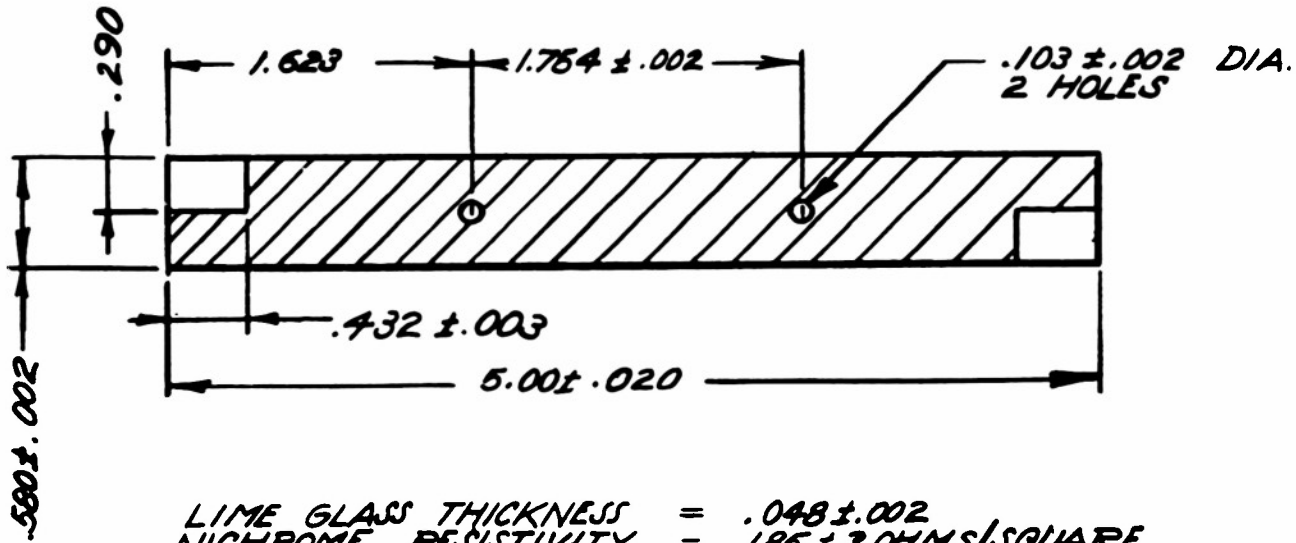

LIME GLASS THICKNESS = .048 ± .002
NICHROME RESISTIVITY = 185 ± 3 OHMS/SQUARE

NOTE:
TO BE USED WITH WAVEGUIDE TUBING RG-50/U WITH NARROW DIMENSION .622 ± .004 AND LENGTH 6 INCHES.

MRI. 12729

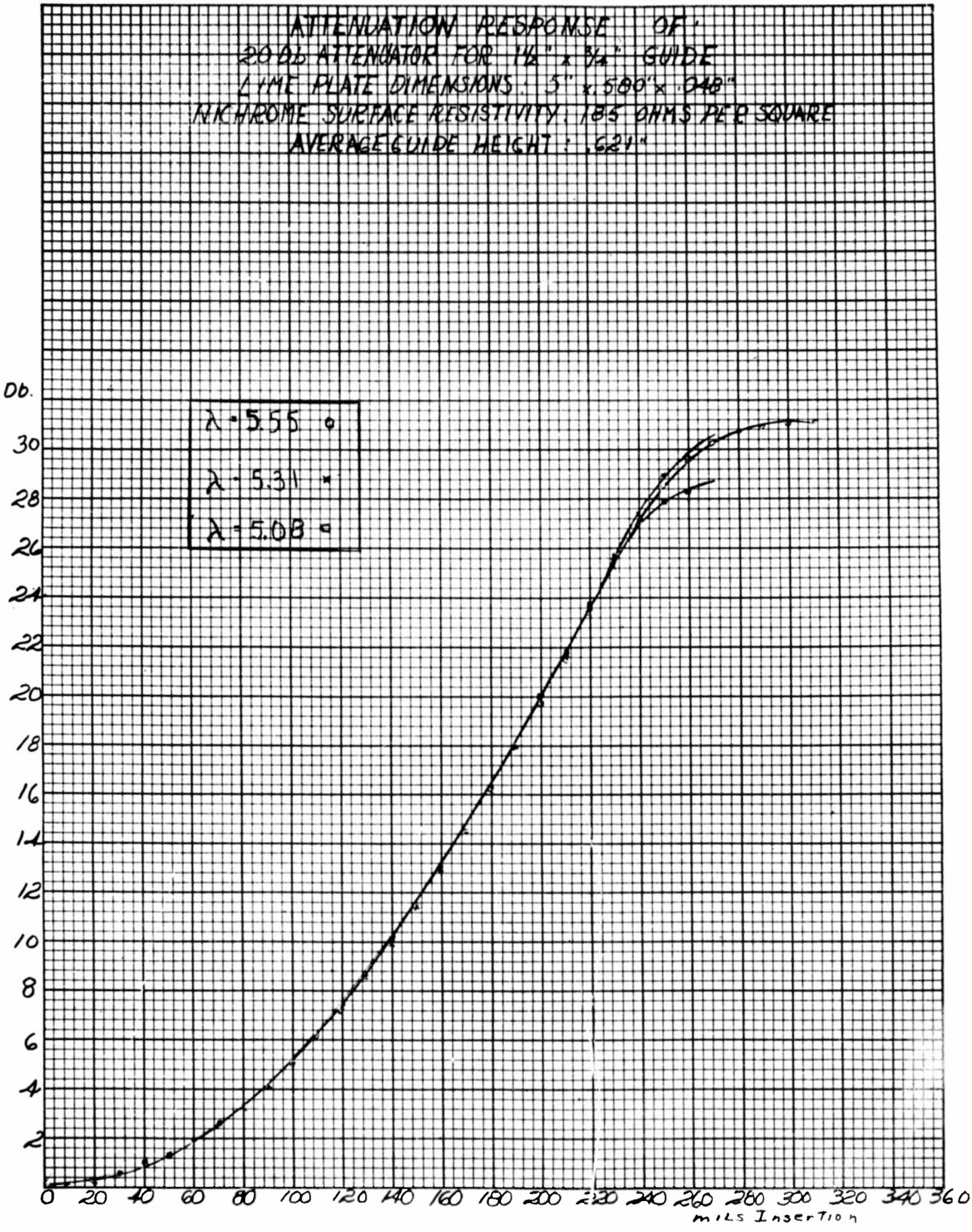
ATTENUATION RESPONSE OF
20 DB ATTENUATOR FOR 1/2" x 1/4" GUIDE
LUCITE PLATE DIMENSIONS: 5" x .580" x .248"
NICHROME SURFACE RESISTIVITY: 185 OHMS PER SQUARE
AVERAGE GUIDE HEIGHT: .621"
λ = 5.55 o
λ = 5.31 x
λ = 5.08 □
Db.
30
28
26
24
22
20
18
16
14
12
10
8
6
4
2
0 20 40 60 80 100 120 140 160 180 200 220 240 260 280 300 320 340 360
MILS Insertion

MRI-12730

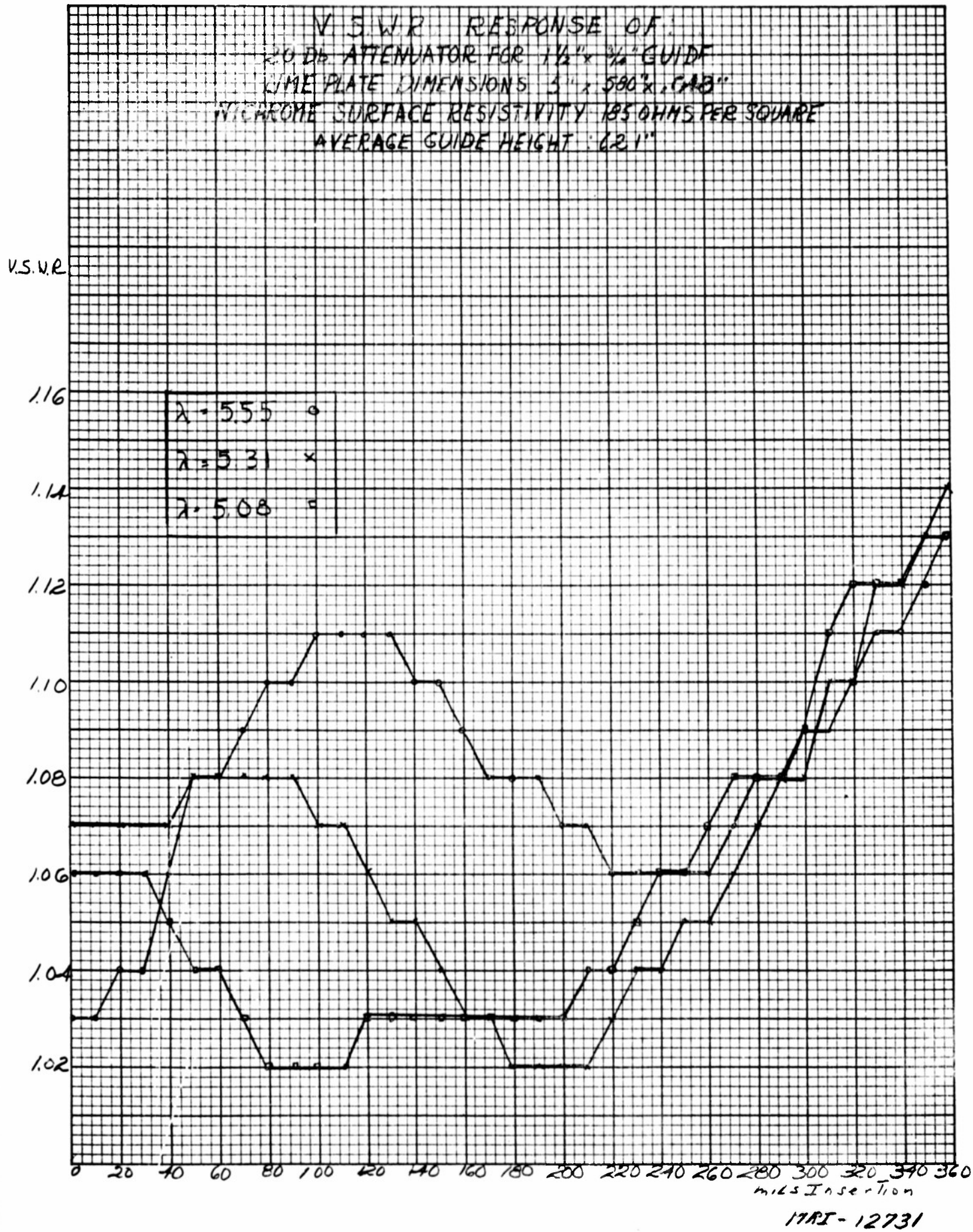
V.S.W.R RESPONSE OF
20 DB ATTENUATOR FOR 1½" x ¾" GUIDE
LIME PLATE DIMENSIONS 3" x .590" x .040"
NICHROME SURFACE RESISTIVITY 185 OHMS PER SQUARE
AVERAGE GUIDE HEIGHT .621"
V.S.W.R
λ = 5.55 o
λ = 5.31 x
λ = 5.08 □
1.16
1.14
1.12
1.10
1.08
1.06
1.04
1.02
0 20 40 60 80 100 120 140 160 180 200 220 240 260 280 300 320 340 360
mils Insertion

ITRI - 12731

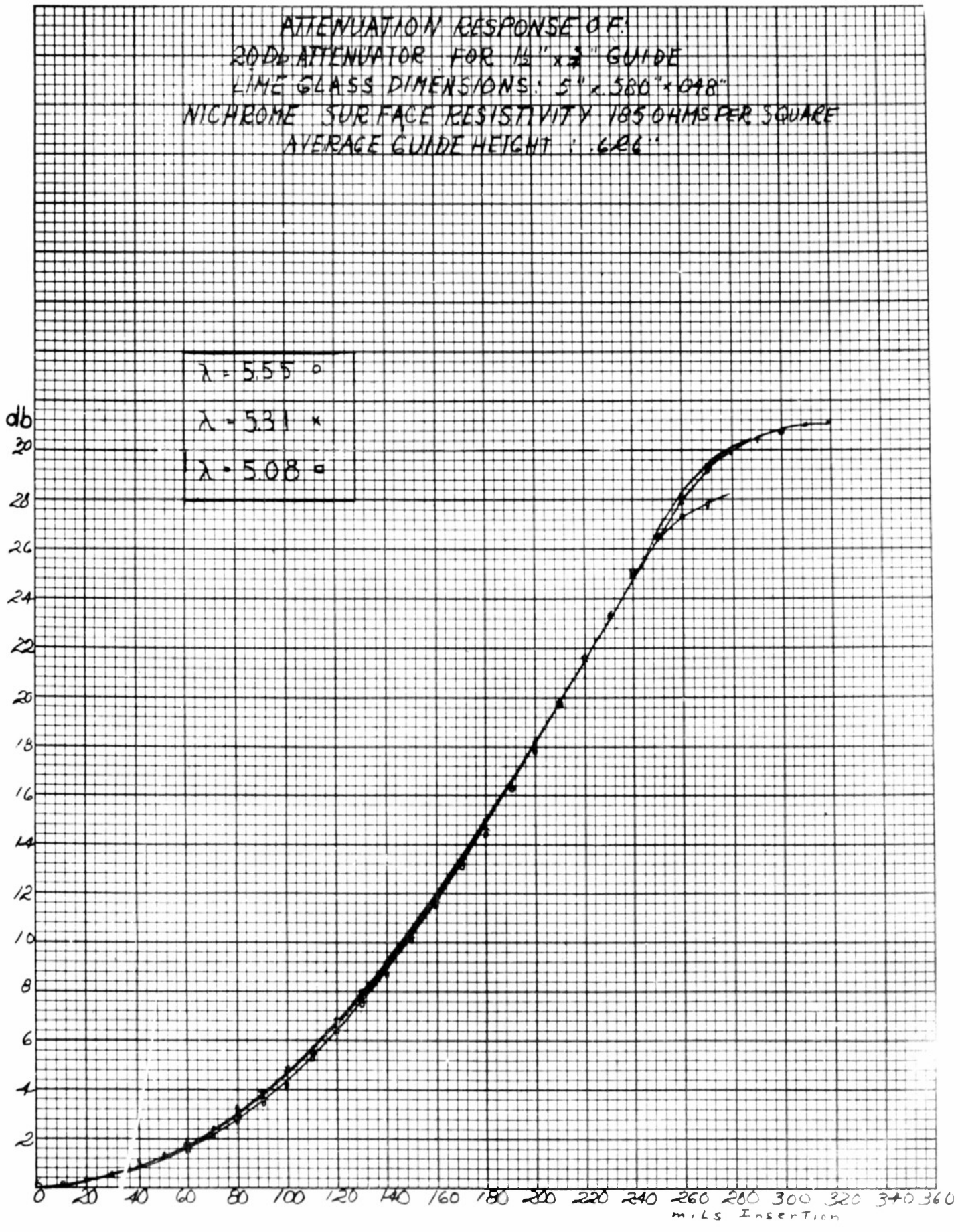
ATTENUATION RESPONSE OF
20 Db ATTENUATOR FOR 1½" x ½" GUIDE
LINE GLASS DIMENSIONS: 5" x .580" x .048"
NICHROME SURFACE RESISTIVITY 185 OHMS PER SQUARE
AVERAGE GUIDE HEIGHT: .626"
λ = 5.55 ○
λ = 5.31 ×
λ = 5.08 □
db
30
28
26
24
22
20
18
16
14
12
10
8
6
4
2
0
20
40
60
80
100
120
140
160
180
200
220
240
260
280
300
320
340
360
mils Insertion

MRT-12732

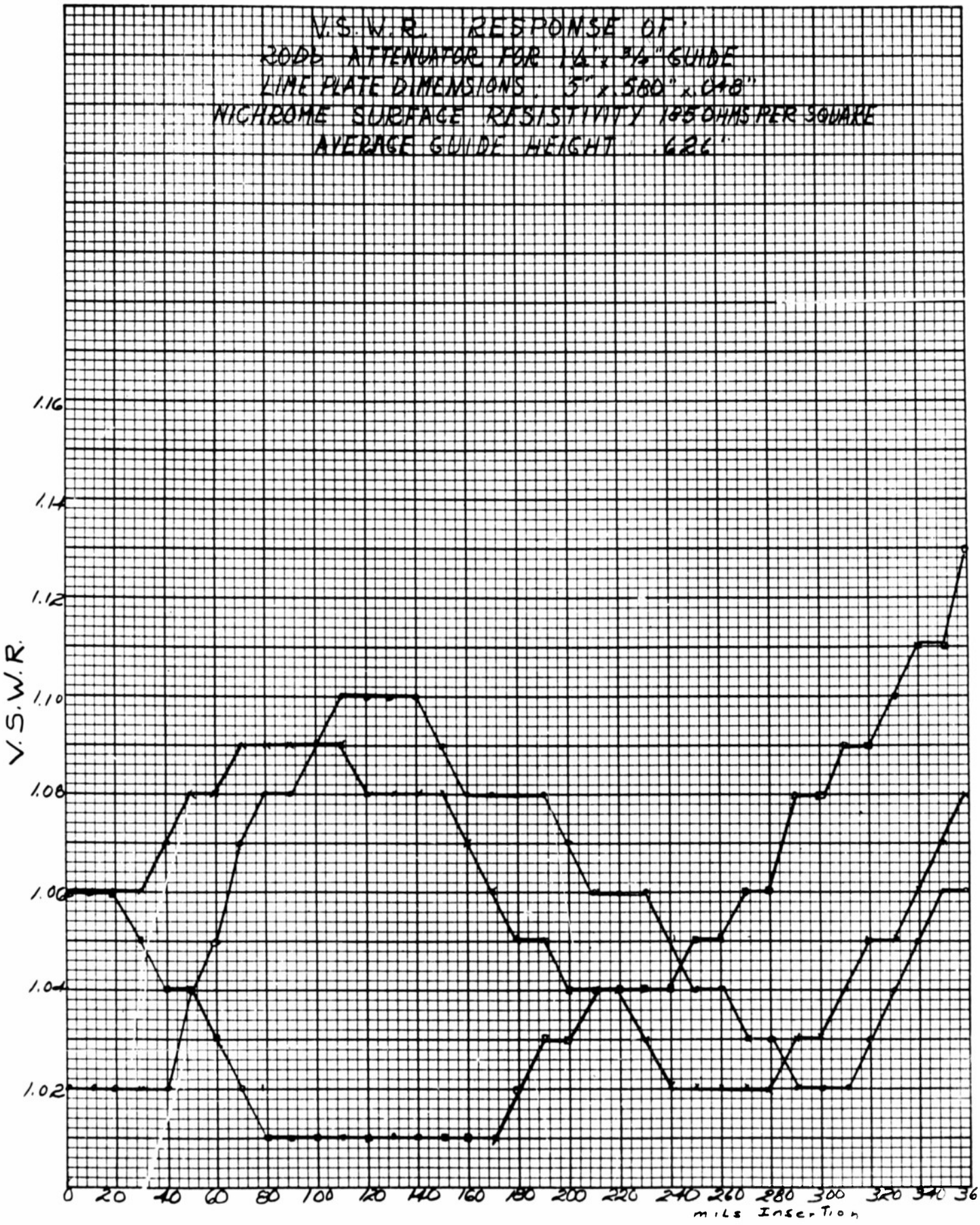
V.S.W.R. RESPONSE OF
20Db ATTENUATOR FOR 1/4" x 3/4" GUIDE
LINE PLATE DIMENSIONS: 3" x .580" x .048"
NICHROME SURFACE RESISTIVITY 185 OHMS PER SQUARE
AVERAGE GUIDE HEIGHT .626"
V.S.W.R.
1.16
1.14
1.12
1.10
1.08
1.06
1.04
1.02
0 20 40 60 80 100 120 140 160 180 200 220 240 260 280 300 320 340 360
mils Insertion

MRI-12733

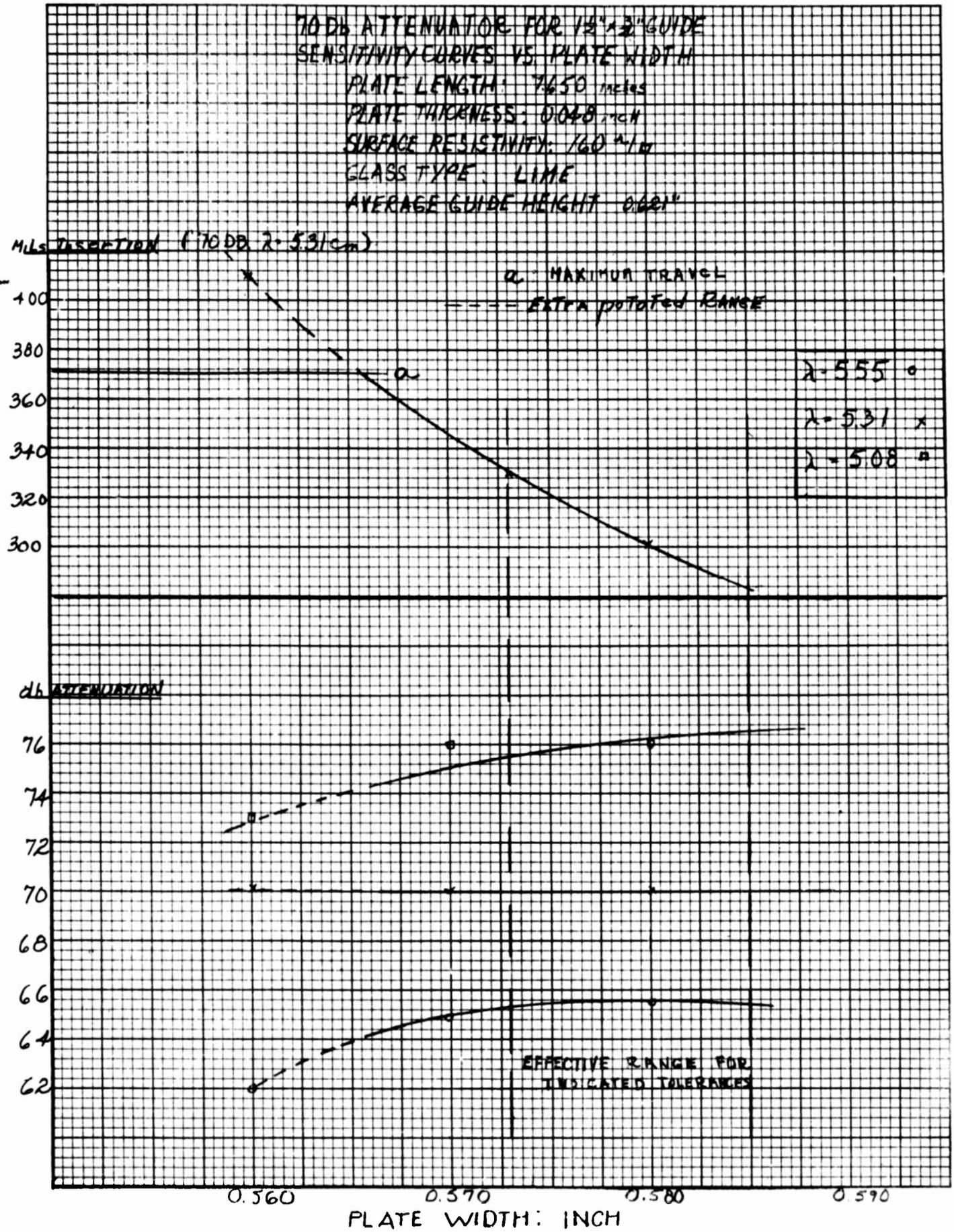
70 Db ATTENUATOR FOR 1/2" x 3" GUIDE
SENSITIVITY CURVES VS. PLATE WIDTH
PLATE LENGTH: 7.650 inches
PLATE THICKNESS: 0.048 inch
SURFACE RESISTIVITY: 160 Ω/□
GLASS TYPE: LIME
AVERAGE GUIDE HEIGHT 0.661"
MILS DEFLECTION (70 DB 2.531 cm)
400
380
360
340
320
300
α: MAXIMUM TRAVEL
EXTRA POTTED RANGE
λ-.555 ○
λ-.531 ×
λ-.508 □
db ATTENUATION
76
74
72
70
68
66
64
62
EFFECTIVE RANGE FOR INDICATED TOLERANCES
0.560
0.570
0.580
0.590
PLATE WIDTH: INCH

MR.1 12734

SPECIFICATIONS OF 70 DB METALLIZED-GLASS PLATE DESIGNED FOR $1\frac{1}{2}$" × $\frac{3}{4}$" × 0.064" WAVEGUIDE

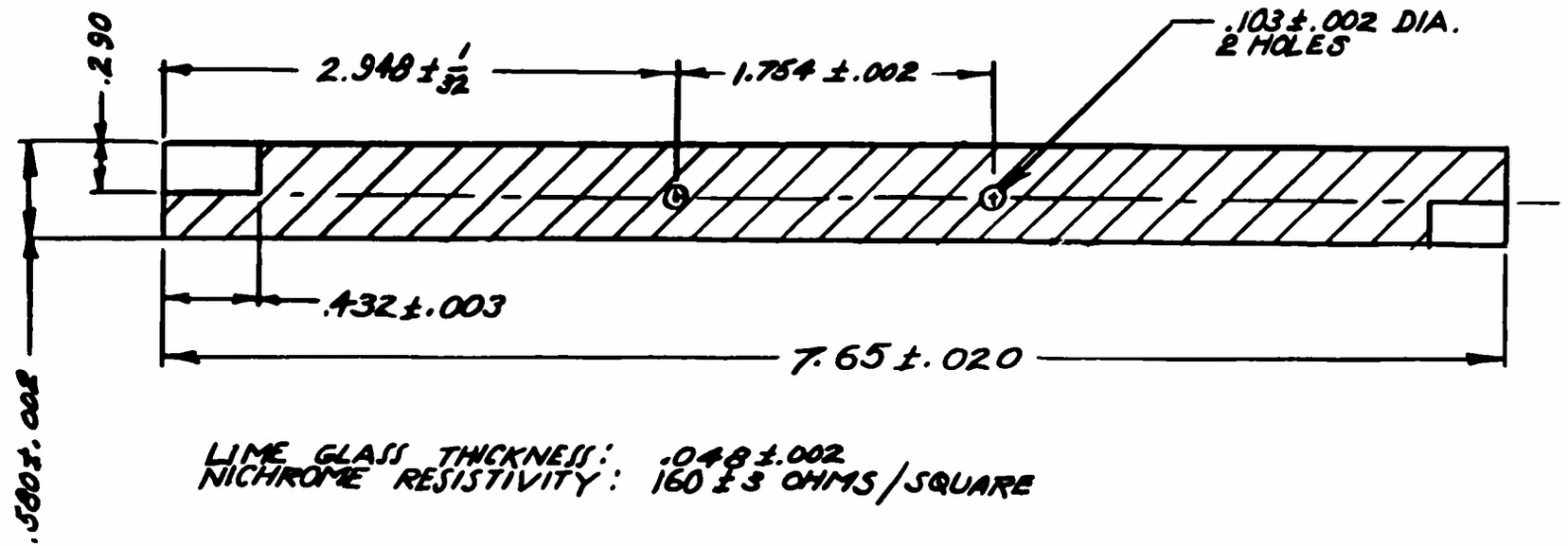

LIME GLASS THICKNESS: .048 ± .002
NICHROME RESISTIVITY: 160 ± 3 OHMS/SQUARE

NOTE:
TO BE USED WITH WAVEGUIDE TUBING RG-50/U WITH NARROW DIMENSION .622 ± .004 AND LENGTH 8.5 INCHES

MRI.-12735

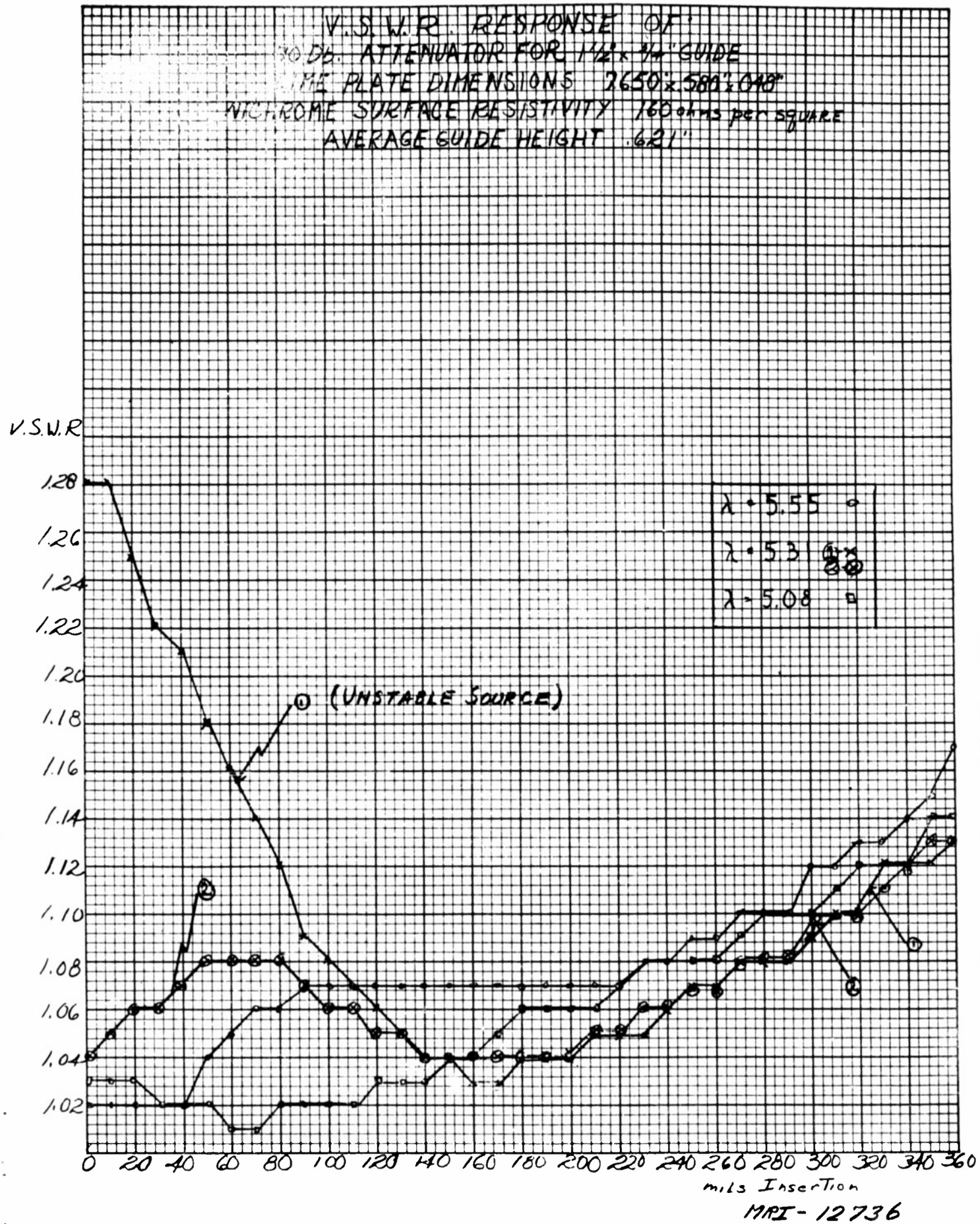
V.S.W.R. RESPONSE OF
10 Db. ATTENUATOR FOR 1½" x ¾" GUIDE
ME PLATE DIMENSIONS .2650" x .580" x .040"
NICHROME SURFACE RESISTIVITY 160 ohms per square
AVERAGE GUIDE HEIGHT .621"
V.S.W.R
1.28
1.26
1.24
1.22
1.20
1.18
1.16
1.14
1.12
1.10
1.08
1.06
1.04
1.02
λ = 5.55
λ = 5.31
λ = 5.08
(UNSTABLE SOURCE)
0 20 40 60 80 100 120 140 160 180 200 220 240 260 280 300 320 340 360
mils Insertion

MRI-12736

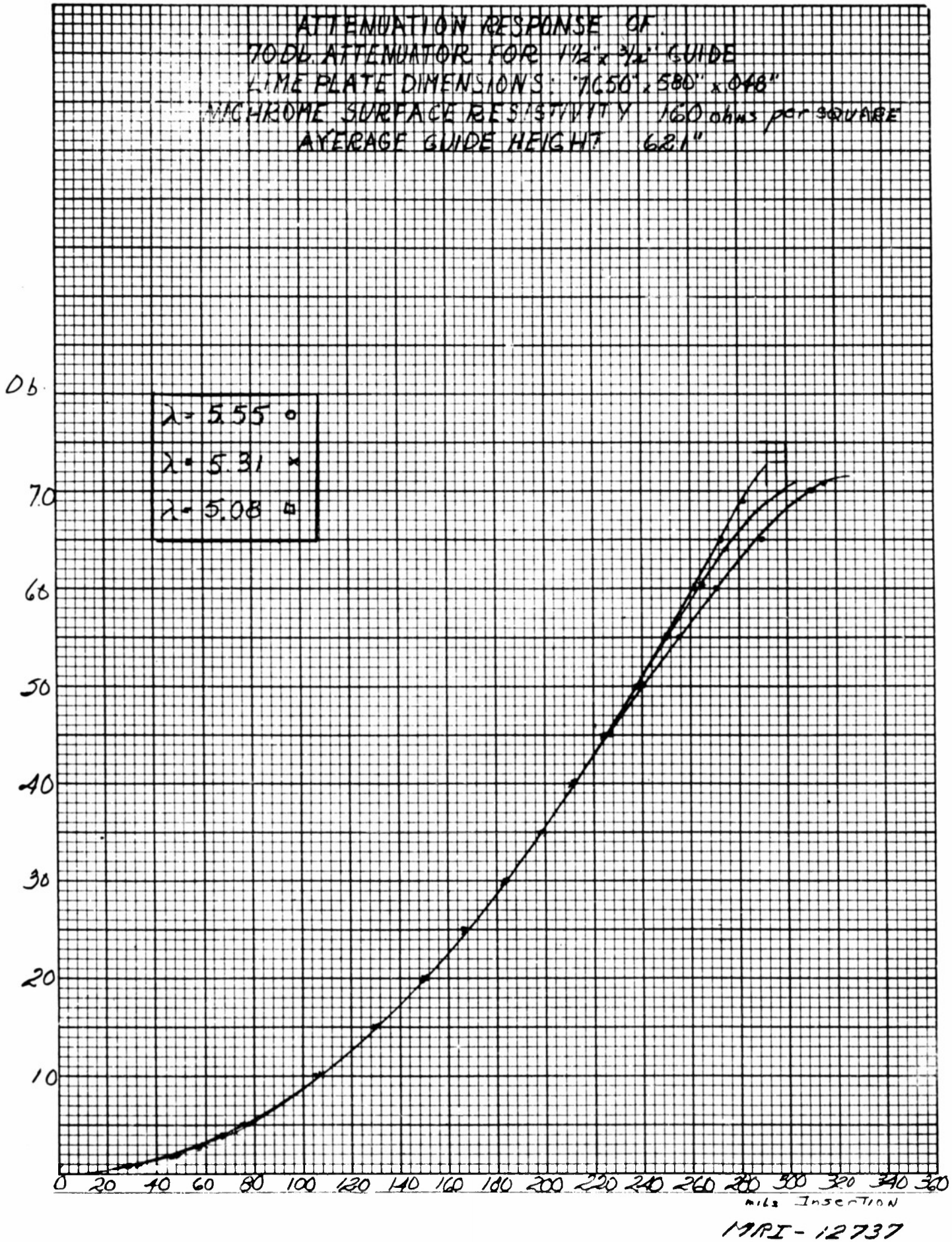
ATTENUATION RESPONSE OF
70 Db ATTENUATOR FOR 1½" x ½" GUIDE
LIME PLATE DIMENSIONS: .7650" x .580" x .048"
NICHROME SURFACE RESISTIVITY 160 ohms per SQUARE
AVERAGE GUIDE HEIGHT .621"
λ = 5.55 o
λ = 5.31 x
λ = 5.08 □
Db
70
60
50
40
30
20
10
0 20 40 60 80 100 120 140 160 180 200 220 240 260 280 300 320 340 360
Mils Insertion

MRI-12737

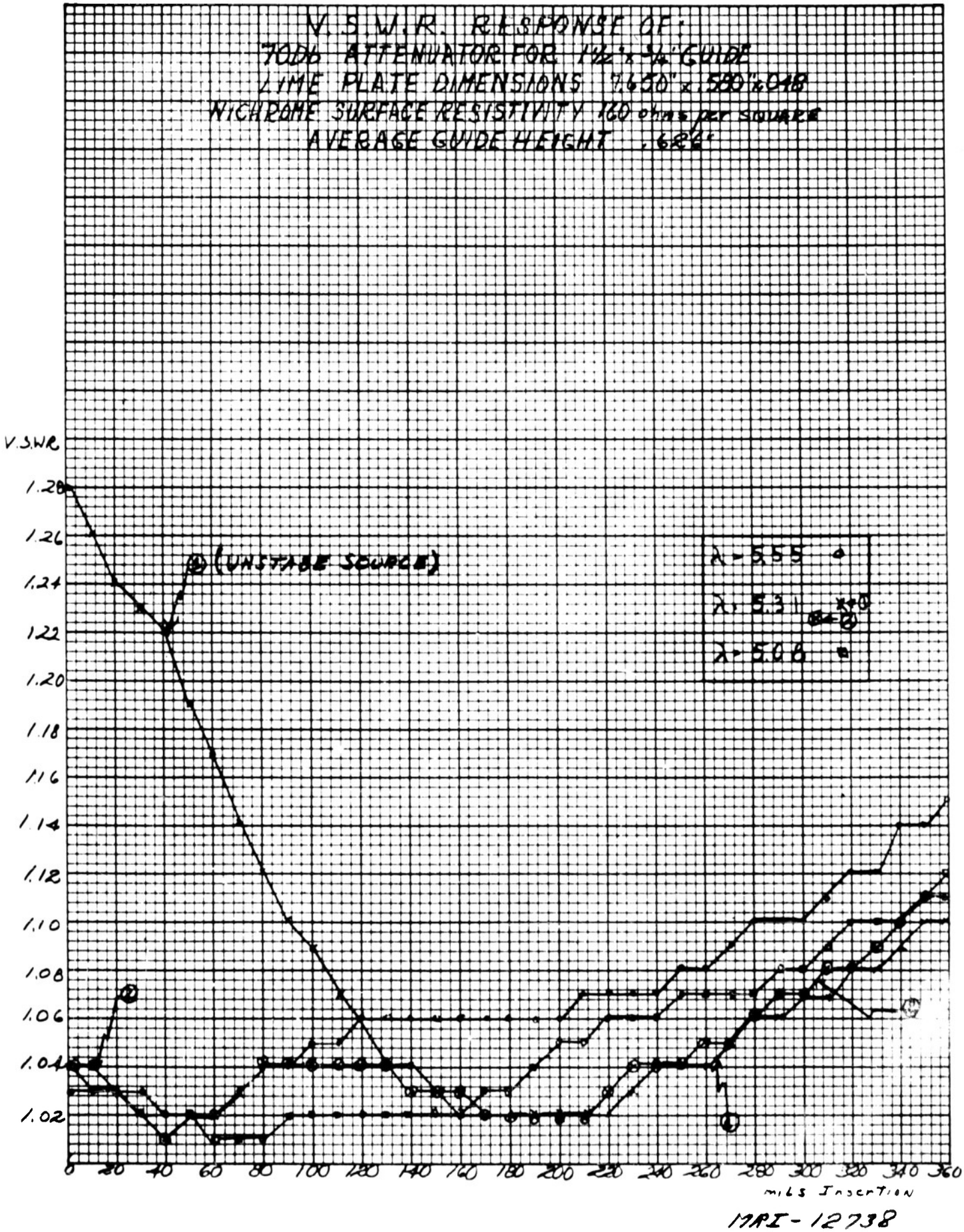

V.S.W.R. RESPONSE OF:
70db ATTENUATOR FOR 1¼" x ¼" GUIDE
LUCITE PLATE DIMENSIONS 7.630" x 580" x .048
NICHROME SURFACE RESISTIVITY 120 ohms per square
AVERAGE GUIDE HEIGHT .166"

MRI-12738

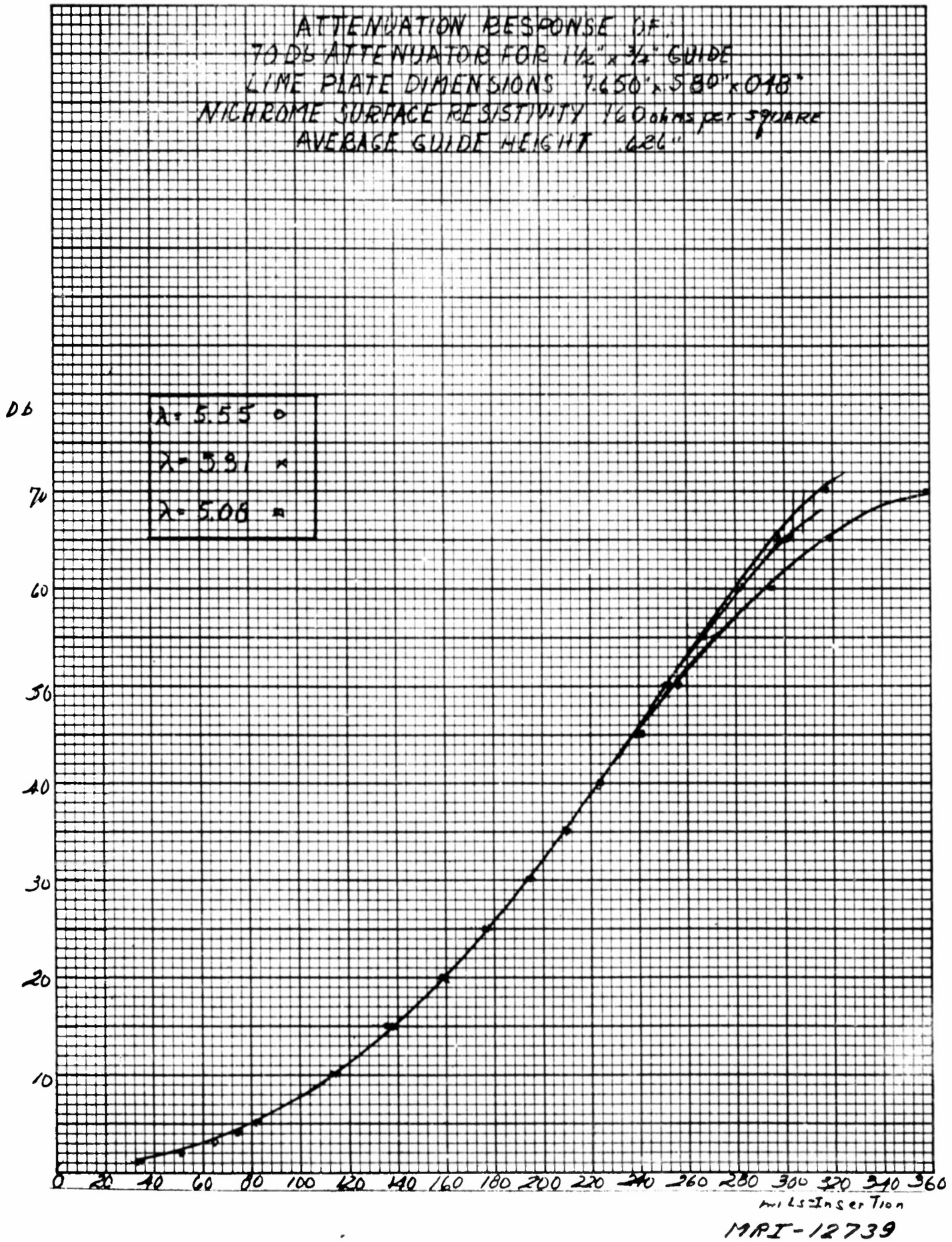
ATTENUATION RESPONSE OF
70 DB ATTENUATOR FOR 1½" x ¾" GUIDE
LIME PLATE DIMENSIONS 7.650" x .580" x .018"
NICHROME SURFACE RESISTIVITY 160 ohms per square
AVERAGE GUIDE HEIGHT .626"
λ = 5.55 o
λ = 5.31 x
λ = 5.08 *
DB
70
60
50
40
30
20
10
0 20 40 60 80 100 120 140 160 180 200 220 240 260 280 300 320 340 360
MILS INSERTION

MRI-12739

MATCHING NETWORKS

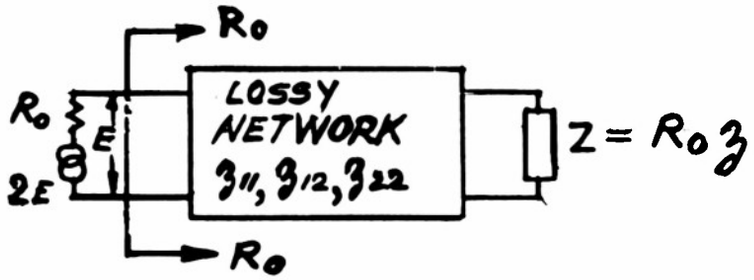

$Z_{11} = R_0 z_{11}$

$Z_{12} = R_0 z_{12}$

$Z_{22} = R_0 z_{22}$

(a) GENERAL MATCHING NETWORK

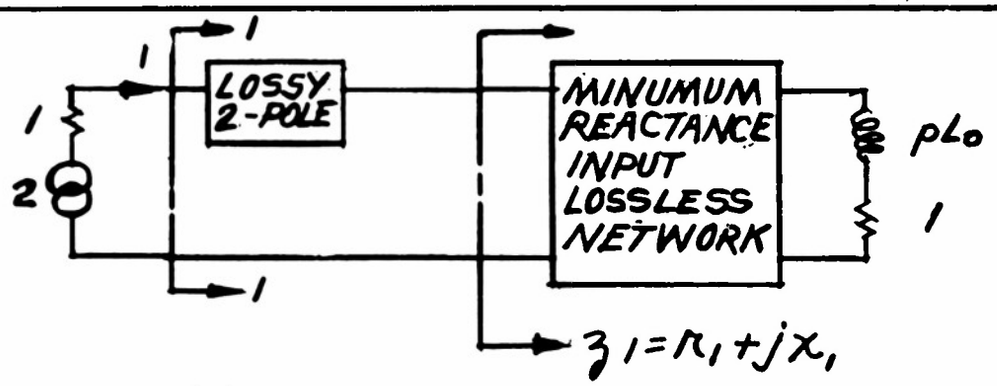

(b) SPECIAL MATCHING STRUCTURE

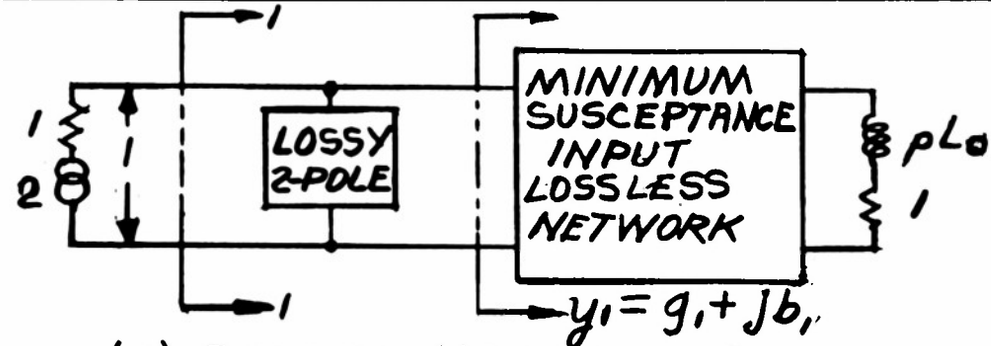

(c) SPECIAL MATCHING STRUCTURE

M.R.I. 1968

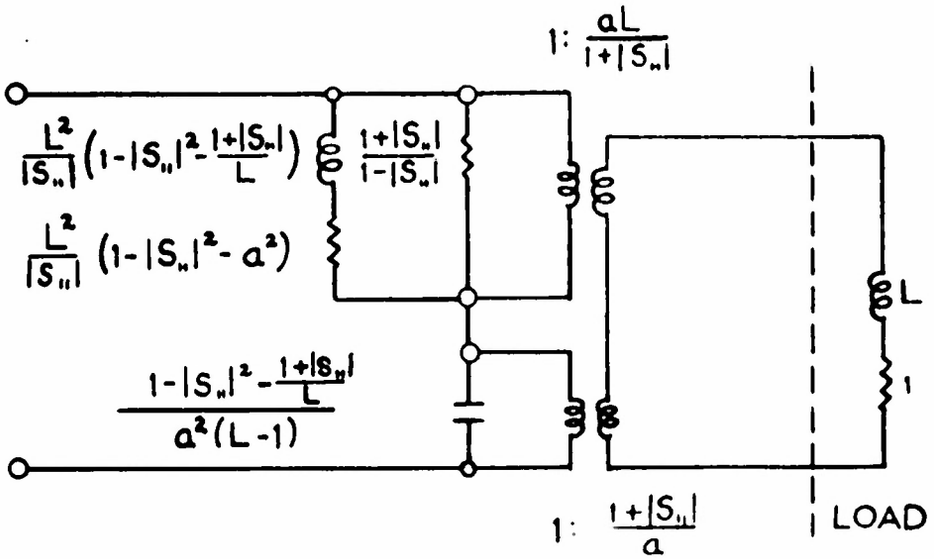

a. MATCHING NETWORK FOR SIMPLE LOAD

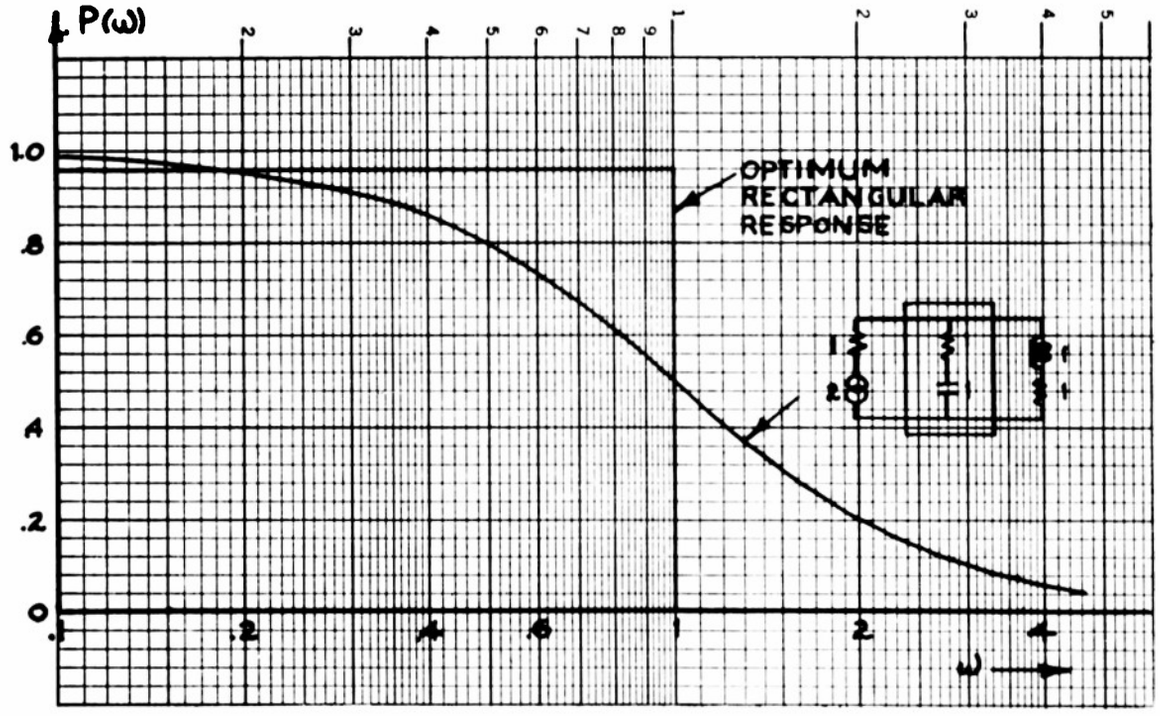

b. PERFORMANCE OF SIMPLE MATCHING NETWORK COMPARED TO BEST POSSIBLE LOW-PASS RESPONSE

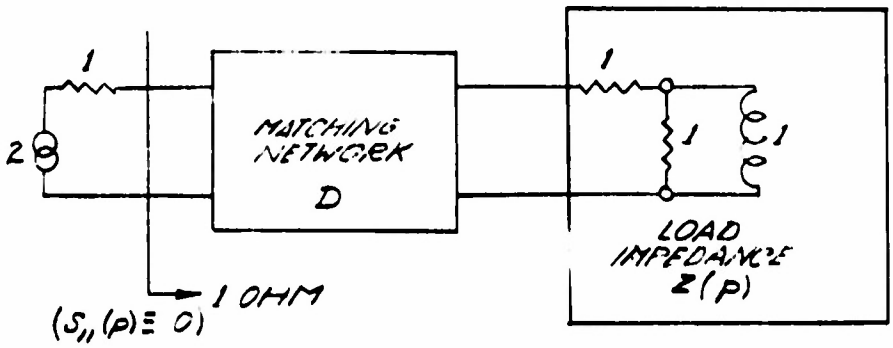

a.

MATCHING NETWORK AND SIMPLE LOAD

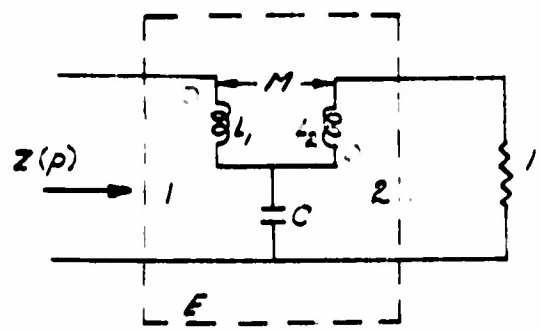

$$L_1 = \frac{2\sqrt{2}}{\sqrt{2}+1}$$

$$L_2 = \frac{\sqrt{2}}{\sqrt{2}+1}$$

$$M = \frac{2}{\sqrt{2}+1}$$

$$C = \sqrt{2}+1$$

$$Z(p) = \frac{2p+1}{p+1}$$

b.

DARLINGTON REPRESENTATION OF Z(p)

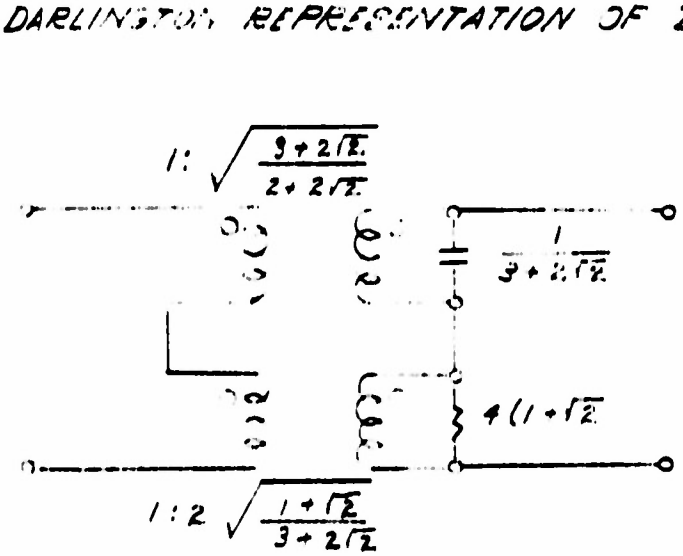

c.

MATCHING NETWORK

SIMPLE LOAD AND MATCHING NETWORK

COMPARISON METHOD OF MEASURING PHASE-SHIFTS

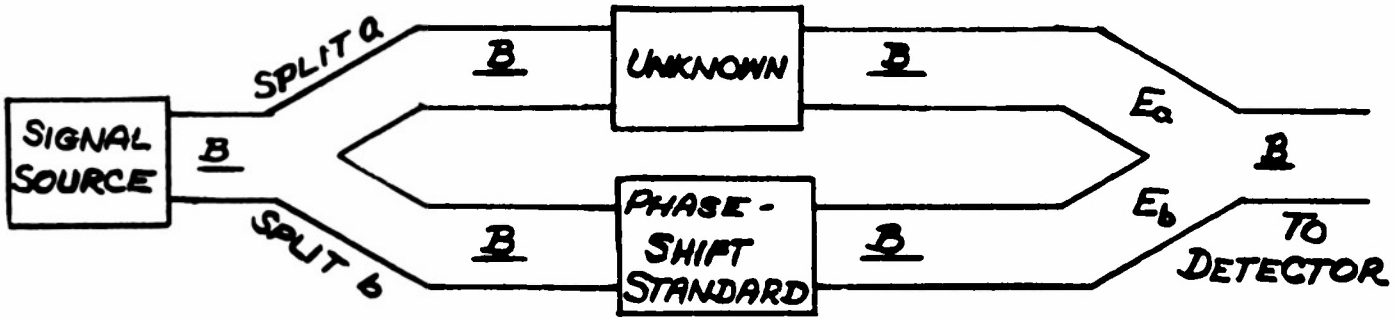

B = MATCHED BUFFER MEASURING ABOUT 15 db.

A

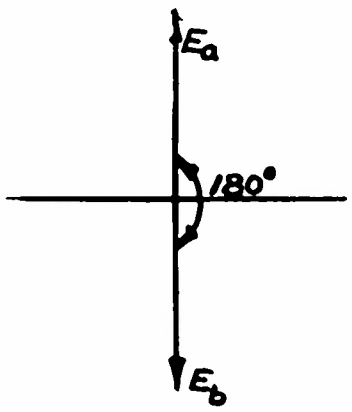

B

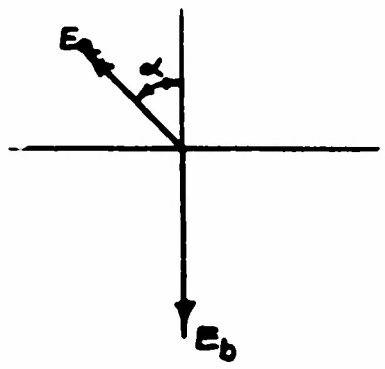

C

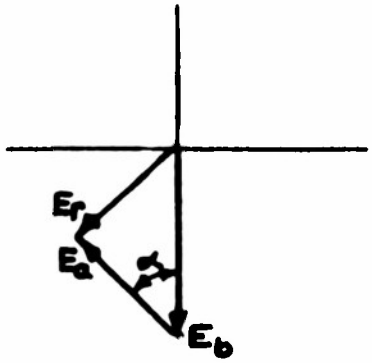

D

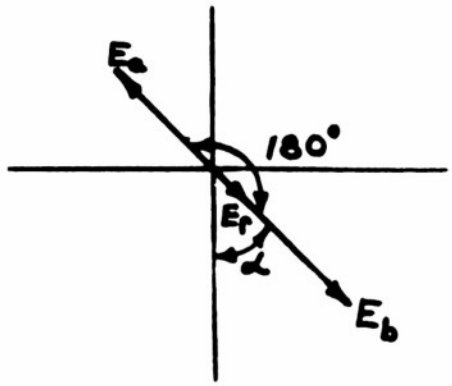

E

M.R.I. 11422

FINAL LINE SET-UP FOR MEASURING PHASE-SHIFTS BY THE COMPARISON METHOD

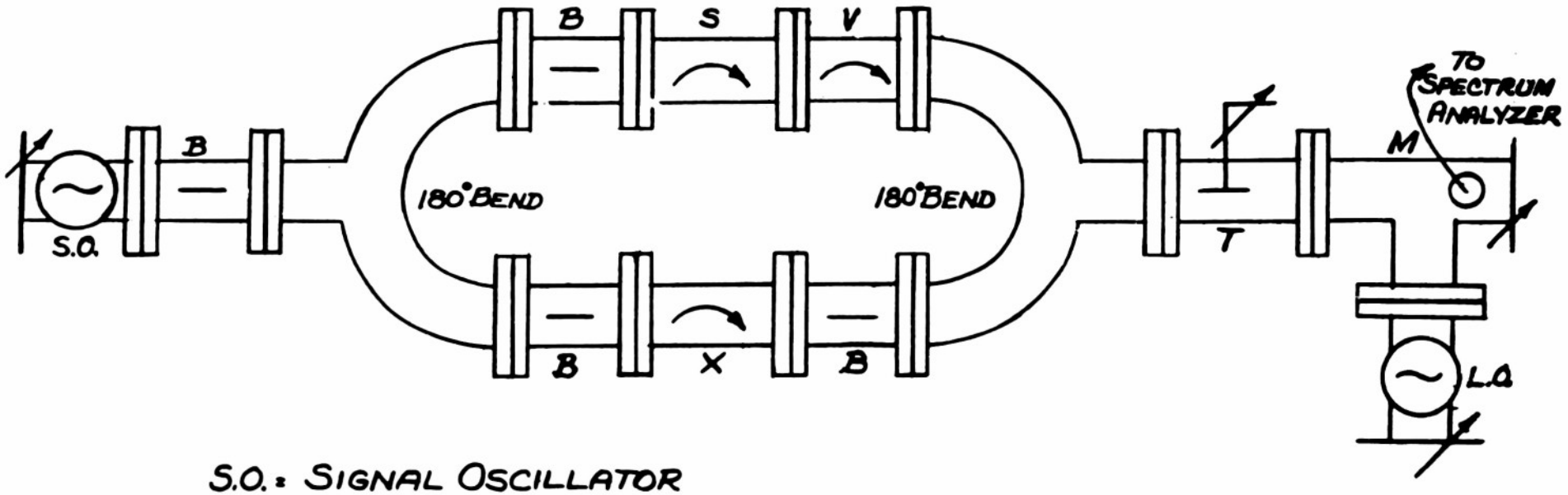

S.O. = SIGNAL OSCILLATOR
L.O. = LOCAL OSCILLATOR
B = FIXED BUFFER
V = VARIABLE BUFFER
S = PHASE-SHIFT STANDARD
X = ATTENUATOR UNDER TEST
T = WAVEGUIDE TUNER
M = CRYSTAL MIXER

M.R.I. 11423

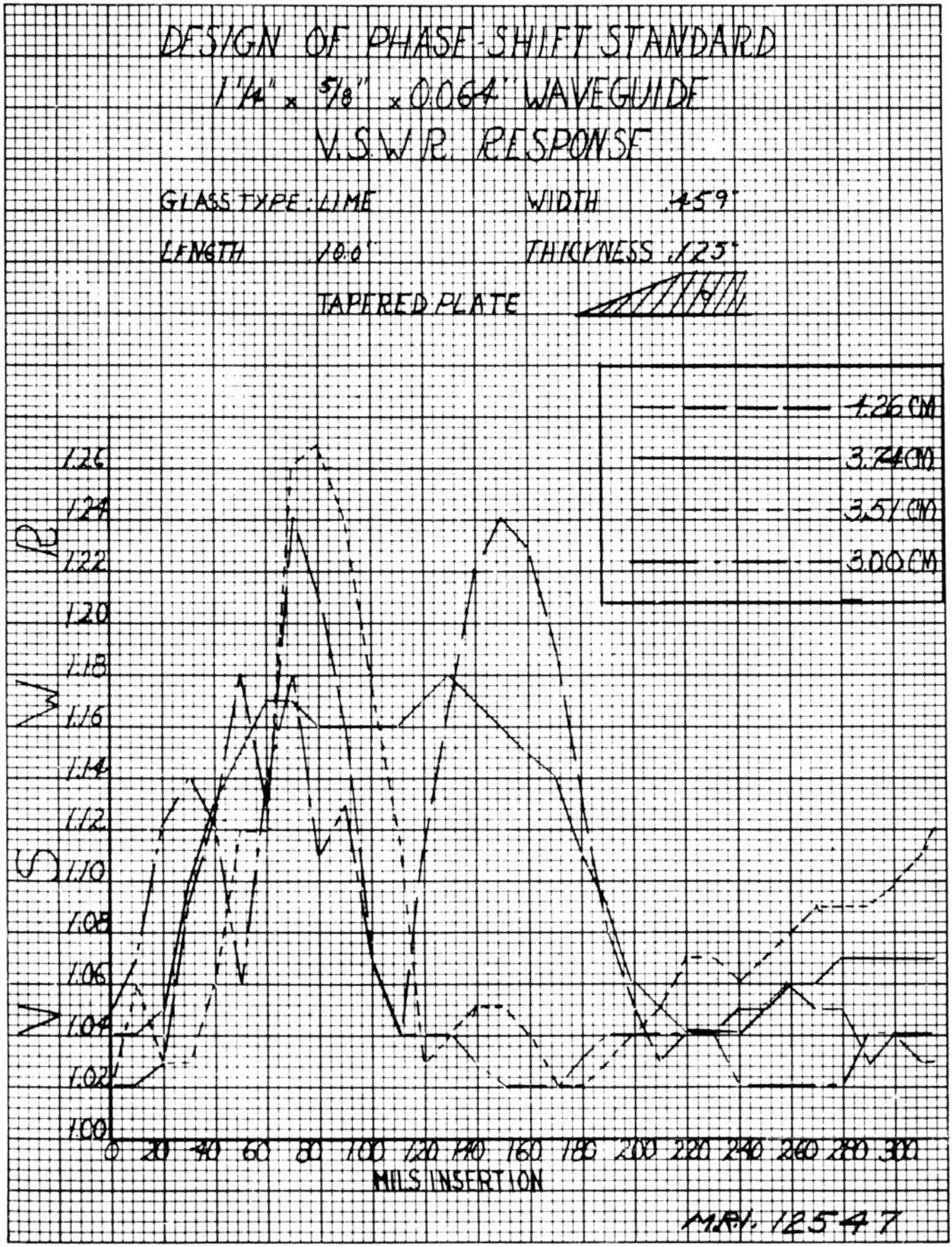
DESIGN OF PHASE-SHIFT STANDARD
1"¼" x 5/8" x 0.064" WAVEGUIDE
V.S.W.R. RESPONSE
GLASS TYPE: LIME
WIDTH .459"
LENGTH 10.6"
THICKNESS .125"
TAPERED PLATE
1.26 CM
3.74 CM
3.51 CM
3.00 CM
VSWR
1.26
1.24
1.22
1.20
1.18
1.16
1.14
1.12
1.10
1.08
1.06
1.04
1.02
1.00
0 20 40 60 80 100 120 140 160 180 200 220 240 260 280 300
MILS INSERTION
MV. 12547

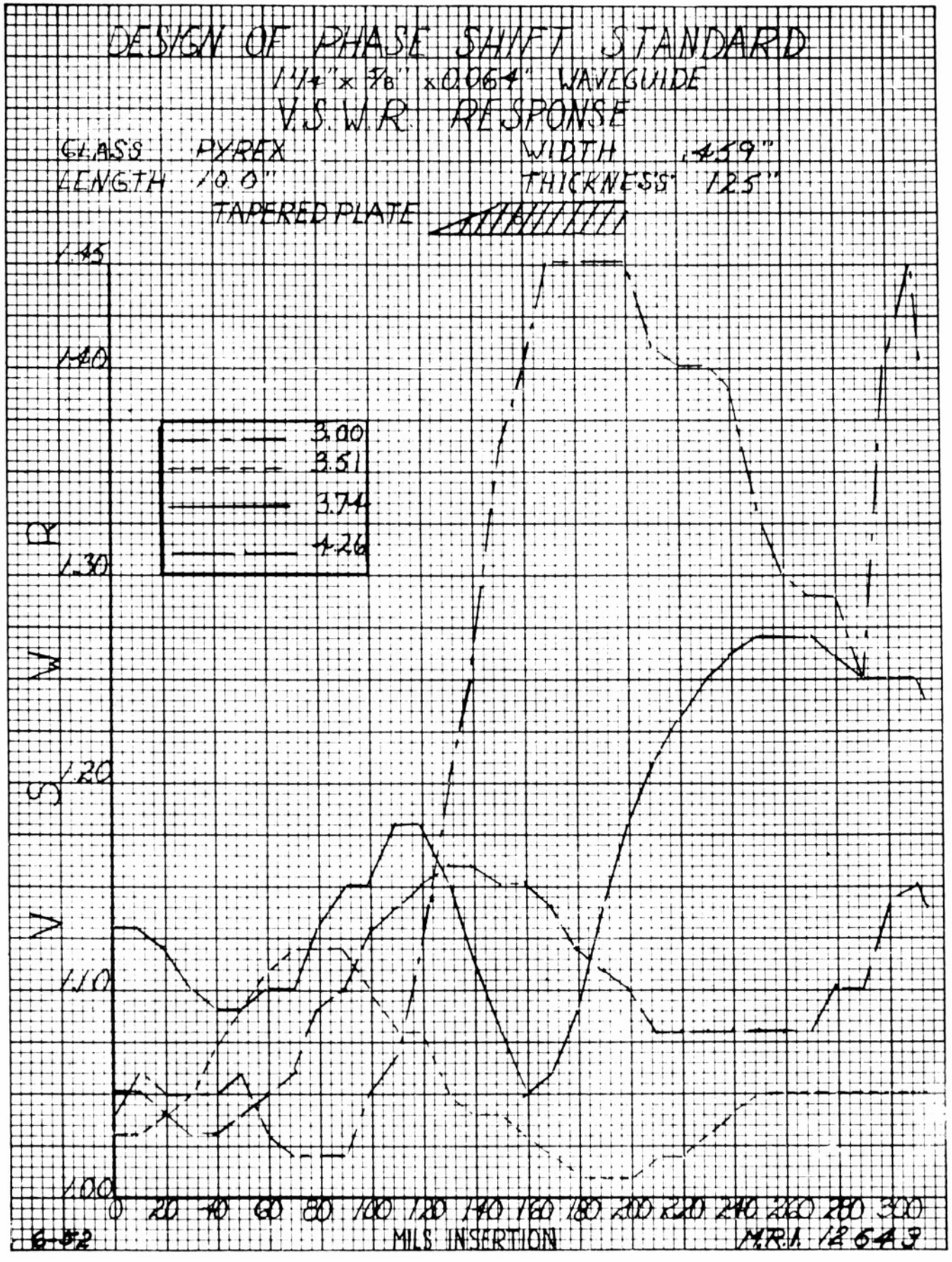
DESIGN OF PHASE SHIFT STANDARD
1 1/4" x 7/8" x 0.064" WAVEGUIDE
V.S.W.R. RESPONSE
GLASS PYREX
LENGTH 10.0"
WIDTH .459"
THICKNESS .125"
TAPERED PLATE
3.00
3.51
3.74
4.26
V.S.W.R.
1.45
1.40
1.30
1.20
1.10
1.00
0 20 40 60 80 100 120 140 160 180 200 220 240 260 280 300
MILS INSERTION
6-52
M.R.I. 12643

DESIGN OF PHASE SHIFT STANDARD

1¼" x ⅝" x .064" WAVEGUIDE

MAXIMUM PHASE SHIFT RESPONSE

GLASS PYREX
LENGTH 10.0"
WIDTH .459"
THICKNESS .125"
TAPERED PLATE

λ	3.00	- 543°
λ	3.51	- 431°
λ	3.74	- 410°
λ	4.26	- 375°

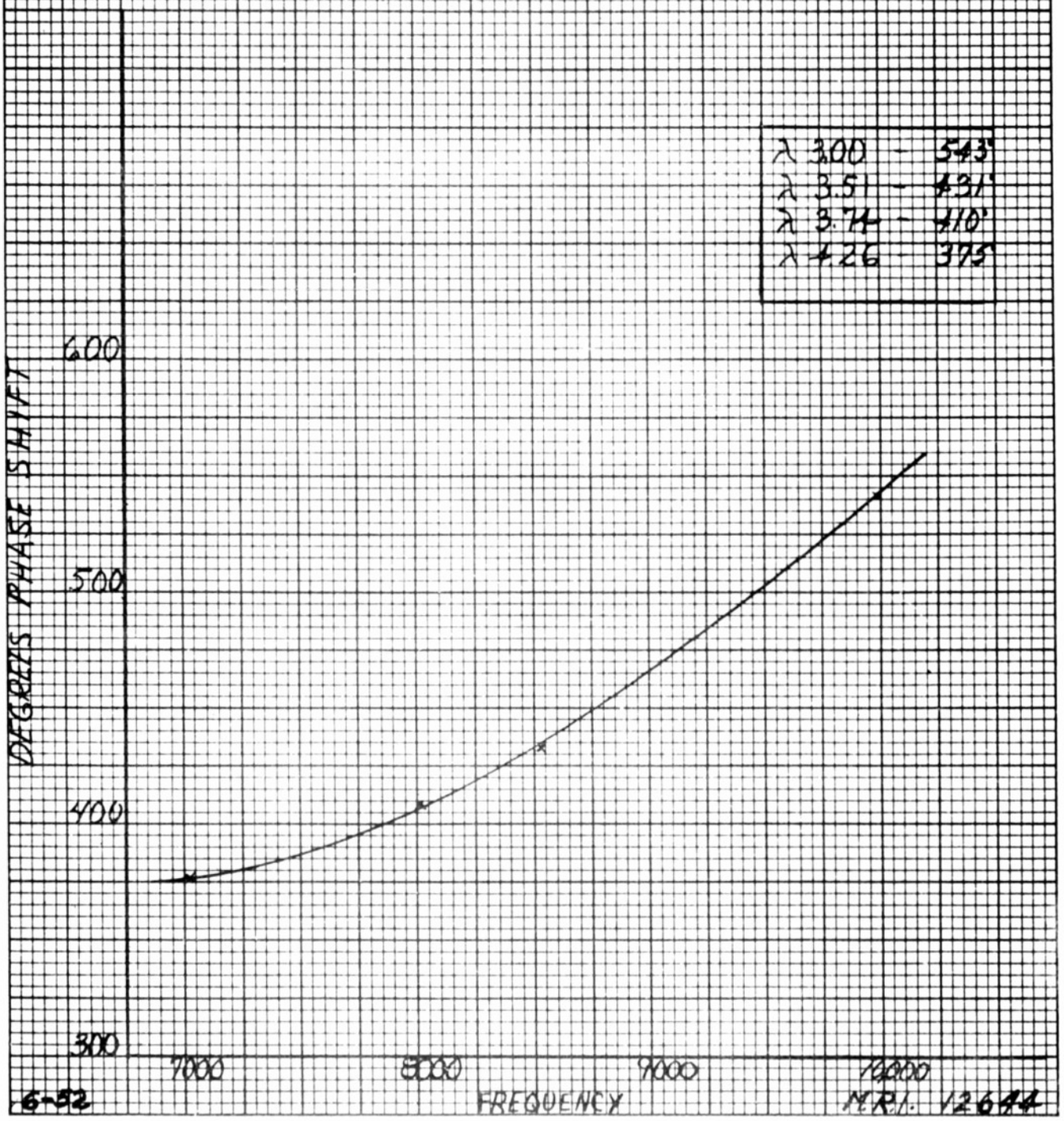

6-52

NRL 12644

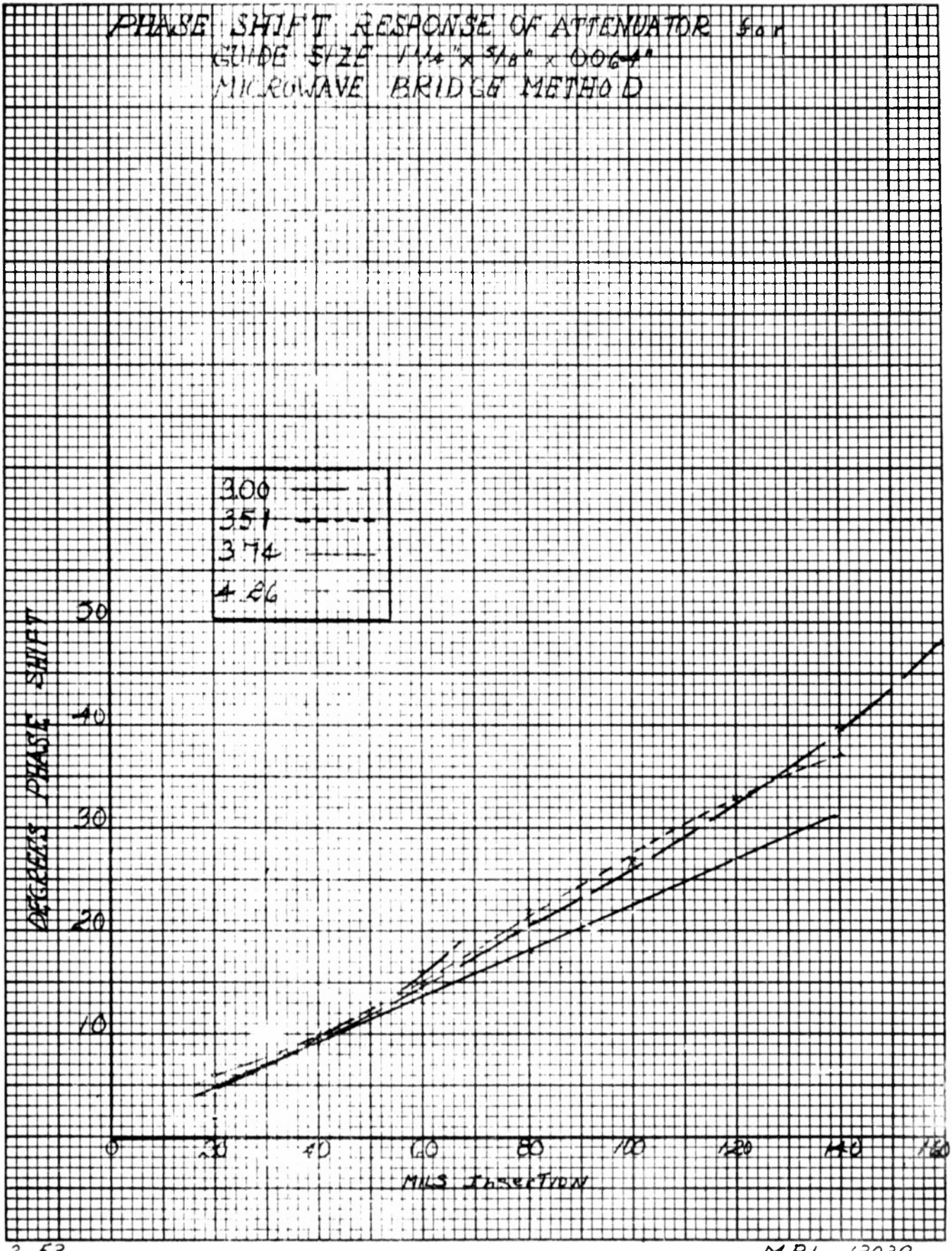
PHASE SHIFT RESPONSE OF ATTENUATOR for
GUIDE SIZE 1.14" x 5/16" x 0064"
MICROWAVE BRIDGE METHOD
3.00
3.51
3.74
4.26
DEGREES PHASE SHIFT
0
10
20
30
40
0
20
40
60
80
100
120
140
160
MILS INSERTION

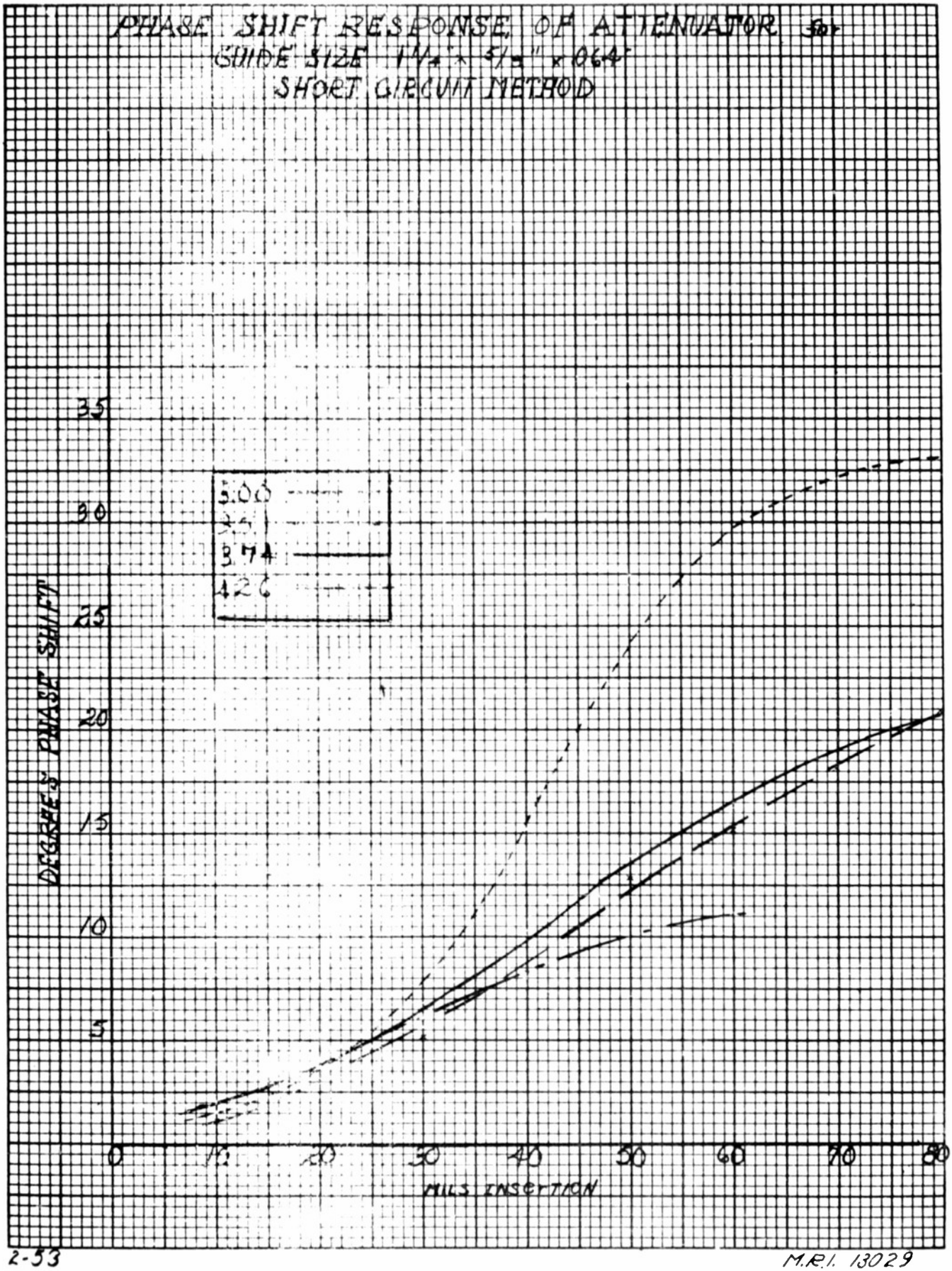

2-53

M.R.I. 13029

ATTENUATION PERFORMANCE OF ATTENUATOR

FOR GUIDE SIZE 1/4" x 5/8" x .064"

NAVY MODEL SERIAL NO. 79

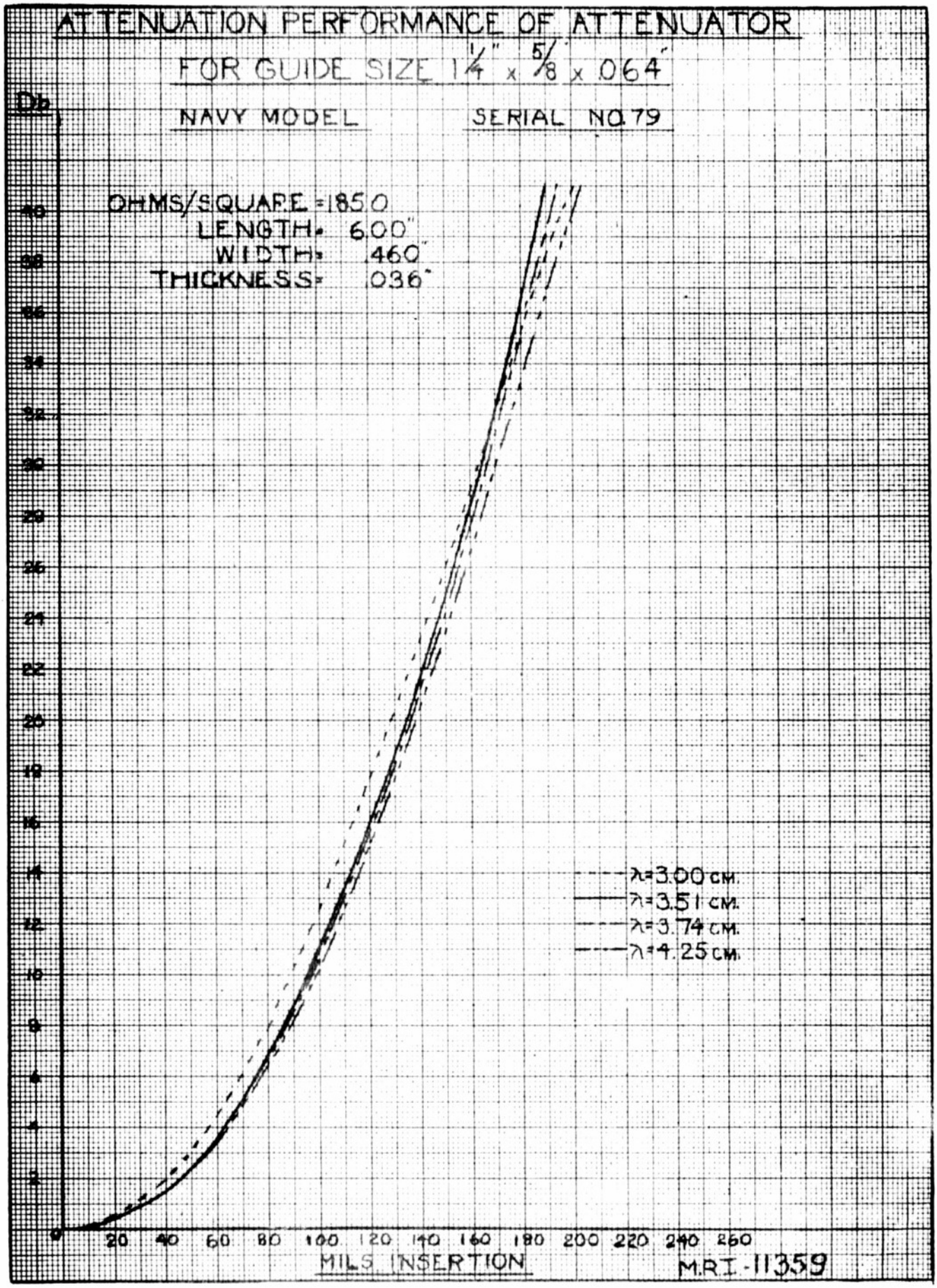

M.R.I.-11359

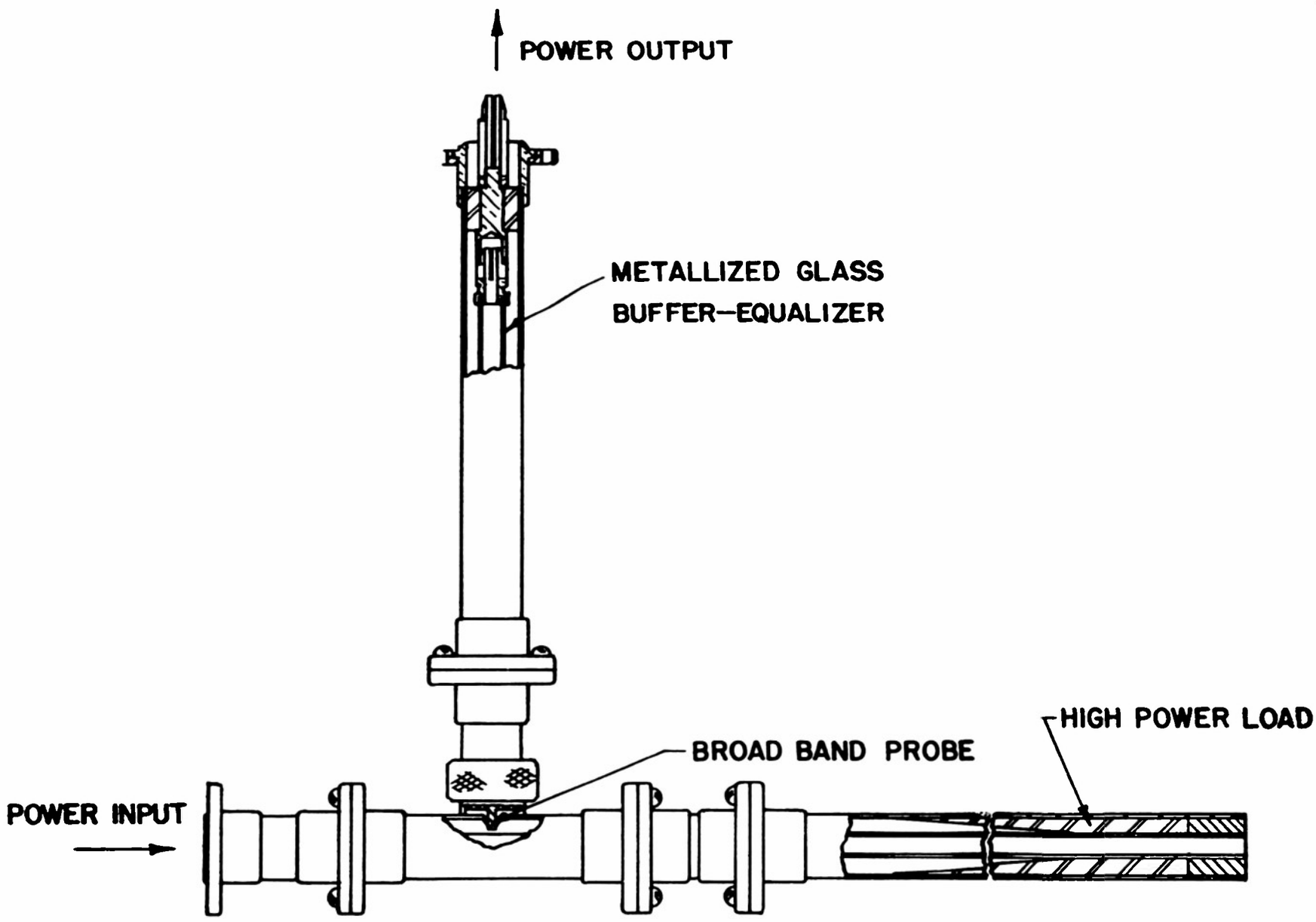

SCHEMATIC OF BROAD BAND HIGH POWER ATTENUATOR

Carlir - Torgow Fig. 5

M.R.I. 11161

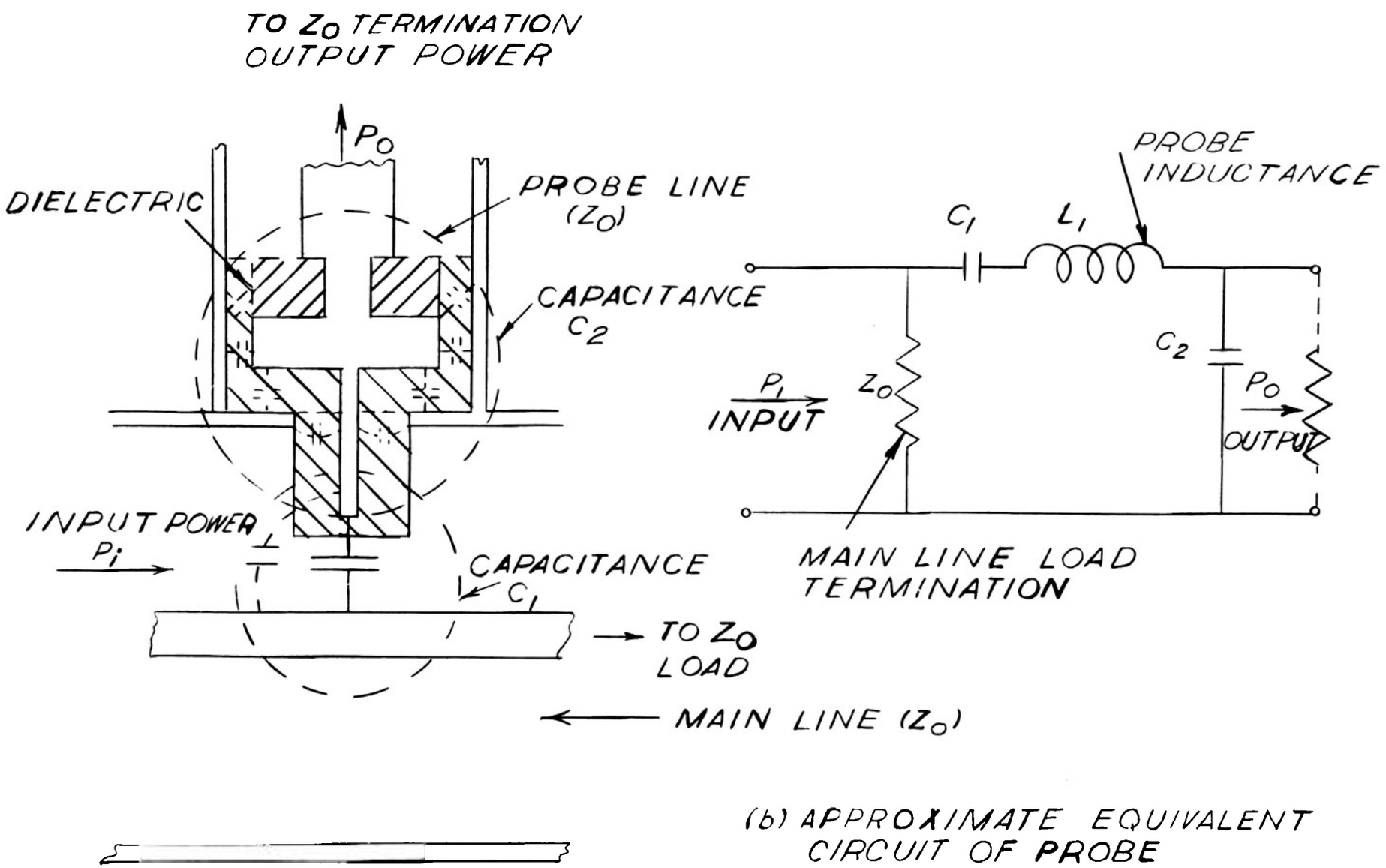

(a) SCHEMATIC DIAGRAM OF PROBE

(b) APPROXIMATE EQUIVALENT CIRCUIT OF PROBE

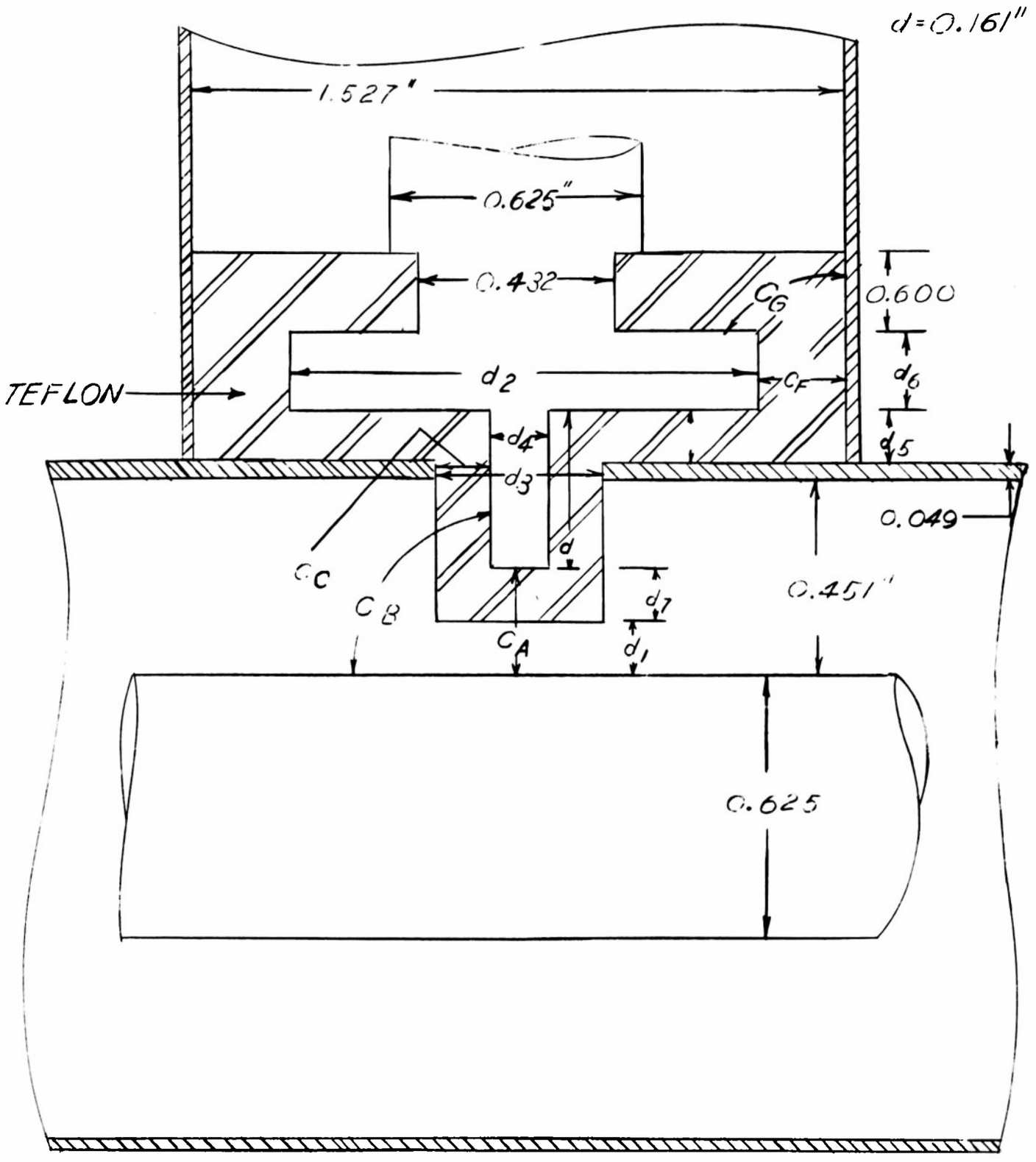

SCHEMATIC DIAGRAM
PROBE SECTION - 1⅝" COAXIAL PROBE
ATTENUATOR

12-53

MRI-13696

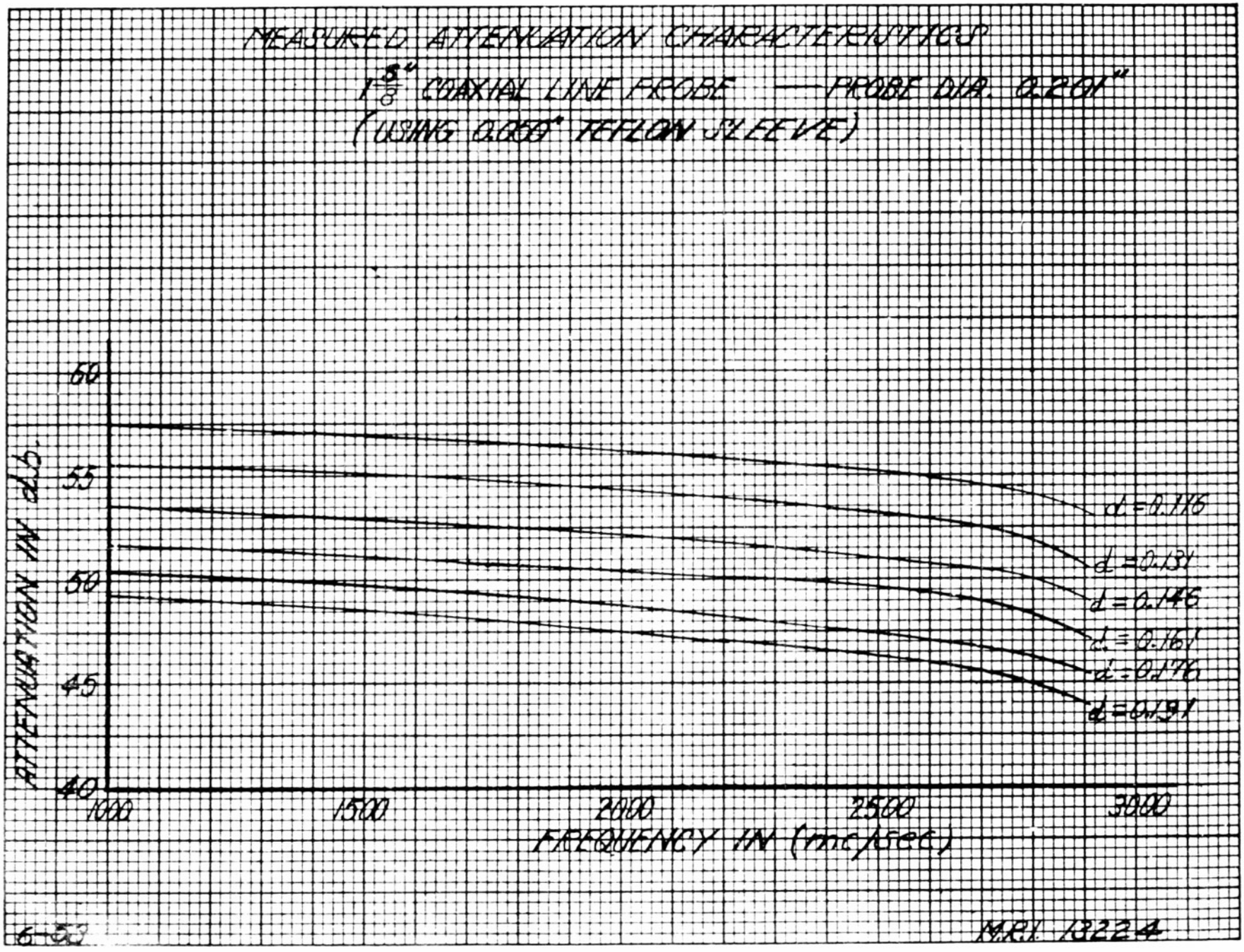
MEASURED ATTENUATION CHARACTERISTICS
1 5/8" COAXIAL LINE PROBE — PROBE DIA. 0.201"
(USING 0.005" TEFLON SLEEVE)
ATTENUATION IN db.
60
55
50
45
40
1000
1500
2000
2500
3000
FREQUENCY IN (mc/sec)
d = 0.115
d = 0.131
d = 0.146
d = 0.161
d = 0.176
d = 0.191
M.R.I. 13224

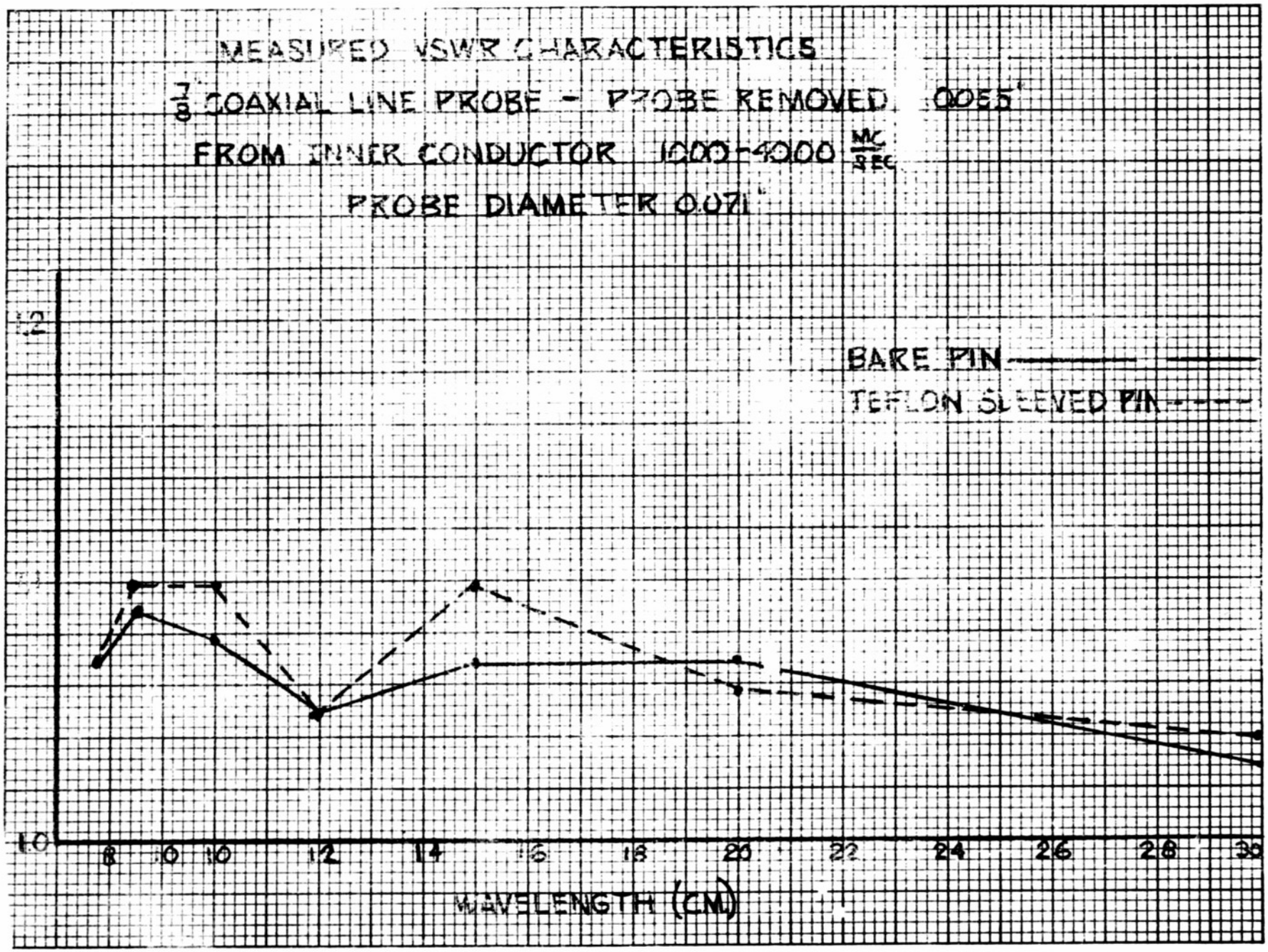
MEASURED VSWR CHARACTERISTICS
7/8 COAXIAL LINE PROBE - PROBE REMOVED .0065"
FROM INNER CONDUCTOR 1000-4000 MC/SEC
PROBE DIAMETER 0.071"
BARE PIN
TEFLON SLEEVED PIN
VSWR
1.2
1.0
8
10
12
14
16
18
20
22
24
26
28
30
WAVELENGTH (CM)

MRI 12746

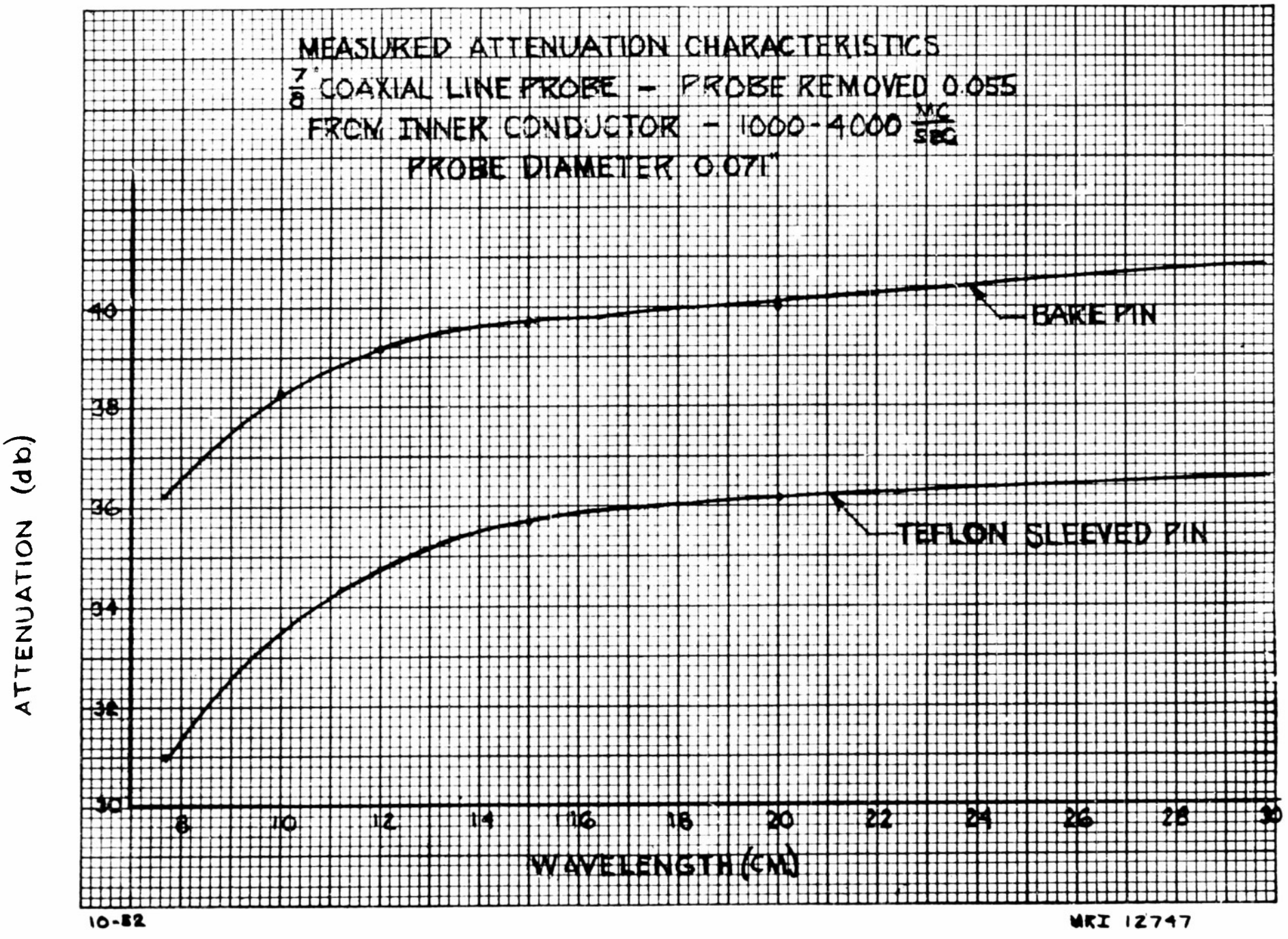

10-52

MRI 12747

COMPENSATED $1\frac{5}{8}$ COAXIAL TEFLON BEAD

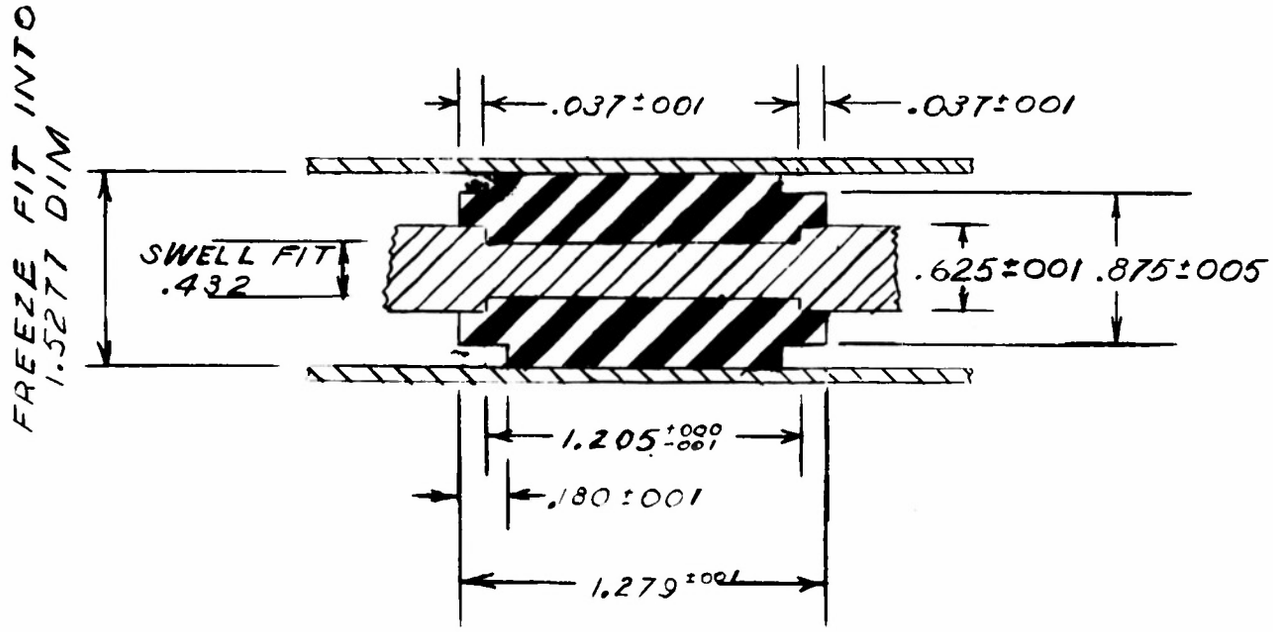

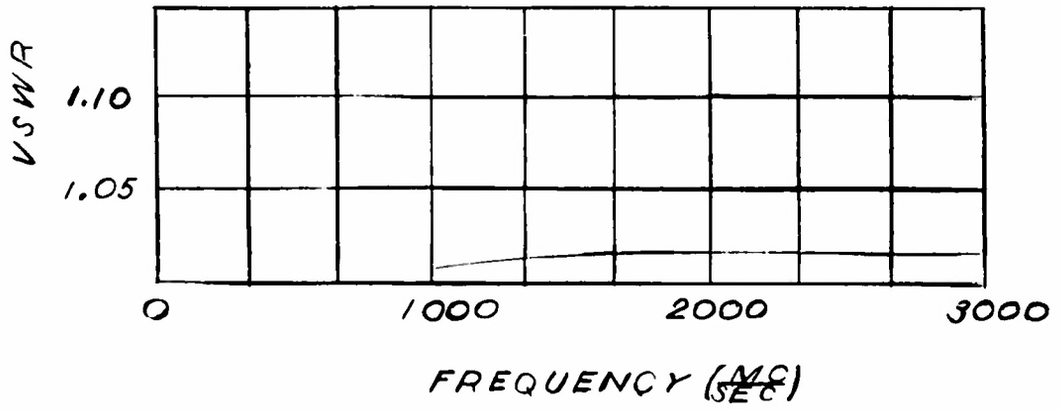

PIB-B-522A

BEFORE ASS'Y OF ITEM 8 & ITEM 10, THE FACE OF ITEM 15 PROTRUDES .002".

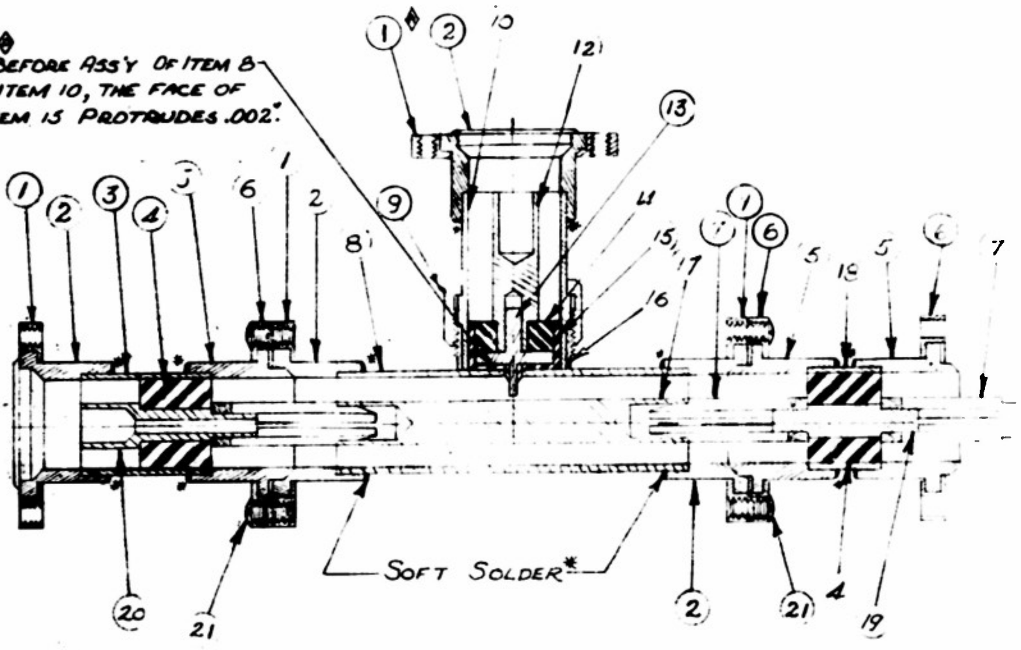

Part No	Dwg No	Stock Item	No Req	Name
	PIB-C-522-P			Sub-Assembly of Parts 12, 13, 14, & 15
	PIB-C-522-N			Sub-Assembly of Parts 12, 13 & 14
	PIB-C-522-M			Sub-Assembly of Parts 8 & 16
21		#10-32	8	Brass Screws, RD HD, ½" LG
20	PIB-C-469-C		1	Inner Conductor
19	PIB-C-521-E		1	Inner Conductor
18	PIB-C-521-K		1	Outer Conductor
17	PIB-C-522-L		1	Inner Conductor
16	PIB-C-522-K		1	Saddle
15	PIB-C-522-J		1	Dielectric Casing
14	PIB-C-522-H		1	Dielectric Bead
13	PIB-C-521-G		1	Brass Disk
12	PIB-C-522-F		1	Stub Inner Conductor
[illegible]	PIB-C-522-D		1	Outer Stub
[illegible]	PIB-C-522-C		1	Locking Nut
[illegible]	PIB-C-522-B		1	Outer Conductor
7	PIB-C-471-D		3	Coupling Bullet
6	PIB-C-195-GG		3	Coupling Flange (Clearance Holes)
5	PIB-C-195-DD		3	Short Receptacle - (Male End)
4	PIB-C-521-F		2	Bead
3	PIB-C-469-B		1	Outer Conductor
2	PIB-C-195-EE		4	Short Receptacle - (Female End)
1	PIB-C-195-FF		4	Coupling Flange - (Tapped Holes)

POLYTECHNIC INSTITUTE OF BROOKLYN
MICROWAVE RESEARCH INSTITUTE

Drawn for PM
Drawn by S. Foster
Checked by
Approved by
Scale 1" = 1"
Date 7-14-48

Change / Date: [illegible] 4-28-49; [illegible] 4-48; [illegible] 2-49; [illegible] 11-48

Title: BROAD BAND ATTENUATOR

File / Dwg No: PIB-B-522A

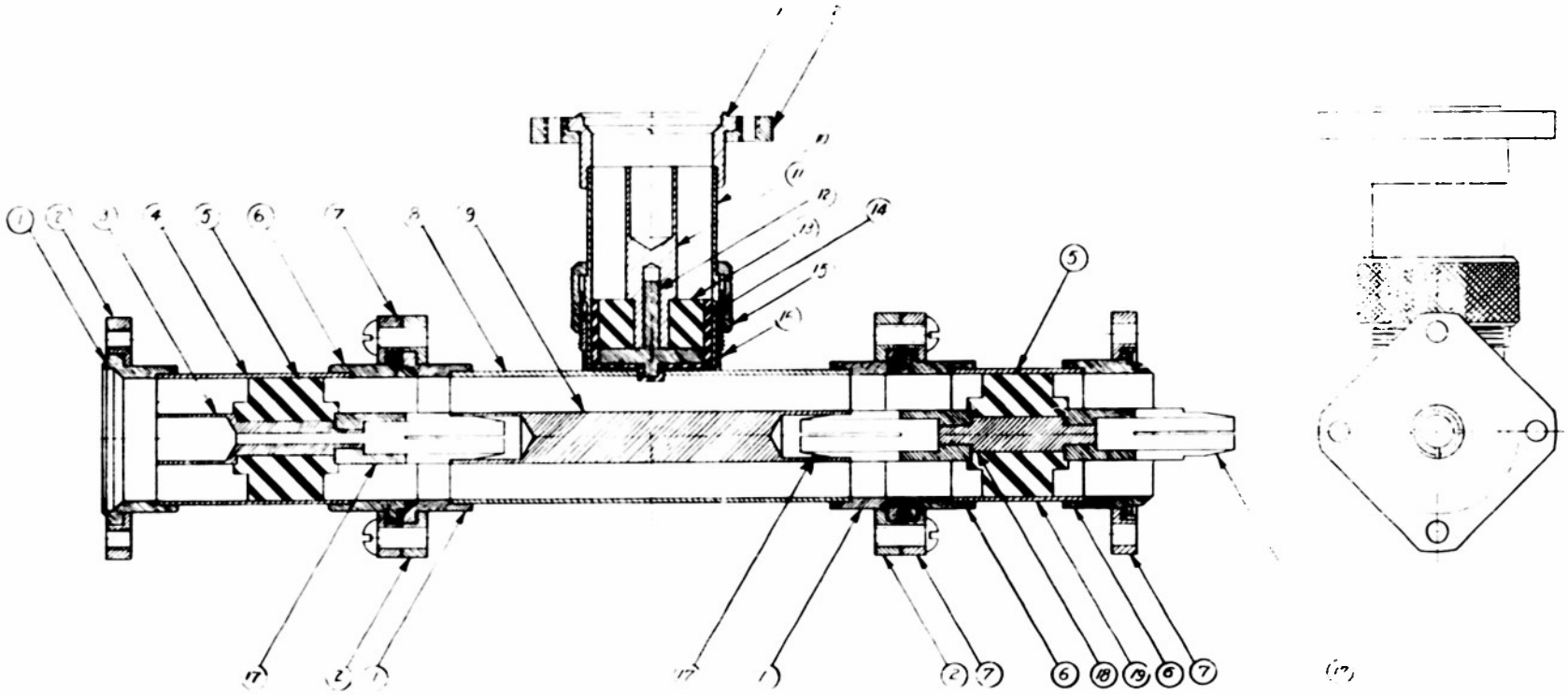

ITM	DWG. NO.	DESCRIPTION	REQD	STOCK ITEMS
19	P.I.B-C713R	OUTER CONDUCTOR	1	
18	P.I.B-C713Q	INNER CONDUCTOR	1	
17	P.I.B-C713P	COUPLING BULLET	3	
16	P.I.B-C713N	SADDLE	1	
15	P.I.B-C713M	LOCKING NUT	1	
14	P.I.B-C713L	DIELECTRIC CASING	1	
13	P.I.B-C713K	DIELECTRIC BEAD	1	
12	P.I.B-C713J	BRASS DISC	1	
11	P.I.B-C713H	STUB INNER CONDUCTOR	1	
10	P.I.B-C713G	OUTER STUB	1	
9	P.I.B-C713F	INNER CONDUCTOR	1	
8	P.I.B-C713E	BRASS TUBING	1	
7	M49512/12-3	COUPLING FLANGE UNTAPPED	3	
6	M49512/12-1	MALE RECEPTACLE	3	
5	P.I.B-C713D	BEAD	2	
4	P.I.B-C713C	OUTER CONDUCTOR	1	
3	P.I.B-C713B	INNER CONDUCTOR	1	
2	M49512/12-4	COUPLING FLANGE TAPPED	4	
1	M49512/12-5	FEMALE RECEPTACLE	4	

CHANGE	DATE

POLYTECHNIC INSTITUTE OF BROOKLYN
MICROWAVE RESEARCH INSTITUTE

DRAWN FOR P.N.	APPROVED BY
DRAWN BY Lindsay	SCALE X
CHECKED BY	DATE

TITLE
1 5/8 PROBE ATTENUATOR

DWG NO. P.I.B-A-713A

VSWR AND DECOUPLING CHARACTERISTICS OF HIGH POWER COAXIAL PROBE ATTENUATOR

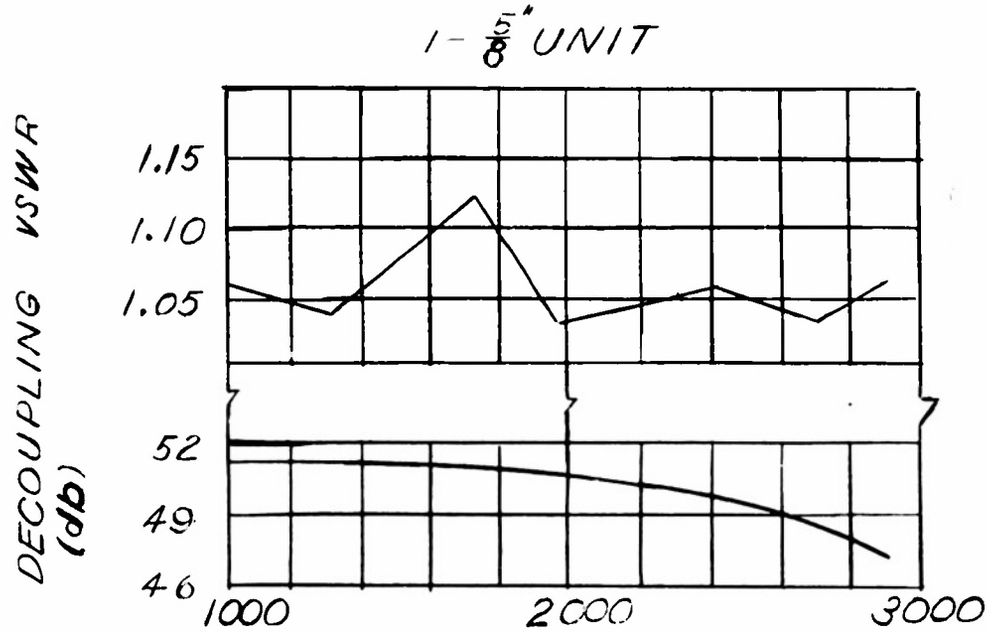

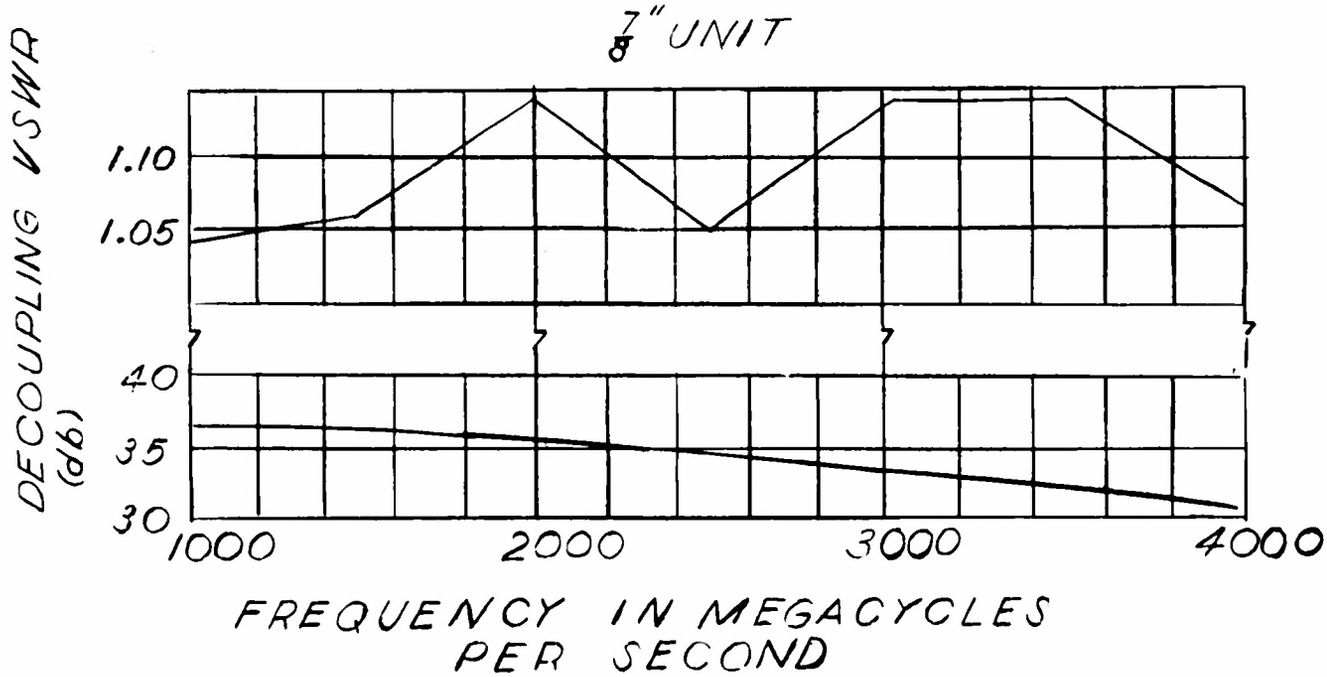

VARIATION OF ELECTRIC FIELD DENSITY RATIO VERSUS ECCENTRICITY

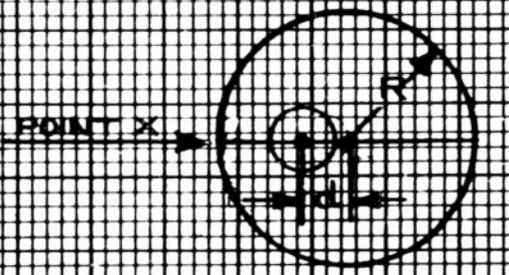

$\epsilon = \frac{d}{R}$

$C = \frac{\text{FIELD DENSITY AT X IN ECCENTRIC LINE}}{\text{FIELD DENSITY AT X IN COAXIAL LINE}}$

$Z_0 = 50\Omega$ FOR ECCENTRIC AND COAXIAL

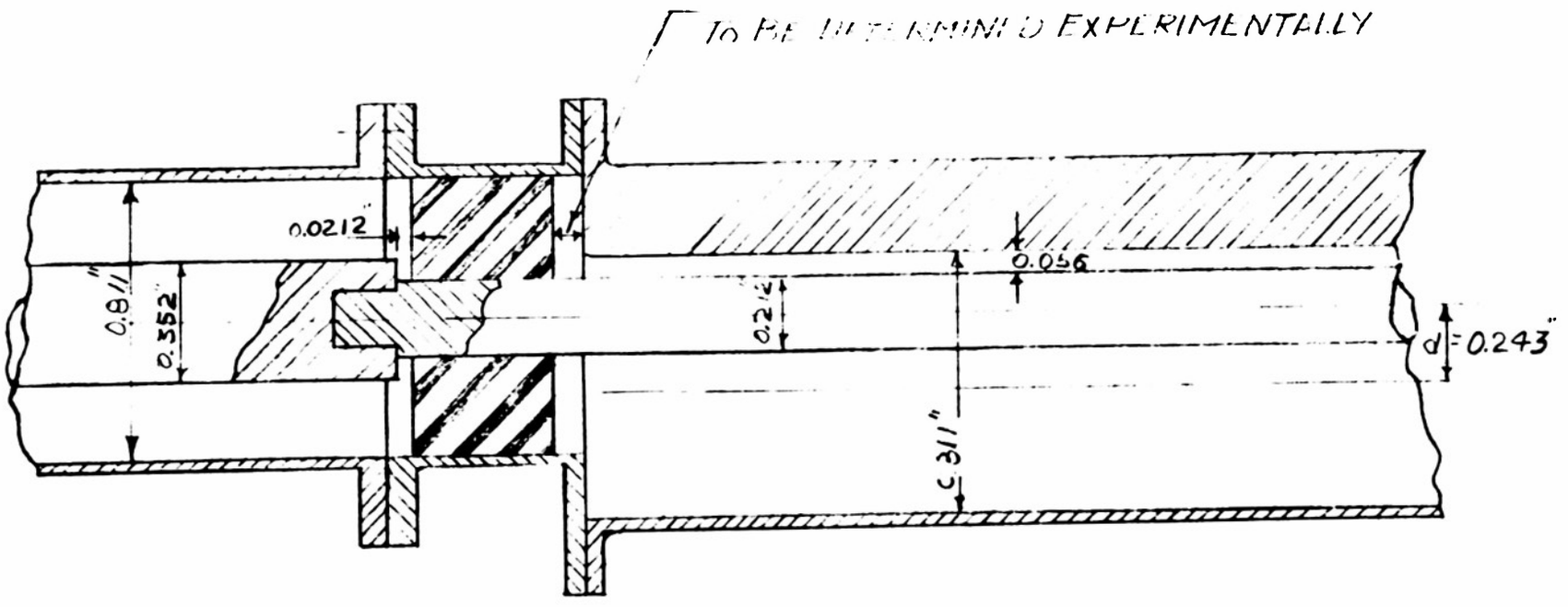

PRELIMINARY DESIGN OF MODIFIED BROAD BAND COAXIAL ATTENUATOR

SCALE 2:1

M.R.I.-12130

7-51

RESISTIVE STRIP FOR VARIABLE COAXIAL ATTENUATOR

IRC CARD - 50 Ω/sq.
SHAPE OF RESISTIVE COATING

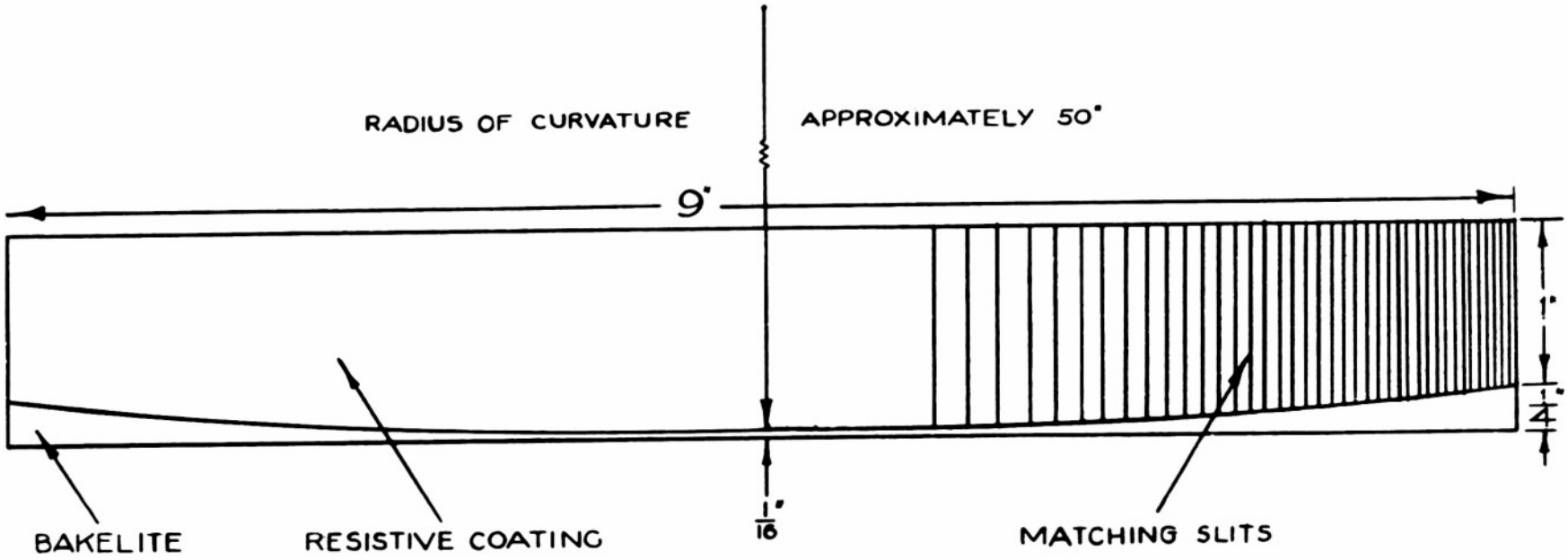

M.R.I. 13706

SCHEMATIC OF CONCENTRIC SLOTTED LINE ATTENUATOR

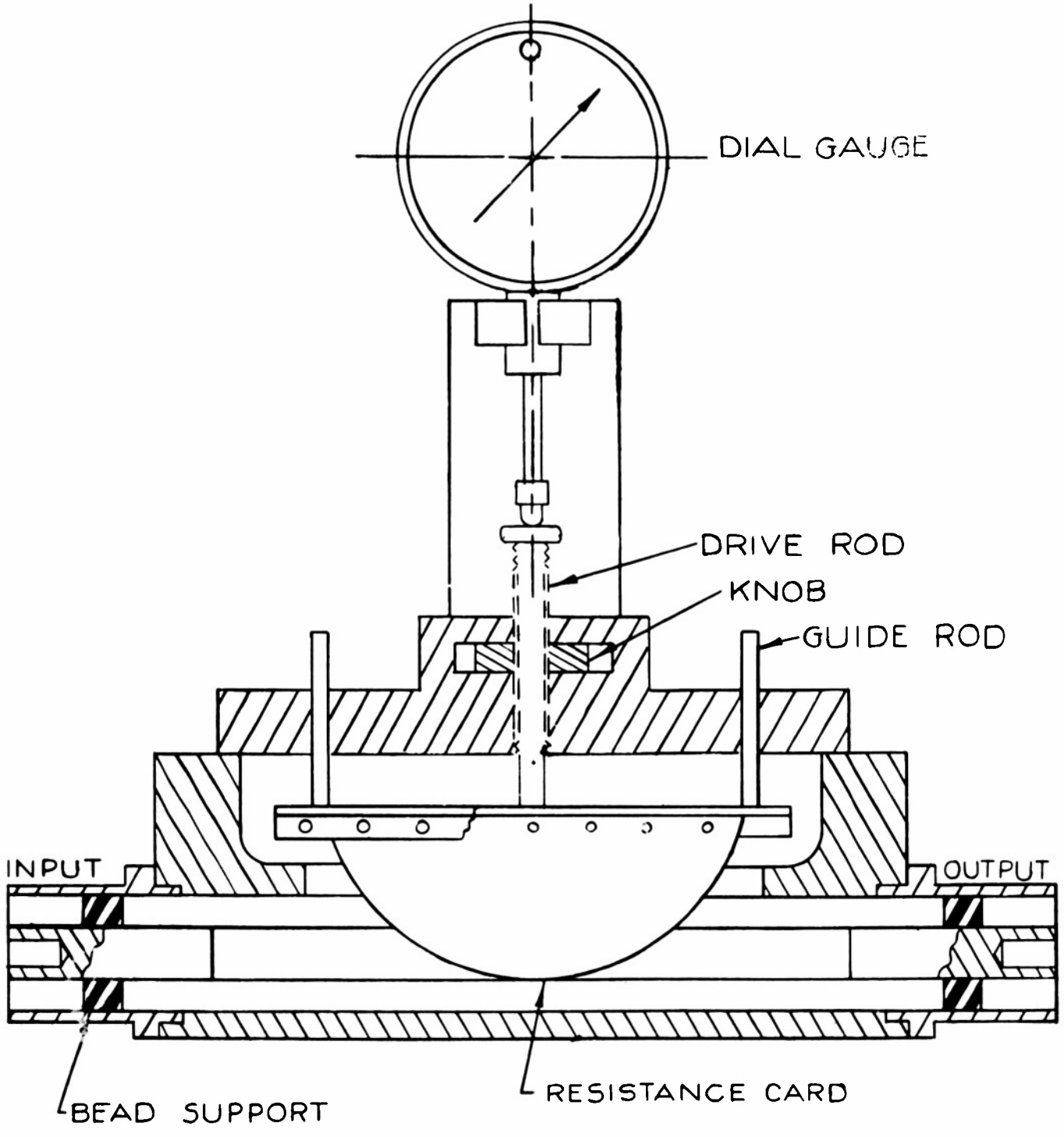

M.R.I. 13697

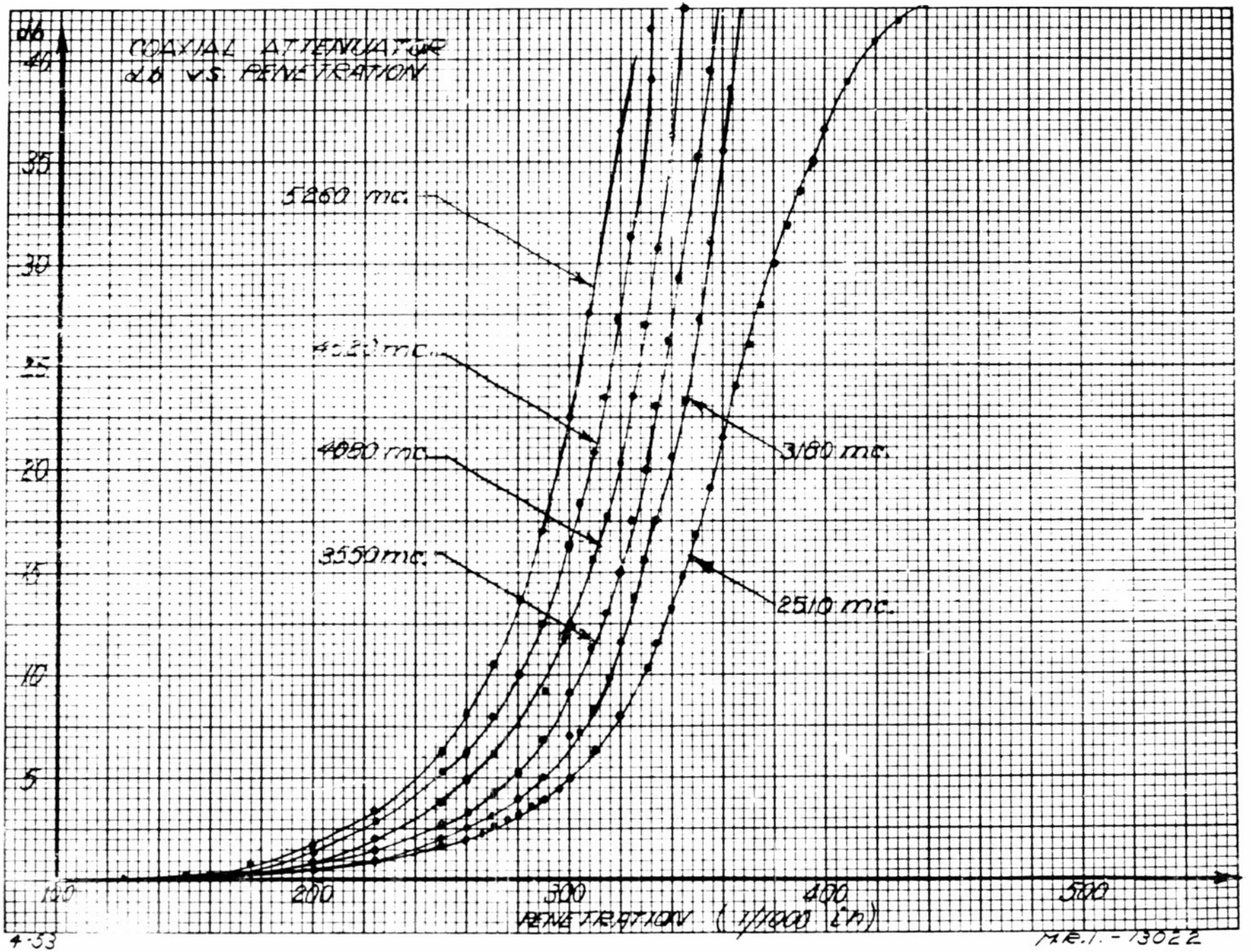

4-53

ME.1. - 13022

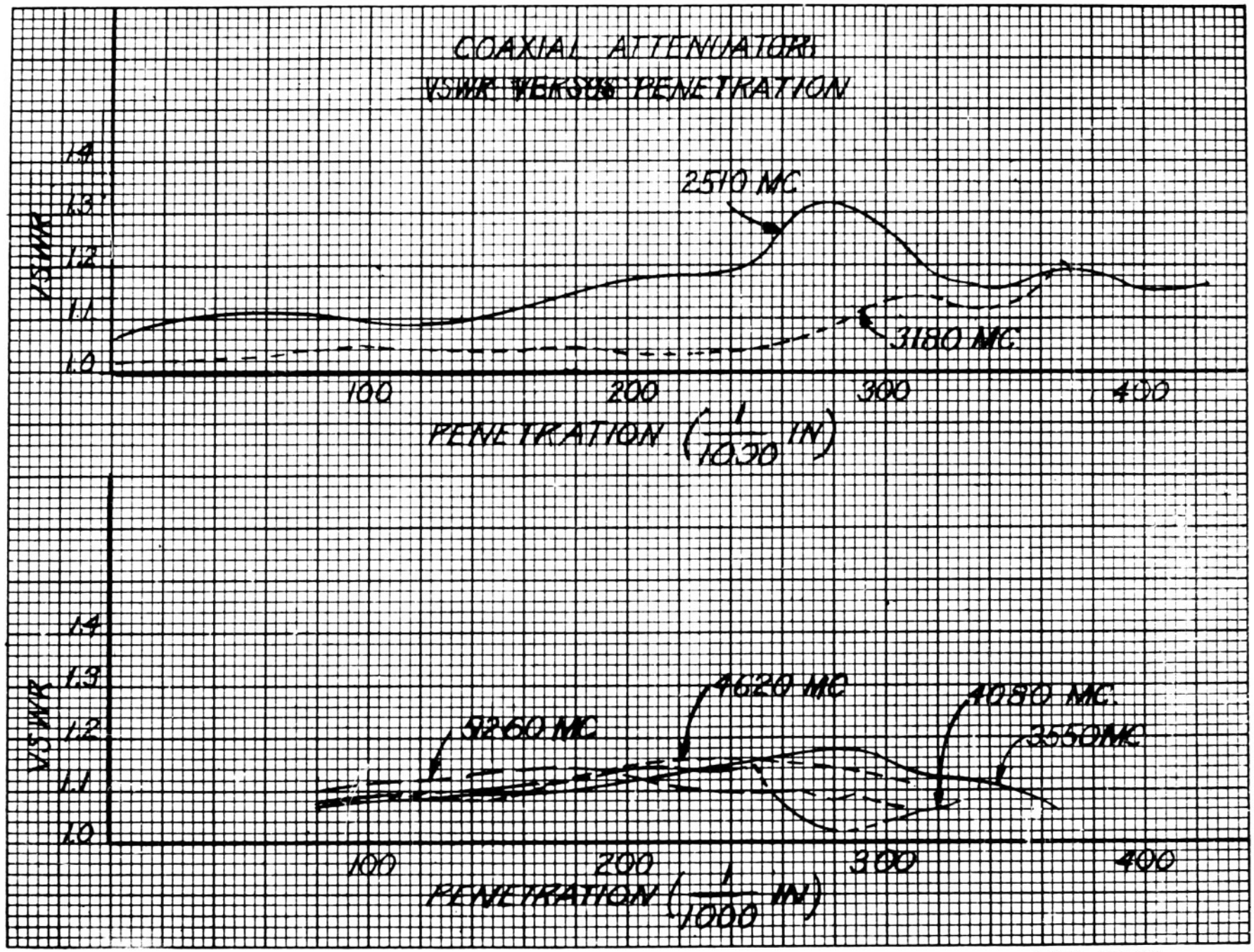
COAXIAL ATTENUATORS
VSWR VERSUS PENETRATION
VSWR
1.4
1.3
1.2
1.1
1.0
2510 MC.
3180 MC.
100
200
300
400
PENETRATION ($\frac{1}{1000}$ IN)
VSWR
1.4
1.3
1.2
1.1
1.0
9260 MC.
4620 MC.
4050 MC.
3550MC.
100
200
300
400
PENETRATION ($\frac{1}{1000}$ IN)

MRI 13023

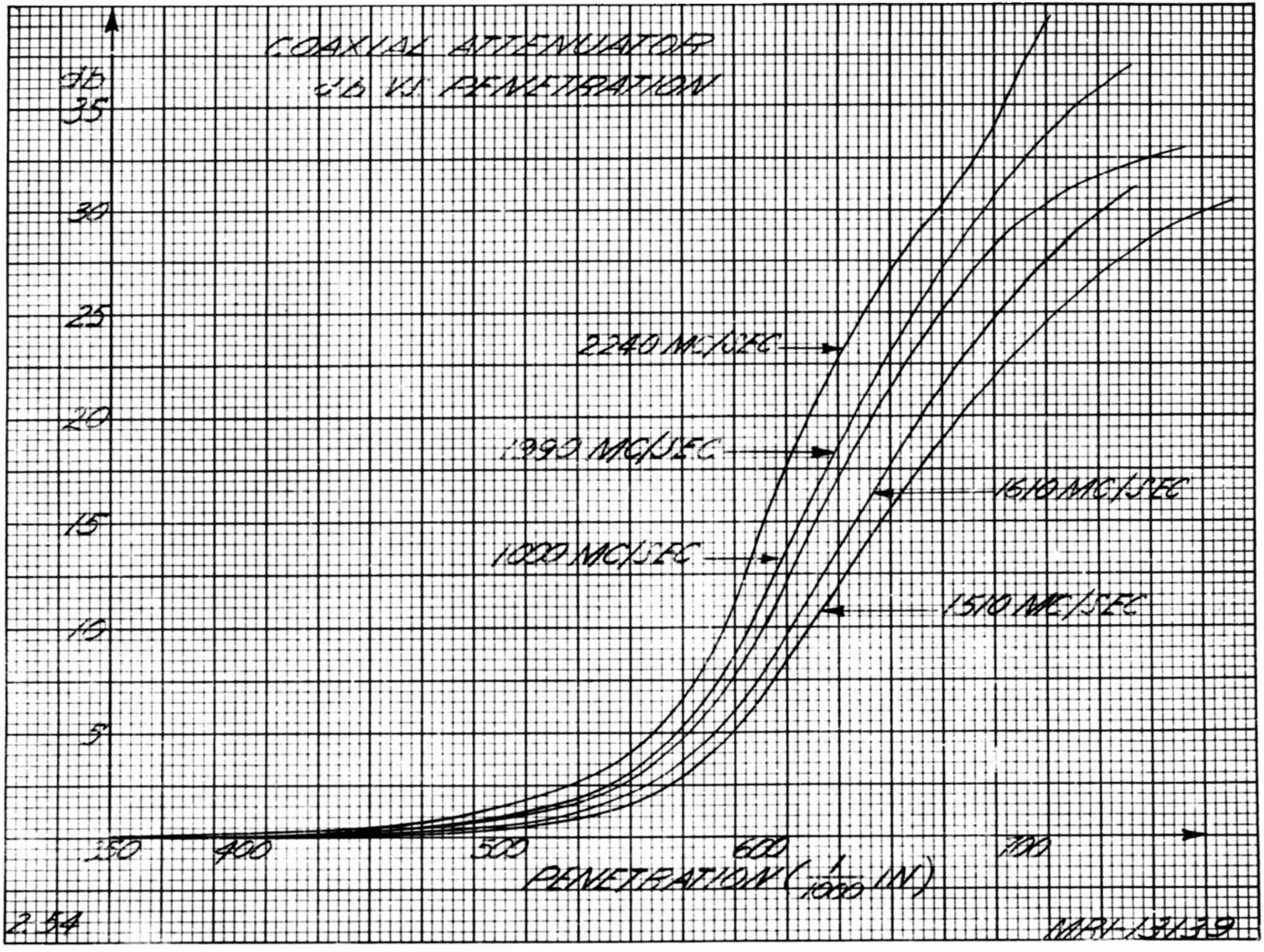
COAXIAL ATTENUATOR
DB VS PENETRATION
35
30
25
20
15
5
2240 MC/SEC
1990 MC/SEC
1510 MC/SEC
1000 MC/SEC
1510 MC/SEC
400
500
600
700
PENETRATION (1/1000 IN)
2.54
MAY 1961

SKETCH OF NEW ATTENUATOR UNIT

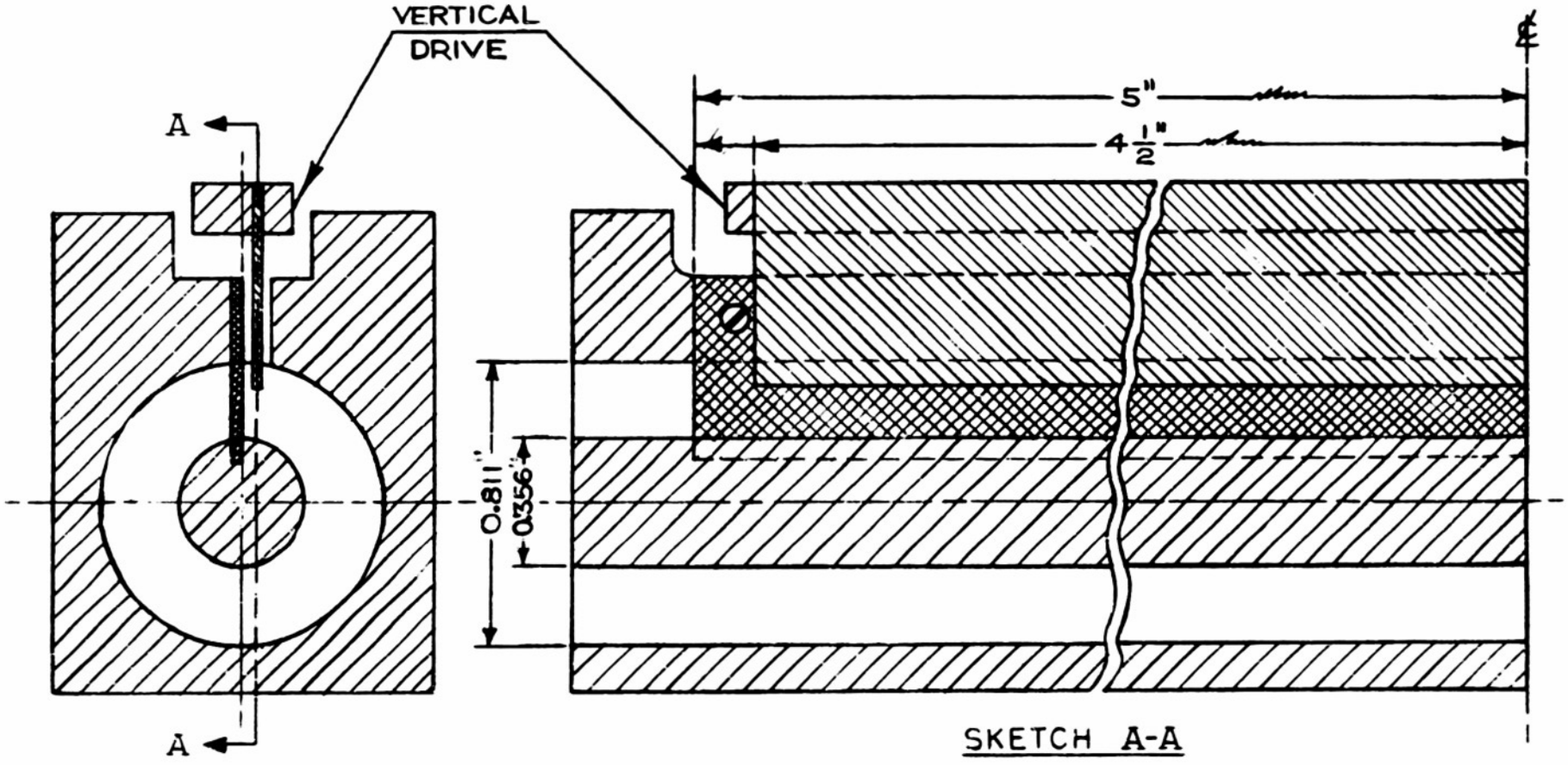

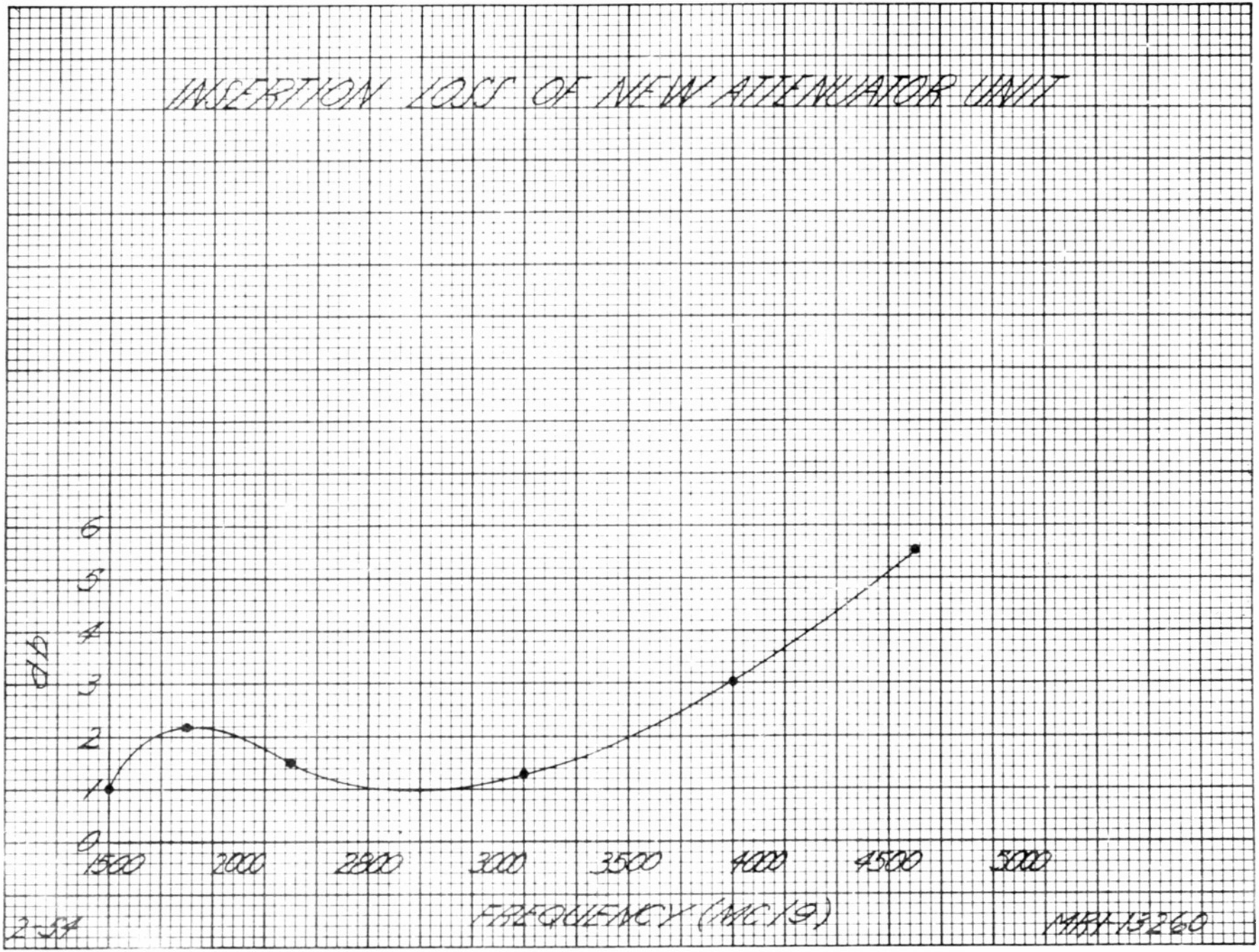
INSERTION LOSS OF NEW ATTENUATOR UNIT
dB
0
1
2
3
4
5
6
1500
2000
2500
3000
3500
4000
4500
5000
FREQUENCY (MC/S)
2-54
MBR 15260

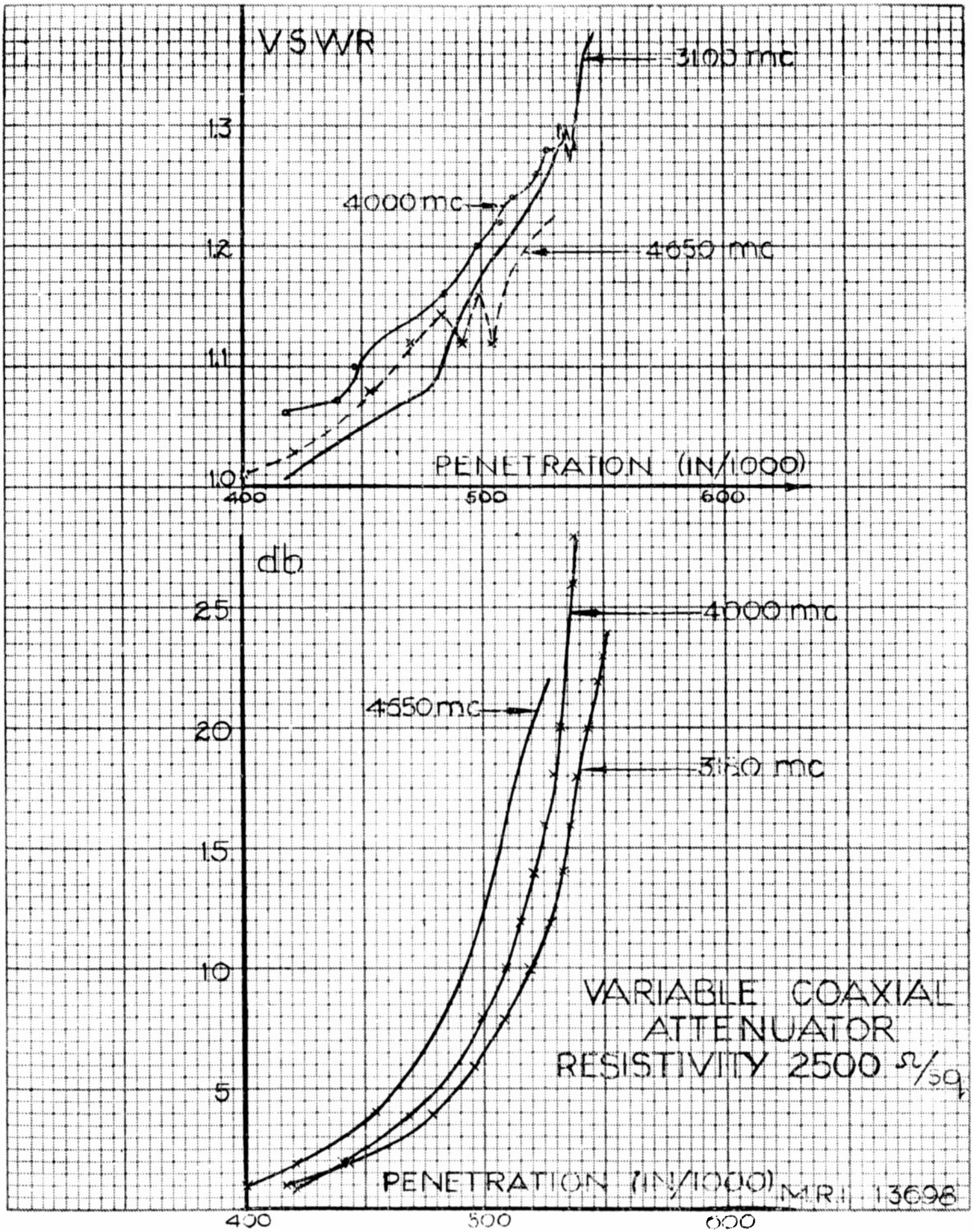
VSWR
3100 mc
1.3
4000 mc
1.2
4650 mc
1.1
1.0
PENETRATION (IN/1000)
400
500
600
db
25
4000 mc
4650 mc
20
3100 mc
1.5
1.0
5
VARIABLE COAXIAL
ATTENUATOR
RESISTIVITY 2500 Ω/sq
PENETRATION (IN/1000)
M.R. 13698
400
500
600

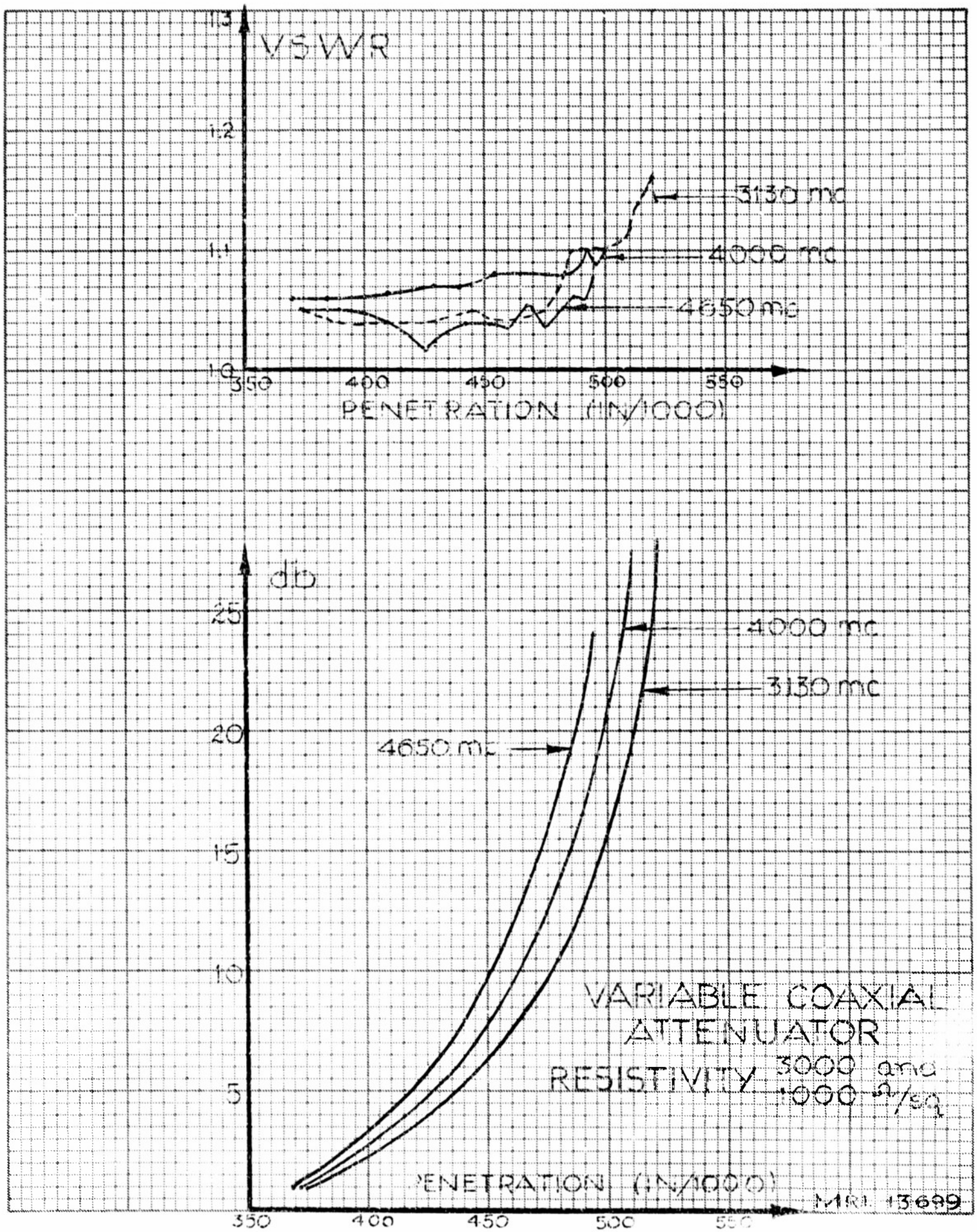
VSWR
1.3
1.2
1.1
1.0
3130 mc
4000 mc
4650 mc
350
400
450
500
550
PENETRATION (IN/1000)
db
25
20
15
10
5
4000 mc
3130 mc
4650 mc
VARIABLE COAXIAL
ATTENUATOR
RESISTIVITY 3000 and
1000 Ω/sq
PENETRATION (IN/1000)
MRL 13699

DWG. NO. P. I. B.-C-

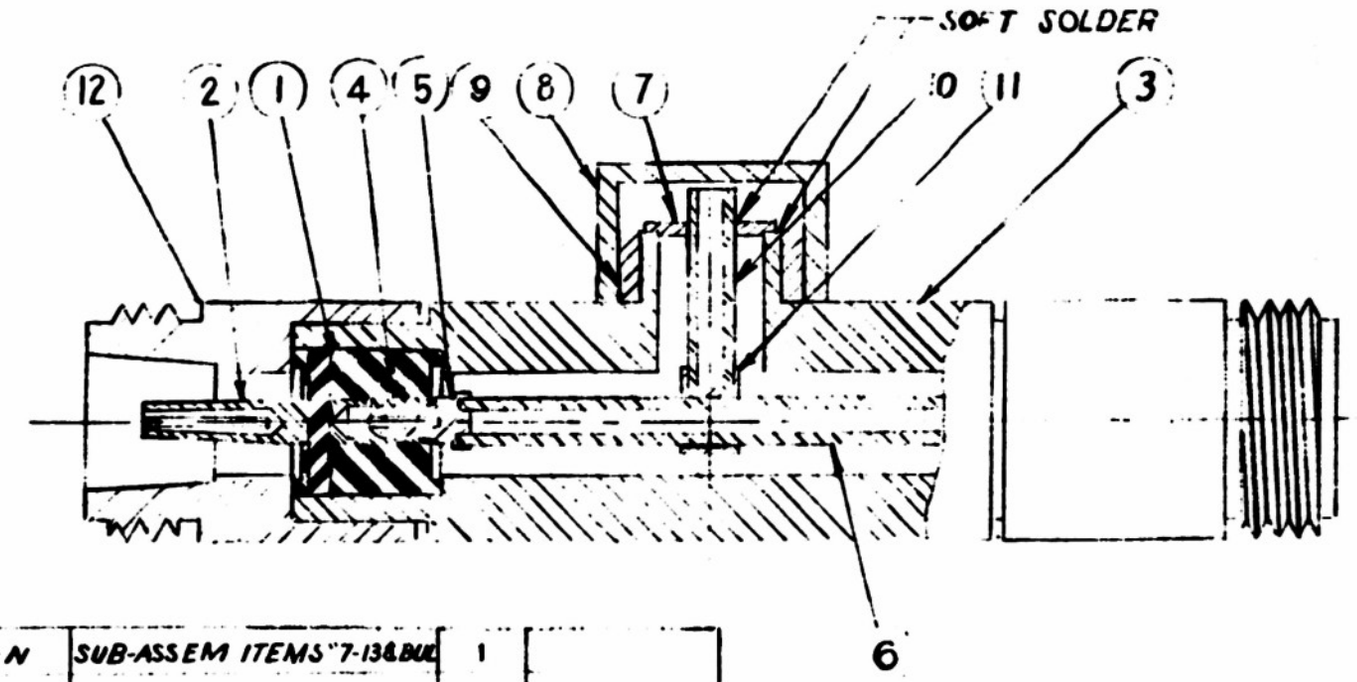

ITEM	DWG. NO.	DESCRIPTION	REQ'D	STOCK ITEMS
14	PIB-C-634-N	SUB-ASSEM ITEMS "7-13 & BUL	1	
13	PIB-C-634-M	SUB ASSEM ITEMS "1-6 & BUL	1	
12	PIB-C-634-L	TYPE N BODY	2	
11	PIB-C-634-K	CHIMNEY T-HOLDER	1	
10	PIB-C-634-J	CHIMNEY SHUNT ELEMENT	1	
9	PIB-C 700-D	CASING CLAMP	1	
8	PIB-C 700-C	CHIMNEY CAP	1	
7	PIB C 634-G	SHORTING CAP	1	
6	PIB-C-634-F	SERIES ELEMENT	1	
5	PIB-C 329	BULLET 3 MI	2	
4	PIB C-634-E	BEAD	2	
3	PIB-C-700B	CHIMNEY T-CASING	2	
2	PIB-C-634 C	JACK PIN	2	
1	PIB-C 634-B	SUB-ASSEM BEAD & JACK PIN	2	

CHANGE	DATE

POLYTECHNIC INSTITUTE OF BROOKLYN
MICROWAVE RESEARCH INSTITUTE

DRAWN FOR PM	APPROVED BY
DRAWN BY E.D	SCALE 2:1
CHECKED BY	DATE 10-53

TITLE
CHIMNEY T-PADS

DWG. NO. P. I. B. -C- 700 A

DWG. NO. P. I. B.-C- 691-A

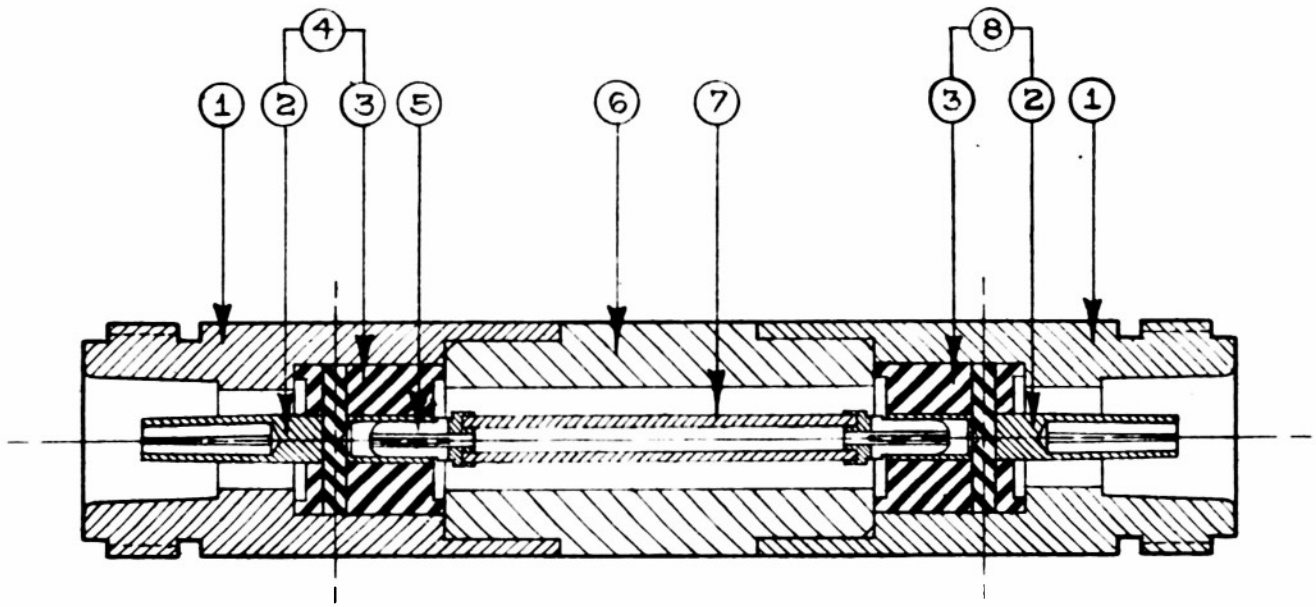

ITEM	DWG. NO	DESCRIPTION	REQ'D	STOCK ITEMS
8	P.I.B.-C-691-H	SUB-ASSEMBLY OF BEAD AND JACK PIN		
7	P.I.B.-C-691-G	ELEMENT	1	
6	P.I.B.-C-691-F	BODY	1	
5	P.I.B.-C-329	3MI BULLET	2	
4	P.I.B.-C-691-E	SUB-ASSEMBLY OF BEAD AND JACK PIN		
3	P.I.B.-C-691-D	BEAD	2	
2	P.I.B.-C-691-C	JACK PIN	2	
1	P.I.B.-C-691-B	TYPE "N" JACK BODY	2	

CHANGE	DATE

POLYTECHNIC INSTITUTE OF BROOKLYN
MICROWAVE RESEARCH INSTITUTE

DRAWN FOR P. M.	APPROVED BY
DRAWN BY M.T.M.	SCALE 2-1
CHECKED BY	DATE 2-53

TITLE
SHORT SERIES 3/8" LINE ATTENUATOR CASING

DWG. NO. P. I. B. -C- 691-A

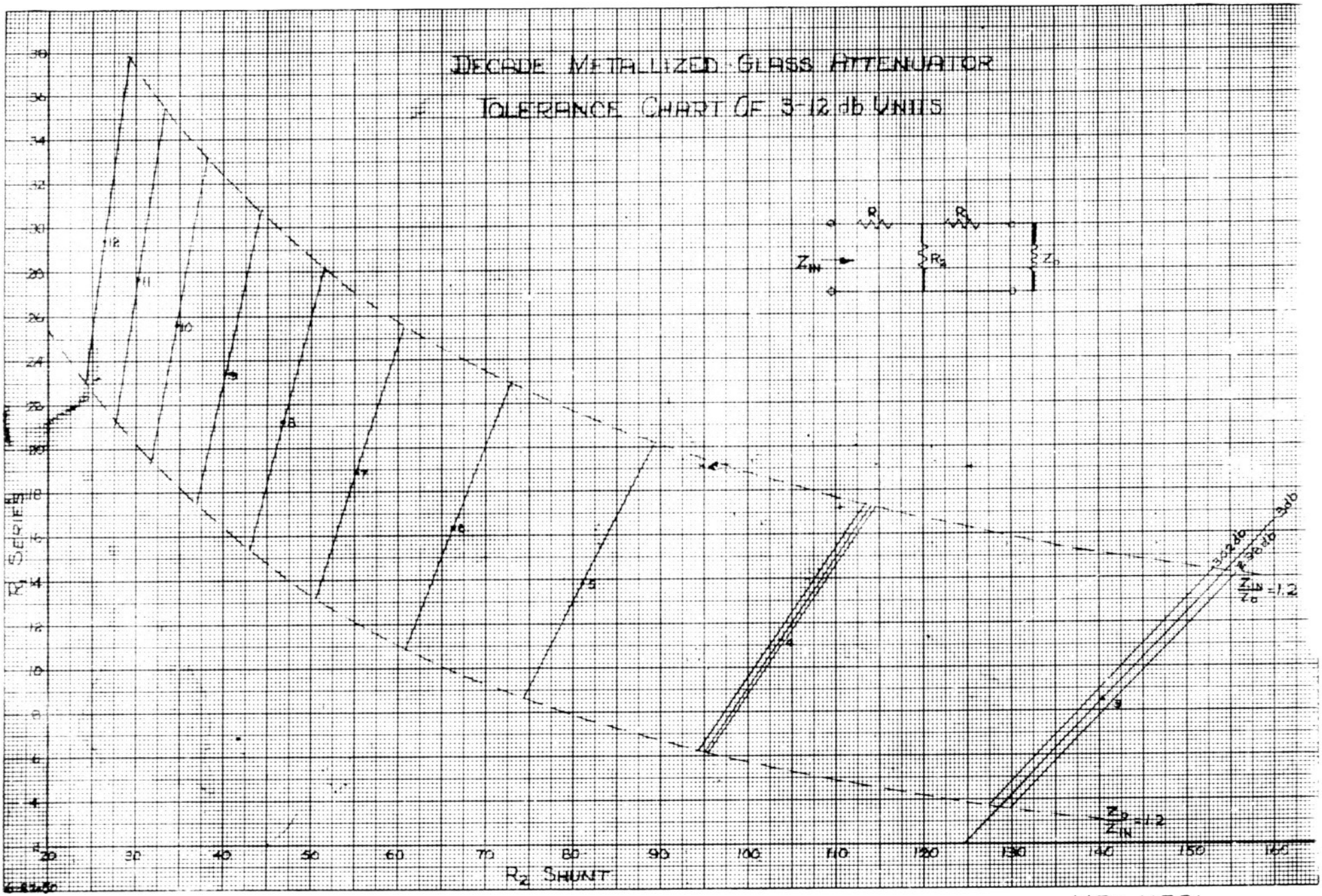
DECADE METALLIZED GLASS ATTENUATOR
TOLERANCE CHART OF 3-12 db UNITS
R
R
Z_{IN}
R_2
Z_0
R_1 SERIES
R_2 SHUNT
$\frac{Z_0}{Z_{IN}} = 1.2$
$\frac{Z_{IN}}{Z_0} = 1.2$
12
11
10
9
8
7
6
5
4
3
2
1
20
30
40
50
60
70
80
90
100
110
120
130
140
150
160
300

M.R.I. 11781

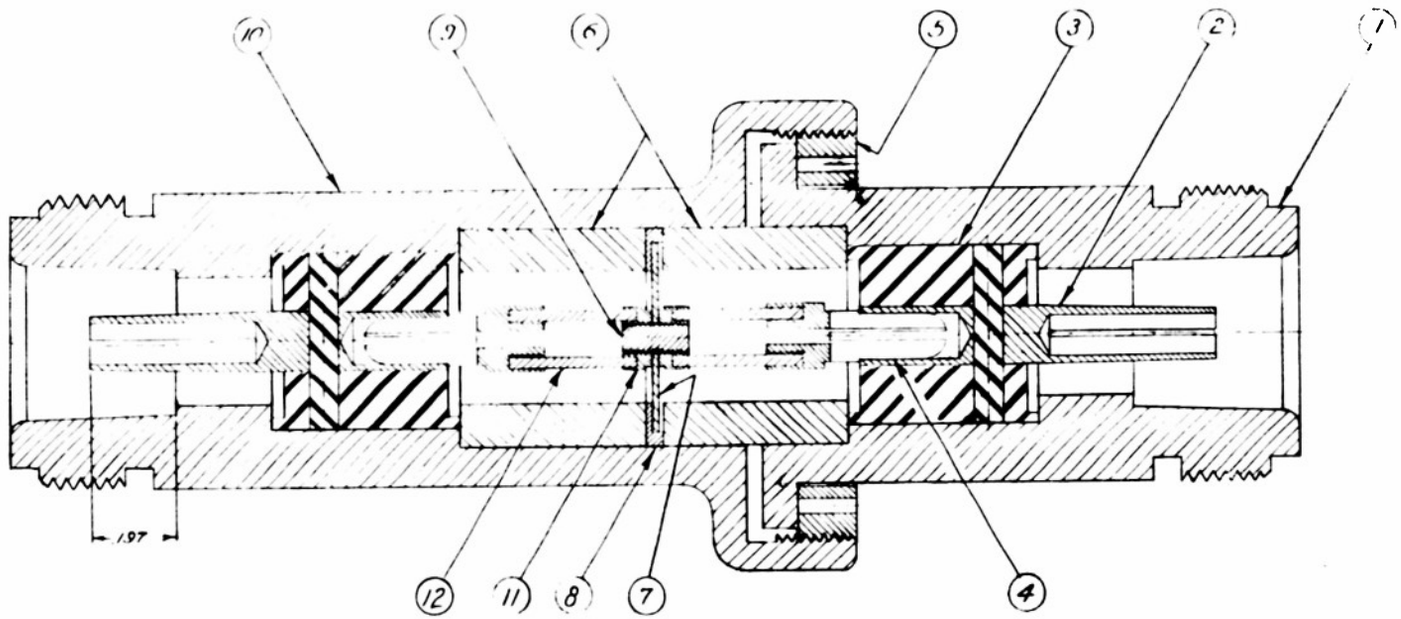

ITEM	DWG. NO.	DESCRIPTION	REQD	STOCK ITEM
12	P.I.B.C-624-N	SERIES ELEMENT		
11	P.I.B.C-624-M	SERIES ELEMENT CONNECTOR		
10	P.I.B.C-624-L	BODY-THREADED END		
9	P.I.B.C-624-K	SERIES ELEMENT SCREW		
8	P.I.B.C-624-J	SHUNT ELEMENT RETAINER		
7	P.I.B.C-624-H	SHUNT ELEMENT		
6	P.I.B.C-624-G	ATTENUATOR OUTER CONDUCTOR		
5	P.I.B.C-624-F	HOLDING NUT		
4	P.I.B.C-211	M-1 STOCK BILLET		
	P.I.B.C-624-E	PINNED BEAD ASSEMBLY		
3	P.I.B.C-624-D	BEAD		
2	P.I.B.C-624-C	JACK PIN		
1	P.I.B.C-624-B	BODY SLIDE END		

POLYTECHNIC INSTITUTE OF BROOKLYN
MICROWAVE RESEARCH INSTITUTE

DRAWN FOR P.M.	APPROVED BY
DRAWN BY Entag	SCALE 4 X
CHECKED BY	DATE 6-5-1

TITLE T-PAD ATTENUATOR TYPE N LINE

CHANGE	DATE	DWG. NO. P.I.B.-624-A

DWG. NO. P. I. B.-C. 624-H

DWG. NO. P. I. B.-C. 624-H

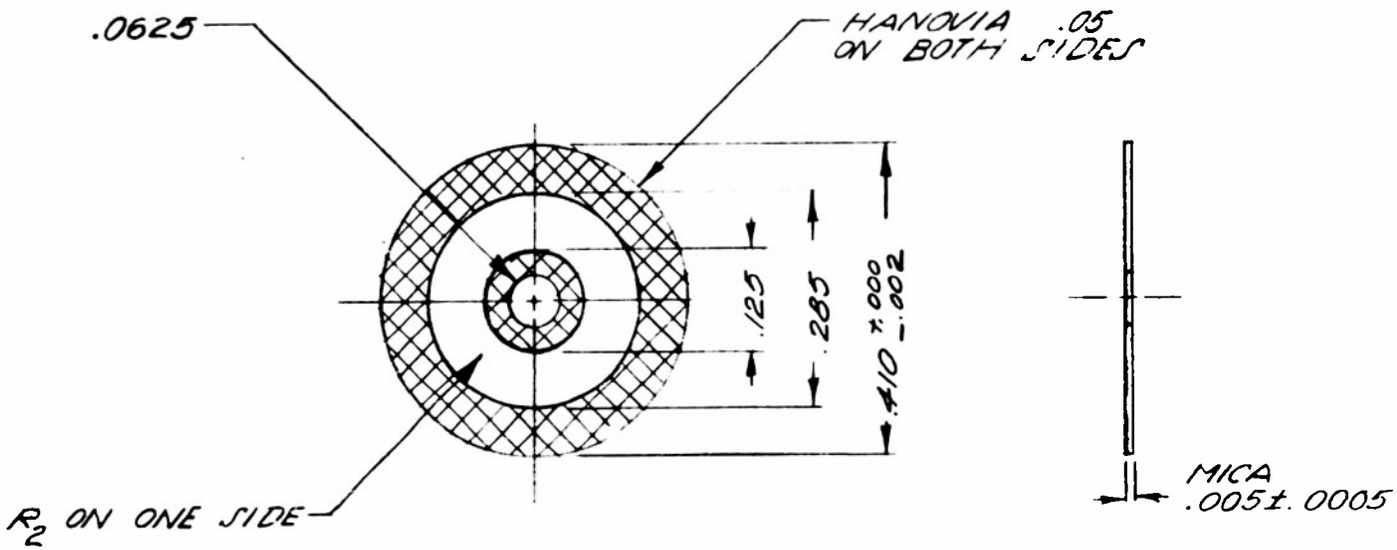

R_2	db	R_2	db Ⓐ
34.67	10	9.98	20
30.25	11	3.20	30
26.5	12	.995	40

ITEM	DWG NO	DESCRIPTION	REQ'D	STOCK ITEMS

CHANGE	DATE
Ⓐ ADD db	10-6-52

POLYTECHNIC INSTITUTE OF BROOKLYN
MICROWAVE RESEARCH INSTITUTE

DRAWN FOR P.M.	APPROVED BY
DRAWN BY Emtag	SCALE 4/1
CHECKED BY	DATE 6-51

TITLE

SHUNT ELEMENT

DWG. NO. P. I. B.-C. 624-H

DWG. NO. P. I. B.-C. 624-N

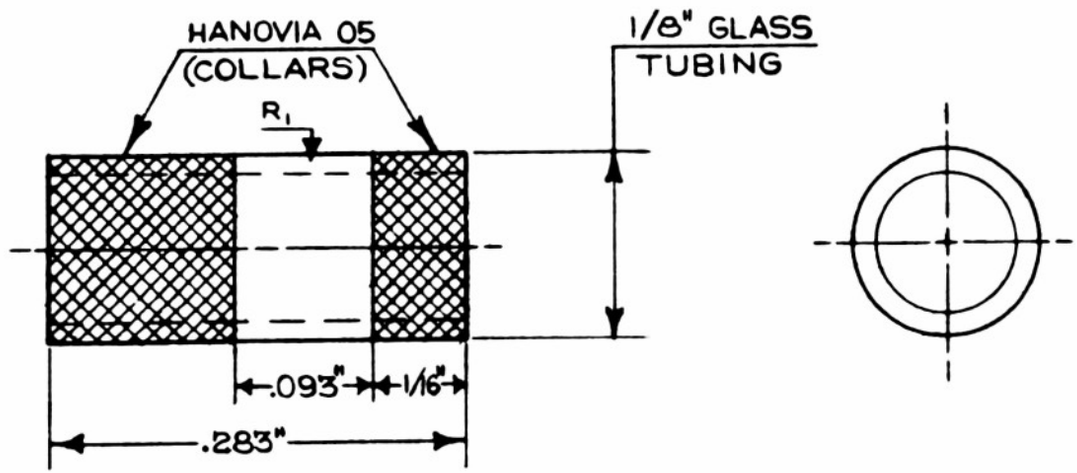

SHOULDER TO SHOULDER .880 $\pm .002$
S BAND BULLETS

R_1	db	R_1	db
25.65	10	40.4	20
27.68	11	46.3	30
29.50	12	48.4	40

(A)

ITEM	DWG. NO.	DESCRIPTION	REQ'D	STOCK ITEMS

CHANGE	DATE
(A) ADD - db	10-4-52

POLYTECHNIC INSTITUTE OF BROOKLYN
MICROWAVE RESEARCH INSTITUTE

DRAWN FOR P.M	APPROVED BY
DRAWN BY M.T.M	SCALE 2 = 1
CHECKED BY	DATE 4-3-52

TITLE
SERIES ELEMENT

DWG. NO. P. I. B.-C. 624-N N

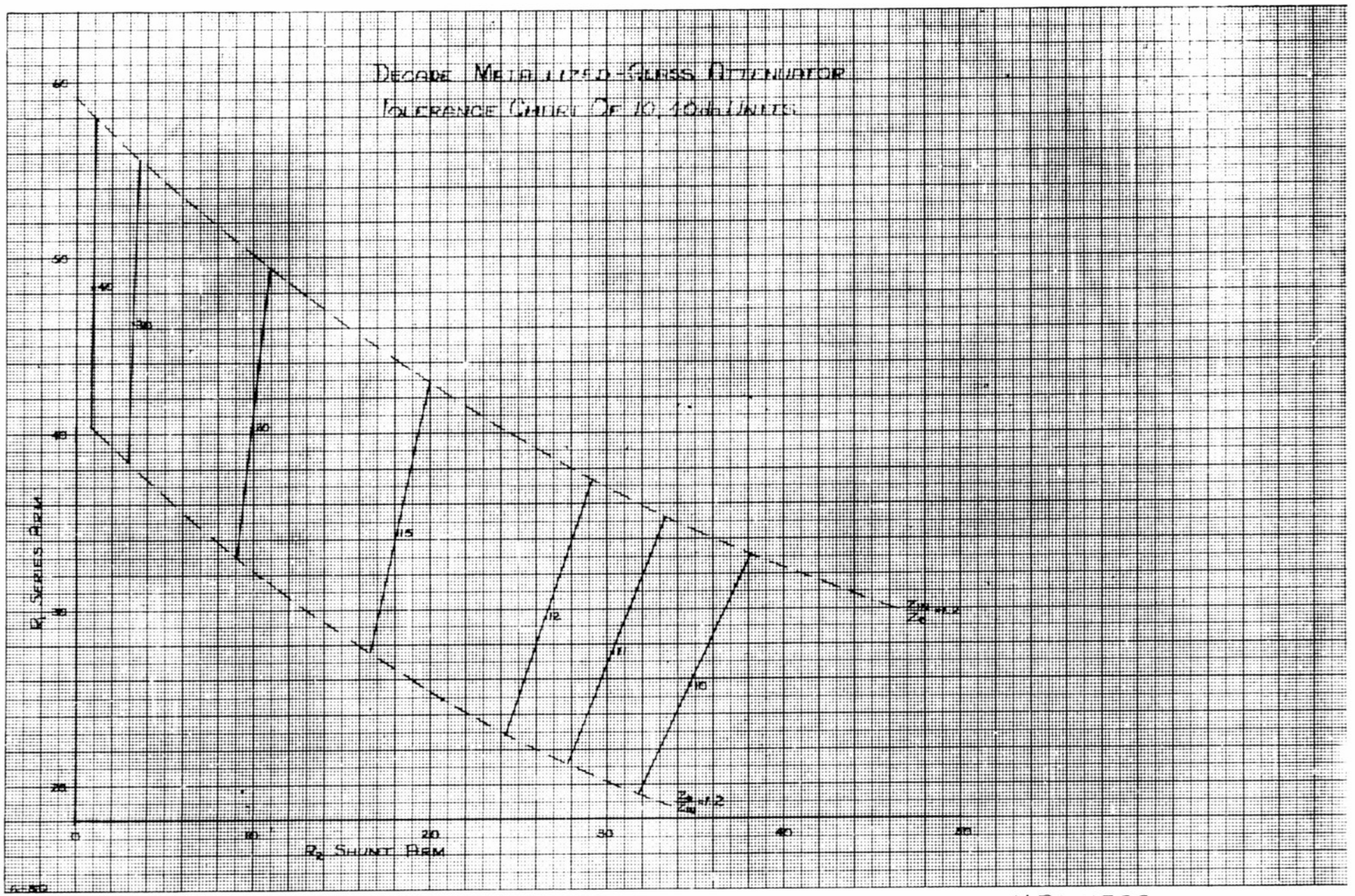
DECADE METALLIZED-GLASS ATTENUATOR
TOLERANCE CHART OF ±0.1db UNITS
R1 SERIES OHMS
R2 SHUNT OHMS
60
50
40
30
20
0
10
20
30
40
50
115
12
11
10
Z1/Z2=1.2
Z1/Z2=1.2

M.R.I. 11783

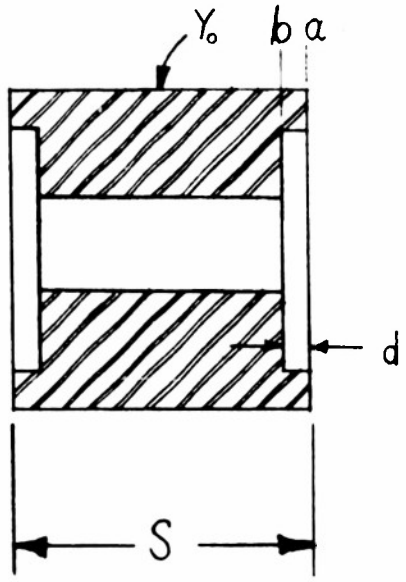

(a)

GROOVED BEAD

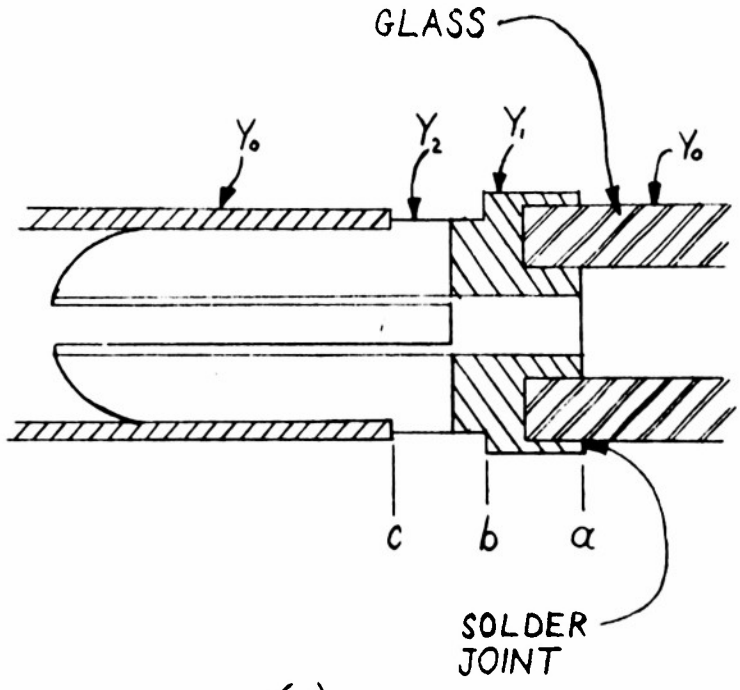

(c)

BULLET FOR ATTENUATOR INSERT

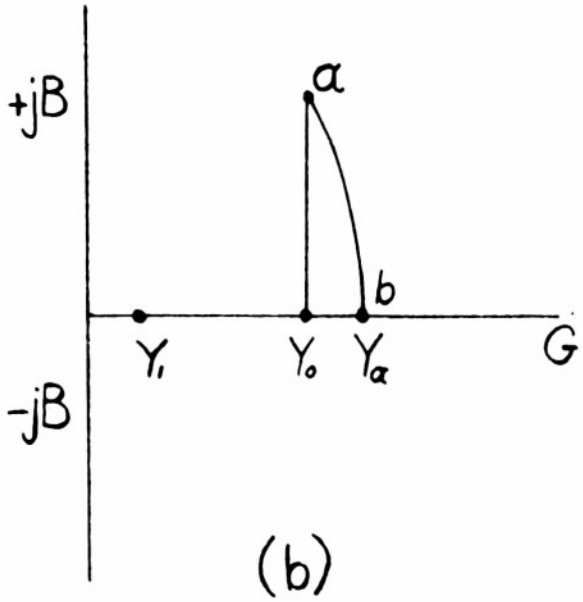

(b)

BEAD REACTIVE CANCELLATION

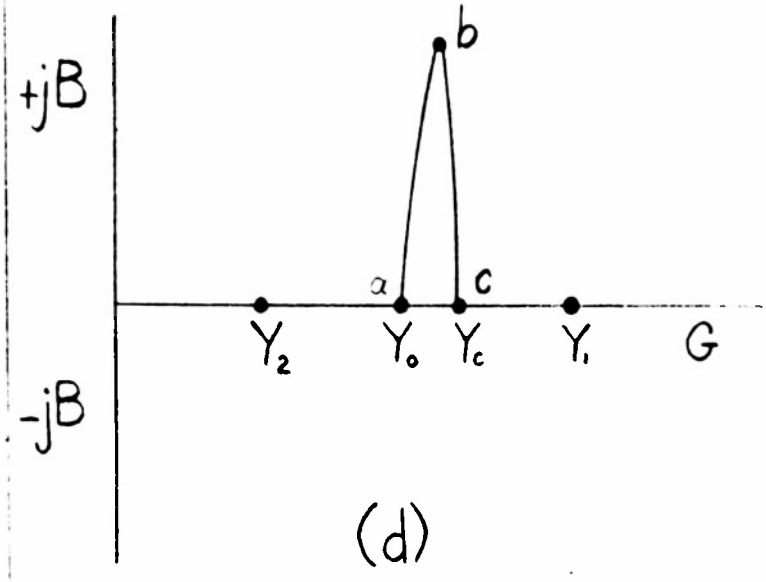

(d)

BULLET SHOULDER CANCELLATION

SCHEMATIC ADMITTANCE DIAGRAMS

MRI 11260

CIRCUIT FOR MEASURING V.S.W.R., INSERTION LOSS, AND VARIATION IN POWER LEVEL AS A FUNCTION OF A.C. & D.C. MAGNETIZING CURRENT FOR FERROMAGNETIC MATERIALS IN COAXIAL

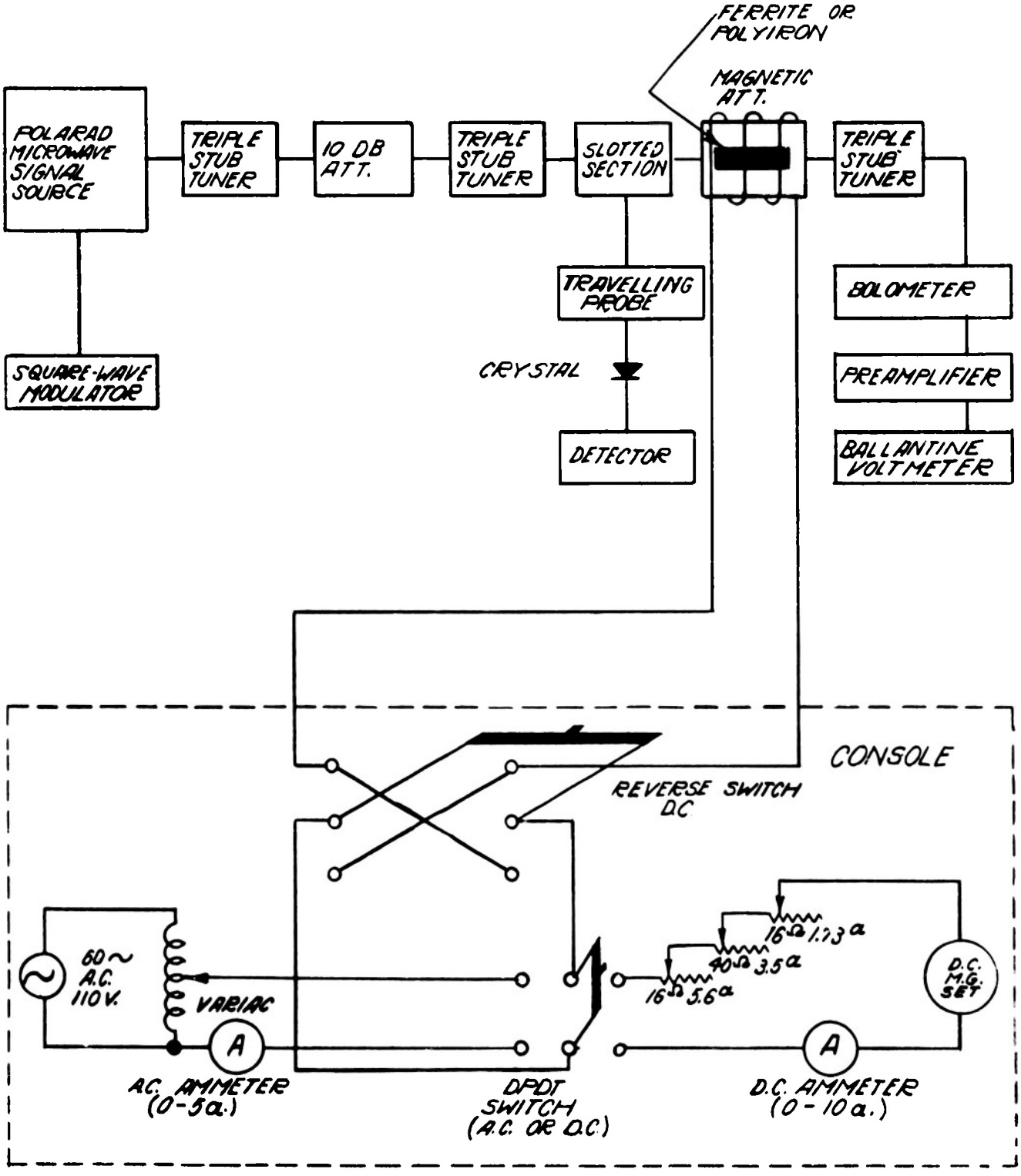

4-53

M.R.I. 13141

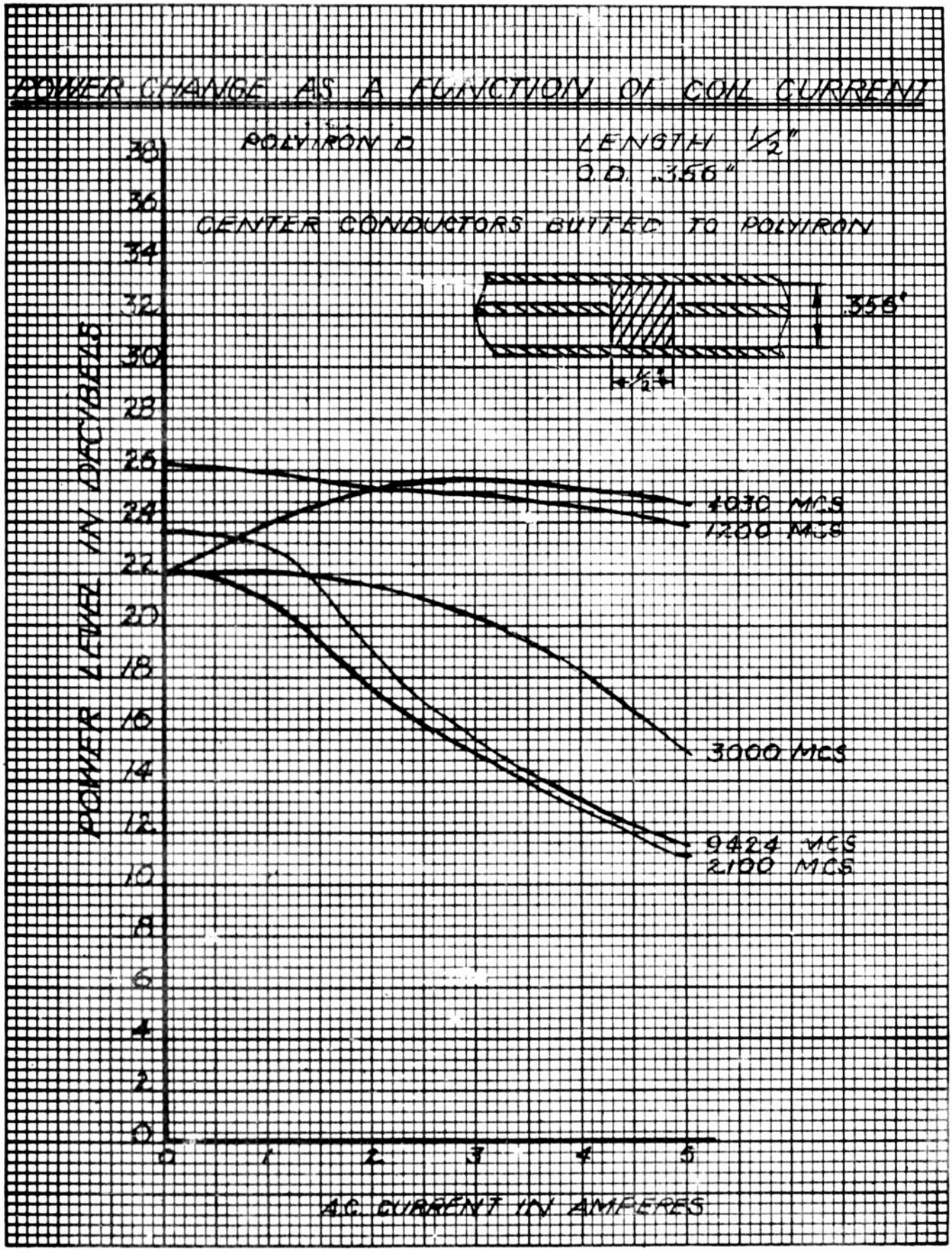
POWER CHANGE AS A FUNCTION OF COIL CURRENT
POLYIRON D
LENGTH 1/2"
O.D. .356"
CENTER CONDUCTORS CUTTED TO POLYIRON
.356"
1/2"
POWER LEVEL IN DECIBELS
38
36
34
32
30
28
26
24
22
20
18
16
14
12
10
8
6
4
2
0
1030 MCS
1200 MCS
3000 MCS
9424 MCS
2100 MCS
0
1
2
3
4
5
A.C. CURRENT IN AMPERES

MRI. 12933

POWER CHANGE AS A FUNCTION OF COIL CURRENT

POLYIRON D

LENGTH 1/4"
O.D. .356"

CENTER CONDUCTOR BUTTED TO POLYIRON

POWER CHANGE IN DECIBELS

27
26
25
24
23
22
21
20
19
18

980 MCS
1500 MCS
2000 MCS

0 1 2 3 4 5

A.C. CURRENT IN AMPERES

MRI 12934

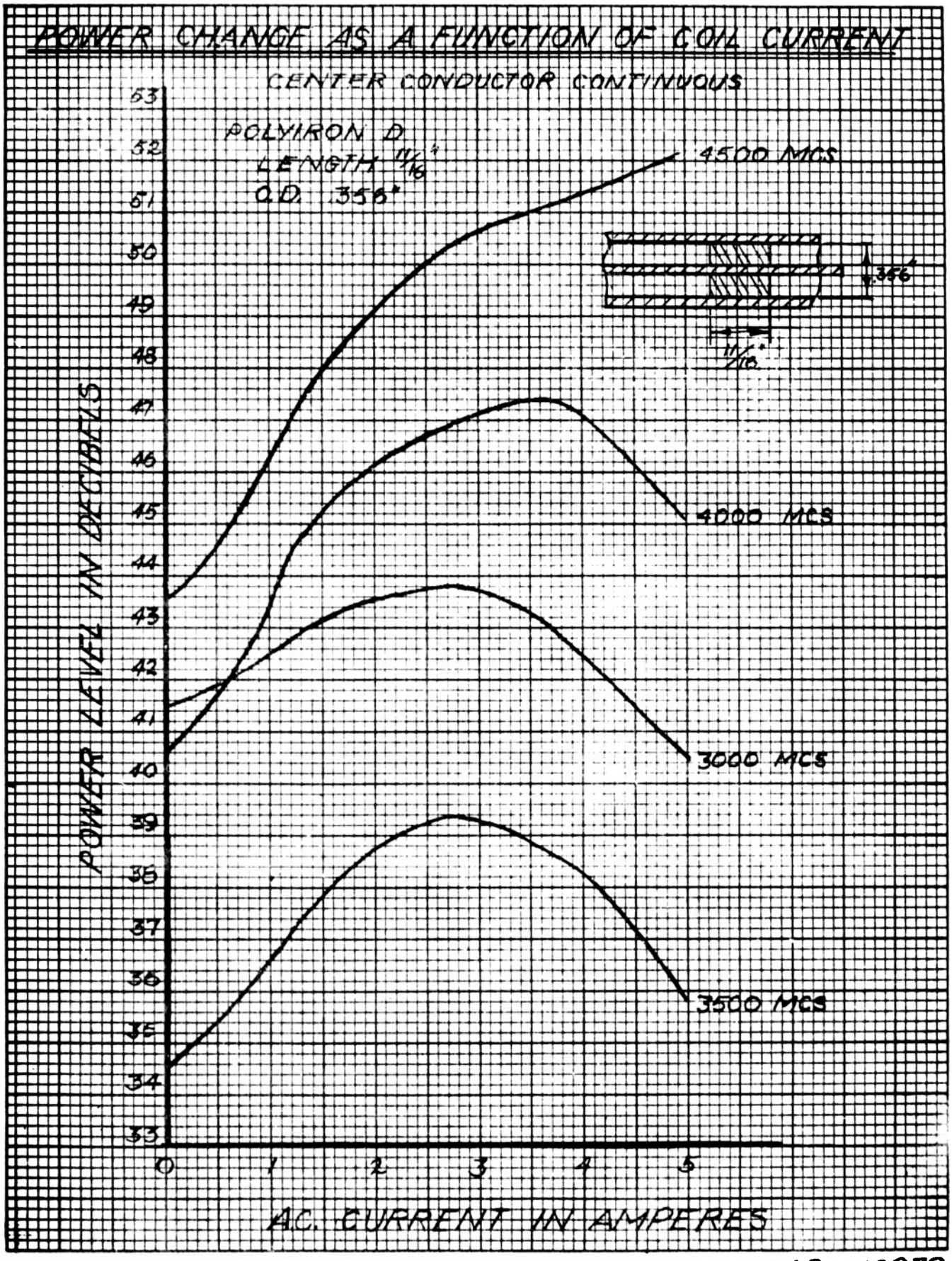
POWER CHANGE AS A FUNCTION OF COIL CURRENT
CENTER CONDUCTOR CONTINUOUS
POLYIRON D
LENGTH 11/16"
O.D. .356"
4500 MCS
4000 MCS
3000 MCS
3500 MCS
.356"
11/16"
POWER LEVEL IN DECIBELS
A.C. CURRENT IN AMPERES
53
52
51
50
49
48
47
46
45
44
43
42
41
40
39
38
37
36
35
34
33
0
1
2
3
4
5

M.R.I. 12939

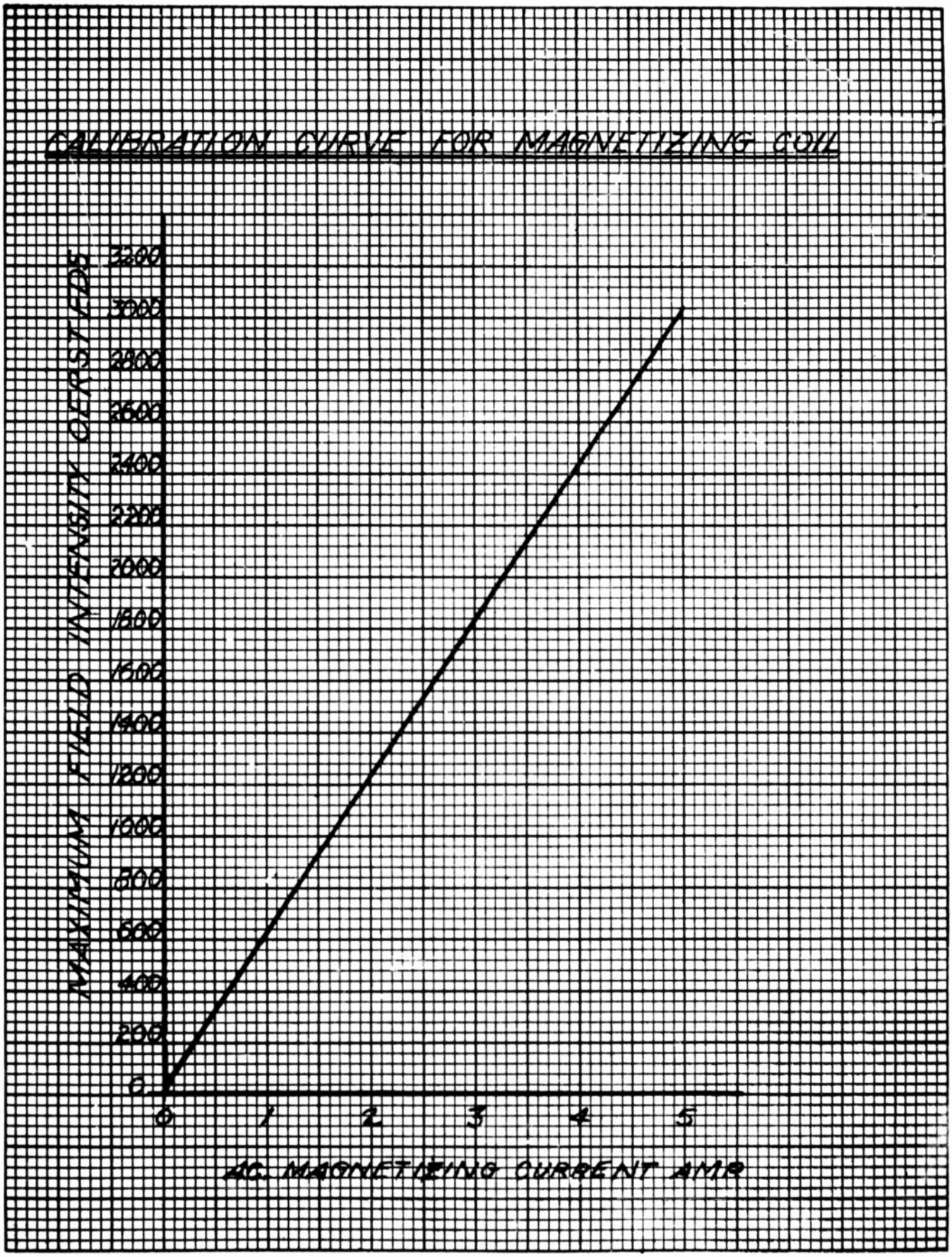
CALIBRATION CURVE FOR MAGNETIZING COIL
MAXIMUM FIELD STRENGTH GAUSS
3200
3000
2800
2600
2400
2200
2000
1800
1600
1400
1200
1000
800
600
400
200
0
0
1
2
3
4
5
AC. MAGNETIZING CURRENT AMP

MRI. 12940

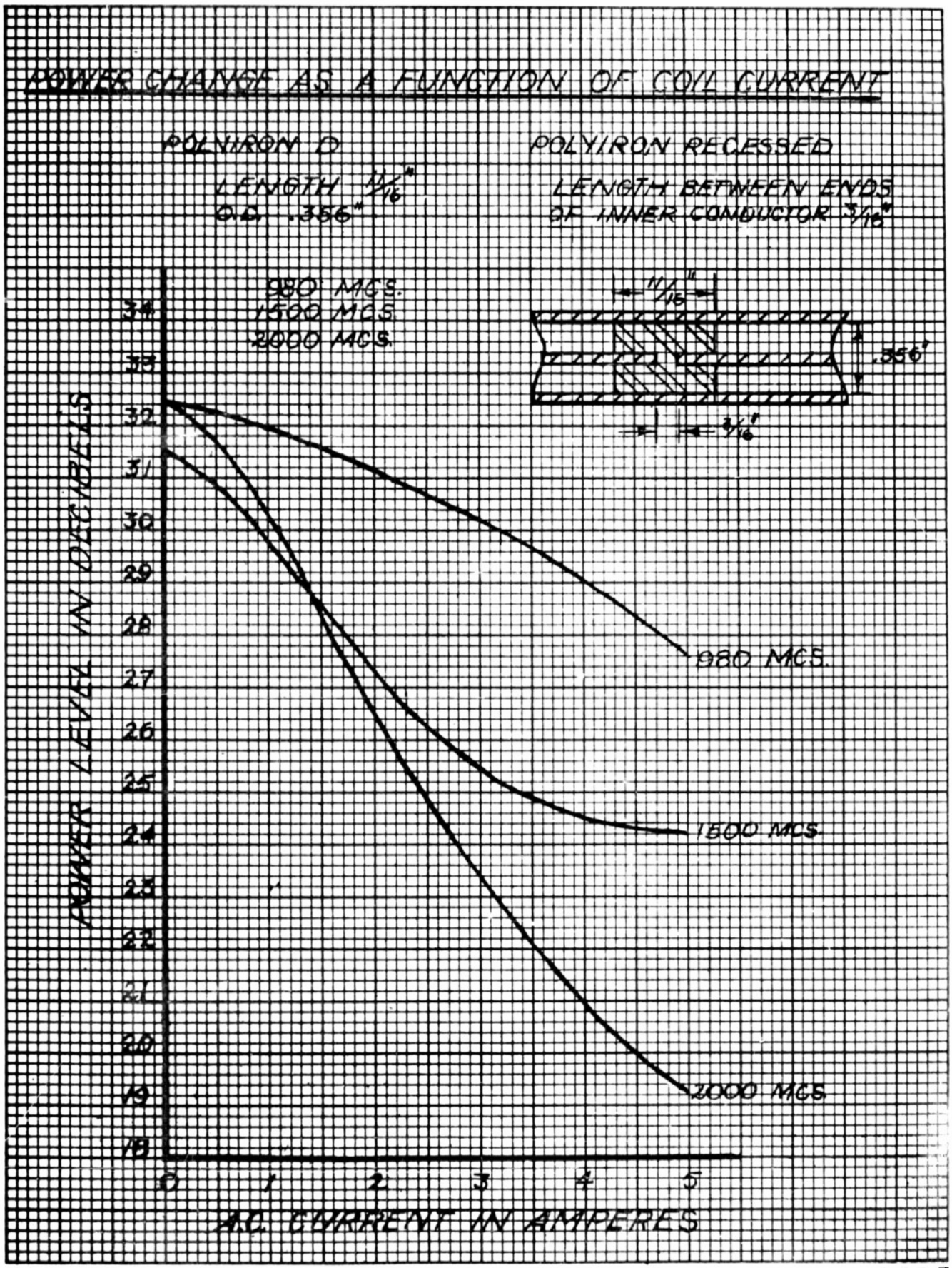
POWER CHANGE AS A FUNCTION OF COIL CURRENT
POLYIRON D
LENGTH 11/16"
O.D. .356"
980 MCS.
1500 MCS.
2000 MCS.
POLYIRON RECESSED
LENGTH BETWEEN ENDS
OF INNER CONDUCTOR 3/16"
11/16"
.356"
3/16"
POWER CHANGE IN MICRO-WATTS
34
33
32
31
30
29
28
27
26
25
24
23
22
21
20
19
18
980 MCS.
1500 MCS.
2000 MCS.
0
1
2
3
4
5
A.C. CURRENT IN AMPERES

M.R.I. 12935

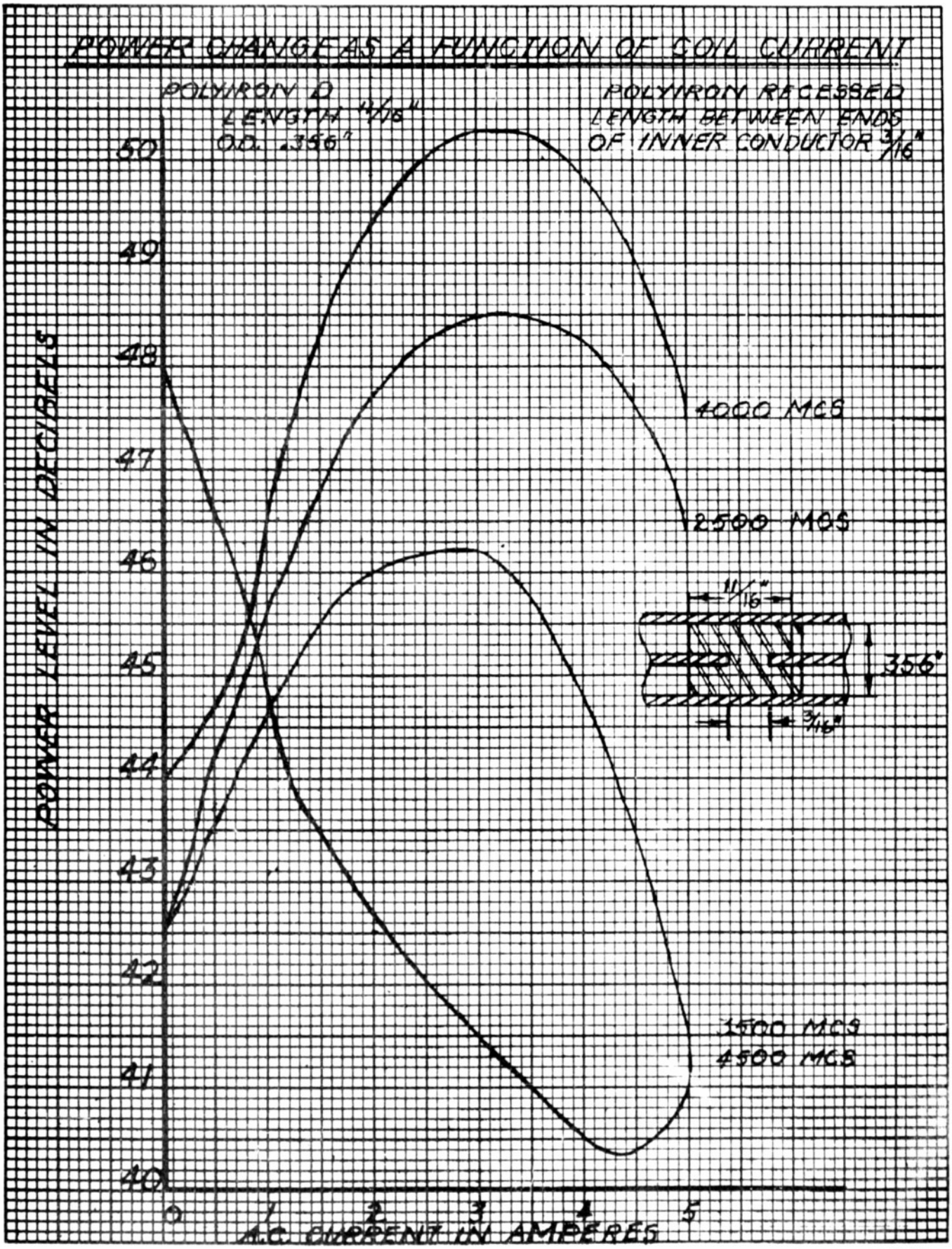
POWER CHANGE AS A FUNCTION OF COIL CURRENT
POLYIRON D
LENGTH 11/16"
O.D. .356"
POLYIRON RECESSED
LENGTH BETWEEN ENDS
OF INNER CONDUCTOR 3/16"
50
49
48
47
46
45
44
43
42
41
40
POWER LEVEL IN DECIBELS
4000 MCS
2500 MCS
1500 MCS
4500 MCS
11/16"
.356"
3/16"
0
1
2
3
4
5
A.C. CURRENT IN AMPERES

M.R.I. 12936

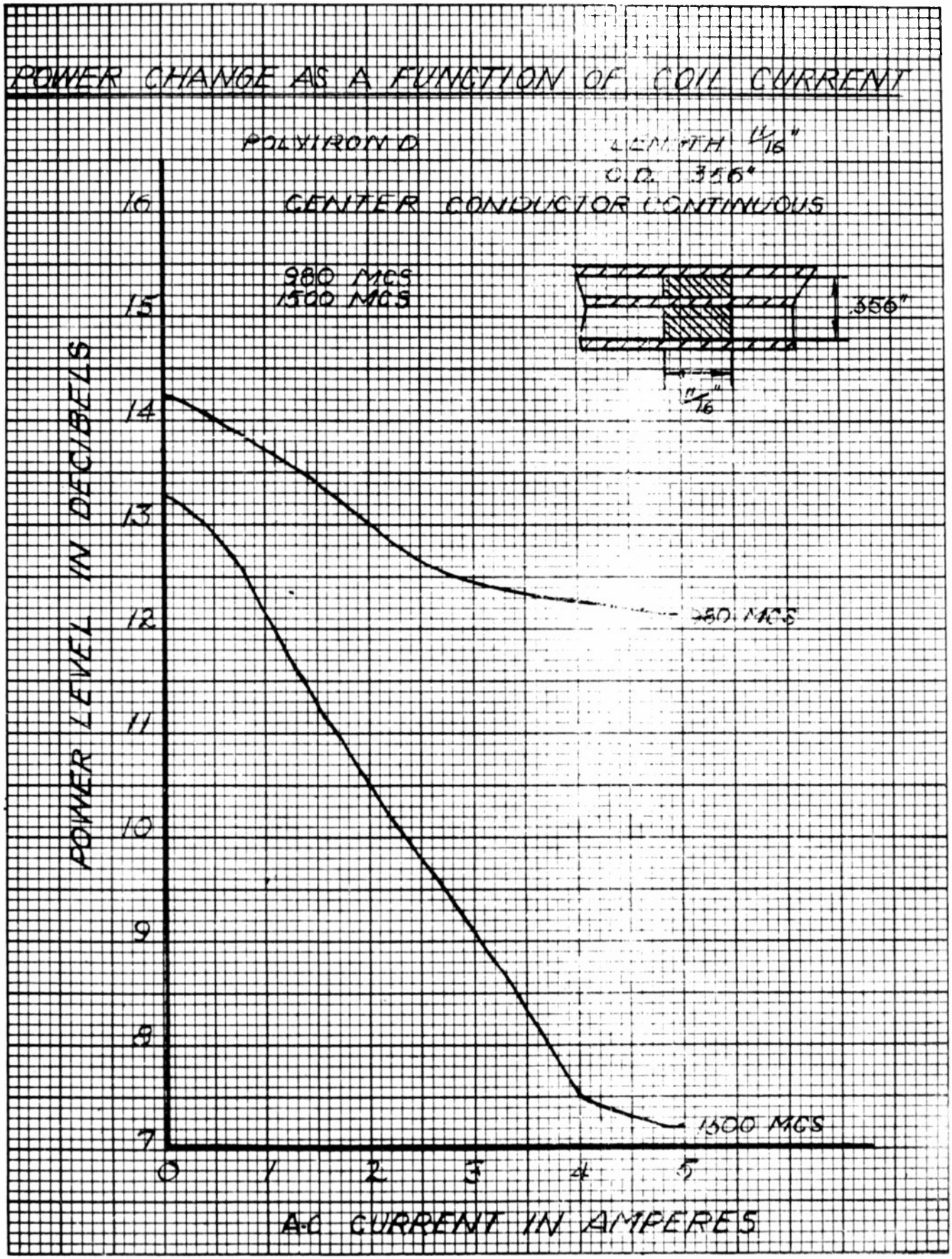
POWER CHANGE AS A FUNCTION OF COIL CURRENT
POLYIRON D
LENGTH 11/16"
O.D. .356"
CENTER CONDUCTOR CONTINUOUS
980 MCS
1500 MCS
.356"
1/16"
250 MCS
1500 MCS
POWER LEVEL IN DECIBELS
16
15
14
13
12
11
10
9
8
7
0
1
2
3
4
5
A-C CURRENT IN AMPERES

M.R.I. 12937

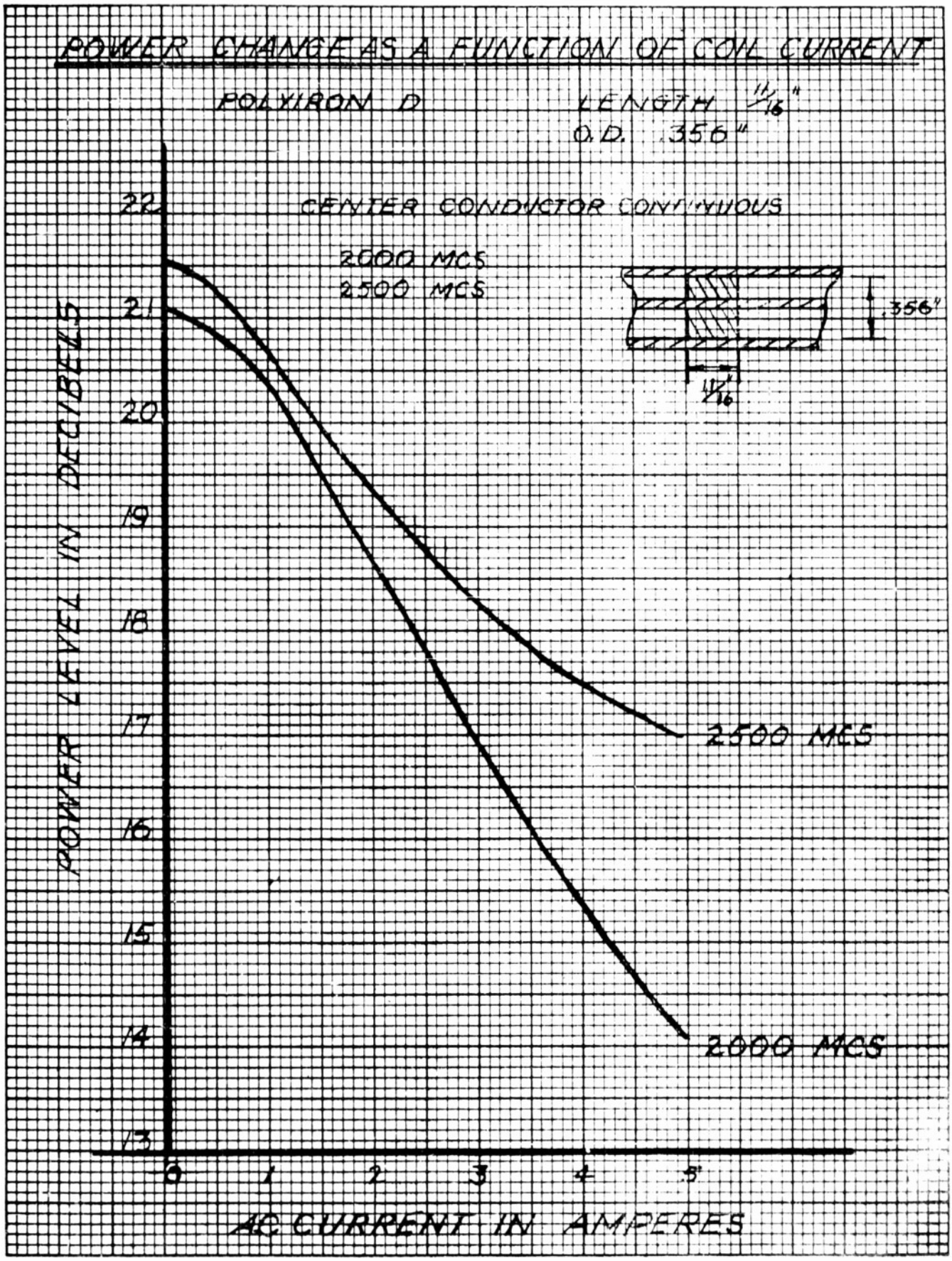
POWER CHANGE AS A FUNCTION OF COIL CURRENT
POLYIRON D
LENGTH 11/16"
O.D. .356"
CENTER CONDUCTOR CONTINUOUS
2000 MCS
2500 MCS
.356"
11/16"
POWER LEVEL IN DECIBELS
22
21
20
19
18
17
16
15
14
13
2500 MCS
2000 MCS
0
1
2
3
4
5
AC CURRENT IN AMPERES

M.R.I. 12938

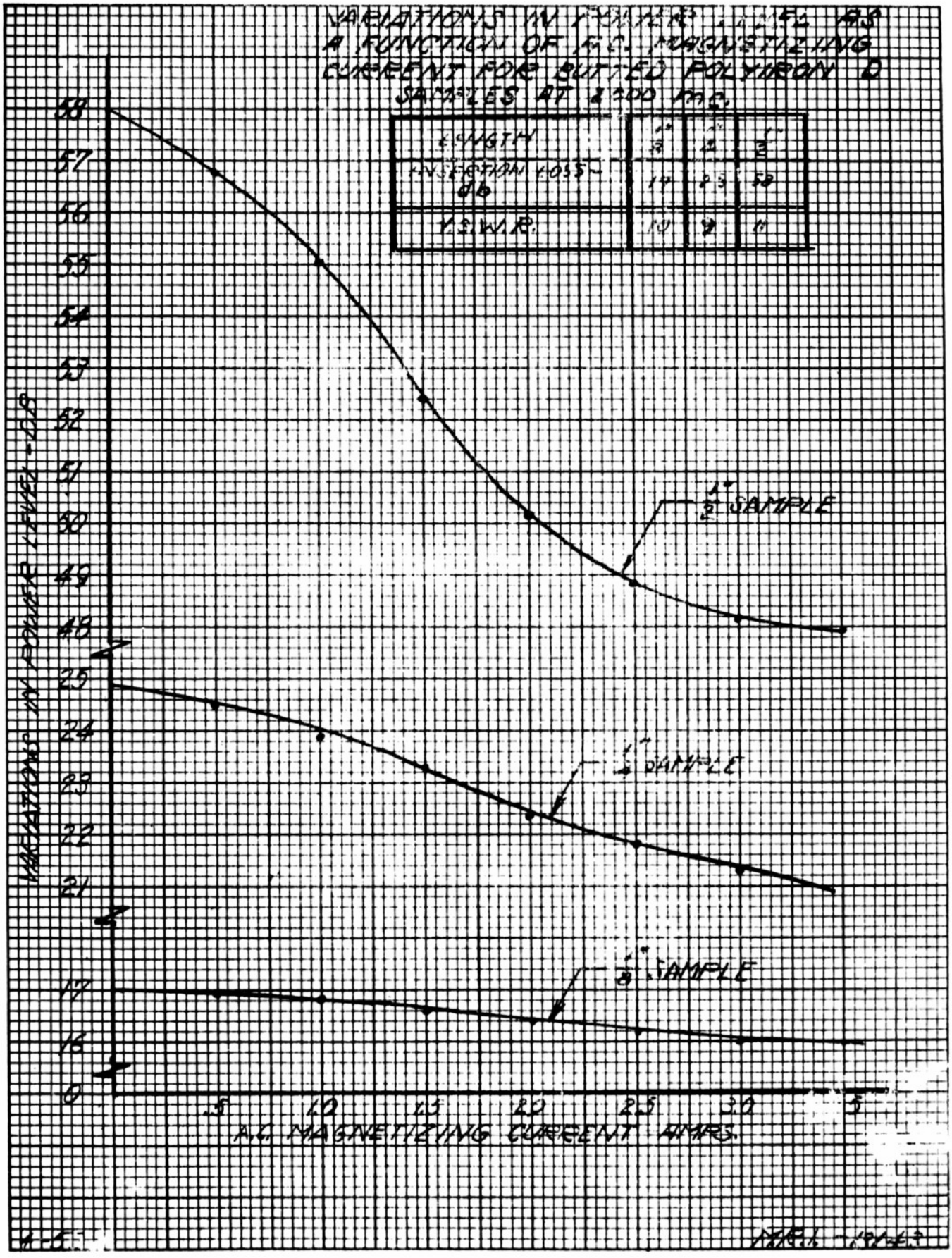
VARIATIONS IN PERMEABILITY AS A FUNCTION OF A.C. MAGNETIZING CURRENT FOR CUT CO POLYIRON D SAMPLES AT 2700 ~ C.
LENGTH
PENETRATION LOSS - db
P.I.W.R.
1"
1/2"
1/8"
1/2" SAMPLE
1/8" SAMPLE
PERMEABILITY - GAUSS/OERSTED
A.C. MAGNETIZING CURRENT AMPS.

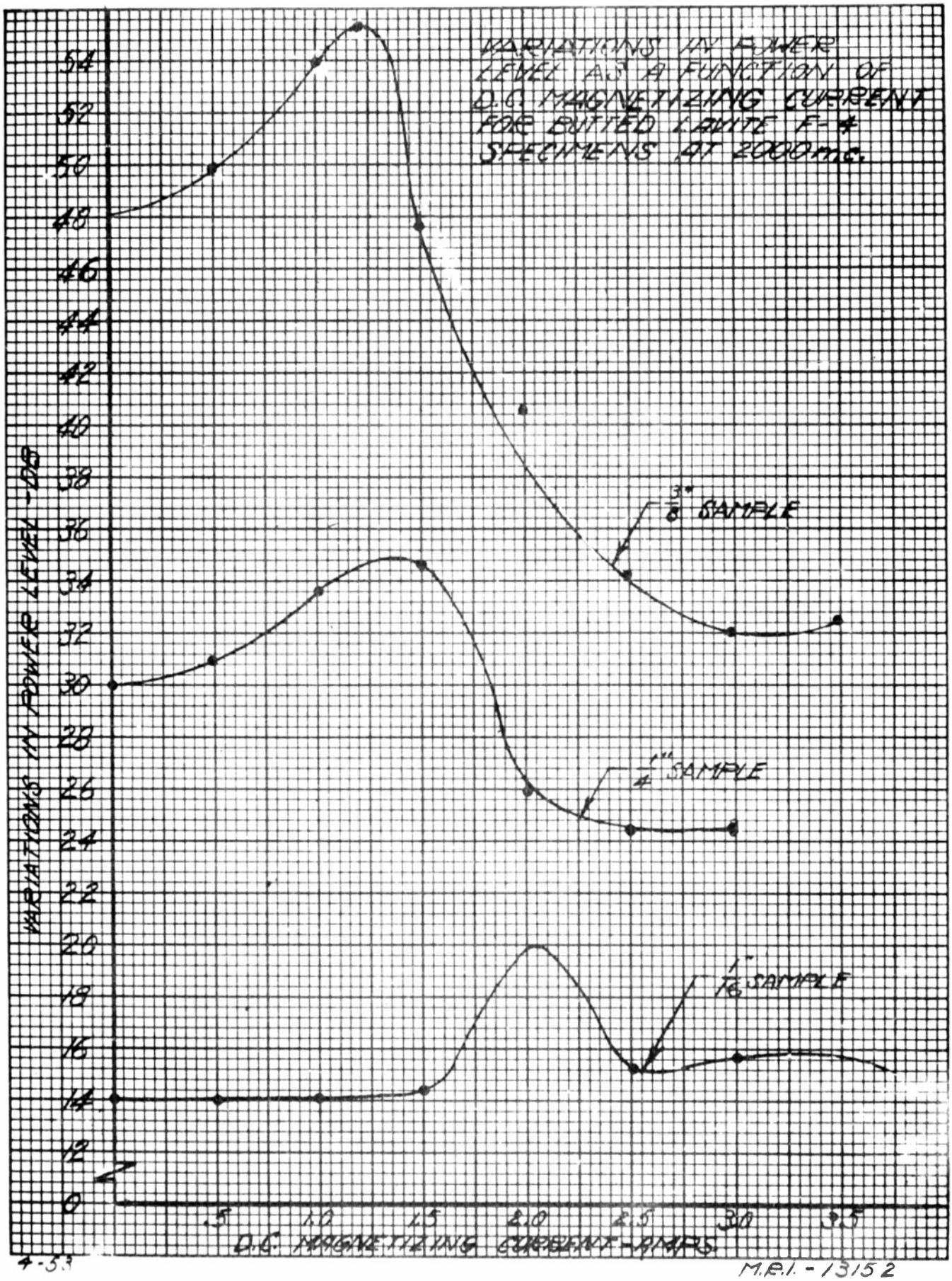
VARIATIONS IN POWER LEVEL - DB
54
52
50
48
46
44
42
40
38
36
34
32
30
28
26
24
22
20
18
16
14
12
0
.5
1.0
1.5
2.0
2.5
3.0
3.5
D.C. MAGNETIZING CURRENT - AMPS.
VARIATIONS IN POWER LEVEL AS A FUNCTION OF D.C. MAGNETIZING CURRENT FOR BUTTED JOINTS OF F-4 SPECIMENS AT 2000mc.
3" SAMPLE
1" SAMPLE
1/16" SAMPLE

4-33

M.E.I. - 1352

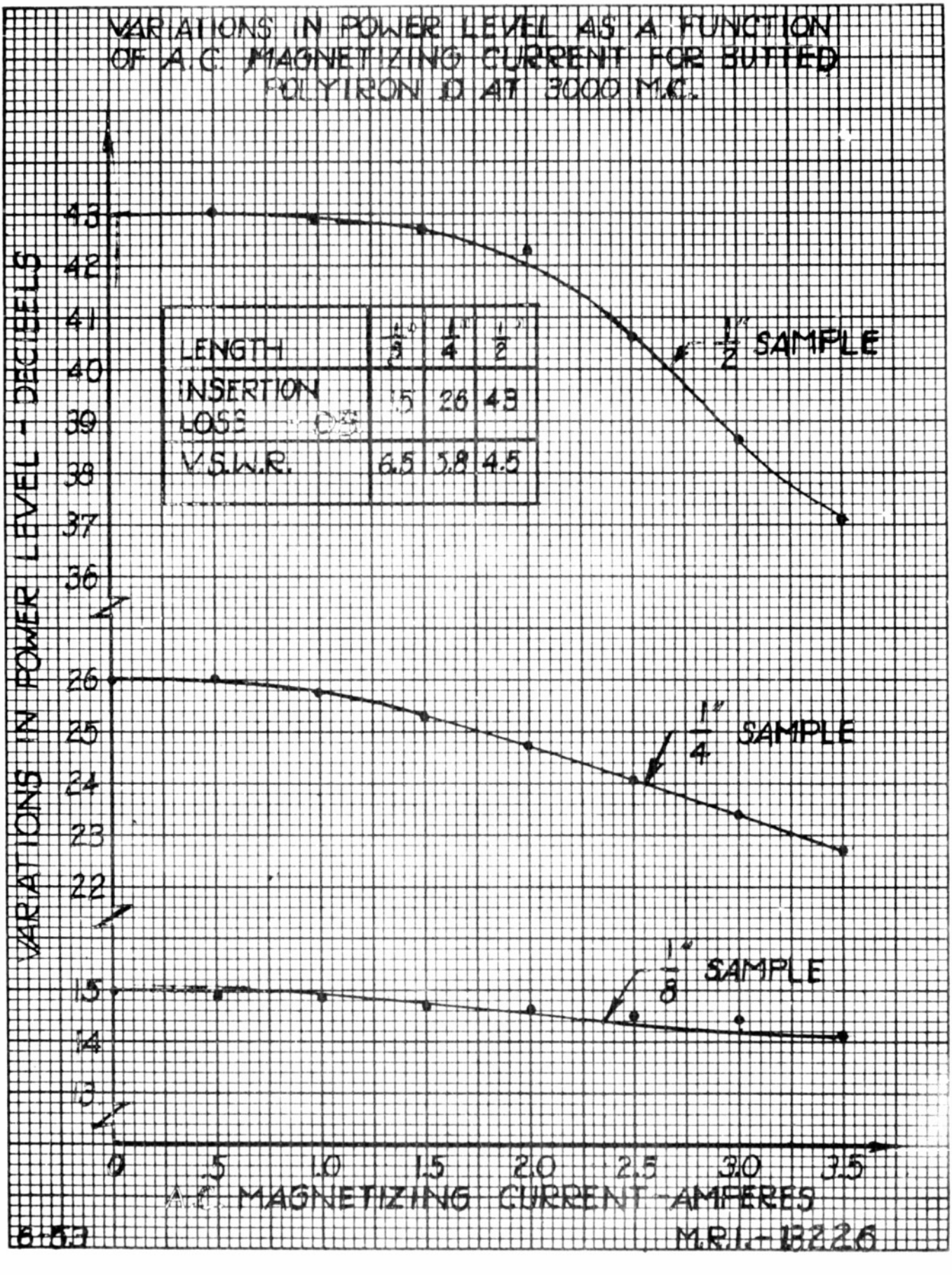
VARIATIONS IN POWER LEVEL AS A FUNCTION OF A.C. MAGNETIZING CURRENT FOR BUTTED POLYIRON ID AT 3000 M.C.
VARIATIONS IN POWER LEVEL IN DECIBELS
43
42
41
40
39
38
37
36
26
25
24
23
22
15
14
13
0
.5
1.0
1.5
2.0
2.5
3.0
3.5
A.C. MAGNETIZING CURRENT - AMPERES
LENGTH
INSERTION LOSE DB
V.S.W.R.
1/8"
1/4"
1/2"
1.5
2.6
4.3
6.5
5.8
4.5
1/2" SAMPLE
1/4" SAMPLE
1/8" SAMPLE
6-53
M.R.I. - B226

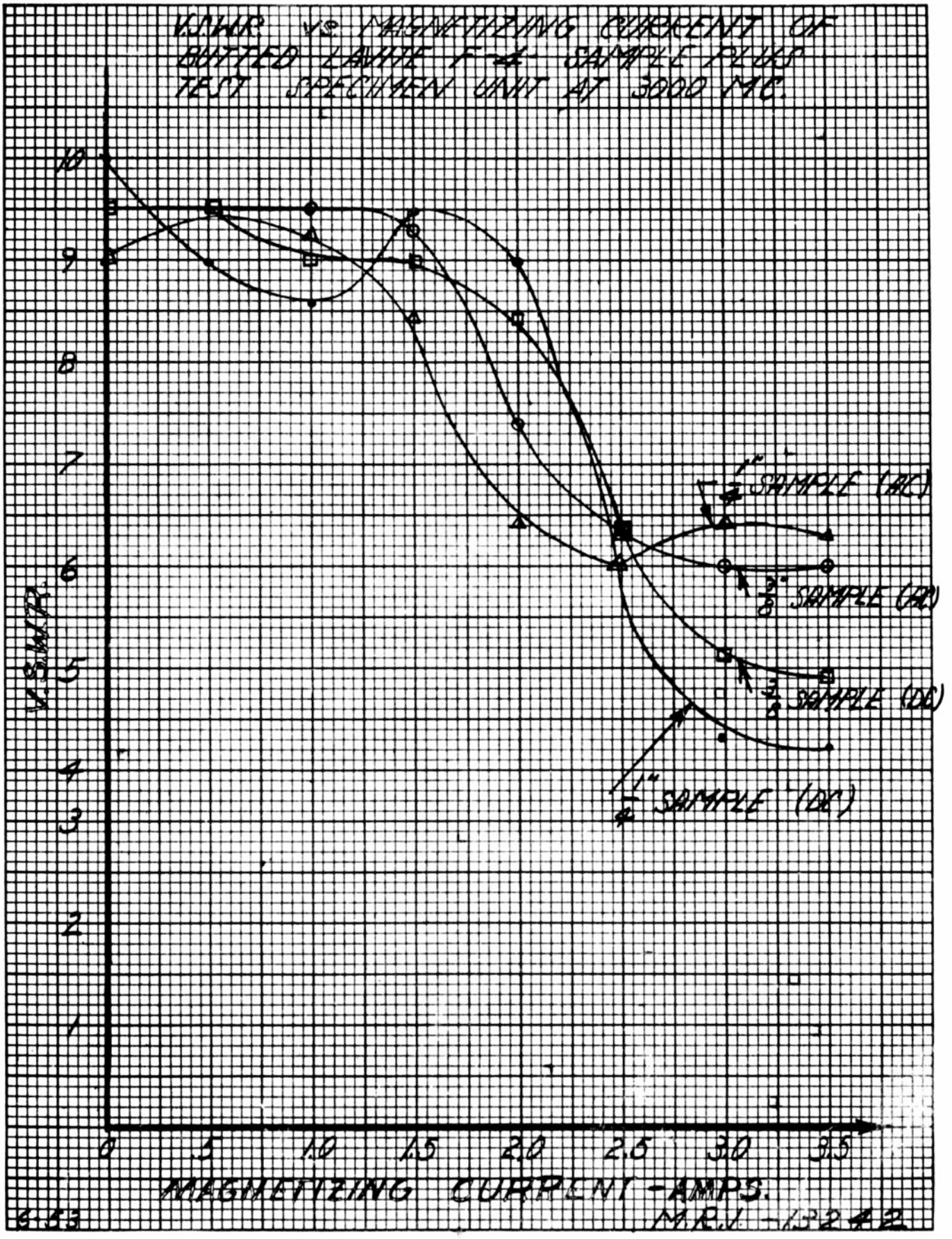
KILNER VS MAGNETIZING CURRENT OF BUTTED LAMINE F-4 SAMPLE PLUS TEST SPECIMEN UNIT AT 3000 MC.
10
9
8
7
6
5
4
3
2
1
0
.5
1.0
1.5
2.0
2.5
3.0
3.5
MAGNETIZING CURRENT - AMPS.
1/2" SAMPLE (AC)
3/8" SAMPLE (AC)
3/8" SAMPLE (DC)
1/2" SAMPLE (DC)
6.83
M.R.L. 1952 #2

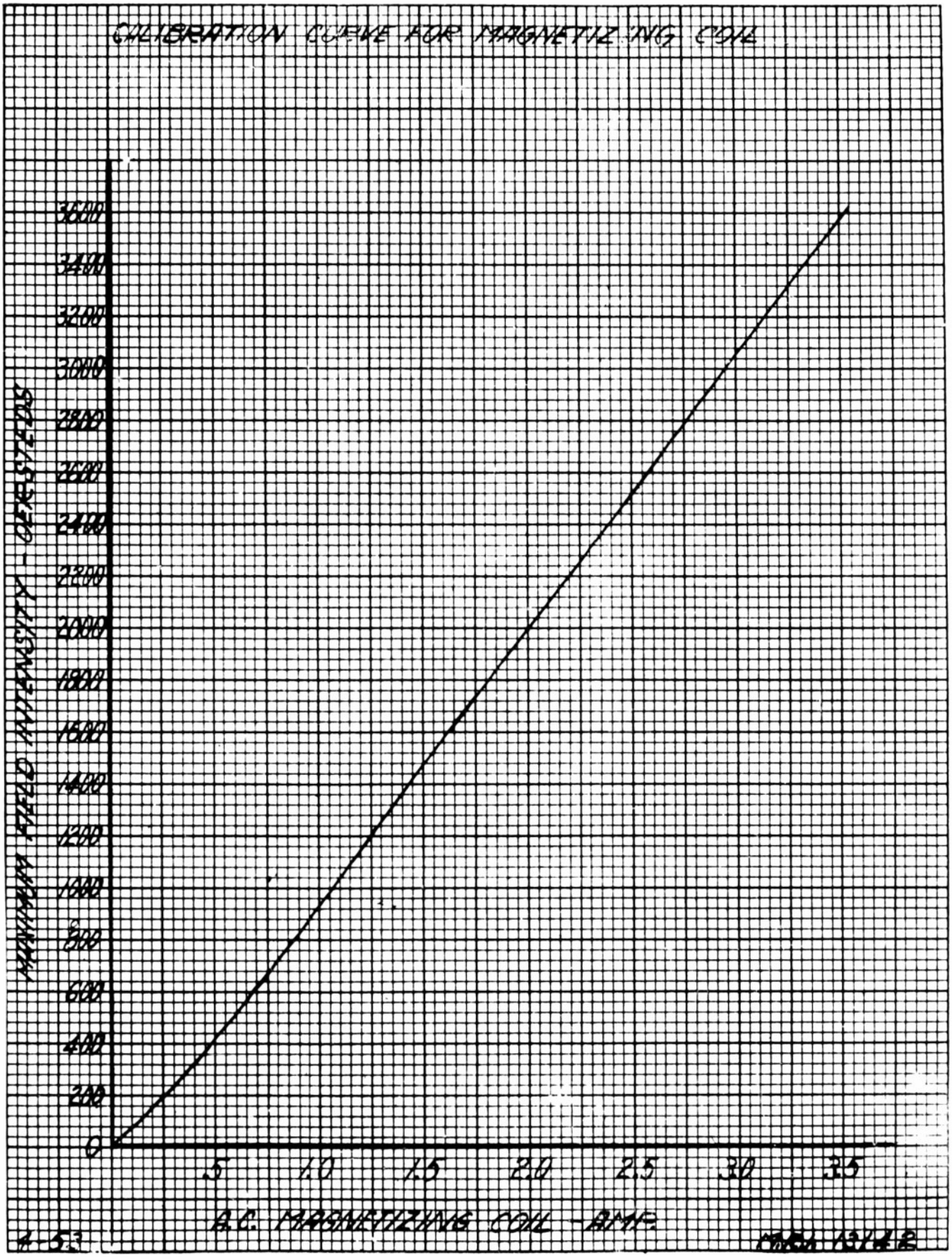
CALIBRATION CURVE FOR MAGNETIZING COIL
3600
3400
3200
3000
2800
2600
2400
2200
2000
1800
1600
1400
1200
1000
800
600
400
200
0
.5
1.0
1.5
2.0
2.5
3.0
3.5
A.C. MAGNETIZING COIL - RMS

V. S.W.R. v.s. A.C. MAGNETIZING CURRENT OF BUTTED LAVITE F – 4 SAMPLES PLUS TEST SPECIMEN UNIT AT 2000 MC

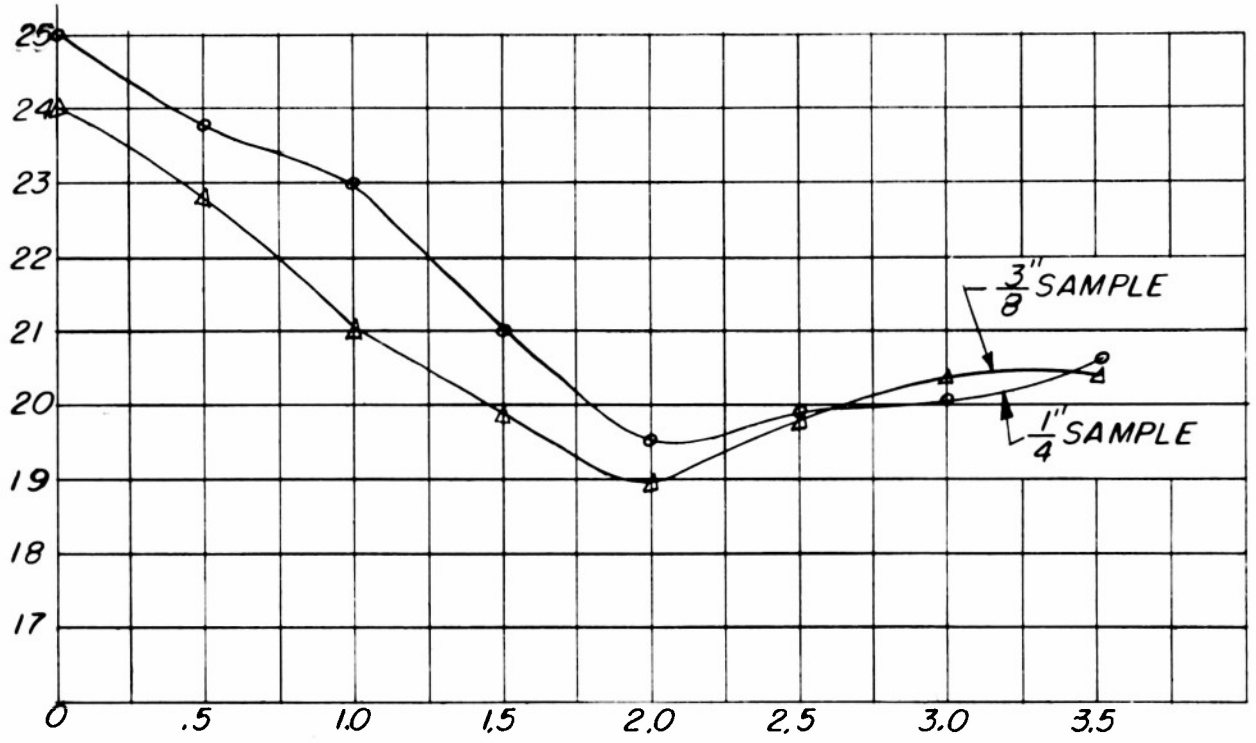

V. S.W.R. v.s D.C. MAGNETIZING CURRENT OF BUTTED LAVITE F – 4 SAMPLES PLUS TEST SPECIMEN UNIT AT 2000 MC

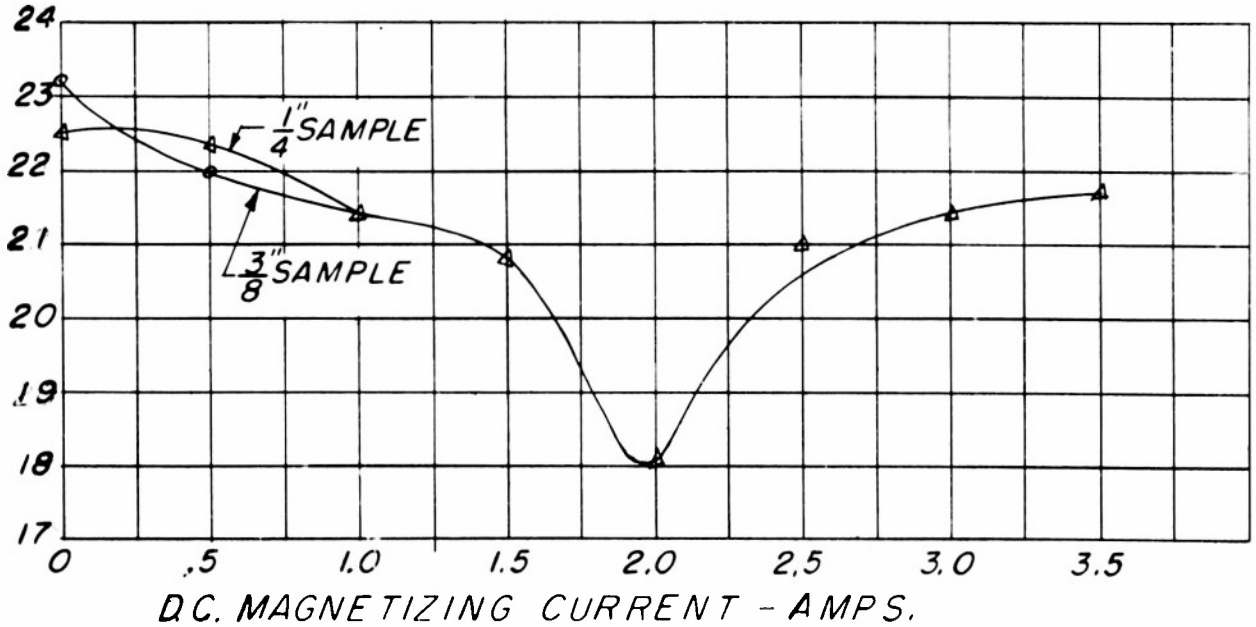

MRI - 13240

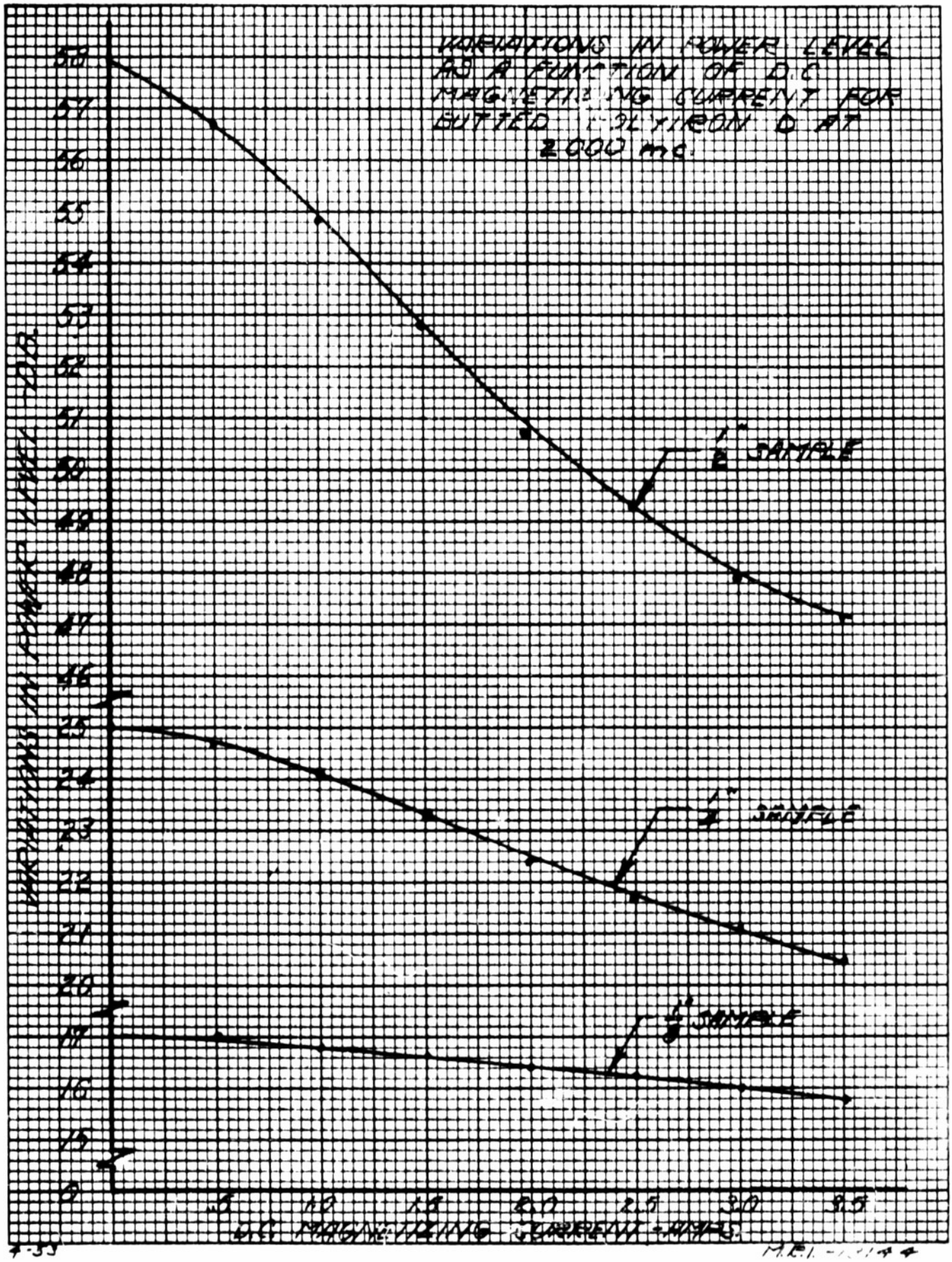
VARIATIONS IN POWER LOSS AS A FUNCTION OF D.C. MAGNETIZING CURRENT FOR SUTTED SILICON D AT 2000 mc.
1" SAMPLE
½" SAMPLE
¼" SAMPLE
D.C. MAGNETIZING CURRENT - AMPS.

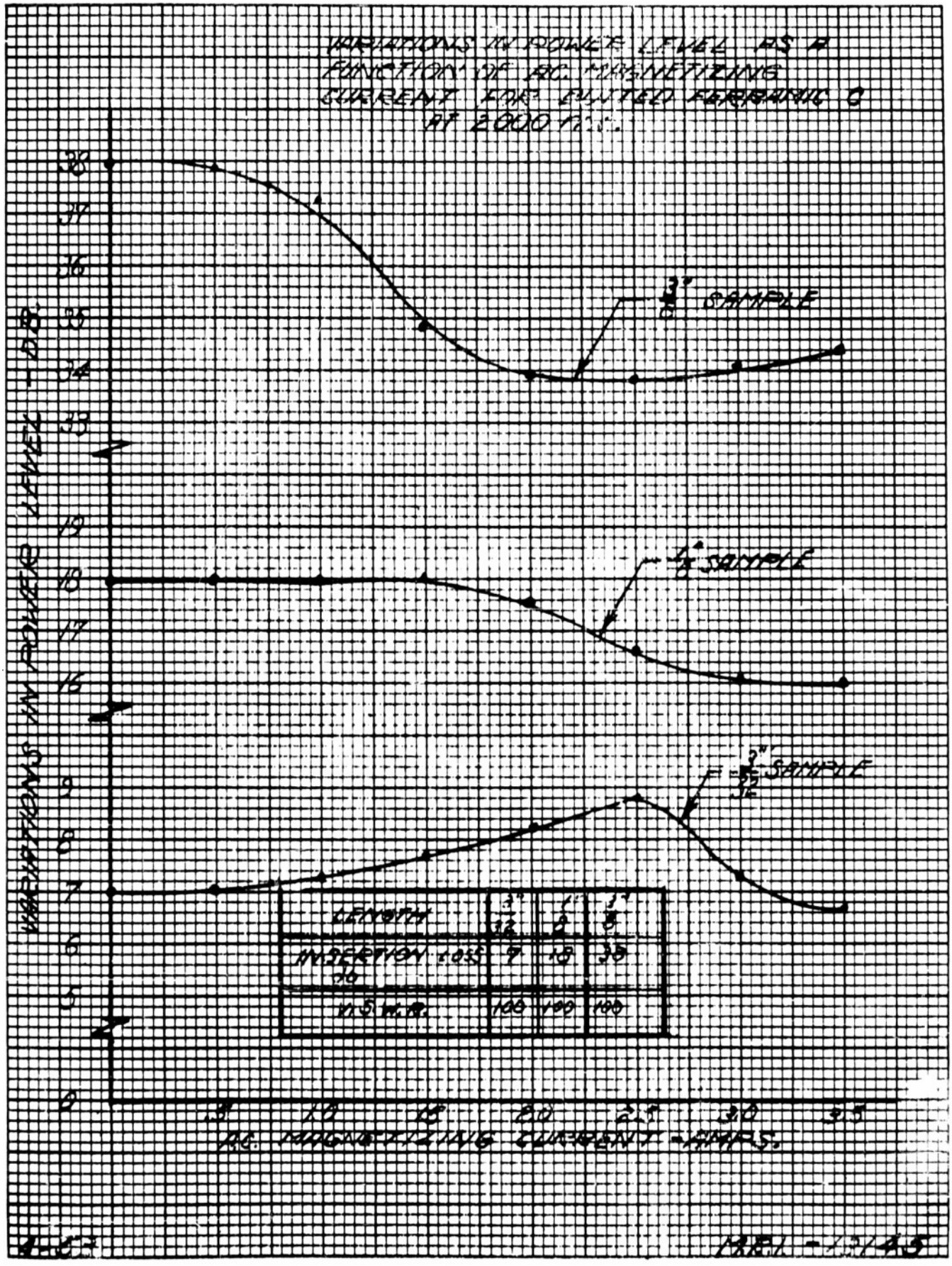
VARIATIONS IN POWER LOSS AS A FUNCTION OF AC. MAGNETIZING CURRENT FOR SINTERED FERROMAGNETIC CORES AT 20000 C.P.S.
VARIATIONS IN POWER LOSS IN WATTS
3" sample
1/2" sample
3/4" sample
LENGTH
3/32"
1/2"
3/4"
INSERTION LOSS IN DB
7
10
30
MAGNETIZING CURRENT IN M.A.
100
100
100
AC. MAGNETIZING CURRENT IN M.A.

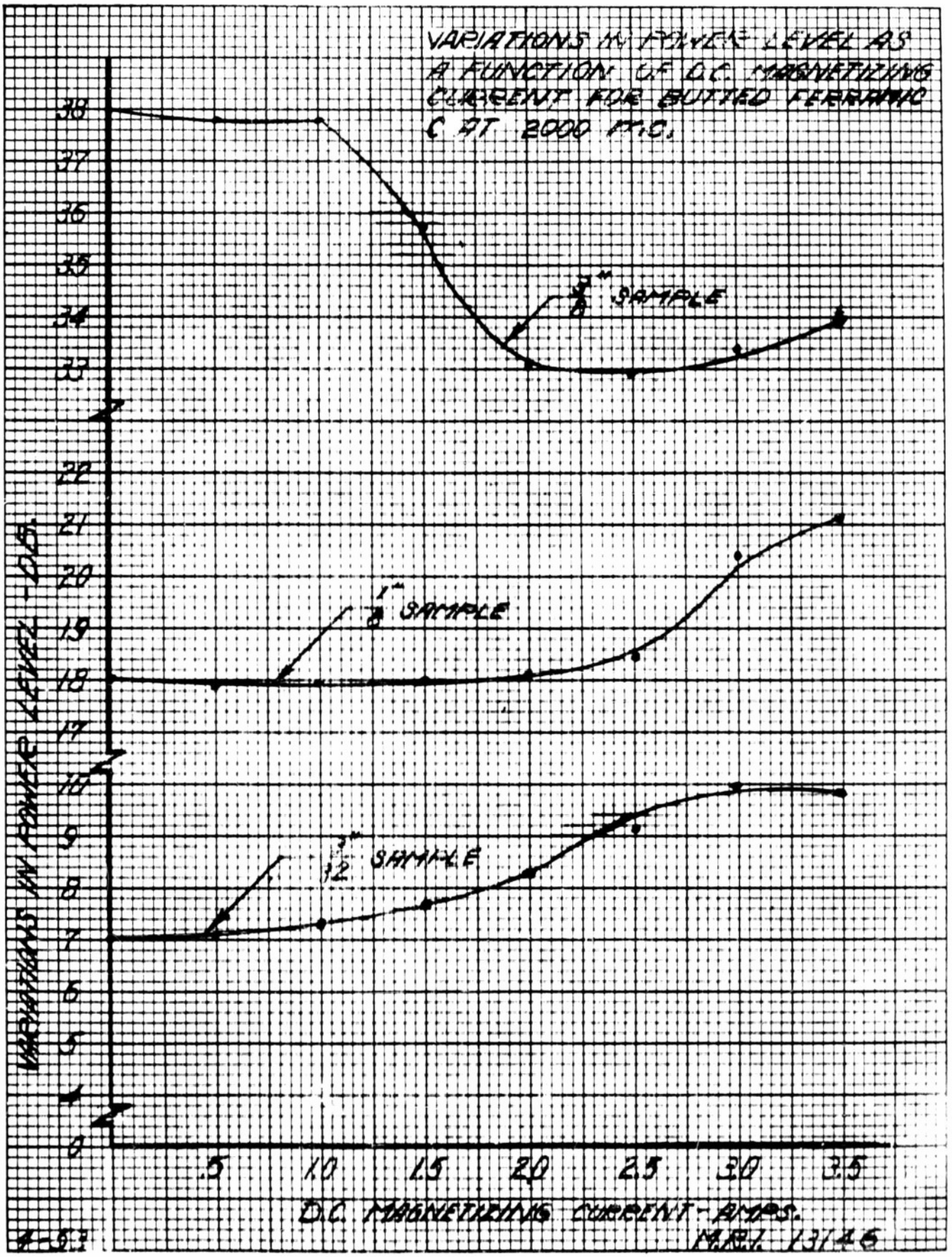
VARIATIONS IN POWER LEVEL AS A FUNCTION OF D.C. MAGNETIZING CURRENT FOR BUTTED FERRAMIC C AT 2000 M.C.
3/8" SAMPLE
1/8" SAMPLE
1/2" SAMPLE
VARIATIONS IN POWER LEVEL - DB.
38
37
36
35
34
33
22
21
20
19
18
17
10
9
8
7
6
5
4
2
0
5
10
15
20
25
30
35
D.C. MAGNETIZING CURRENT - AMPS.
4-5.2
MR. 13146

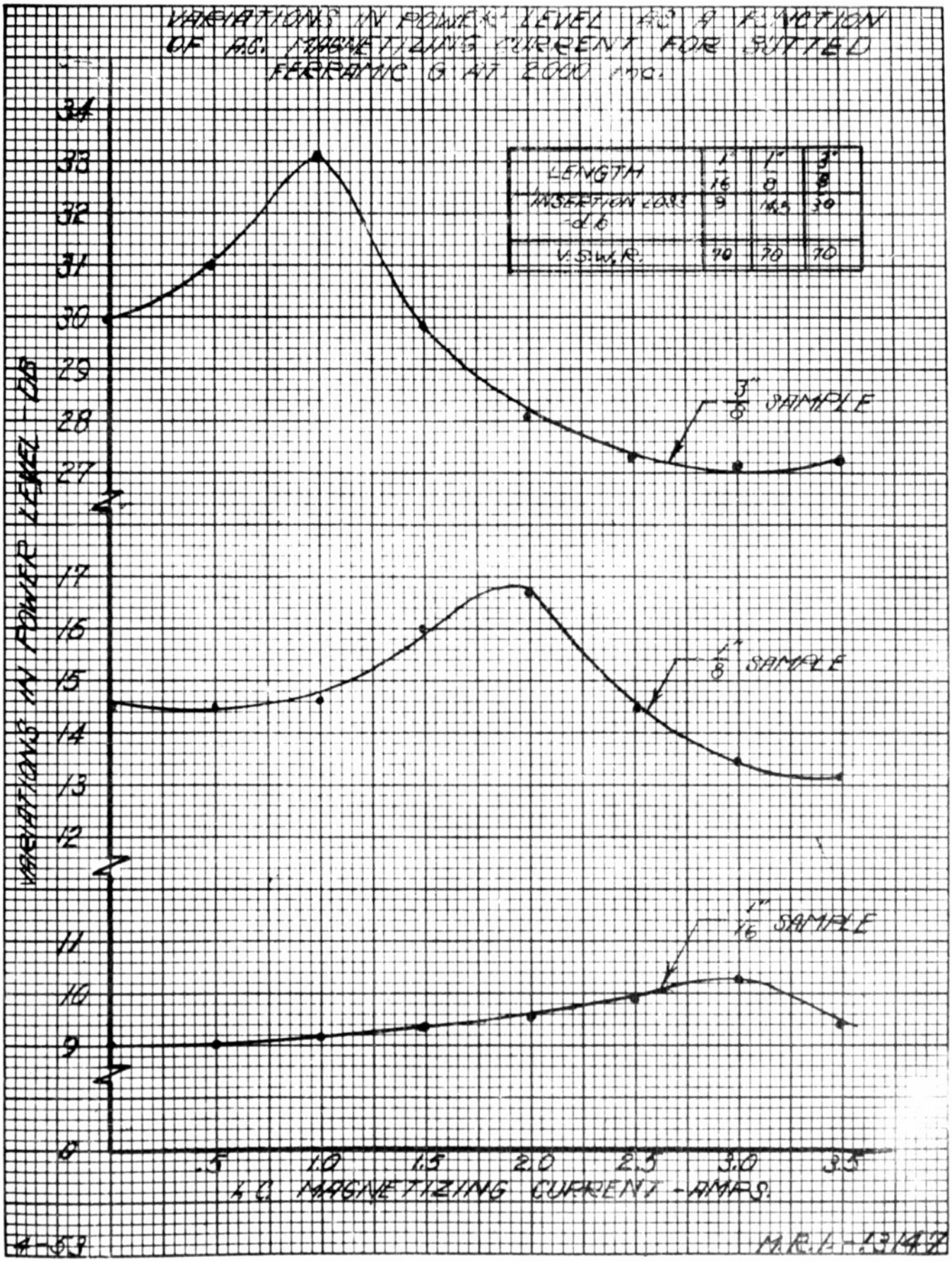
VARIATIONS IN POWER LEVEL AS A FUNCTION OF A.C. MAGNETIZING CURRENT FOR SINTERED FERRAMIC G AT 2000 KC.
LENGTH
INSERTION LOSS -d.b
V.S.W.R.
1/16
3
70
1"
8
14.5
70
3"
8
30
70
VARIATIONS IN POWER LEVEL DB
34
33
32
31
30
29
28
27
17
16
15
14
13
12
11
10
9
8
3/8" SAMPLE
1/8" SAMPLE
1/16" SAMPLE
.5
1.0
1.5
2.0
2.5
3.0
3.5
A.C. MAGNETIZING CURRENT - AMPS.
4-63
M.E.L. - 13448

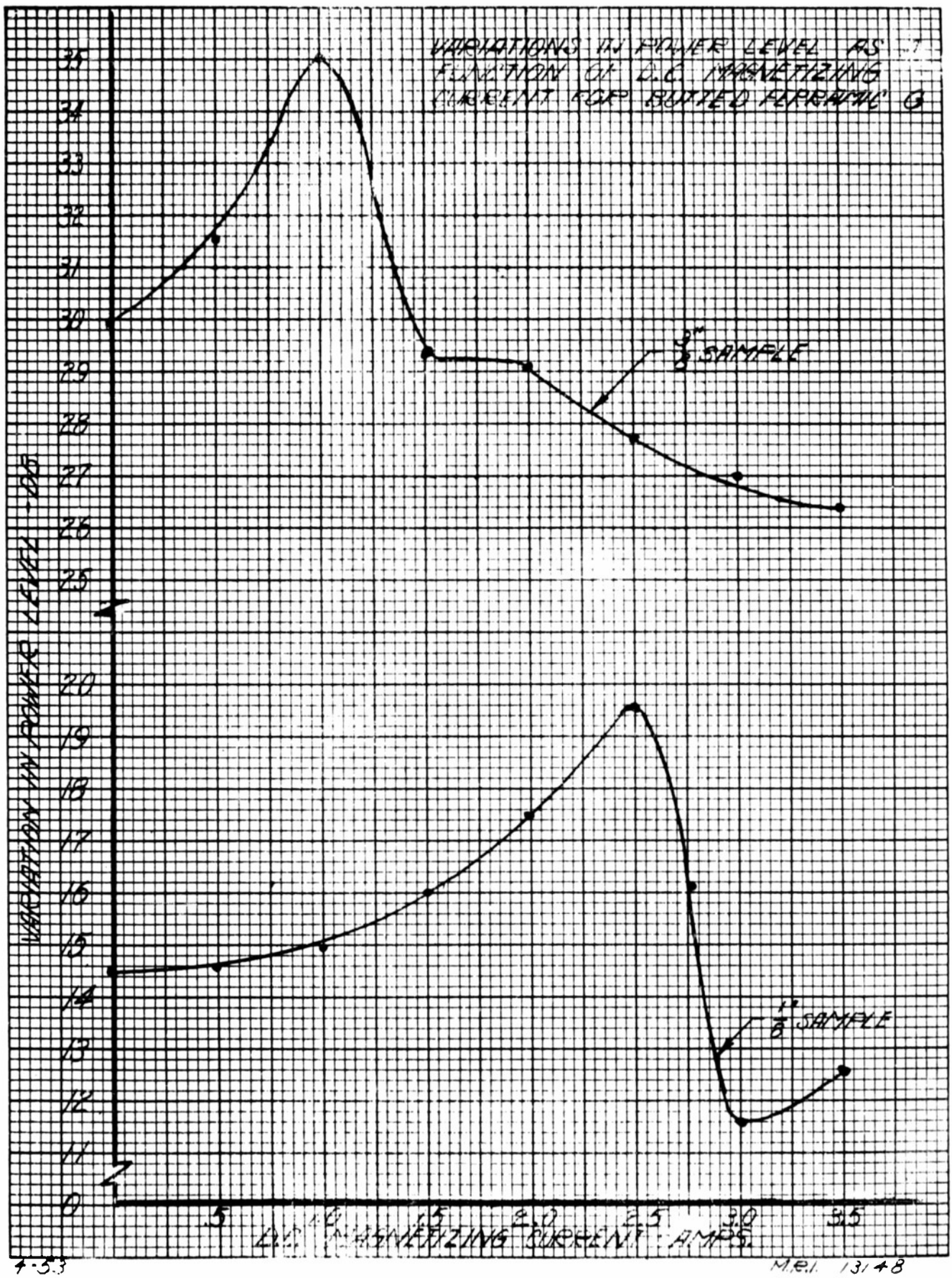

4-5-3

M.E.I. 13148

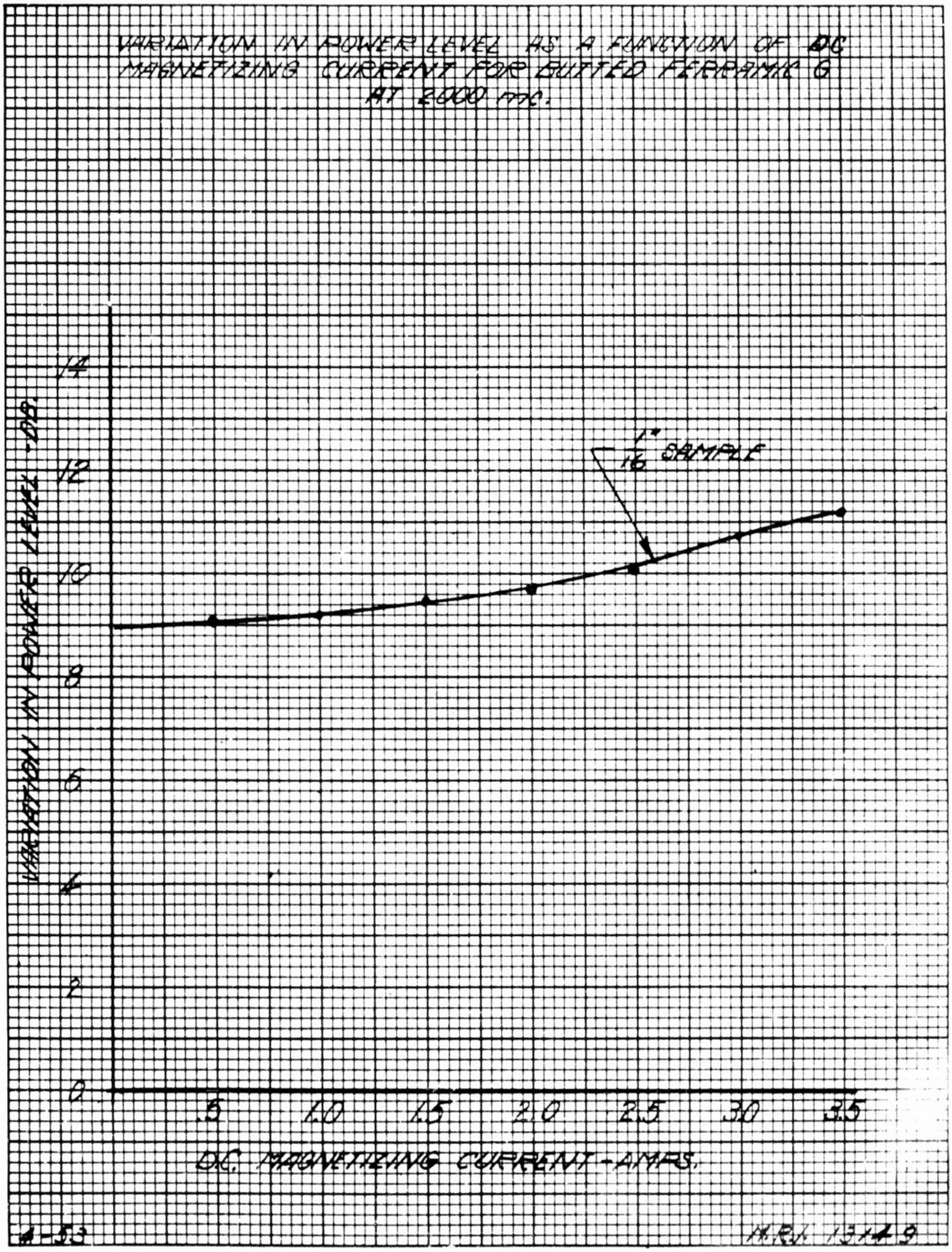
VARIATION IN POWER LEVEL AS A FUNCTION OF DC
MAGNETIZING CURRENT FOR BUTTED FERRAMIC G
AT 2000 mc.
VARIATION IN POWER LEVEL -DB.
14
12
10
8
6
4
2
0
.5
1.0
1.5
2.0
2.5
3.0
3.5
D.C. MAGNETIZING CURRENT - AMPS.
1/16" SAMPLE
A-53

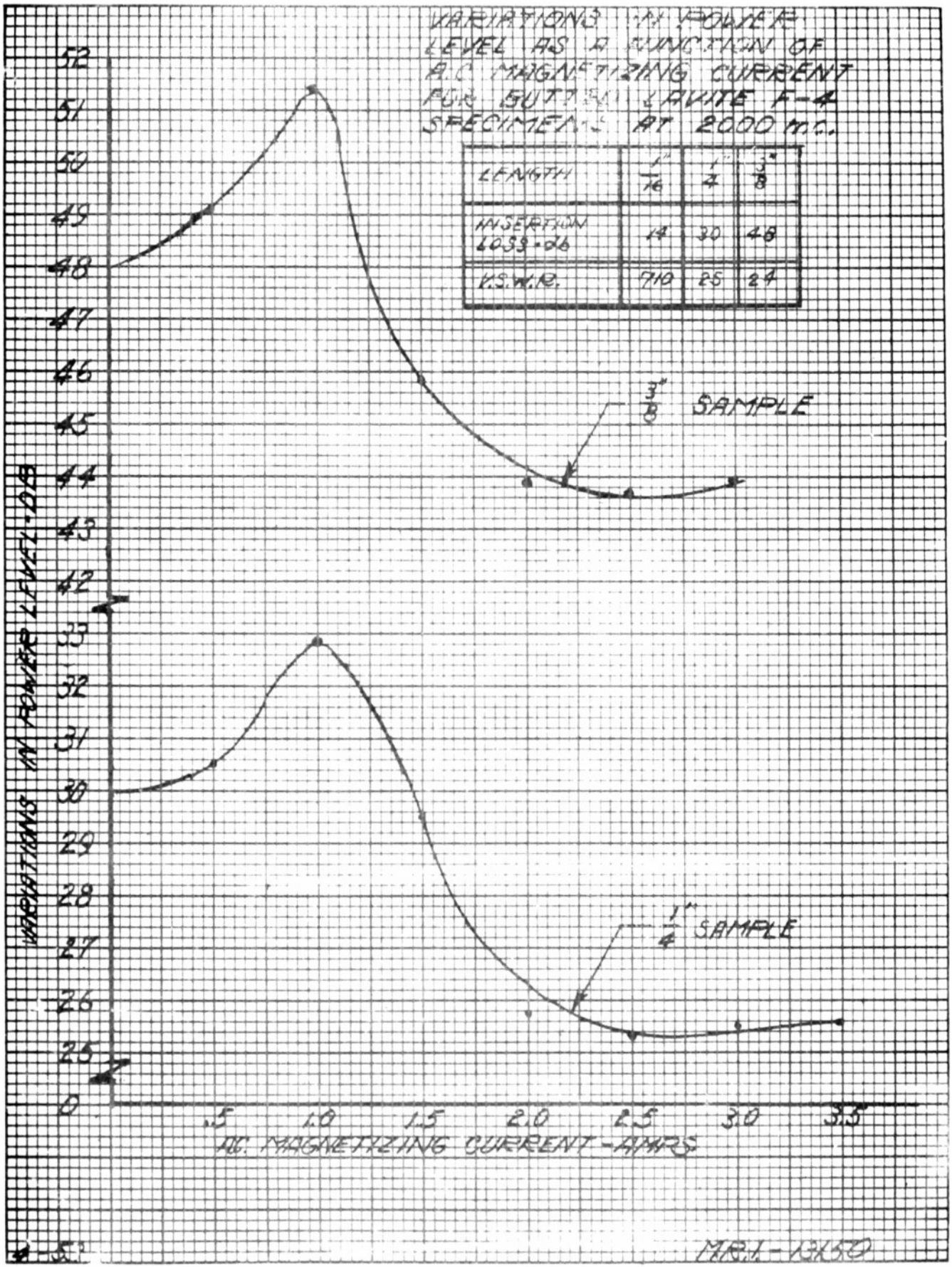
VARIATIONS IN POWER LEVEL AS A FUNCTION OF A.C. MAGNETIZING CURRENT FOR GUTTA PERCHA SPECIMENS AT 2000 MC.
LENGTH
1/16"
1/4"
3/8"
INSERTION LOSS - DB
14
30
48
V.S.W.R.
7.10
2.5
2.4
3/8" SAMPLE
1/4" SAMPLE
VARIATIONS IN POWER LEVEL - DB
52
51
50
49
48
47
46
45
44
43
42
33
32
31
30
29
28
27
26
25
0
.5
1.0
1.5
2.0
2.5
3.0
3.5
A.C. MAGNETIZING CURRENT - AMPS.
MR.1-13650

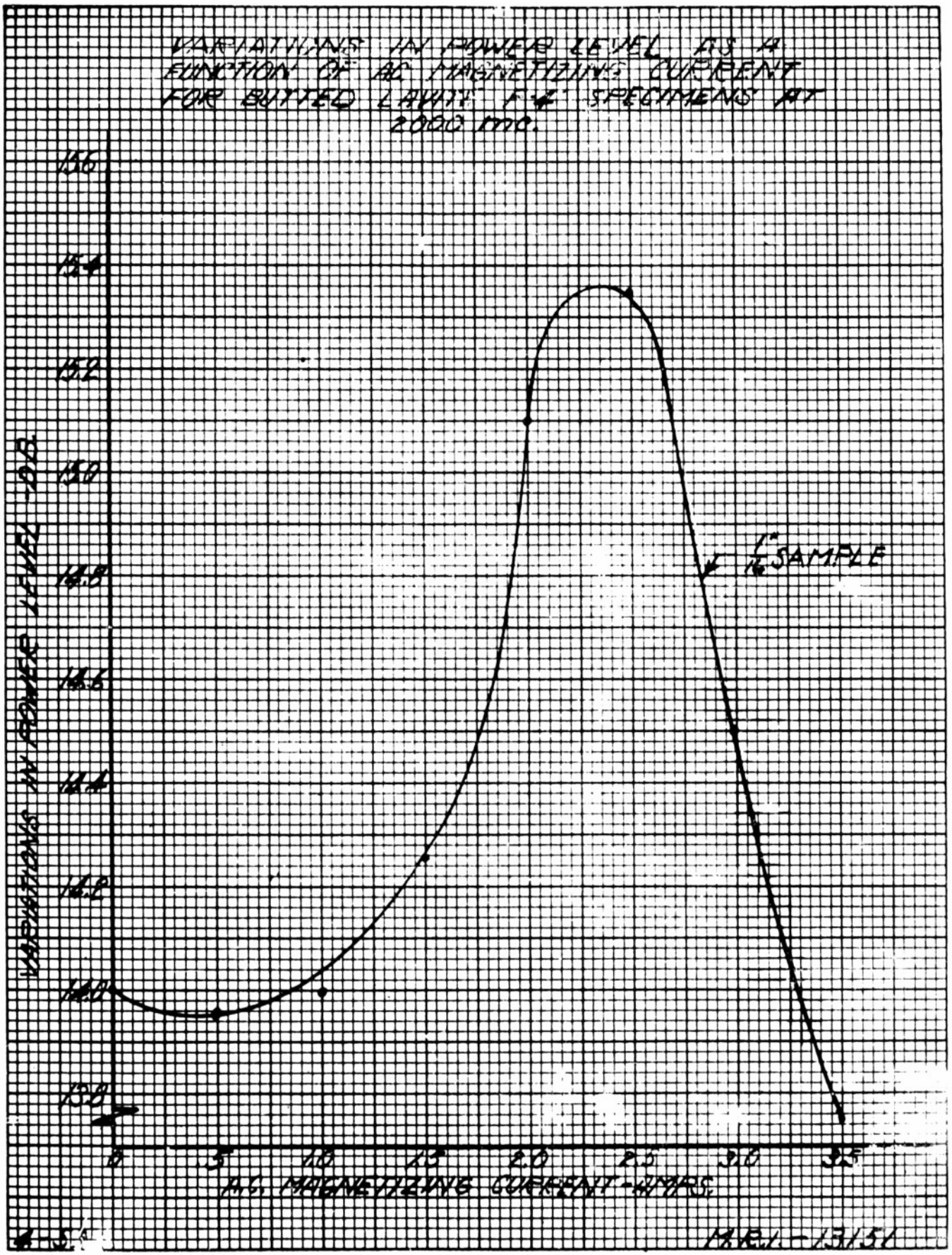
VARIATIONS IN POWER LEVEL AS A FUNCTION OF AC MAGNETIZING CURRENT FOR BUTTED LAYUP OF SPECIMENS AT 2000 PPG.
15.6
15.4
15.2
15.0
14.8
14.6
14.4
14.2
14.0
13.8
VARIATIONS IN POWER LEVEL - DB
SAMPLE
0
.5
1.0
1.5
2.0
2.5
3.0
3.5
A.C. MAGNETIZING CURRENT - AMPS.
4-5
NAVAL - 13151

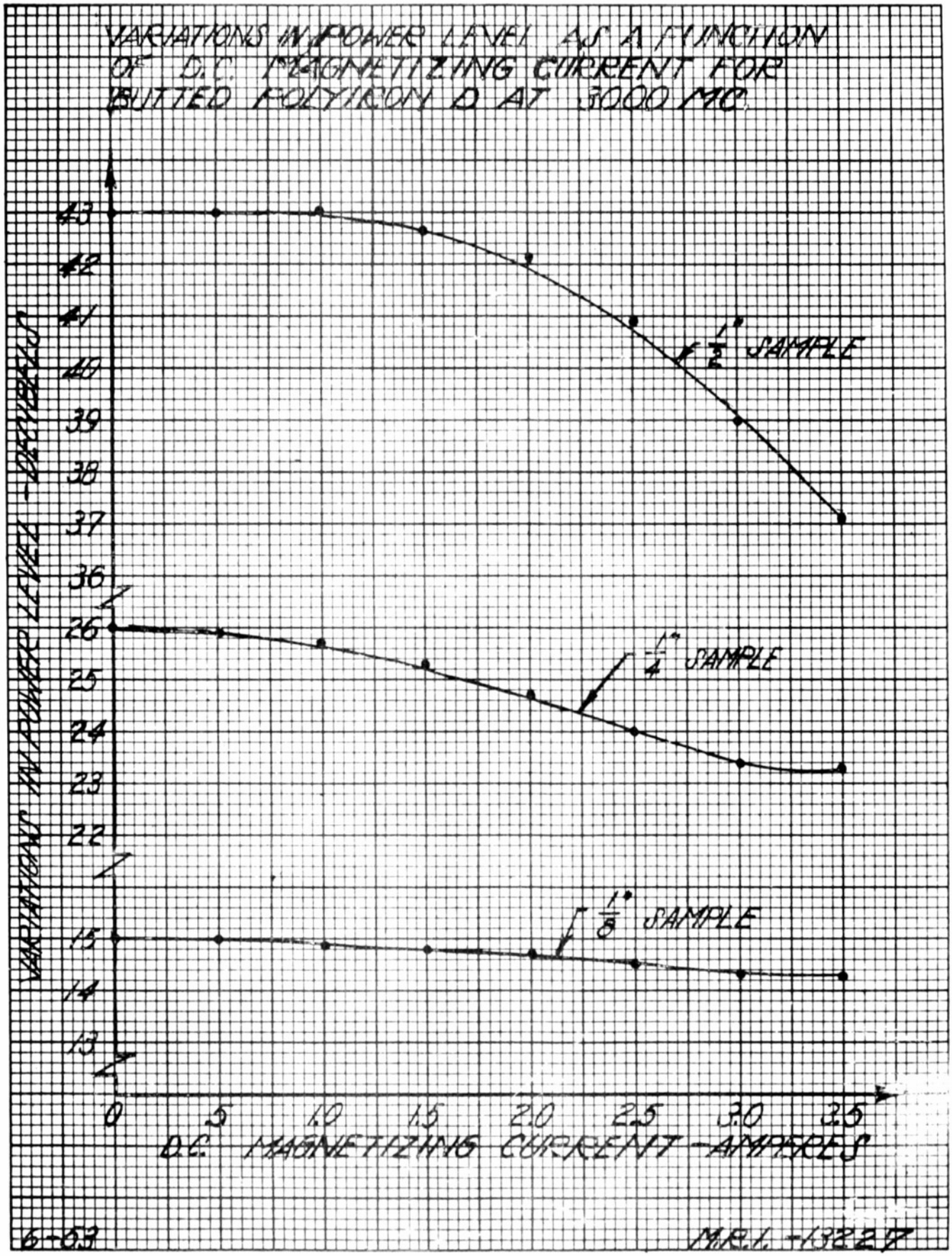
VARIATIONS IN POWER LEVEL AS A FUNCTION OF D.C. MAGNETIZING CURRENT FOR BUTTED FOSTERITE DISC AT 3000 MC.
43
42
41
40
39
38
37
36
26
25
24
23
22
15
14
13
0
.5
1.0
1.5
2.0
2.5
3.0
3.5
1/2" SAMPLE
1/4" SAMPLE
1/8" SAMPLE
VARIATIONS IN POWER LEVEL - DECIBELS BELOW 1 MILLIWATT
D.C. MAGNETIZING CURRENT - AMPERES
6-53
M.R.L. -13228

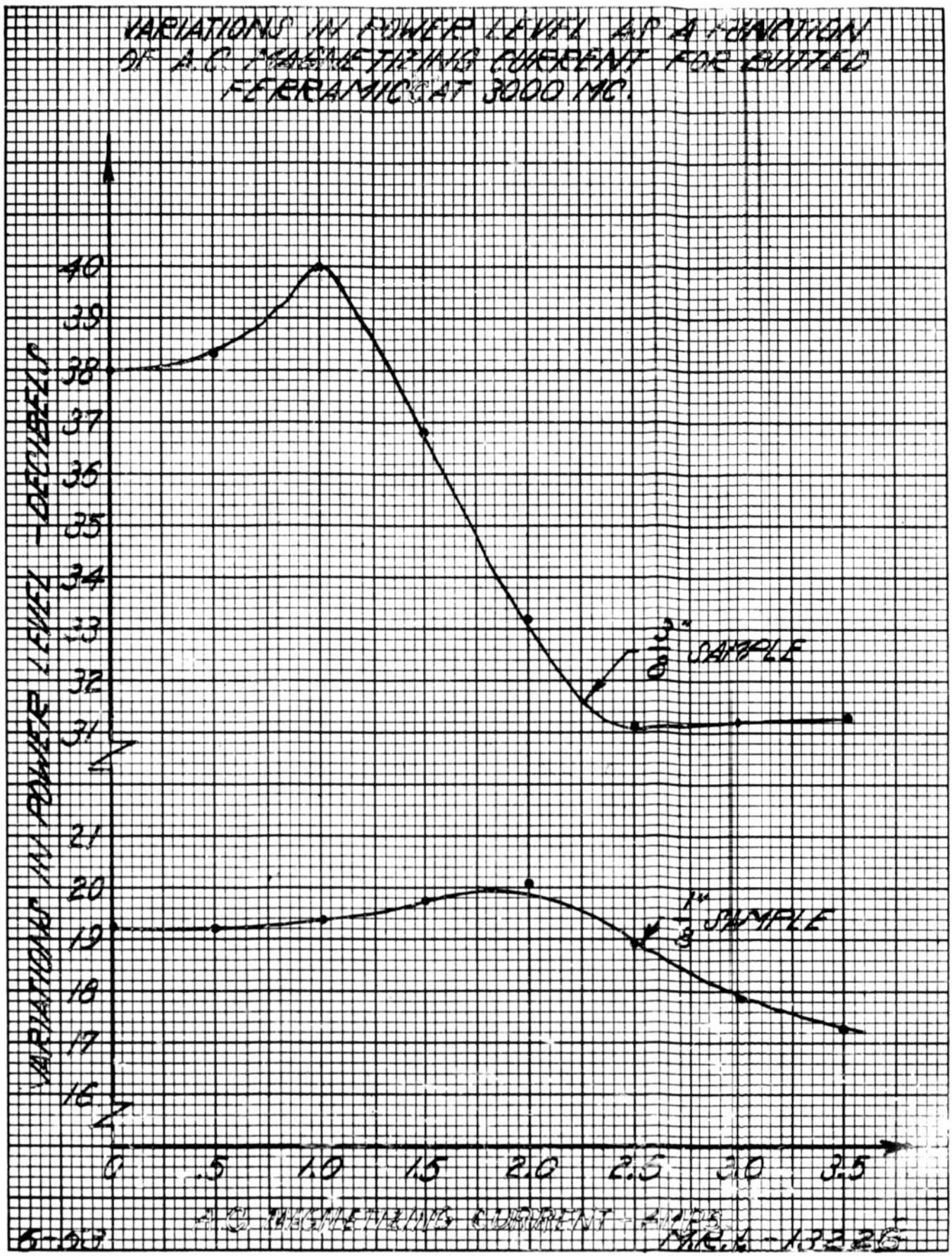
VARIATIONS IN POWER LEVEL AS A FUNCTION OF A.C. MAGNETIZING CURRENT FOR CUT #2 FERRAMIC AT 3000 MC.
VARIATIONS IN POWER LEVEL - DECIBELS
40
39
38
37
36
35
34
33
32
31
21
20
19
18
17
16
3/8" SAMPLE
1" SAMPLE
0
.5
1.0
1.5
2.0
2.5
3.0
3.5
A.C. MAGNETIZING CURRENT - AMPS
6-53
FIG. 4 - 13326

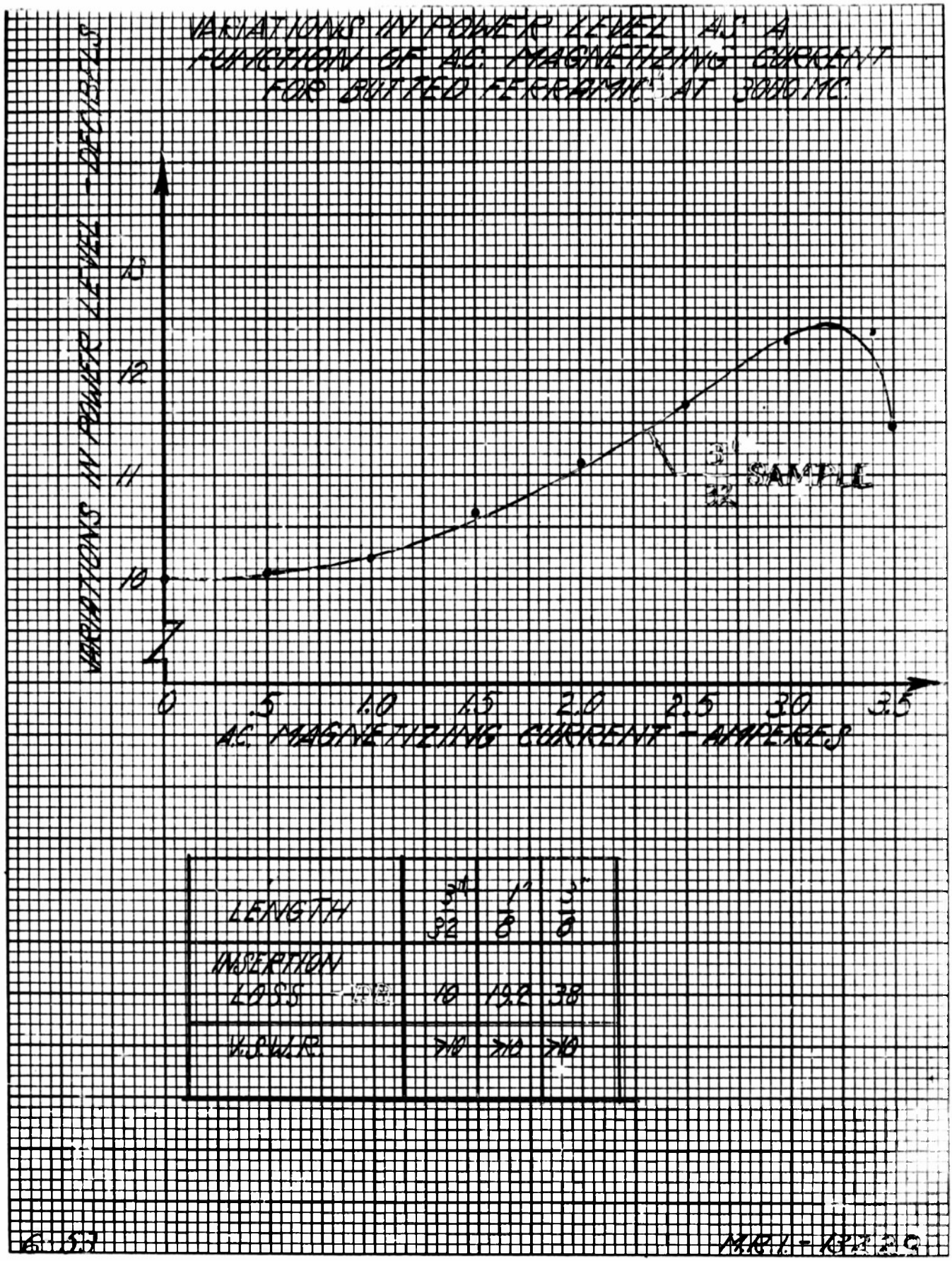

VARIATIONS IN POWER LEVEL AS A FUNCTION OF A.C. MAGNETIZING CURRENT FOR RUTILE FERRITE AT 3000 MC.

LENGTH	3/4"	1"	3"
INSERTION LOSS - DB.	10	19.2	38
V.S.W.R.	>10	>10	>10

6.53

MR1-6R2.2

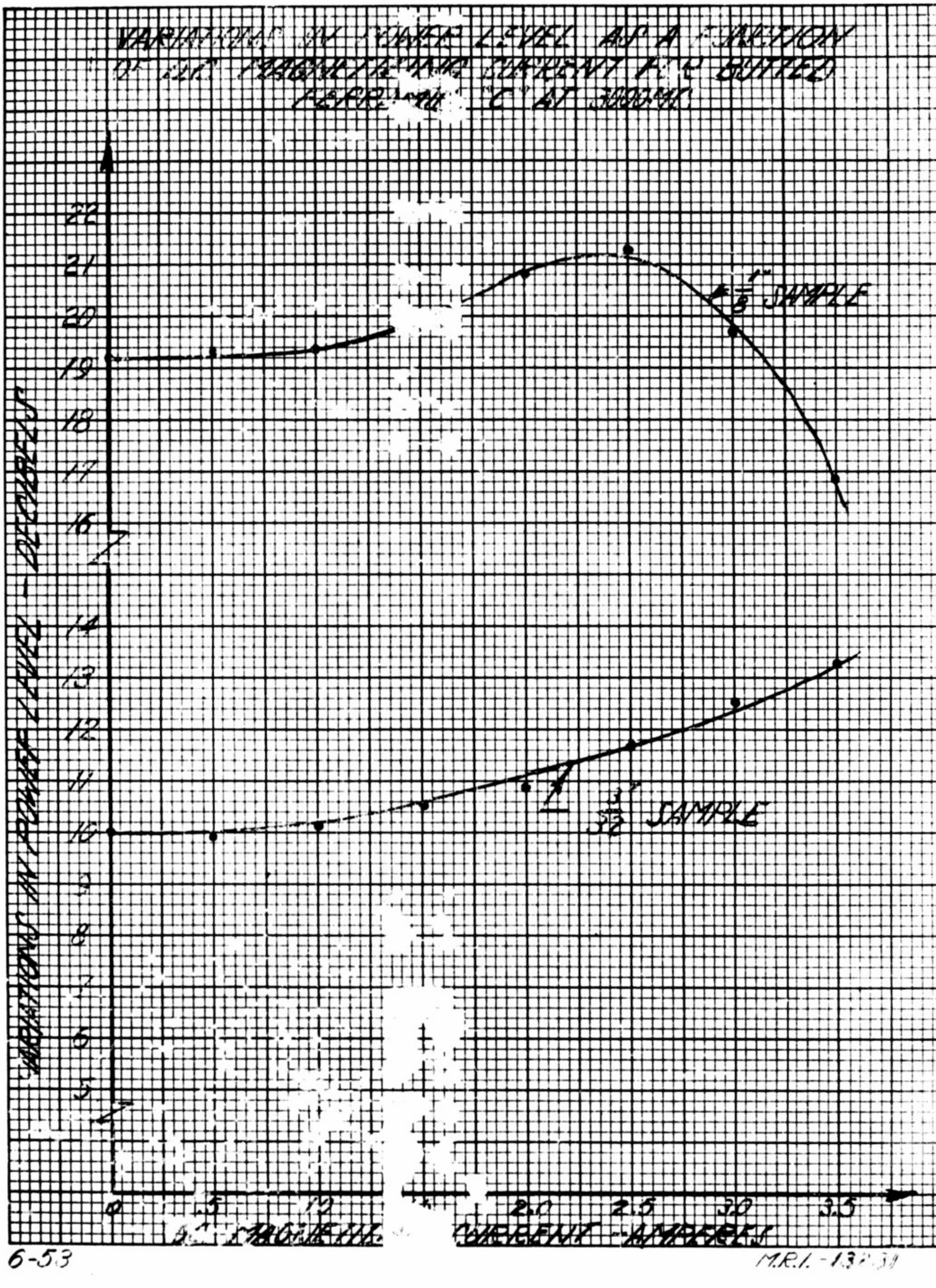
VARIATIONS IN POWER LEVEL AS A FUNCTION OF DC MAGNETIZING CURRENT FOR BUTTED FERRAMIC "C" AT 3000 MC
VARIATIONS IN POWER LEVEL - DECIBELS
1/8" SAMPLE
3/32" SAMPLE
CURRENT - AMPERES
0
.5
1.0
2.0
2.5
3.0
3.5
22
21
20
19
18
17
16
14
13
12
11
10
9
8
7
6
5

6-53

M.R.I.-13P3

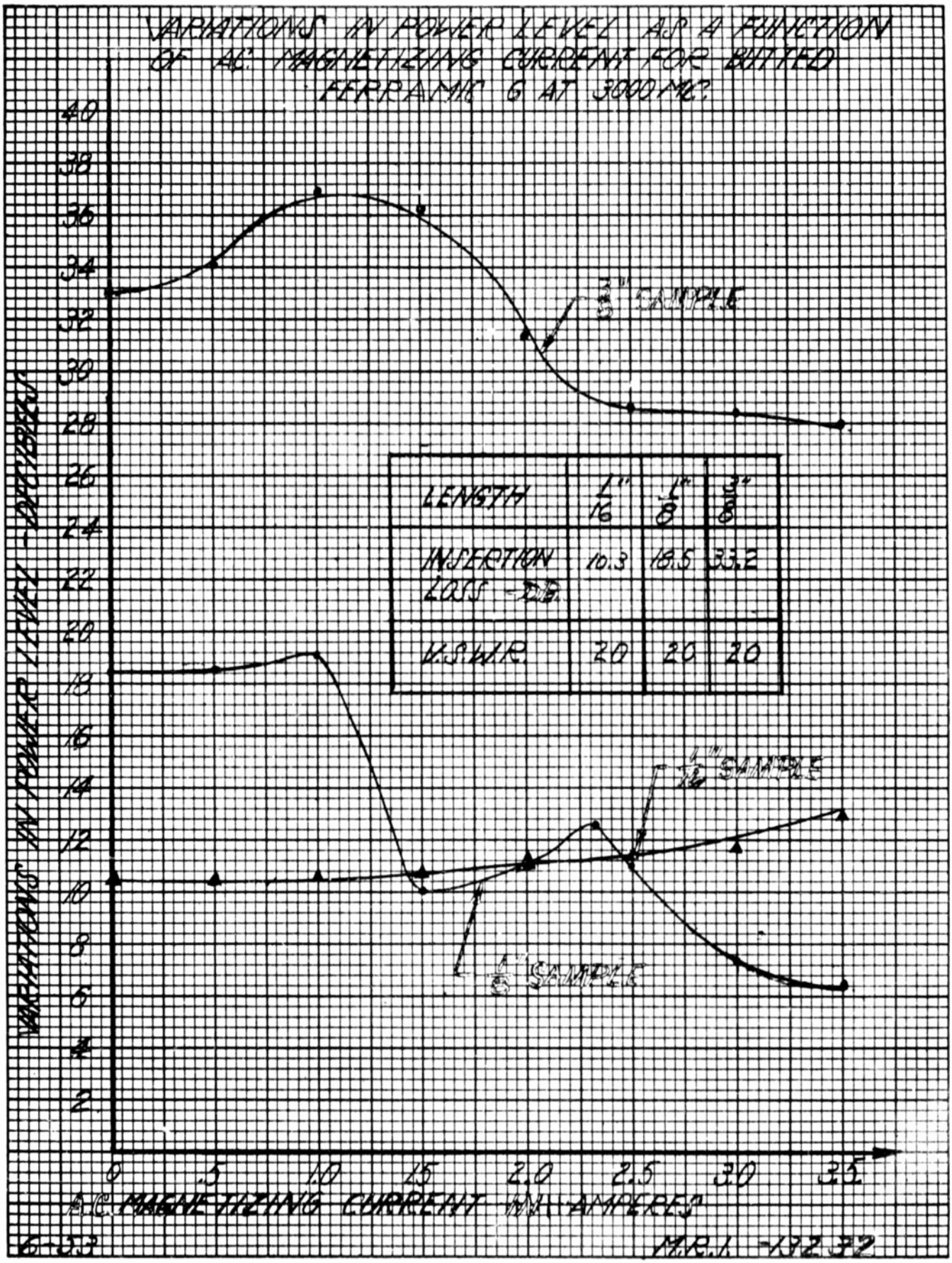
VARIATIONS IN POWER LEVEL AS A FUNCTION OF AC. MAGNETIZING CURRENT FOR MATCHED FERRAMIC 6 AT 3000 MC.
3" SAMPLE
1/16" SAMPLE
1/8" SAMPLE
LENGTH | 1/16" | 1/8" | 3/8"
INSERTION LOSS - DB. | 10.3 | 18.5 | 33.2
V.S.W.R. | 20 | 20 | 20
MAGNETIZING CURRENT IN MILLIAMPERES
A.C. MAGNETIZING CURRENT IN AMPERES
M.R.I. -132-32
6-53

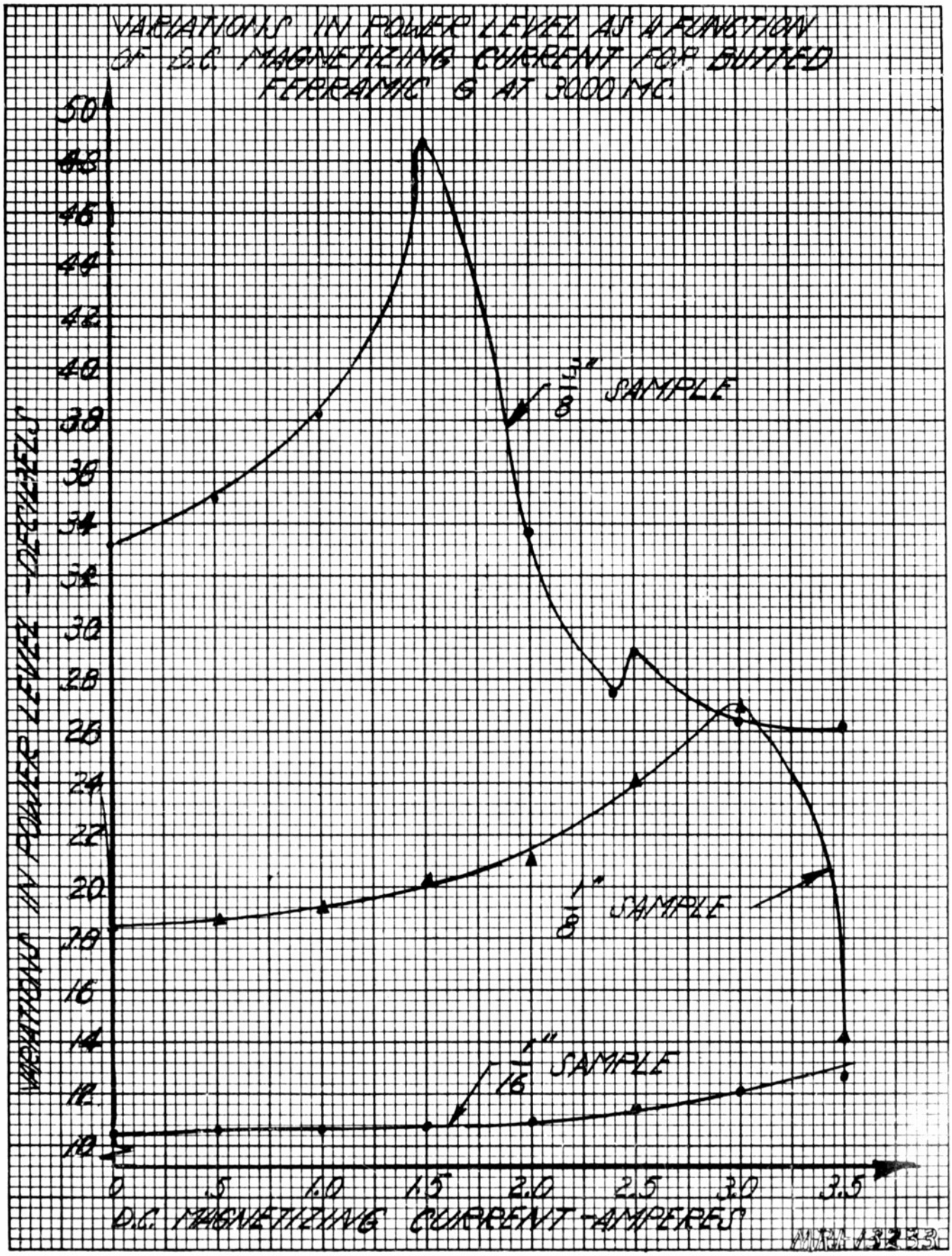
VARIATIONS IN POWER LEVEL AS A FUNCTION OF D.C. MAGNETIZING CURRENT FOR BUTTED FERRAMIC 6 AT 3000 MC.
50
48
46
44
42
40
38
36
34
32
30
28
26
24
22
20
18
16
14
12
10
0
.5
1.0
1.5
2.0
2.5
3.0
3.5
D.C. MAGNETIZING CURRENT - AMPERES
MAXIMUM INPUT POWER LEVEL - WATTS
1/8" SAMPLE
1/8" SAMPLE
1/16" SAMPLE

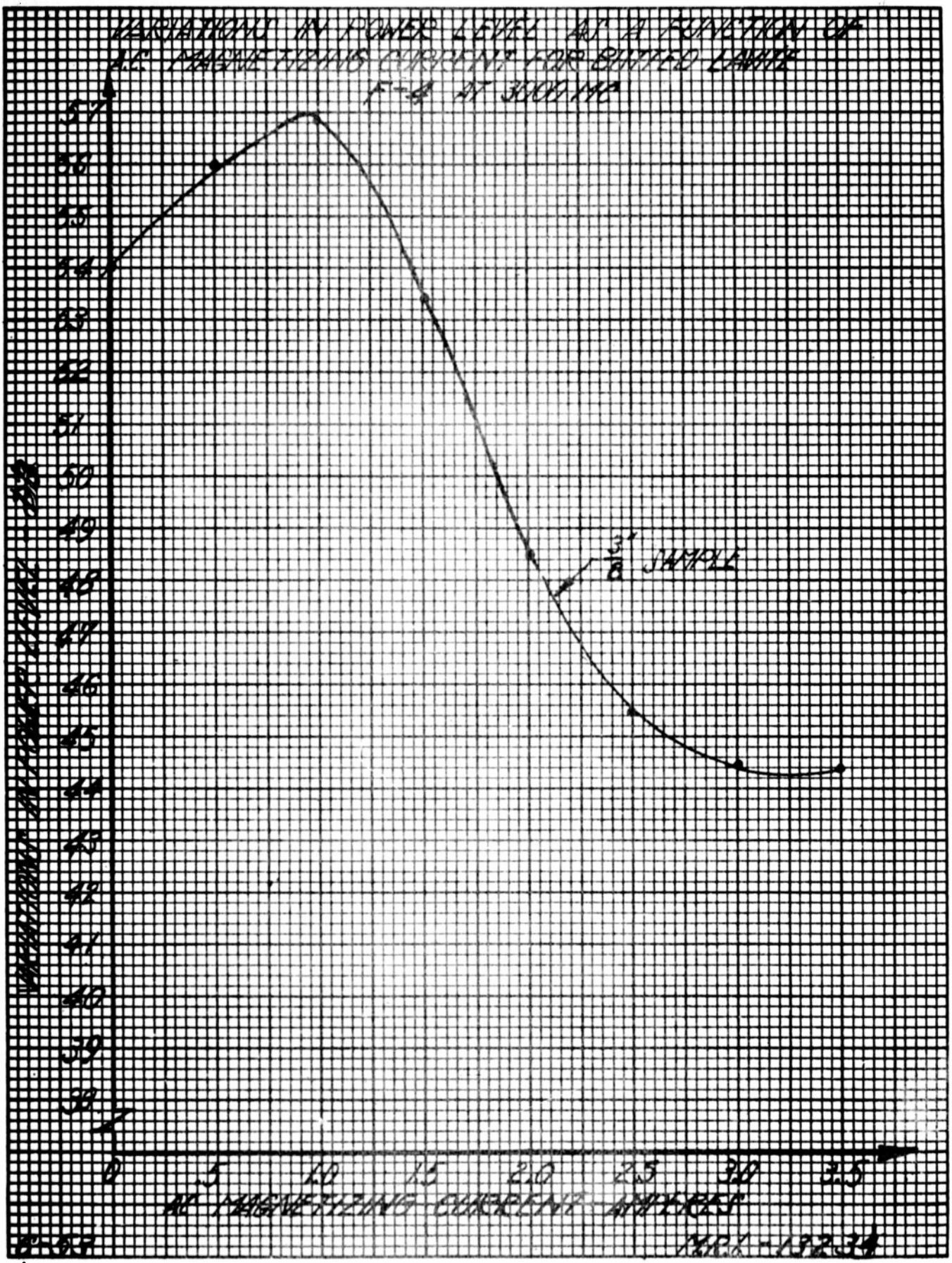
3/8" SAMPLE
0
.5
1.0
1.5
2.0
2.5
3.0
3.5

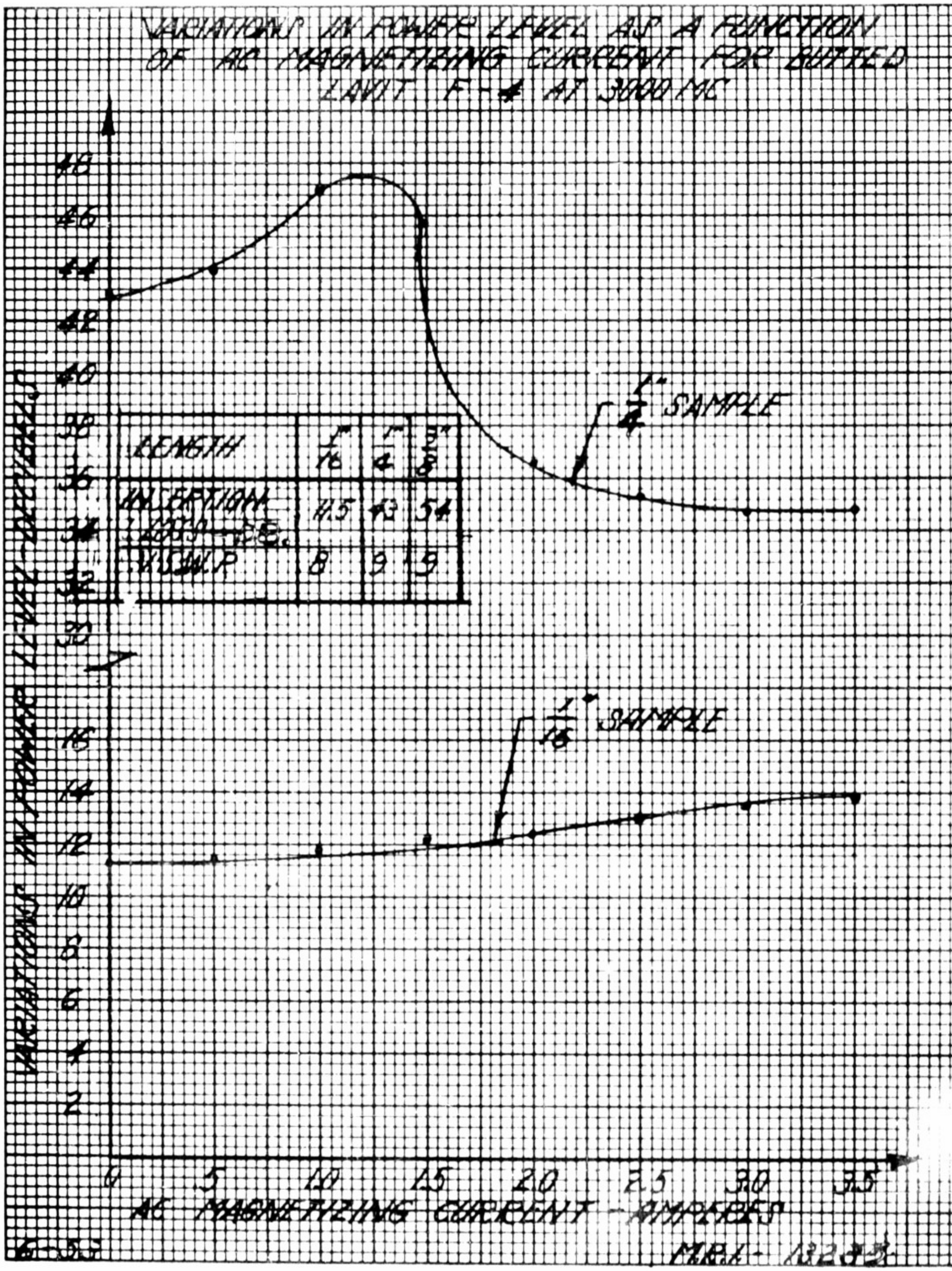
VARIATIONS IN POWER LEVEL AS A FUNCTION OF AC MAGNETIZING CURRENT FOR BUTTED UNIT F-4 AT 3000 MC
VARIATIONS IN POWER LEVEL - DECIBELS
AC MAGNETIZING CURRENT - AMPERES
1/4" SAMPLE
1/16" SAMPLE
LENGTH 1/16" 1/4" 5/8"
INSERTION LOSS - DB. 11.5 43 54
VSWR 8 9 9
48
46
44
42
40
38
36
34
32
30
16
14
12
10
8
6
4
2
0
5
10
15
20
25
30
35
MRL-13233

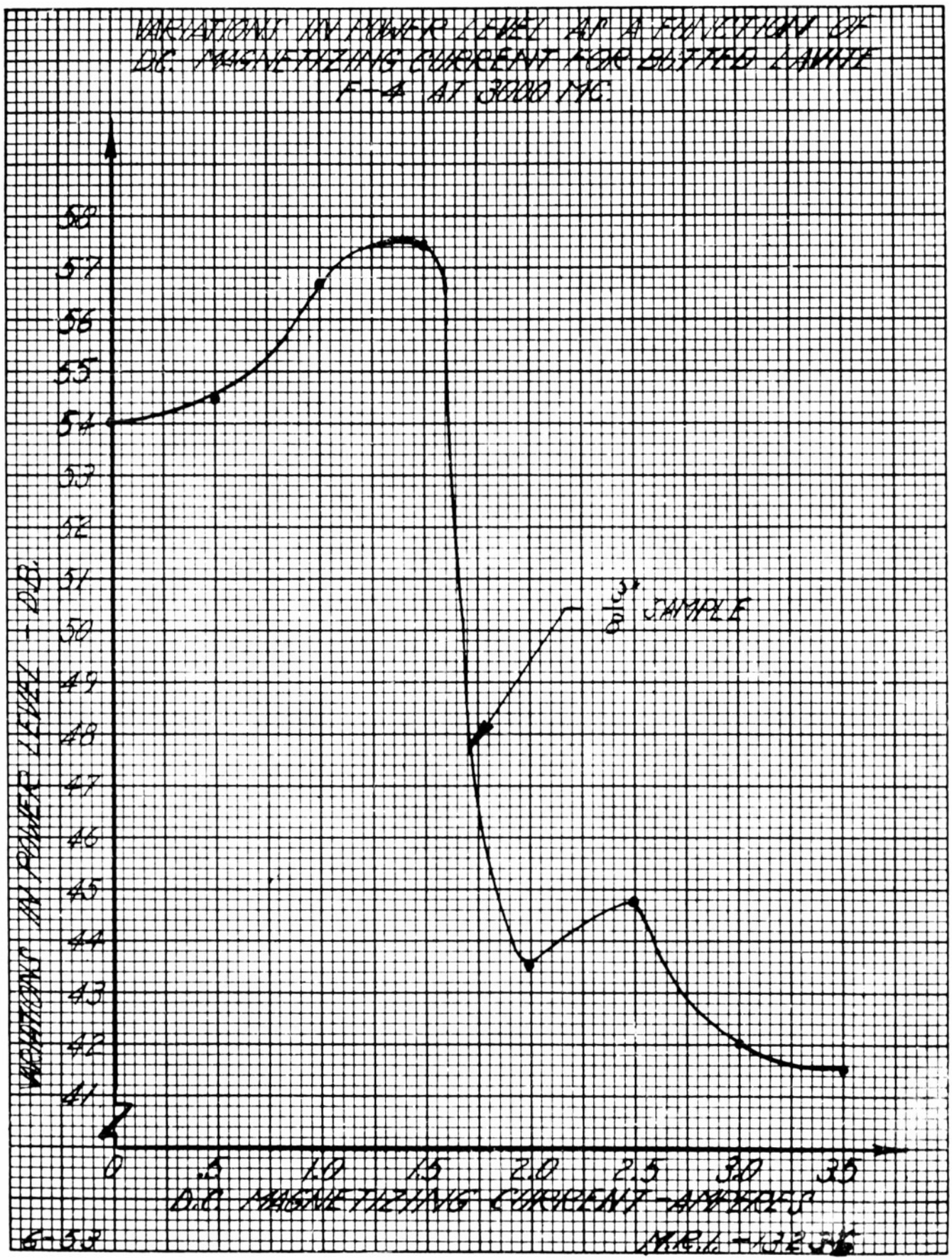

MAGNETIZING CURRENT AT A FUNCTION OF DC. MAGNETIZING CURRENT FOR OUTER CAMAC E-A AT 3000 NC.

6-53

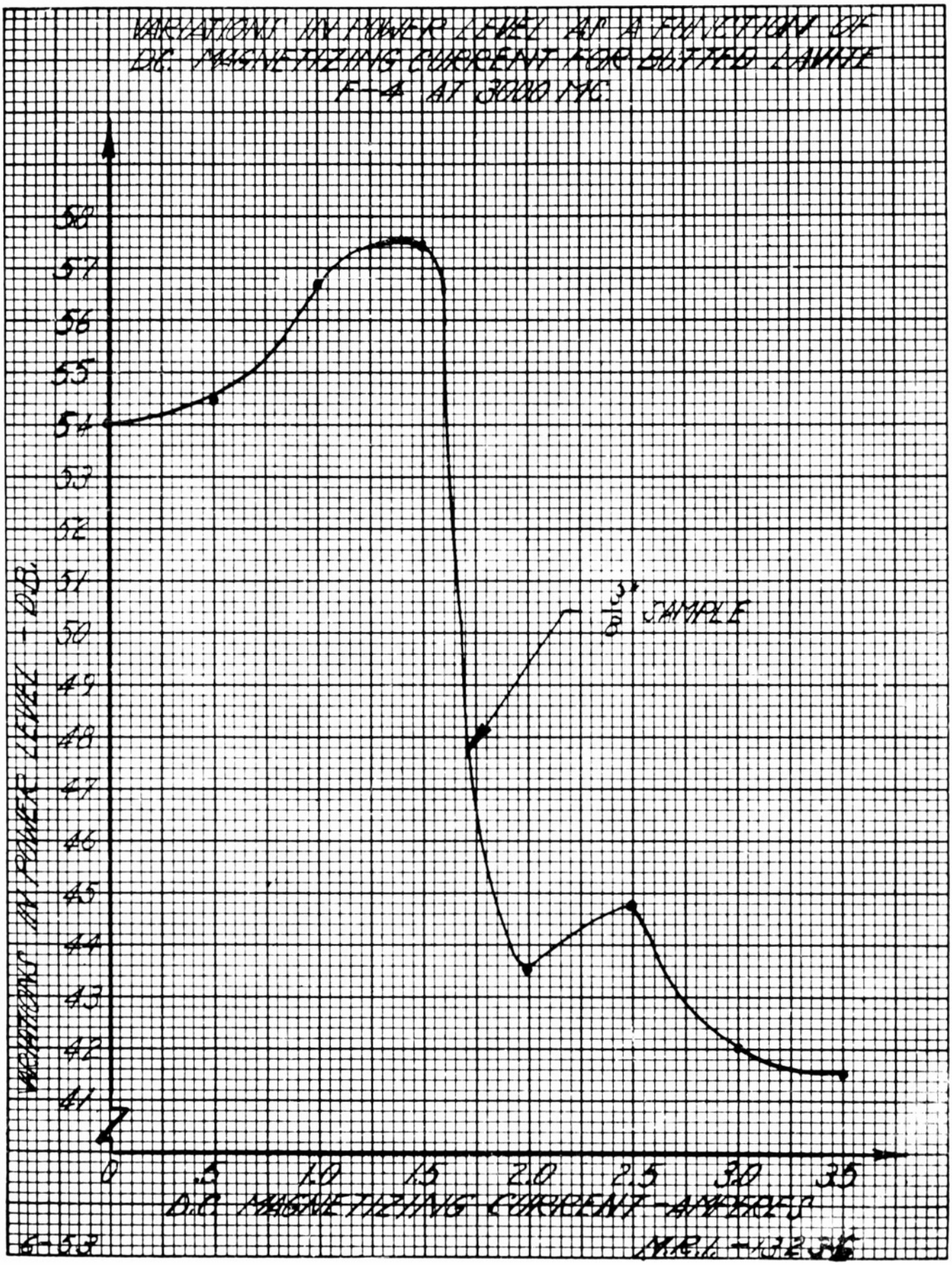
VARIATION IN POWER LEVEL ΔP AS A FUNCTION OF
DC MAGNETIZING CURRENT FOR SATIN LAMINE
F-4 AT 3000 MC.
58
57
56
55
54
53
52
51
50
49
48
47
46
45
44
43
42
41
VARIATION IN POWER LEVEL - DB
$\frac{\partial P}{\partial I}$ SAMPLE F
0
.5
1.0
1.5
2.0
2.5
3.0
3.5
D.C. MAGNETIZING CURRENT - AMPERES
6-53

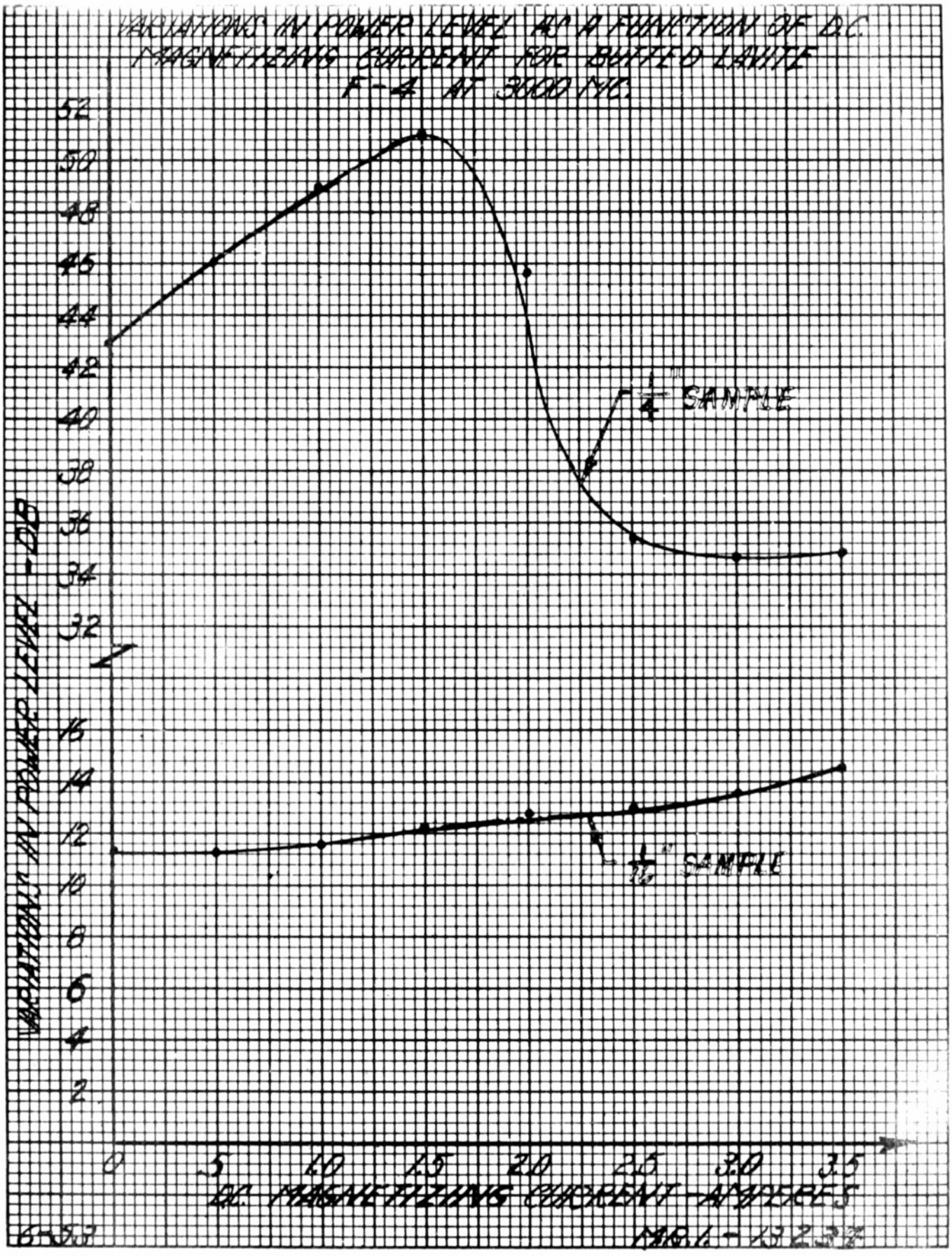
VARIATIONS IN POWER LEVEL AS A FUNCTION OF D.C. MAGNETIZING CURRENT FOR BUTTON LAMP F-4 AT 3000 MC.
F 1/4" SAMPLE
1/2" SAMPLE
POWER LEVEL IN DECIBELS BELOW 1 MILLIWATT
52
50
48
46
44
42
40
38
36
34
32
16
14
12
10
8
6
4
2
0
.5
1.0
1.5
2.0
2.5
3.0
3.5
D.C. MAGNETIZING CURRENT - AMPERES
6-58
MIC. - 13233

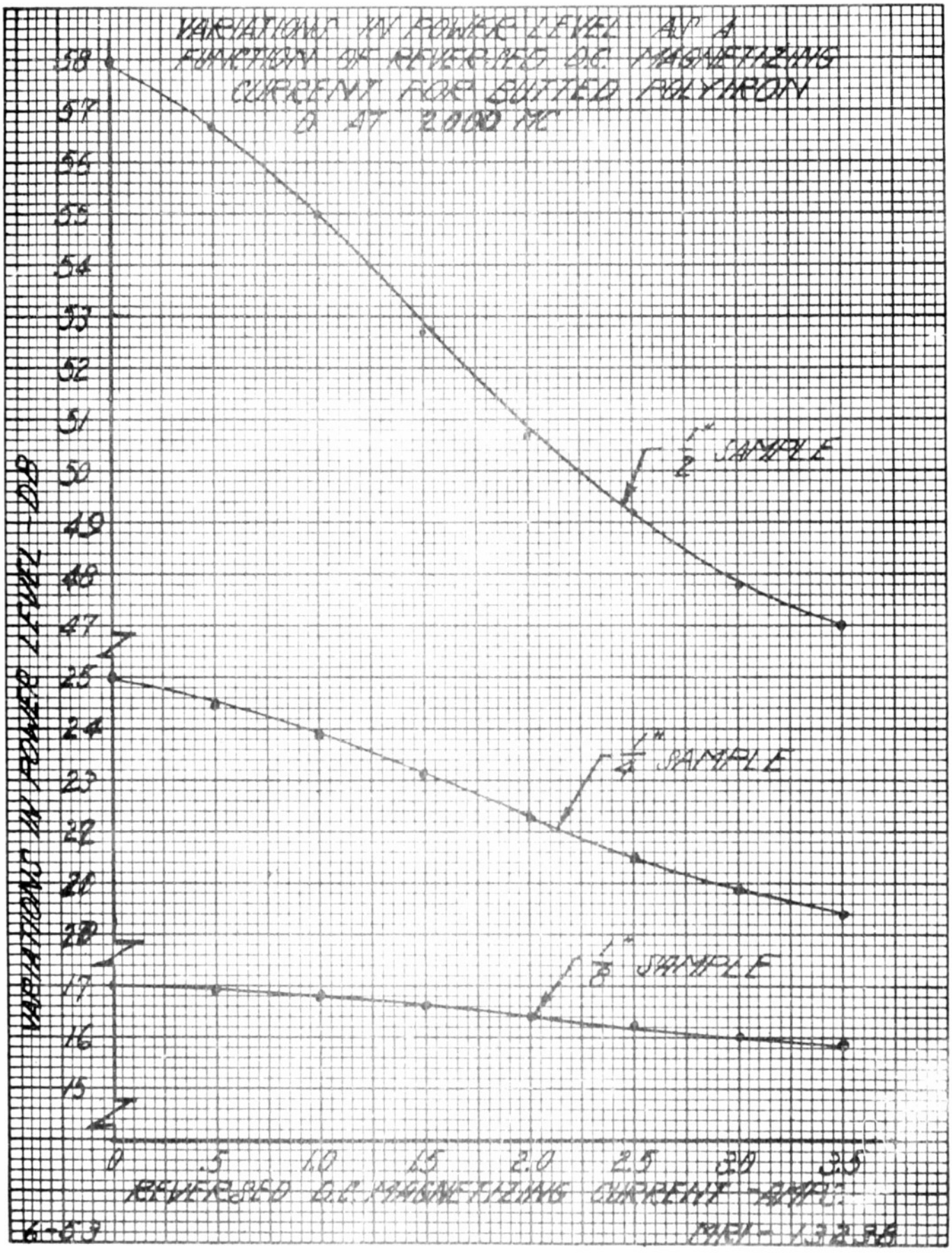
VARIATION IN POWER LEVEL AS A FUNCTION OF REVERSED D.C. MAGNETIZING CURRENT FOR SINTERED POLYKRON D AT 2000 MC
1/2" SAMPLE
1/4" SAMPLE
1/8" SAMPLE
POWER LEVEL IN DECIBELS BELOW MAXIMUM
REVERSED D.C. MAGNETIZING CURRENT - AMPS.
58
57
56
55
54
53
52
51
50
49
48
47
25
24
23
22
20
19
17
16
15
0
.5
1.0
1.5
2.0
2.5
3.0
3.5

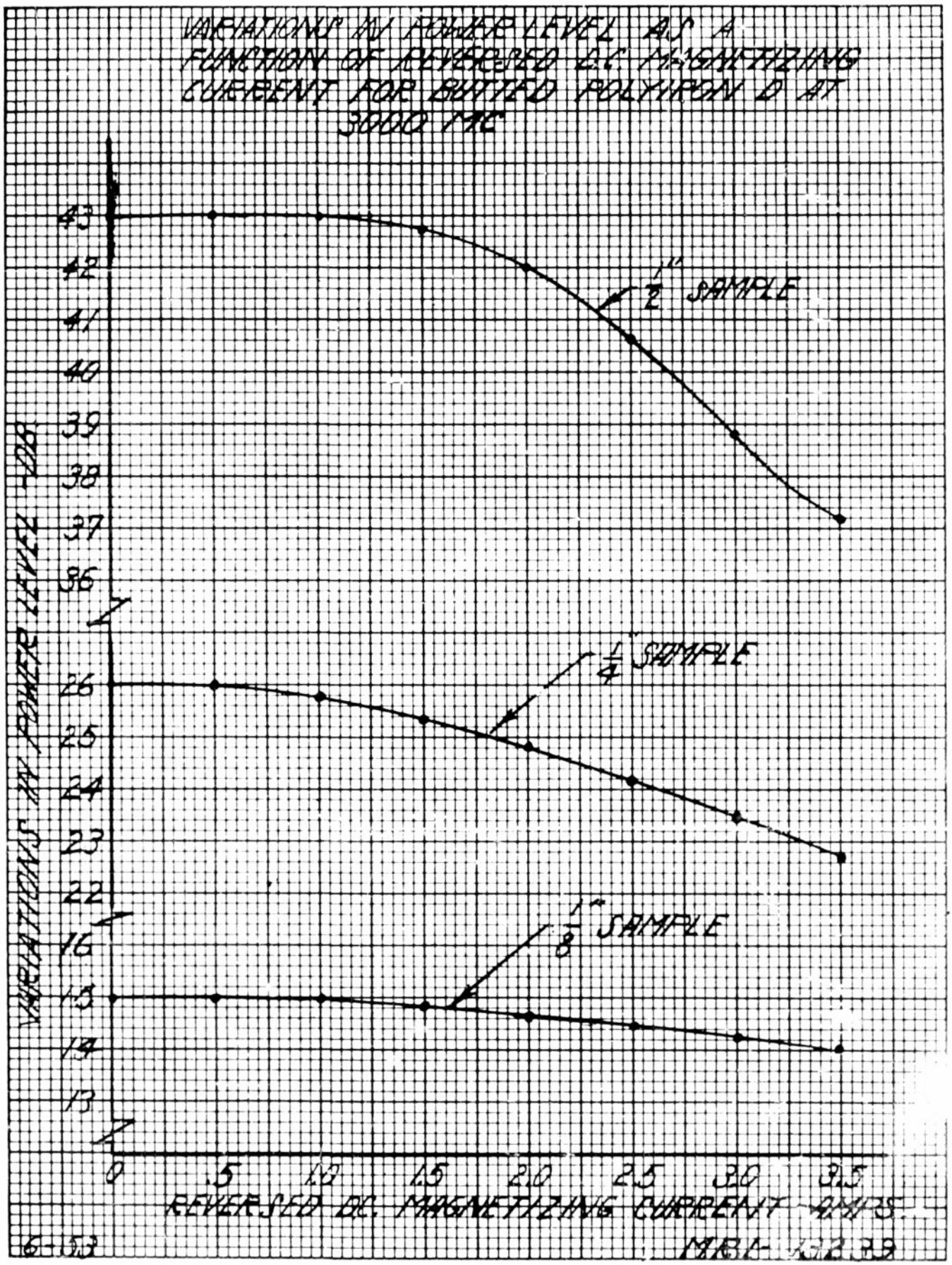
VARIATIONS IN POWER LEVEL AS A FUNCTION OF REVERSED A.C. MAGNETIZING CURRENT FOR SINTERED POLYIRON D AT 30000 RPC
43
42
41
40
39
38
37
36
26
25
24
23
22
16
15
14
13
0
.5
1.0
1.5
2.0
2.5
3.0
3.5
1/2" SAMPLE
1/4" SAMPLE
1/8" SAMPLE
REVERSED AC. MAGNETIZING CURRENT AMPS.
6-53
MBA-12239

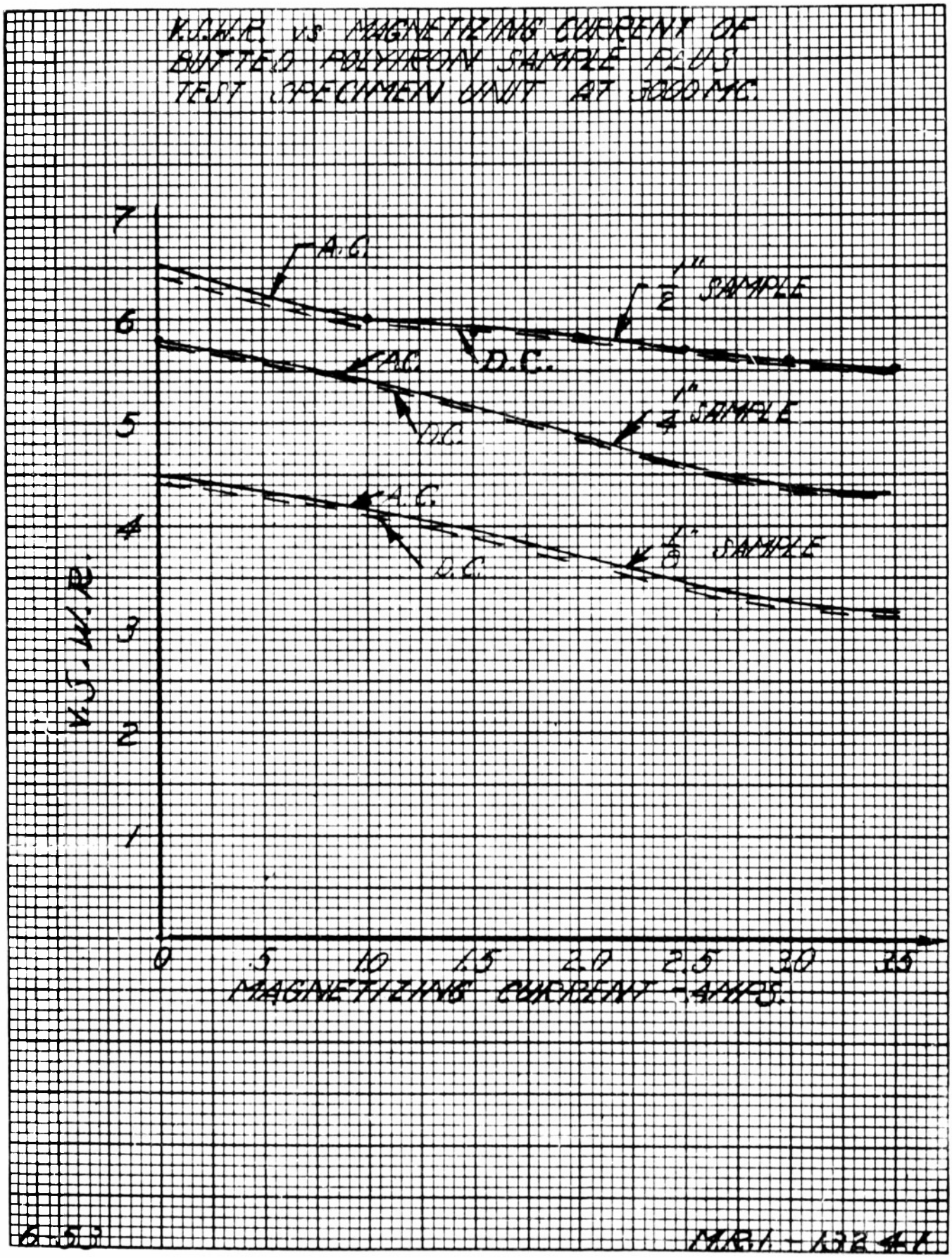
K.M.R. VS MAGNETIZING CURRENT OF
BUTTED POLYRON SAMPLE FROM
TEST SPECIMEN UNIT AT 3000 MC.
A.C.
D.C.
1" SAMPLE
A.C.
D.C.
1/2" SAMPLE
A.C.
D.C.
1/4" SAMPLE
K.M.R.
MAGNETIZING CURRENT - AMPS.
0
5
10
15
2.0
2.5
3.0
3.5
1
2
3
4
5
6
7

DWG. NO. P. I. B.-C- 634-F

DWG. NO. P. I. B.-C- 634-1

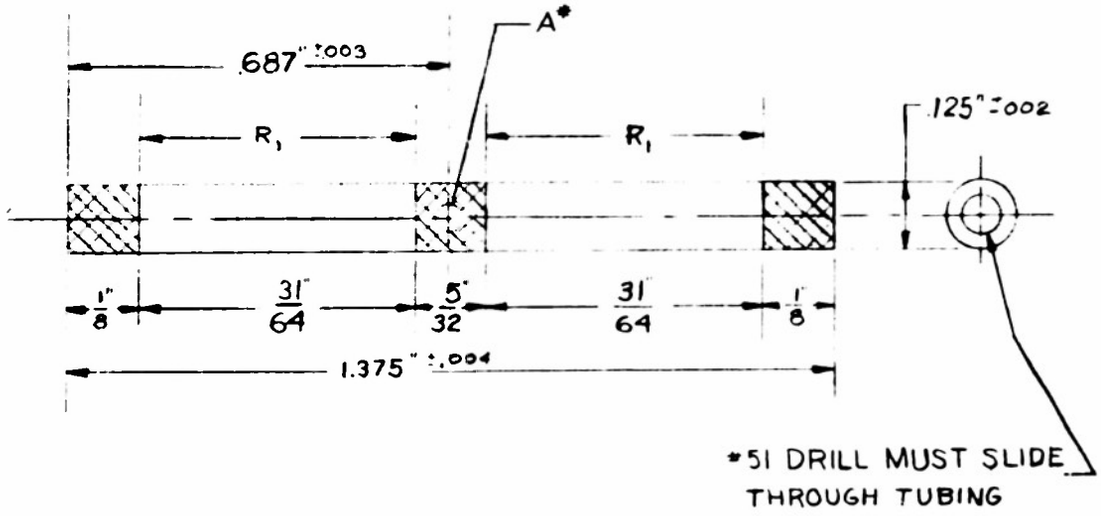

ITEM	R* FOR db
1	2.24 .8
2	2.58 .9
3	2.84 1.0
4	8.45 3.0
5	11.16 4.0
6	13.85 5.0
7	16.4 6
8	18.9 7
9	21.3 8
10	23.5 9
11	25.7 10
12	27.7 11
13	29.5 12

FOR TOLERANCE SEE M.R.I. 11781

MATERIAL - LIME GLASS TUBING

* DRILL HOLE FOR ITEMS 1,2,3,4,5, & 6 ONLY
DIA. HOLE .046" +.002 -.000

POLYTECHNIC INSTITUTE OF BROOKLYN
MICROWAVE RESEARCH INSTITUTE

DRAWN FOR PM	APPROVED BY
DRAWN BY RE	SCALE 3=1
CHECKED BY	DATE 11-51

TITLE: SERIES ELEMENT

DWG. No. P. I. B.-C- 634-F

ITEM	DWG. NO	DESCRIPTION	REQ'D	STOCK ITEMS

CHANGE	DATE

DWG. NO. P. I. B.-C-634-J

DWG. NO. P. I. B.-C-634-J

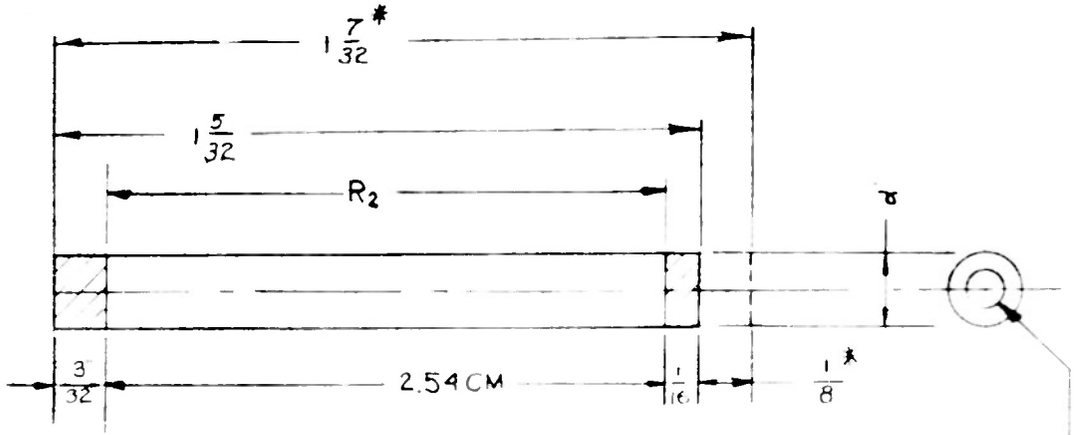

*5| DRILL MUST SLIDE THROUGH TUBING

ITEM	R_2 *	$d^{\pm .002}$ TUBING	FOR db
1	542.	.044	.8
2	476.	.044	.9
3	427.	.044	1.0
4	140.4	.044	3
5	103.6	.044	4
6	81.1	.044	5
7	66.3	.125	6
8	55.1	.125	7
9	46.8	.125	8
10	40.2	.125	9
11	34.6	.125	10
12	30.3	.125	11
13	26.5	.125	12

* FOR TOLERANCE SEE DWG MRI 11781

MATERIAL - LIME GLASS TUBING

* FOR ITEMS 1 THRU 6 INCLUSIVE

POLYTECHNIC INSTITUTE OF BROOKLYN
MICROWAVE RESEARCH INSTITUTE

DRAWN FOR PM	APPROVED BY
DRAWN BY R E	SCALE 3-1
CHECKED BY	DATE 11-51

TITLE

CHIMNEY SHUNT ELEMENT

ITEM	DWG. NO	DESCRIPTION	REQ'D	STOCK ITEMS	CHANGE	DATE	DWG. NO. P. I. B.-C-634-J

Armed Services Technical Information Agency

Because of our limited supply, you are requested to return this copy WHEN IT HAS SERVED YOUR PURPOSE so that it may be made available to other requesters. Your cooperation will be appreciated.

AD 36782

NOTICE: WHEN GOVERNMENT OR OTHER DRAWINGS, SPECIFICATIONS OR OTHER DATA ARE USED FOR ANY PURPOSE OTHER THAN IN CONNECTION WITH A DEFINITELY RELATED GOVERNMENT PROCUREMENT OPERATION, THE U. S. GOVERNMENT THEREBY INCURS NO RESPONSIBILITY, NOR ANY OBLIGATION WHATSOEVER; AND THE FACT THAT THE GOVERNMENT MAY HAVE FORMULATED, FURNISHED, OR IN ANY WAY SUPPLIED THE SAID DRAWINGS, SPECIFICATIONS, OR OTHER DATA IS NOT TO BE REGARDED BY IMPLICATION OR OTHERWISE AS IN ANY MANNER LICENSING THE HOLDER OR ANY OTHER PERSON OR CORPORATION, OR CONVEYING ANY RIGHTS OR PERMISSION TO MANUFACTURE, USE OR SELL ANY PATENTED INVENTION THAT MAY IN ANY WAY BE RELATED THERETO.

Reproduced by

DOCUMENT SERVICE CENTER

KNOTT BUILDING, DAYTON 2, OHIO

UNCLASSIFIED